Possible thunderstorm modifications caused by the Athabasca oil sands development and the Canadian Shield

by

Daniel Martin Brown

A thesis submitted in partial fulfillment of the requirements for the degree of

Doctor of Philosophy

Department of Earth and Atmospheric Sciences
University of Alberta

Abstract

Thunderstorms are common in boreal forest regions and can cause dangerous hazards such as lightning, forest fires, hail, wind, and flooding. Significant research has been conducted to help predict thunderstorms to mitigate or avoid the hazards and damage. The development of thunderstorms depends on many factors, including land cover variations. In this thesis, the Athabasca oil sands development (an anthropogenic land cover modification), and the Canadian Shield (a natural land cover variation), will be examined. The oil sands development creates a massive almost 1000 km^2 land disturbance, changing boreal forest to barren land, tailings ponds, and bitumen upgrading facilities. The Canadian Shield is a drastic land cover change from lusher boreal forest on soil to sparser boreal forest on exposed Precambrian bedrock interspersed with intermittent deep, cold lakes. The effect of land disturbances in the boreal forest is relatively unexplored, and cooler, drier climatic conditions and land cover could result in unexpected effects on thunderstorms.

The first results chapter in this thesis compares temperature, humidity, precipitation, and lightning near and away from the oil sands development, searching for temporal trends as the oil sands development increases in size. Comparing how weather near the oil sands development changes over time, with respect to weather away from it, eliminates differences due to local effects and general climate variation. The precipitation and lightning did not change over time, thus, the oil sands development does not appear to affect thunderstorm climatology. However, a strengthening heat island and dry island were detected within the oil sands development. In particular, the overnight temperatures have increased about 1.2°C relative to the surroundings. These phenomena are thought to be caused by clearing the land, causing a higher Bowen ratio, and emissions of waste heat from oil upgrading, which might be able to trigger thunderstorms in rare situations.

The second results chapter in this thesis used the Weather Research and Forecasting (WRF) model to perform sensitivity experiments. Factor separation was used to quantify the effect of adding/removing two major environmental factors caused by the oil sands development: the land cover disturbance, and the emissions of waste heat. The effect of the oil sands development on thunderstorm intensity was insignificant on all ten days investigated. However, on two of the case study days, the oil sands development appeared to cause thunderstorms to occur one to two hours earlier. The analysis indicates that the oil sands likely triggered storms earlier in these cases, but they appear to be rare. Aircraft measurements indicated that the oil sands development affects thunderstorms mostly when the vertical totals index is greater than 30°C. However, there are probably not enough of these cases to measurably affect climatology.

The third results chapter in this thesis analyzed the variation of detected cloud-to-ground lightning density near the Canadian Shield boundary. The results show that significantly less lightning occurs inside the Canadian Shield than just outside, and a strong cloud-to-ground lightning density gradient exists along the boundary. Various statistical analyses suggest that the lightning density gradient is statistically significantly higher near the Canadian Shield boundary than away from it. However, the signal was not detected in regions with large lakes or more complex topography, which seemed to dominate over the Canadian Shield effect. In one region, the Lightning density decreased from 10 strikes per square km down to 6 over less than 100 km. This effect may be caused by a lower detection efficiency in the Canadian Shield. However, it also could be caused by the sudden change in land cover from more lush, moist, higher transpiring broadleaf forest to sparser, lower transpiring needle-leaf forests on bare bedrock.

This thesis shows that two unique land cover variations in the boreal forest can affect thunderstorms. However, the magnitude of the effect was not always what was expected. The Athabasca oil sands were expected to enhance thunderstorms significantly, but their effect was

much weaker than expected. The Canadian Shield was not anticipated to have much effect at all; however, it significantly diminished thunderstorms. It seems that because thunderstorms occur less in a shorter season and are generally weaker in the boreal forest, that land cover variations could cause thunderstorms to be more difficult to enhance, and easier to diminish.

Preface

Chapters 1, 2, and 3 are introductory and literature review chapters, and Chapter 7 is the conclusions chapter. All are the original work of the author, Daniel Brown. Chapter 4 has been published in the journal *Earth Interactions*. Daniel Brown was the lead author, and was responsible for data collection, data analysis, and the manuscript preparation. Gerhard Reuter was the thesis supervisor, and provided guidance, assisted with data analysis and interpretation, and assisted with editing the manuscript. Thomas Flesch assisted with data analysis, results interpretation, and editing the manuscript.

Brown, D. M., G. W. Reuter, and T. K. Flesch, 2011: Temperature, precipitation, and lightning modification in the vicinity of the Athabasca oil sands. *Earth Interactions*, 15, 1–14. DOI: 10.1175/2011EI412.1.

Chapter 5 is the original work of the author, Daniel Brown. It has been submitted to the journal *Earth Interactions* in June 2017. Chapter 6 has been published in the journal *Atmosphere-Ocean*. Daniel Brown was the lead author, and was responsible for data collection, data analysis, and the manuscript preparation. Gerhard Reuter was the thesis supervisor, and provided guidance, assisted with data analysis and interpretation, and assisted with editing the manuscript.

Brown, D. M. and G. W. Reuter, 2017: The effect of the Canadian Shield on cloud-to-ground lightning density. *Atmosphere-Ocean*, 53, 3, 133-143. DOI: 10.1080/07055900.2017.1316699.

A version of Appendix A has been posted on the University of Utah WRF user's webpage.

Dedication

This thesis is dedicated to our future children, the first of whom is due to be born in mid-October 2017.

Acknowledgements

First, I would like to acknowledge my thesis supervisor, Gerhard Reuter, who spent significant amounts of time helping me learn the research process from formulating a research plan to writing up the final results. He helped me learn how to organize my thoughts into clear and concise writing. Gerhard was always available if I needed to talk to him about anything. If a suitable employment opportunity arose, Gerhard encouraged me to accept it and suggested that we could finish the thesis alongside it. Even once I was employed full-time, Gerhard encouraged me to continue working on the thesis and never lost hope that I would eventually finish.

Additionally, I would like to thank my thesis supervisory committee and Thomas Flesch. Tom Flesch helped me organize some of my complex thoughts into concise sentences suitable for publication. Tom was always available for thoughtful discussion on my research topics. He supported my research and had valuable input on research methods, statistical analysis, and final conclusions. My thesis supervisory committee consisted of John Wilson, Paul Myers, and my supervisor, Gerhard Reuter.

I would also like to thank both Bill Burrows and Bob Kochtubajda from Environment and Climate Change Canada for their helpful input. Bill's experience with lightning parameters and analysis, and general weather knowledge, helped improve our analysis and interpretation of the results (Specifically for Chapters 4 and 5). Bob was extremely helpful in diagnosing possible causes for reduced lightning in the Canadian Shield region (Chapter 6). Bob's understanding of the workings of lightning detection networks and thunderstorm-land surface interactions greatly improved the discussion section of the paper and helped to address the reviewers' comments.

I am grateful to everyone at the Department of Atmospheric Sciences at Texas A&M University who providing me with the opportunity to take all of my required PhD coursework in College Station, Texas. I learned many new techniques for analyzing atmospheric science data while I was there. I especially would like to thank Russ Schumacher (now at Colorado State University) for agreeing to be my supervisor at Texas A&M during my 5 months there, and for being available to answer my questions.

I must acknowledge the data contributors, whose data was used throughout this thesis. I wish to thank Environment and Climate Change Canada for their generous permission to use Canadian Lightning Detection Network (CLDN) data and software. I also thank Alberta Environment for providing land cover data for the oil sands development. The WRF simulations

used data from the North American Regional Reanalysis. Some data from Environment and Climate Change Canada weather stations were also used in various parts of the PhD.

I am also grateful to Environment and Climate Change Canada for providing some paid time for me to work on this thesis during some of my project time at work. As well, I was encouraged by my supervisors to continue working on it. I also received lots of support from my work colleagues. I would also like to thank Wildfire Management in Saskatchewan for supporting my continuing work on the PhD. Chapter 6 in this thesis was developed from research I was encouraged to pursue during project time in the off-season when I was employed there. I especially would like to thank Daniel Poirier for encouraging my early work on the variation of lightning near the Canadian Shield (Chapter 5). Without the support of my employers and colleagues, it would have been much more difficult to finish this thesis.

I received significant assistance from the researchers at the Department of Atmospheric Sciences at the University of Utah, specifically for making modifications to the WRF model to properly simulate the sensible heat output from an industrial facility. Various students and researchers there had experimented modifying the FORTRAN code from the WRF model, and their input helped me to make the modifications I needed to get the results for Chapter 5 in the thesis.

Finally, I would like to thank my family for their inexhaustible support throughout this process. In particular, I am eternally indebted to my loving fiancée, Freja, who stood by me and encouraged me to keep working on the thesis, and helped with the final editing. Her support throughout this process is what allowed me to finish this thesis, and I look forward to being there for her as she continues work on her own thesis. I am also thankful for the many walk requests by our dog, Bella, which helped to clear my head while writing.

Table of Contents

List of Tables

Table 5.3: The results of the factor separation for each case study day. The factor separation method was applied for three variables: maximum reflectivity (dBZ), average total condensate (g/kg), and the total average rainfall (mm).

Table 5.4: The initiation time (UTC), and the storm duration (hours) for each model run for each case study day. The initiation time and duration difference columns are the difference between the "0" and the "HB" cases. The two days with the largest initiation time and duration differences are bolded and italicized. The initiation times are from the innermost domain only, and thus might not match the numbers from table 5.2.

Table 5.5: The results of the factor separation analysis on the initiation time and duration data for 29 July 2010 and 29 July 2014 for each of the model runs. The factor separation results are bolded.

Table 6.1: Various statistical analyses of the mean cloud-to-ground lightning density gradient near the Canadian Shield boundary. The units on the means and standard deviations are 10^{-3} flashes km^{-2} km^{-1} yr^{-1}. The mean ratio is the ratio of the mean near the Canadian Shield divided by the mean away from it. In the last three rows, statistically significant values at the 0.05 threshold are identified by an asterisk. The one-tailed t-statistic requires values greater than 1.73 to be significant. The one tailed U-statistic requires values less than 21 to be significant. The KS statistic requires values greater than 0.664 to be significant.

List of Figures

Figure 4.2: Lightning analysis boxes. The smallest lightning box was designed to approximately include the area of the oil sands disturbance (about 2500 km^2). The two larger boxes are approximately 10000 km^2 and 22500 km^2.

Figure 4.3: Summer temperatures at Mildred Lake and Fort McMurray. a) The average high and low temperatures by year. b) The difference between Mildred Lake and Fort McMurray for the average high and low temperatures, including the linear trend and 95 % confidence intervals.

Figure 4.4: Summer precipitation at Mildred Lake and Fort McMurray. a) The total precipitation by year. b) The difference in precipitation between Mildred Lake and Fort McMurray, including the linear trend and 95 % confidence intervals.

Figure 4.5: Summer humidity at Mildred Lake and Fort McMurray. A) The average water vapor mixing ratio by year. B) The water vapor mixing ratio difference between Mildred Lake and Fort McMurray including the linear trend and 95 % confidence intervals.

Figure 4.6: a) Summer cloud-to-ground lightning strike density (strikes per 10 km^2) in northeast Alberta from 1999 to 2010. b) Cloud-to-ground lightning days. The main disturbance due to the Athabasca oil sands is located at -111.5° and 57.0°, and is outlined in black.

Figure 4.7: Summer lightning trends near the oil sands from 1999 to 2010. a) The number of lightning strikes each year in the biggest box (defined in Figure 2). b) Blue lines are the ratio (percentage) of the lightning density in the innermost area to that in the middle ring. The bottom panel is the ratio of the lightning density in the innermost area to that in the outer ring. The areas and rings are defined in Figure 2.

Figure 5.1: Left: the location of the oil sands and Fort McMurray in Alberta (Brown et al., 2011). Centre: the oil sands land cover in 2007 (Brown et al., 2011). Right: the model modifications. We modelled the oil sands development approximately as a circular 650 km^2 disturbance of barren ground (pink area). We added waste heat to the atmosphere in a smaller area in the centre of the disturbance (blue area).

Figure 5.2: A map of the three nested model domains in relation to the oil sands development in northeastern Alberta.

Figure 5.3: Upper left: a cross section of the model simulated temperature (°C) near the oil sands development from the case with no barren modifications or waste heat. Next three upper row images: the difference between the three modified simulations and the first one. Bottom row: same as above, but with the water vapour mixing ratio (g kg^{-1}) instead of the temperature. All images are at 1815 UTC 29 July 2010, and the cross section was take at latitude 57.1 °N.

Figure 6.2: Cloud-to-ground lightning flash density (flashes km^{-2} yr^{-1}) from 1999 until 2015 along the Canadian Shield boundary between Great Bear Lake and Lake of the Woods. The Canadian Shield boundary is identified by the purple line. Upper left: The Northwest Territories. Upper Right: Alberta and Saskatchewan. Lower Left: Saskatchewan and Manitoba. Lower Right: Southern Manitoba. Note that the colour scales had to be different because of the large variation in lightning density between the northern and southern regions.

Figure 6.3: Lightning density and density gradient versus distance from the Canadian Shield boundary for selected regions. The units of lightning density are flashes km^{-2} yr^{-1}, and the units of the lightning density gradient are 10^{-3} flashes km^{-2} km^{-1} yr^{-1}. Note that the scales are different on some regions because of the large differences in lightning density between the northern and southern regions.

Figure 6.4: Maps of various parameters of lightning flashes and strokes in 10 by 10 km grid boxes in the Canadian Shield area. Top: the average normalized chi-square error from 1999-2015. Bottom-left: the waveform rise-time (μs) from 2011-2015. Bottom-right: the waveform peak-to-zero time (μs) from 2011-2015.

Figure 6.5: Histograms of various lightning stroke parameters within and outside of the Canadian Shield. Top: Normalized chi-square value. Middle: Waveform rise-time (μs). Bottom: Waveform peak-to-zero time (μs).

1. Introduction

1.1. Setting the stage

Summertime thunderstorms are common across the Canadian Prairies and boreal forest, and sometimes they pose a risk to lives and property. Most large wildfires in the boreal forest have been ignited by lightning from thunderstorms (Stocks et al. 2003). In Canada, lightning causes about 100 injuries and 10 casualties annually (Mills et al. 2008). Severe thunderstorms also cause major destruction to property, livestock, and injure people from hail, wind gusts, flooding, and tornadoes. Large hail is particularly common in Alberta (Smith et al. 1998). For example, the 1991 Calgary hailstorm had insured damages of $400 million (Charlton et al. 1995). Hail is such a concern for Calgary and Red Deer that commercial hail seeding has been in operation for the past 15 years. Weather Modification Incorporated regularly seeds thunderstorms in these regions with silver iodide in an attempt to reduce the size of hailstones to reduce their damage (Krauss and Renick 1997). Although less common, tornadoes have also caused heavy damage and casualties in Alberta. The 1987 Edmonton tornado caused $250 million in damage and killed 27 people (Dupilka and Reuter, 2005), and produced the largest hailstone recorded in Alberta at 264 grams (Charlton et al. 1995). Given the impact that thunderstorms can have on everyday life, researchers are continually trying to improve thunderstorm forecasting. However, thunderstorms are notoriously difficult to predict.

This thesis is concerned with two cases of boreal forest land cover variations that may affect thunderstorm initiation and development: the Athabasca oil sands development near Fort McMurray, and the Canadian Shield in western Canada. The oil sands development is a localized, but massive almost 1000 km^2 anthropogenic surface disturbance in the boreal forest. The

Canadian Shield is a widespread natural land cover and geological change predominantly in the boreal forest.

There are two main methods by which the land surface can affect thunderstorms: triggering and widespread changes in surface conditions. For triggering, smaller land cover changes that add heat to the air near the surface or generate lift can cause thunderstorms to be triggered that may not have otherwise formed. Thunderstorms require warm humid air at lower layers with cool air aloft. However, often a warmer nose of air (the capping inversion) blocks the humid air at the surface from interacting with the air aloft. Then thunderstorm initiation becomes very sensitive to triggers in the boundary layer, which are needed for air parcels in the boundary layer to punch through the capping inversion and initiate convection (Strong 1986). Widespread land cover changes work differently in that they influence the amount of heat and humidity available to thunderstorms. For example, large scale conversion of grasslands to farmland has led to a shorter, more intense, more focused thunderstorm season on the Canadian Prairies (Raddatz 1998).

Many researchers have documented various land cover variations affecting thunderstorms. King et al. (2003) found that the climatology of tornadoes in Ontario was affected by lake breeze fronts. Burrows and Kochtubajda (2010) showed that lightning density rapidly drops downwind of large lakes. Rabin et al. (1990) showed that cumulus clouds formed earlier over wheat stubble than forested areas. Raddatz (1998) showed that the large-scale land cover change from prairie to cropland on the Canadian Prairies has affected the thunderstorm season. Brown and Arnold (1998) found that cumulus clouds tended to be focused near land cover boundaries. Even tornadoes tended to cluster near land cover boundaries (Kellner and Niyogi, 2015). The previous examples are just a small sample of the research on how thunderstorms are affected by the land cover.

Additionally, some research has shown that anthropogenic land disturbances caused by concentrations of industrial facilities can affect thunderstorms. Steiger and Orville (2003) found that concentrations of oil refineries in Louisiana caused enhanced cloud-to-ground lightning. Guan and Reuter (1995) showed that waste heat from refineries can influence convective clouds. The Athabasca oil sands development is a massive land disturbance in northeastern Alberta that consists of barren ground, tailings ponds, roads, and bitumen upgrading facilities. There has been a large focus on the environmental impact of the oil sands, yet there were no investigations that focused on the impact of the Athabasca oil sands development on thunderstorms.

1.2. Objectives

This thesis will investigate how natural and artificial land cover variations affect the initiation and sustenance of thunderstorms. The main theme of this thesis will be broken into two sub-themes: artificial land cover variation and natural land cover variation, which will be addressed by the following questions:

1) To what extent are temperature, humidity, precipitation, and lightning modified in the vicinity of the oil sands development,
2) How much do the land cover modifications and the waste heat emitted by the oil sands development affect thunderstorm initiation and development, and
3) How is the distribution of lightning and thunderstorms affected by the Canadian Shield boundary?

One of the biggest summertime forecast challenges in continental climates is narrowing down the risk area for showers and thunderstorms. Understanding the interactions between land cover and thunderstorms allows operational weather forecasters to be more specific with their forecasts and

provide more useful information to their users. However, a review of thunderstorm processes, including land cover effects and lightning formation and detection, needs to be presented to facilitate understanding of the following research.

1.3. Thesis structure

The investigations in this thesis are separated into two separate land cover impacts on thunderstorms: the artificial Athabasca oil sands development, and the natural Canadian Shield boundary. The investigation of the effect of the Athabasca oil sands development are documented in two chapters: one looking at past meteorological observations and lightning detection, and another using numerical modelling to compare thunderstorms simulated with and without the oil sands development. The third paper quantifies the effect of the Canadian Shield on cloud-to-ground lightning density, and speculates why the effect exists.

This thesis is separated into a total of seven chapters. The first chapter is the introduction. The second chapter presents a review of relevant literature on artificial and natural land cover effects on thunderstorms. The third chapter reviews relevant literature on lightning formation and detection. Both the origins of lightning, and methods of lightning detection will be explored. The main body of original research in this thesis is separated into three papers which each investigate a different aspect of artificial and natural land cover variations on thunderstorms. At the end of the thesis, a general conclusions section ties all the three main areas of novel research together. Following the conclusions, various appendices describe methodology, techniques, and datasets in more detail.

The first paper uses past temperature, humidity, rainfall, and lightning measurements to investigate how the oil sands development affects the weather and thunderstorms. In the paper,

differences in the temperature, precipitation, humidity, and lightning trends are explored between areas near the oil sands development versus areas away from it. A statistical test is used to quantify the change in the weather near the oil sands development compared with that away as the oil sands development increases in size and intensity.

The second paper builds on the results from the first paper. A numerical model is used to simulate the effect on thunderstorms by adding or removing the oil sands development on several case study days. Sensible waste heat and land cover changes are added in the model each on their own, and then both together, to investigate the processes involved in thunderstorm enhancement. The method of factor separation is used to quantify changes to modelled thunderstorms as the different effects of the oil sands are added to the simulation.

The third paper focuses on how and why the Canadian Shield affects cloud-to-ground lightning density. Lightning density maps along with some statistical tests were used to quantify the magnitude of the effect. Two possibilities were speculated as to why the effect occurs: there is less lightning because the land cover affects the temperature and humidity at the surface, and there is less lightning detected because the Canadian Shield interferes with lightning detection and causes lower detection efficiency.

1.4. Overview of thunderstorm development

The formation and development of thunderstorms has been researched extensively. During many field projects, investigators have looked at the initiation of thunderstorms, different types of thunderstorms, hail, and tornadoes. For example, Wurman et al. (2012) discuss the Verification of the Origins of Rotation in Tornadoes Experiment (VORTEX, VORTEX2), Weckwerth et al. (2004) discuss the International H_2O Project (IHOP), Geerts et al. (2017) discuss the Plains

Elevated Convection at Night field project (PECAN), and Taylor et al. (2011) discuss the Understanding Severe Thunderstorms and Alberta Boundary Layer Experiment (UNSTABLE).

Thunderstorms are caused by convection, for which buoyancy is the driving force. Positive buoyancy occurs when a parcel of air is warmer than its surroundings. This warm air rises, cools by expansion, and the water vapour condenses into cloud droplets forming a cumulus cloud. The warm bubble of rising air is heated as the latent heat of condensation is released when the cloud droplets condense. Thus, in addition to warmer temperatures, higher surface humidity can lead to more buoyancy because the latent heat of condensation is released as the cloud forms. As the cloud grows, precipitation forms and begins to fall. Air cooled by evaporating precipitation has negative buoyancy, and falls as a downdraft. Thunderstorms require three ingredients: surface humidity, convective instability, and a trigger to release the instability. Severe thunderstorms a fourth ingredient: vertical wind shear. The ingredients for thunderstorms will be discussed in greater detail in the following text.

Humid air is important for the development of thunderstorms. There are two main sources of low-level humidity for thunderstorms in western Canada: moisture advection, and evapotranspiration (Raddatz 2005). Brimelow and Reuter (2008) showed that moisture trajectories for significant rainfall events in northern Alberta often came from the Gulf of Mexico. Strong (1997) showed that transpiration from crops could raise the mixing ratio significantly (Figure 1.1), and could significantly increase thunderstorm potential. Crops tend to transpire the most in the afternoon, which further increases the possibility of thunderstorms at the time of peak surface temperatures (Raddatz 1993). Land surface effects on thunderstorm initiation and development will be discussed further in the Chapter 2. In the lee of the Rocky Mountains, the humidity from both of these effects can be pooled and enhanced with an easterly component to

the surface wind because the Rocky Mountains block the westward flow at the surface (Smith and Yau 1993).

Convective instability is crucial for the development of thunderstorms. The concept of convective instability is shown in the upper air sounding in Figure 1.2, where the area of instability is shaded in light red. Relatively warm air at the surface and relatively cool air aloft is required to create the buoyancy to drive the convective overturning. Forecasters often try to align a thermal ridge at the surface with a thermal trough aloft when formulating a thunderstorm risk area. Convective instability also requires sufficient low-level humidity. When the buoyant surface air is lifted, the humidity warms the air further due to the release of latent heat. Forecasters often look for areas of high surface humidity when forecasting thunderstorms. Convective instability is most common in the summer, when strong daytime heating creates warm air in the low levels, and transpiration from abundant vegetation causes high humidity.

Thunderstorms are affected by the presence of a capping inversion. A capping inversion is a layer of warm air that can form above the surface, but still in the low levels of the atmosphere (Strong 1986). This layer of warm air does not allow the slightly cooler air at the surface to rise through it until it is sufficiently warm or is pushed by a trigger (Figure 1.3). The capping inversion can completely inhibit thunderstorm development if it is strong. The upper air sounding in Figure 1.2 has a moderately strong capping inversion. However, a weaker inversion can be penetrated by a surface updraft, especially with strong surface heating or a trigger. The capping inversion can make thunderstorms much stronger by delaying storm initiation until late afternoon when daytime heating and transpiration are at their peak. The inversion also limits the number of storms so that they do not interfere with each other (Strong 1986). Both Smith and Yau (1993) and Strong (1986) stress the importance that the capping inversion has on the development of severe thunderstorms in Alberta.

Even given all of the previous ingredients for thunderstorm development, thunderstorms will not form without a trigger. A trigger is an atmospheric or terrain feature that enhances lift and allows the thunderstorm updraft to break through the capping inversion. An example of a trigger is a dark field amongst many light-coloured fields that enhances daytime heating and causes a stronger updraft. Land cover variation, such as land-water boundaries (King et al. 2003) and vegetation boundaries (Carleton et al. 2008), can trigger thunderstorms because of varying albedo and evapotranspiration. Hills or valleys can trigger storms because the sun-facing slope is heated more intensely (Thielan and Gadian 1997). The tops of hills can have a higher potential temperature than the surrounding air, initiating an updraft (Hanesiak et al. 2004). Meteorological features such as thermal fronts, drylines, outflow boundaries, and short-wave upper troughs can also trigger thunderstorms.

All of the previously discussed conditions will cause thunderstorms to form, but they will not necessarily cause severe and damaging thunderstorms. An additional ingredient, vertical wind shear, is required for severe thunderstorms (Figure 1.4). Thunderstorms consist of a warm moist updraft and a rain cooled downdraft. Wind shear separates the updraft and downdraft so that they do not interfere with each other. The separation give the updraft more consistent access to warm moist air because the cool dry downdraft is blown downstream and out of the way. A 20 to 30 m/s vector wind difference between the surface and 500 mb is generally considered sufficient to cause severe thunderstorms (Weismann and Kemp 1982), which is present in the upper air sounding in Figure 1.2. The effect of wind shear can be complex. Straight line wind shear and directional wind shear can cause different types of storms. However, that is beyond the scope of this discussion.

Thunderstorms in western Canada are strongly affected by the Rocky Mountain barrier. Smith and Yau (1993) describe the following conceptual model for the development of summer

severe thunderstorms in the Alberta foothills. A long-wave upper trough or upper low in western British Columbia combined with a long-wave upper ridge in Saskatchewan create a southwesterly flow over the Rocky Mountain barrier in Alberta. The southwesterly flow causes a lee trough or lee cyclogenesis, which results in an easterly wind component at the surface and increases surface convergence. The easterly component can be enhanced in the morning by the mountain-plain circulation; when the morning sun preferentially heats the east slopes of the Rocky Mountains causing low pressure and an easterly flow towards the mountains. The easterly flow is an upslope flow which helps to both trigger thunderstorms near the foothills, and provide wind shear to help severe thunderstorms to form. The easterly flow also causes humid air to pool along the foothills, increasing the instability. As upper-level cooling occurs, instability is increased further, and severe storms can develop (Strong 1986, Smith and Yau 1993).

The vast majority of thunderstorm research has been conducted in the southern half of Alberta, mainly along the foothills of the Rocky Mountains. Researchers tend to focus on the foothills because most of the severe thunderstorms and lightning in Alberta form in this region (Taylor et al. 2011). Research also tends to focus on the devastating effects that these storms can have on the heavily populated Edmonton-Calgary corridor. There has been little focus on thunderstorms farther north in the parkland and boreal forest regions of the Prairie Provinces. However, severe thunderstorms are recorded in those regions. For example, the 2007 Fort McMurray hailstorm caused $15 million in damages (Crewe 2008). Thunderstorms in northern regions are less common than in southern regions, but they also may not be recorded as often due to poor radar coverage and a much lower population density (Cheng et al. 2013). In fact, there are areas in northern Alberta that have a higher lightning strike density than that of southern Alberta, away from the foothills (Burrows and Kochtubajda 2010).

There has, however, been some research in northern regions. For example, Burrows and Kochtubajda (2010) found higher lightning density near hills such as the Swan Hills and the Caribou Mountains in northern Alberta, and also found that large lakes such as Great Slave Lake and Lake Winnipeg inhibited lightning downwind. Kochtubajda et al. (2011) discussed positive cloud-to-ground lightning in the Yukon enhanced by forest fire smoke. The conceptual model by Strong (1986) and Smith and Yau (1993) suggests that thunderstorms tend to develop early in the afternoon when they are triggered in the Alberta and Montana foothills, and then track west and northwestward into Saskatchewan in the evening then through Manitoba overnight. Brown (2012) found that, on average, thunderstorms occurred one to two hours earlier in western Saskatchewan than in eastern Saskatchewan. Cheng et al. (2013) created a possible tornado frequency map corrected for low populated northern regions in Canada using lightning detection data. However no researchers have commented on industrial activities or specific land cover topics that could influence thunderstorms in the boreal forest.

1.5. The Athabasca oil sands development

One of the largest known oil deposits in the world is found in northeastern Alberta. The most dramatic extraction method is open-pit surface mining (Kelly et al. 2009). Oil sands deposits are mined, then bitumen is extracted and is upgraded into synthetic crude oil. The large-scale surface mines, located about 30 km north of Fort McMurray (Figure 1.5 – right), cover almost 900 km^2 (Government of Alberta 2016) and continue to grow at a rapid pace. The landscape of the disturbed area is an assortment of barren land, open pit mines, tailings ponds, and industrial upgrading facilities (Figure 1.5 – left). Mine waste is disposed of in tailings ponds, which cover

about 150 km^2. Oil production from the oil sands is forecast to rise from 1.3 million barrels per day in 2008 to almost 3 million barrels per day in 2020 (Kelly et al. 2009).

Scientists and environmental organizations have expressed concern about the environmental impacts of the oil sands development. The oil sands development has caused massive changes to the land cover and contributes to less prolific vegetation (Latifovic et al. 2005). Pollution emitted by the oil sands could cause acid rain and increase the pH of lakes downwind (Hazewinkel et al. 2008). The oil sands development also causes air pollution and water pollution in the Athabasca River that flows through the development (Grant et al. 2010, Kelly et al. 2009).

Extraction and upgrading of the bitumen requires massive amounts of energy. De Bruijn (2010) estimated that about 1 GJ of energy is required to produce one barrel of oil from oil sands deposits. Much research discusses the carbon dioxide emissions related to this energy use (Charpentier et al. 2009). However, there is very little data or discussion on the amount of the energy used in the oil sands processing that is emitted into the atmosphere as waste heat. The amount of emitted waste heat along with the large-scale land disturbances could cause inadvertent weather modification; the focus of this thesis.

After large scale industrial activity began, interest has grown regarding the transport of air pollution. Fanaki (1986) investigated the structure and evolution of temperature inversions using an acoustic sounder and minisondes. Leahey and Hansen (1982) correlated winds derived from 850 mb maps with winds at 400 metres altitude, and found that the topography significantly influenced these winds. Walmsley and Bagg (1978) found that the wind at the Fort McMurray weather station correlated well with the wind at the Mildred Lake weather station, aside from some small differences caused by topography. There has not been any research into the effect of the oil sands development on thunderstorms.

Data sparsity is a major limitation to weather analysis and forecasting in general, and it is particularly limiting in the Fort McMurray and oil sands development area (Figure 1.6). Weather radar is crucial for detecting, tracking, and analyzing thunderstorms. However, the nearest radar to Fort McMurray is 220 km away, giving very poor resolution, no velocity measurements, and no low-level measurements. The lowest angle of the weather radar is 0.3 degrees (Joe and Lapczack 2002). Thus, at 220 km the radar beam is about 1 km above the original height of the radar tower, plus another 4 km above the surface of the earth because of the curvature of the Earth at the long distances. The nearest weather radar cannot detect precipitation at the oil sands development below about 5 km above the Earth's surface, and can only see the top half of thunderstorms. Other information can be gleaned from geostationary satellites; however, the high latitude of Fort McMurray gives poor resolution and large parallax errors, particularly for thunderstorms.

Upper air data (mainly from balloon soundings) is important for diagnosing atmospheric stability and severe thunderstorm parameters, but the nearest atmospheric soundings are in Stony Plain and Fort Smith; both almost 400 km away. However, Aircraft Meteorological Data Relay (AMDAR) measurements provide temperature and wind profiles from the Fort McMurray airport a number of times per day (less on weekends). There are also very few surface weather stations, and many of the forestry stations only operate in the summer. All of this makes observational studies very difficult, which is why a large portion of this research consisted of numerical modelling.

1.6. The Weather Research and Forecasting (WRF) model

The Weather Research and Forecasting (WRF) model is a non-hydrostatic local-area numerical weather prediction model. Given a set of initial and boundary conditions, the WRF model can forecast the future state of the atmosphere by numerically solving the primitive equations of motion. The WRF model outputs data (such as temperature, humidity, and wind) in a four dimensional array which consists of the three spatial dimensions and one temporal dimension. Each grid cell in the array will have one value of each meteorological variable. The size of the domain of the WRF model can range from as small as a city to as large as a continent. Depending on computer processing power, it is possible to have a horizontal spatial resolution of less than 1 km. Furthermore, WRF has the capability to nest domains within each other. Model output from a low-resolution outermost nest (domain) is used as a boundary condition for a higher-resolution inner nest, and so forth (Shamarock et al. 2008). The WRF model allows grid nests to interact with each other, thus small scale features in the smallest nest can have an effect on the evolution of the flow in the larger nests. The WRF model is suited for simulating synoptic and mesoscale weather. In addition, WRF can be used to simulate past case study events by ingesting initial and boundary conditions from the North American Regional Reanalysis dataset available from the National Centre for Atmospheric Research. WRF uses a terrain following vertical grid, and the horizontal Arakawa-C grid (Shamarock et al. 2008).

Researchers have been using the WRF model to gain further understanding of atmospheric processes. Kumar et al. (2008) used WRF to simulate a case study event of heavy rainfall in Mumbai, India. Mölders (2008) calculated fire weather indices for Alaska using weather forecasts generated by the WRF model. Lin et al. (2008) simulated a case study of an urban heat

island in Taipei, Taiwan, and found that the urban heat island could influence land and sea breezes. Flesch and Reuter (2012) used WRF to simulate Alberta flooding events and to quantify the role of topography in organizing the precipitation. WRF has been shown to adequately simulate Alberta weather (Pennelly et al. 2014, Pennelly and Reuter 2017).

Many atmospheric phenomena occur on a scale much smaller than the grid cells of the model (such as individual wind gusts, or vegetative transpiration from individual plants). Since it is computationally difficult to explicitly model these sub-grid scale phenomena, they are included in the model via parameterisation schemes. The WRF model has options for using different parameterisation schemes. For example, shortwave and longwave radiation is parameterized, along with the atmospheric boundary layer. Cloud and precipitation microphysics were parameterized using the Lin et al. (1983) microphysics scheme. The aim of this thesis is not to test the differences between the various parameterization schemes. However, these schemes do need to be selected in order to run WRF, and thus, in most cases, the default scheme was chosen. The schemes that are more relevant to thunderstorm initiation and development will be discussed next in more detail.

The most important parameterization choice for thunderstorm modelling is the cumulus parameterization scheme. In these simulations the Grell-Freitas convective scheme was used because it is designed for modelling convective processes at high resolutions. Processes caused by convective instability happen on very small scales; often smaller than the grid spacing of the numerical model. Most convective parameterizations assume that convection only exists in a small portion of the grid cell. However, in models with a grid spacing of less than 10 km, convection begins to occupy a substantial proportion of the grid cell (Grell and Freitas 2014). Grell and Freitas (2014) speculated that when subsidence occupies a substantial portion of the grid cell, it may artificially dissipate the convection. They solve this issue by spreading the subsidence over

neighbouring grid cells in cases with grid spacings less than 10 km. In this way, the convective scheme is applicable at varying grid spacings and tends towards no convective scheme (explicit convection) at scales less than 1 km (Grell and Freitas 2014). The Grell-Freitas convective scheme relies on a "closure" assumption, which determines how the scheme removes the buoyancy and converts it to cloud water and rainfall. Many methods can be used for the "closure", including using moisture convergence to determine the rainfall, or just removing the buoyancy (Grell et al. 1994). The Grell-Freitas scheme uses the abundance of "closure" methods to its advantage and actually calculates the ensemble mean of many methods (Grell and Dévényi 2002).

The land surface model is an important factor in modelling the surface weather conditions that provide the "fuel" for thunderstorm development and the trigger for initiating thunderstorms. The Noah Land Surface Model is probably the most complex and realistic of the parameterisation schemes available in WRF that describes the evolution of the surface boundary (Chen et al. 1996, Chen and Dudhia 2001). Remotely sensed land cover images are used to classify the world land surface into 24 land cover types. Each type has various parameters associated with it, such as the albedo, leaf area index, snow depth coverage thresholds, emissivity, roughness, and transpiration parameters. These values are used to model the interactions of the mostly vegetated land surface with the atmospheric boundary layer. Transpiration is modelled in the Noah Land Surface Model using the canopy resistance strategy outlined by Jacquemin and Noilhan (1990). The model includes both evaporation from rainfall intercepted by the plant canopy, and transpiration from the plants' stomata. The transpiration component is modeled using the stomatal resistance, and the leaf area index. The stomatal resistance depends on the plant species, and is specified in the land cover types. The leaf area index is the spatial density of the exposed leaf surfaces, and depends on the plant species and the time of year (Jacquemin and

Noilhan 1990). The maturity of the plants is defined using a static pre-determined monthly greenness amount (Shamarock et al. 2008).

The WRF system does not include a method for modelling output from large industrial complexes. For this thesis, a new module was added to the WRF system that describes how waste heat emitted from the oil sands development interacts with the atmosphere. The amount of waste heat (W/m^2) is specified in a configuration file. The geographical distribution of the waste heat is specified by assigning an unused land cover type to the oil sands development, and adding the waste heat to the lowest model layer at those grid cells (more details are given in Appendix A). The waste heat is added directly to the model temperature in the grid cells. The land cover for all of the oil sands development is set to barren. However, the waste heat is only added to a fraction of the area of the oil sands development. Thus, two unused land cover types were given the properties of barren land, but the waste heat was only added to one of them.

1.7. References

Brimelow, J. C., and G. W. Reuter, 2008: Moisture sources for extreme rainfall events over the Mackenzie Basin. Cold Regions and Hydrologic Studies: The Mackenzie GEWEX Experience, Volume 1, Atmospheric Dynamics, edited by M.-K. Woo, pp 127-136, Springer, Berlin.

Brown, D. M., 2012: Analysis of spatial and temporal lightning frequency and patterns in Saskatchewan. Internal Report for the Saskatchewan Ministry of the Environment.

Brown, M. E., and D. L. Arnold, 1998: Land-surface – atmosphere interactions associated with deep convection in Illinois. *International Journal of Climatology*, **18**, 1637-1653.

Burrows, W. R., and B. Kochtubajda, 2010: A decade of cloud-to-ground lightning in Canada: 1999-2008. Part 1: Flash Density and occurrence. *Atmosphere-Ocean*, **48**, 3, 177-194.

Carleton, A. M., D. J. Travis, J. O. Adegoke, D. L. Arnold, and S. Curran, 2008: Synoptic circulation and land surface influences on convection in the Midwest U.S. "Corn Belt" during the summers of 1999 and 2000. Part II: role of vegetative boundaries. *Journal of Climate*, **21**, 3617-3640. DOI: 10.1175/2007JCLI1584.1

Charlton, R. B., B. M. Kachman, and L. Wojtiw, 1995: Urban hailstorms: A view from Alberta. *Natural Hazards*, **12**, 29-75.

Charpentier, A. D., J. A. Bergerson, and H. L. MacLean, 2009: Understanding the Canadian oil sands industry's greenhouse gas emissions. *Environmental Research Letters*, **4**, 1-11.

Chen, F., and J. Dudhia, 2001: Coupling an advanced land surface hydrology model with the Penn State-NCAR MM5 modelling system. *Monthly Weather Review*, **129**, 569-604.

Chen, F., K. Mitchell, J. Schaake, Y. Zue, H.-L. Pan, V. Koren, Q. Y. Duan, M. Ek, and A. Betts, 1996: Modelling of land surface evaporation by four schemes and comparison with FIFE observations. *Journal of Geophysical Research*, **101**, 7251-7268

Cheng, V. Y. S., G. B. Arhonditsis, D. M. L. Sills, H. Auld, R. W. Shephard, W. A. Gough, and J. Klaassen, 2013: Probability of tornado occurrence across Canada. *Journal of Climate*, **26**, 9415-9428.

Crewe, A., 2008: Hailstorm a year later: It can happen again. Fort McMurray Today. Accessed 01 February 2016. [Available online at http://www.fortmcmurraytoday.com/2008/07/29/hailstorm-a-year-later-it-can-happen-again-2.]

De Bruijn, T.J.W., 2010: Estimated life cycle GHG emissions and energy use for oil sands derived crudes versus conventional light crude using GHGenius, NRC, Canmet Energy, 38 pp.

Dupilka, M. L., and G. W. Reuter, 2005: An examination of three severe convective storms that produced significant tornadoes in central Alberta. *National Weather Digest*, **29**, 47-59.

Fanaki, F., 1986: Simultaneous acoustic sounder measurements at two locations. *Boundary Layer Meteorology*, **37**, 197-207.

Flesch, T.K. and G.W. Reuter, 2012: WRF model simulation of two Alberta flooding events and the impact of topography. *Journal of Hydrometeorology*, **13**, 695-708.

Geerts, B., D. Parsons, C. L. Ziegler, T. M. Weckwerth, M. I. Biggerstaff, R. D. Clark, M. C. Coniglio, B. B. Demoz, R. A. Ferrare, W. A. Gallus Jr., K Haghi, J. M. Hanesiak, P. M. Klein, K. R. Knupp, K. Kosiba, G. M. McFarquhar, J. A. Moore, A. R. Nehrir, M. D. Parker, J. O. Pinto, R. M. Rauber, R. S. Schumacher, D. D. Turner, Q. Wang, X. Wang, Z. Wang, and J. Wurman, 2017:

The 2015 plains elevated convection at night field project. *Bulletin of the American Meteorological Society*, April, 767-786.

Government of Alberta, 2016: Alberta Energy: Facts and statistics. Accessed 31 January 2016. [Available online at http://www.energy.alberta.ca/OilSands/791.asp.]

Grant, J., J. Dagg, S. Dyer, and N. Lemphers, 2010: Northern lifeblood: Empowering northern leaders to protect the Mackenzie River basin from oil sands risks. *Pembina Institute*, Drayton Valley, Alberta, Canada. 77 pp.

Grell, G. A. and D. Dévényi, 2002: A generalized approach to parameterizing convection combining ensemble and data assimilation techniques. *Geophysical Research Letters*, **29**, 14, 38-1 – 38-4.

Grell, G. A., J. Dudhia, and D. R. Stauffer, 1994: A description of the Fifth-Generation Penn State/NCAR Mesoscale Model (MM5). *NCAR Technical Note*.

Grell, G. A., and S. R. Freitas, 2014: A scale and aerosol aware stochastic convective parameterization for weather and air quality monitoring. *Atmospheric Chemistry and Physics*, **14**, 5233-5250.

Guan, S., and G. W. Reuter, 1995: Numerical simulation of a rain shower affected by waste energy released from a cooling tower complex in a calm environment. *Journal of Applied Meteorology*, **34**, 131-142. DOI: 10.1175/1520-0450-34.1.131.

Hanesiak, J. M., R. L. Raddatz, and S. Loban, 2004: Local initiation of deep convection on the Canadian Prairie Provinces. *Boundary Layer Meteorology*, **110**, 455-470.

Hazewinkel, R. R. O., A. P. Wolfe, S. Pla, C. Curtis, and K Hadley, 2008: Have atmospheric emissions from the Athabasca oil sands impacted lakes in northeastern Alberta, Canada? *Canadian Journal of Fisheries and Aquatic Sciences*, **65**, 1554-1567, doi:10.1139/F08.074

Jacquemin, B., and J. Noilhan, 1990: Sensitivity study and validation of a land surface parameterization using the Hapex-Mobilhy data set. *Boundary Layer* Meteorology, **52**, 93-134.

Joe, P., and S. Lapczak, 2002: Evolution of the Canadian operational radar network. *Proceedings of the 2002 European Conference on Radar in Meteorology and Hydrology (ERAD)*, Delft, Netherlands.

Kellner, O. and D. Niyogi, 2015: Land surface heterogeneity signature in tornado climatology? An illustrative analysis over Indiana, 1950-2012. *Earth Interactions*, **18**, 10, 1-32.

Kelly, E. N., J. W. Short, D. W. Schindler, P. V. Hodson, M. Ma, A. K. Kwan, and B. L. Fortin, 2009: Oil sands development contributes polycyclic aromatic compounds to the Athabasca River and its tributaries. *Proceedings of the National Academy of Science*, 106, **52**, 22346–22351. DOI: 10.1073/pnas.0912050106.

King, P. W. S., M. J. Leduc, D. M. L. Sills, N. R. Donaldson, D. R. Hudak, P. Joe, and B. P. Murphy, 2003: Lake breezes in southern Ontario and their relation to tornado climatology. *Weather and Forecasting*, **18**, 795-807.

Kochtubajda, B., W. R. Burrows, D. Green, A. Liu, K. R. Anderson, and D. McLennan, 2011: Exceptional cloud-to-ground lightning during an unusually warm summer in Yukon, Canada. *Journal of Geophysical Research*, **116**, D21206, 1-20, doi:10.1029/2011JD016080.

Krauss, T. W., and J. Renick, 1997: The new Alberta hail suppression project. *Journal of Weather Modification*, **29**, 100-105.

Kumar, A., J. Dudhia, R. Rotunno, D. Niyogi, and U. C. Mohanty, 2008: Analysis of the 26 July 2005 heavy rain event over Mumbai, India using the Weather Research and Forecasting (WRF) model. *Quarterly Journal of the Royal Meteorological Society*, **134**, 1897-1910.

Latifovic, R., K Fytas, J. Chen, and J. Paraszczak, 2005: Assessing land cover change resulting from large surface mining development. *International Journal of Applied Earth Observation and Geoinformation*, **7**, 29-48.

Leahey, D. M., and M. C. Hansen, 1982: Influences of terrain on plume level winds in the Athabasca oil sands area. *Atmospheric Environment*, **16**, 12, 2849-2854.

Lin, C.-Y., F. Chen, J. C. Huang, W.-C. Chen, Y.-A. Liou, W.-N. Chen, S.-C. Liu, 2008: Urban heat island effect and its impact on boundary layer development and land-sea circulation in northern Taiwan. *Atmospheric Environment*, **42**, 5635-5649.

Lin, Y.-L., R. D. Rarley, and H. D. Orville, 1983: Bulk parameterisation of the snow field in a cloud model. *Journal of Climate and Applied Meteorology*, **22**, 1065-1092.

Mills, B., D. Unrau, C. Parkinson, B. Jones, J. Yessis, K. Spring, L. Pentelow, 2008: Assessment of lightning-related fatality and injury risk in Canada. *Natural Hazards*, **47**, 157-183.

Mölders, N., 2008: Suitability of the Weather Research and Forecasting (WRF) model to predict the June 2005 fire weather for interior Alaska. *Weather and Forecasting*, **23**, 953-973.

Pennelly, C., G. W. Reuter, and T. Flesch, 2014: Verification of the WRF model for simulating heavy precipitation in Alberta. *Atmospheric Research*, **135-136**, 172-192. DOI: 10.1016/j.atmosres.2013.09.004.

Pennelly, C. and G. W. Reuter, 2017: Verification of the Weather Research and Forecasting Model when forecasting daily surface conditions in southern Alberta. *Atmosphere-Ocean*, **55**, 1, 31-41.

Rabin, R. M., S. Stadler, P. J. Wetzel, D. J. Stensrud, and M. Gregory, 1990: Observed effects of landscape variability on convective clouds. *Bulletin of the American Meteorological Society*, **71**, 3, 272-280.

Raddatz, R. L., 1993: Prairie agroclimate boundary-layer model: A simulation of the atmosphere/crop-soil interface, *Atmosphere-Ocean*, **31**, 4, 399-419.

Raddatz, R. L., 1998: Anthropogenic vegetation transformation and the potential for deep convection on the Canadian Prairies. *Canadian Journal of Soil Science*, **78**, 4, 657-666.

Raddatz, R. L., 2005: Moisture recycling on the Canadian Prairies for summer droughts and pluvials from 1997 to 2003. *Agriculture and Forest Meteorology*, **131**, 13-26.

Shamarock, W. C., J. B. Klemp, J. Dudhia, D. O. Gill, D. M Barker, M. G. Duda, X.-Y. Huang, W. Wang, and J. G. Powers, 2008: A description of the Advanced Research WRF Version 3. *NCAR Technical Note.*

Smith, S. B., G. W. Reuter, M. K. Yau, 1998: The episodic occurrence of hail in central Alberta and the Highveld of South Africa. Research Note: *Atmosphere-Ocean*, **36**, 2, 169-178. DOI: 10.1080/07055900.1998.9649610.

Smith, S. B., and M. K. Yau, 1993: The causes of severe convective outbreaks in Alberta. Part I: A comparison of a severe outbreak with two non-severe events and part II: Conceptual model and statistical analysis. *Monthly Weather Review*, **121**, 1099-1133.

Steiger, S. M., and R. E. Orville, 2003: Cloud-to-ground lightning enhancement over southern Louisiana. *Geophysical Research Letters*, **30**, 1975, DOI: 10.1029/2003GL017923.

Stocks, B. J., J. A. Manson, J. B. Todd, E. M. Bosch, B. M. Wotton, B. D. Amiro, M. D. Flannigan, K. G. Hirsch, K. A. Logan, D. L. Martell, and W. R. Skinner, 2003: Large forest fires in Canada, 1959-1997. *Journal of Geophysical Research*, **108**, D1, 8159, 1-12.

Strong, G. S., 1986: Synoptic to mesoscale dynamics of severe thunderstorm environments: A diagnostic study with forecasting applications. *PhD Thesis*, University of Alberta, Edmonton.

Strong, G. S., 1997: Atmospheric moisture budget estimates of regional evapotranspiration from RES-91. *Atmosphere-Ocean*, **35**, 1, 29-63

Taylor, N. M., D. M. L. Sills, J. M. Hanesiak, J. A. Milbrandt, C. D. Smith, G. S. Strong, S. H. Scone, P. J. McCarthy, and J. C. Brimelow, 2011: The understanding severe thunderstorms and Alberta boundary layer experiment (UNSTABLE) 2008. *Bulletin of the American Meteorological Society*, June, 739-763

Thielan, J., and A. Gadian, 1997: Influence of topography and urban heat island effects on the outbreak of convective storms under unstable meteorological conditions: A numerical study. *Meteorology Applications*, **4**, 139-149.

Walmsley, J. L., and D. L. Bagg, 1978: A method of correlating wind data between two stations with application to the Alberta oil sands. *Atmosphere-Ocean*, **16**, 4, 333-347.

Weckwerth, T. M., D. B. Parsons, S. E. Koch, J. A. Moore, M. A. LeMone, B. B. Demoz, C. Flamant, B. Geerts, J. Wang, and W. F. Feltz, 2004: An overview of the international H_2O project (IHOP_2002) and some preliminary highlights. *Bulletin of the American Meteorological Society*, February, 253-277.

Weismann, M. L., and J. B. Klemp, 1982: The dependence of numerically simulated convective storms on vertical wind shear and buoyancy. *Monthly Weather Review*, **110**, 504-520.

Wurman, J., D. Dowell, Y. Richardson, P. Markowski, E. Rasmussen, D. Burgess, L. Wicker, and H. B. Bluestein, 2012: The second verification of the origins of rotation in tornadoes experiment. *Bulletin of the American Meteorological Society*, August, 1147-1170.

1.8. Figures

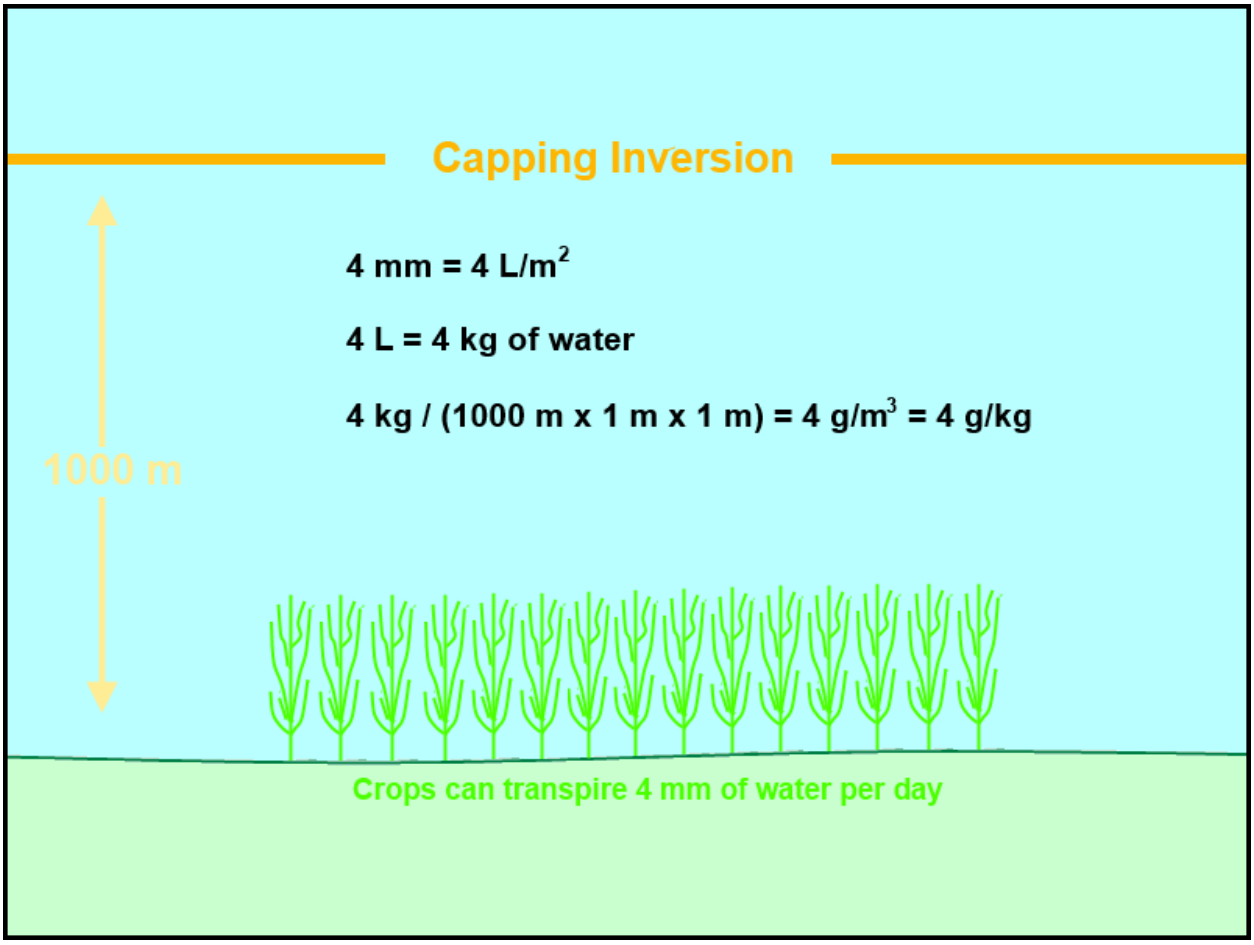

Figure 1.1: The modification of the boundary layer humidity by crop evapotranspiration. Strong (1997) calculated many different values for crop transpiration. 4 mm was picked as a mid-range value.

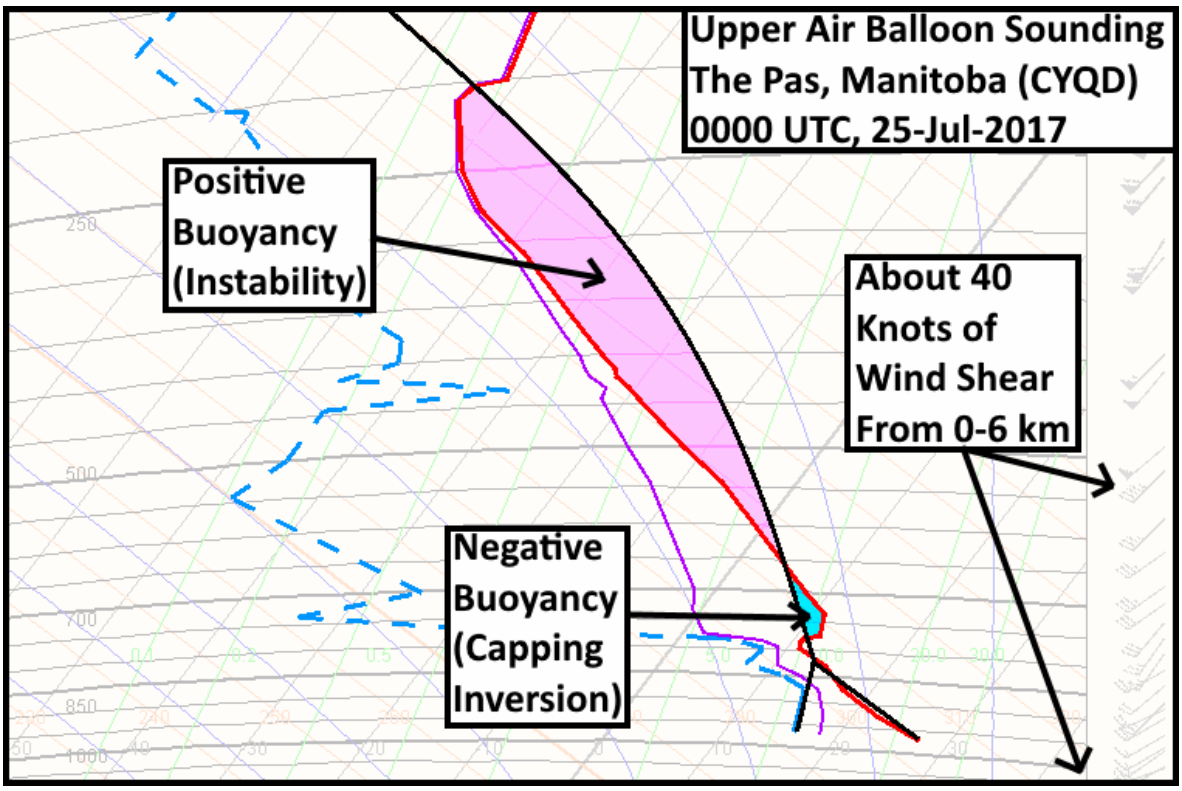

Figure 1.2: Tephigram showing a sounding from The Pas, Manitoba at 0000 UTC on 25 July 2017. The lifted parcel is traced by the black line. The area of positive buoyancy is shaded in pink. The area of negative buoyancy (the capping inversion) is shaded in light blue, and the parcel of air will sink in this region because it is cooler than it surroundings.

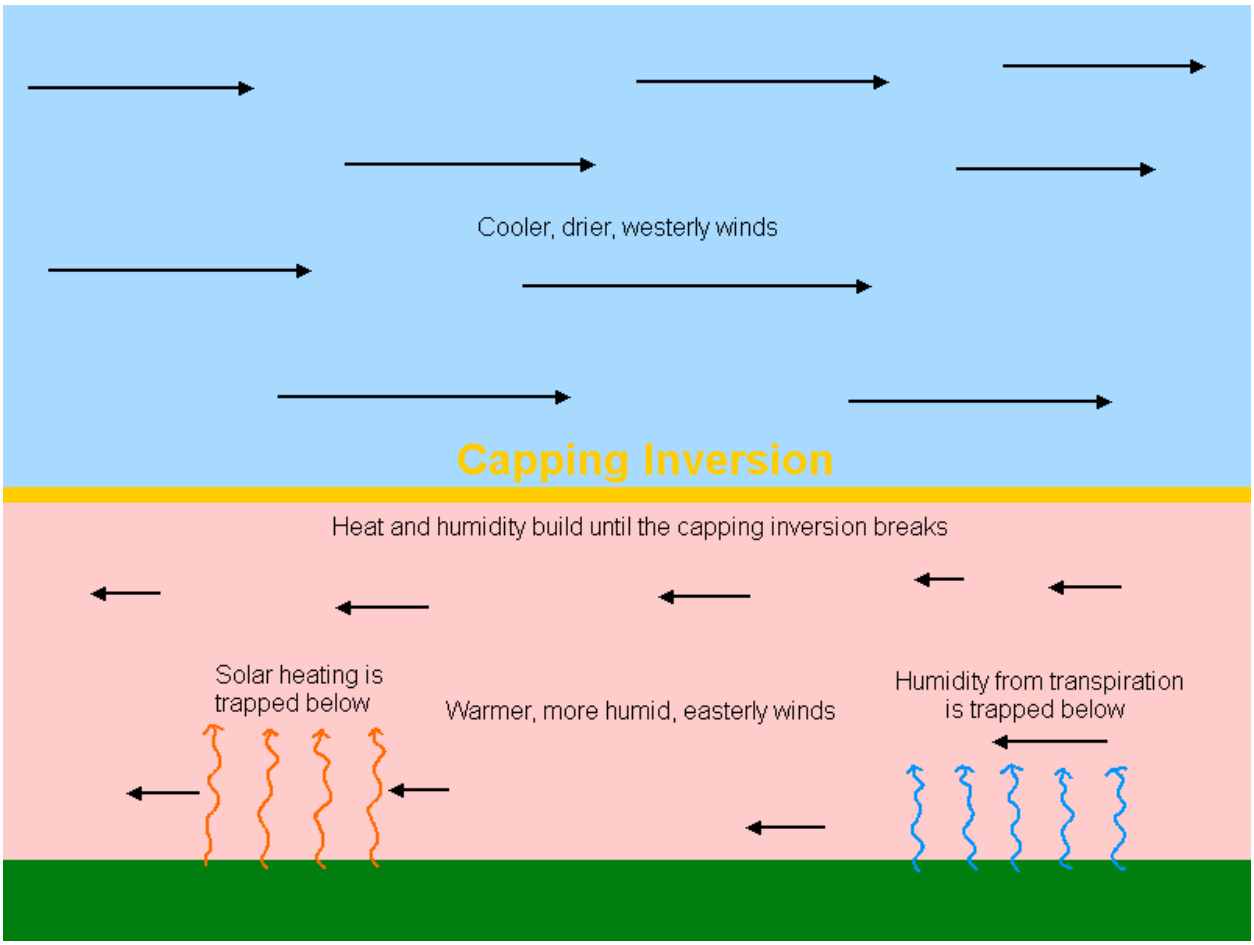

Figure 1.3: The capping inversion. The capping inversion traps heat and moisture underneath itself until thunderstorms form.

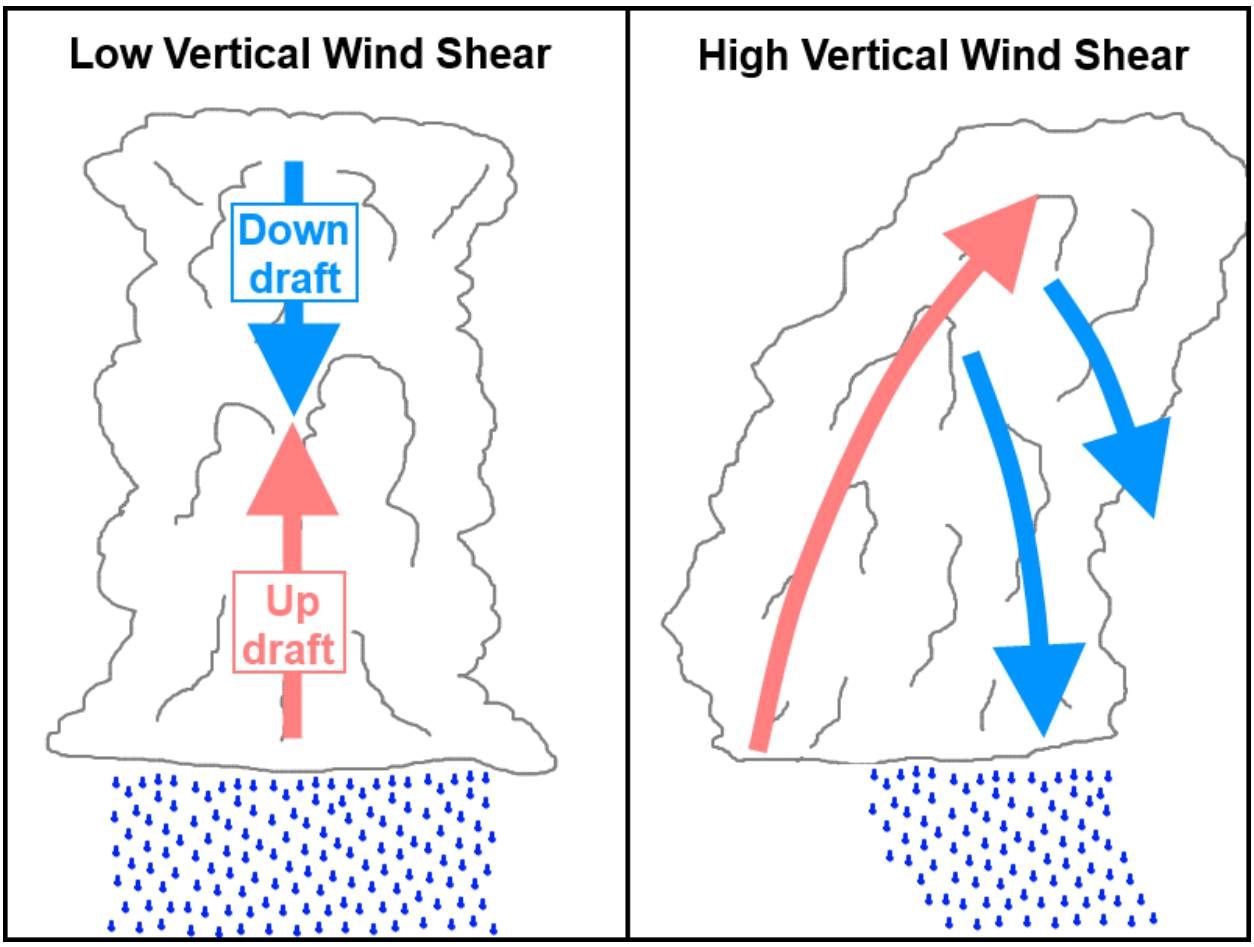

Figure 1.4: A diagram showing the consequences of low vertical wind shear versus high vertical wind shear. With higher vertical wind shear, the updraft continues to have access to warm moist air at the surface and can continue to push it aloft without interference by the precipitation-cooled downdraft.

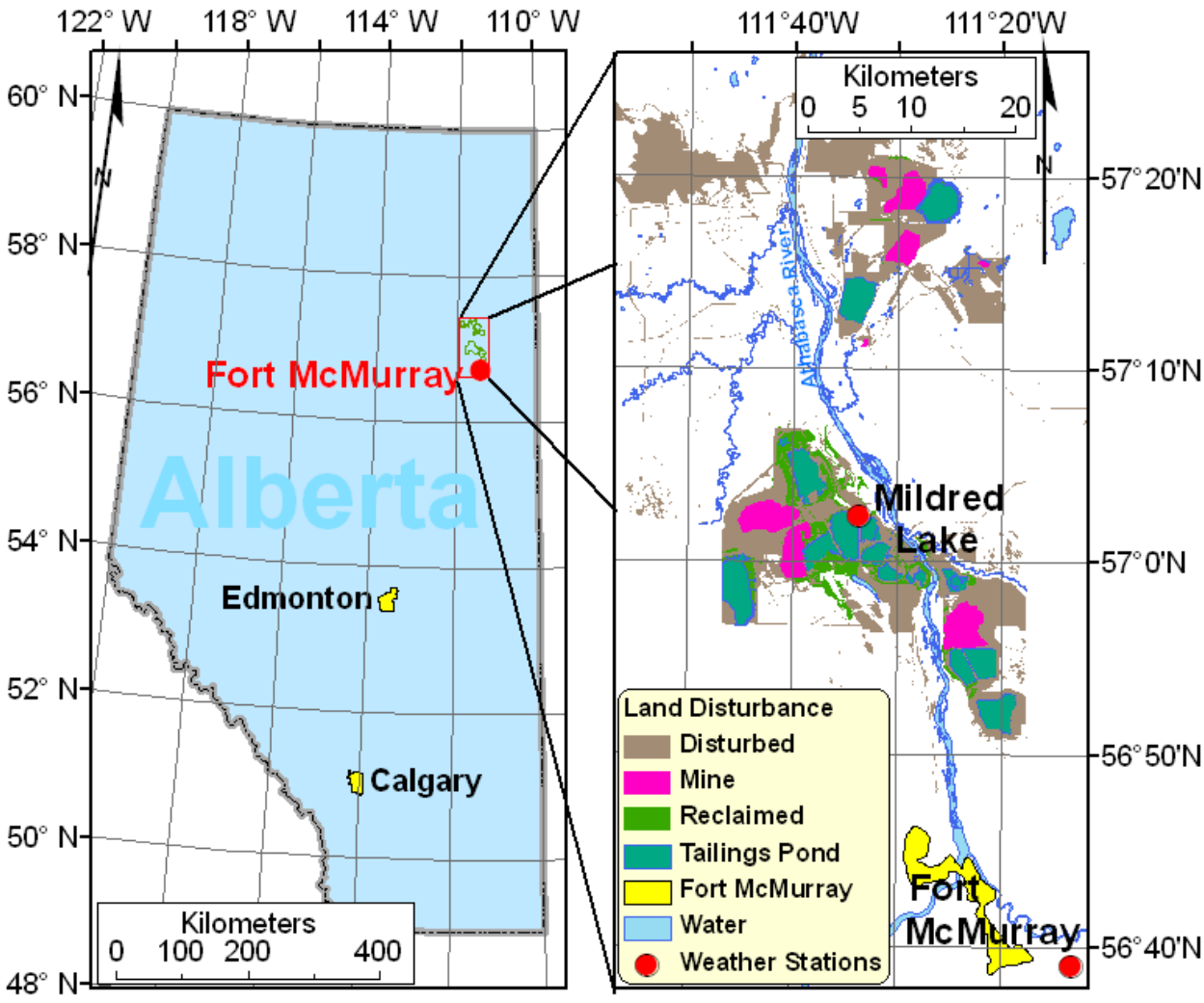

Figure 1.5: The massive oil sands land disturbance. The location of the oil sands development within Alberta is shown on the left. The land cover map of the oil sands disturbance is shown on the right. Reprinted from Brown et al. (2011).

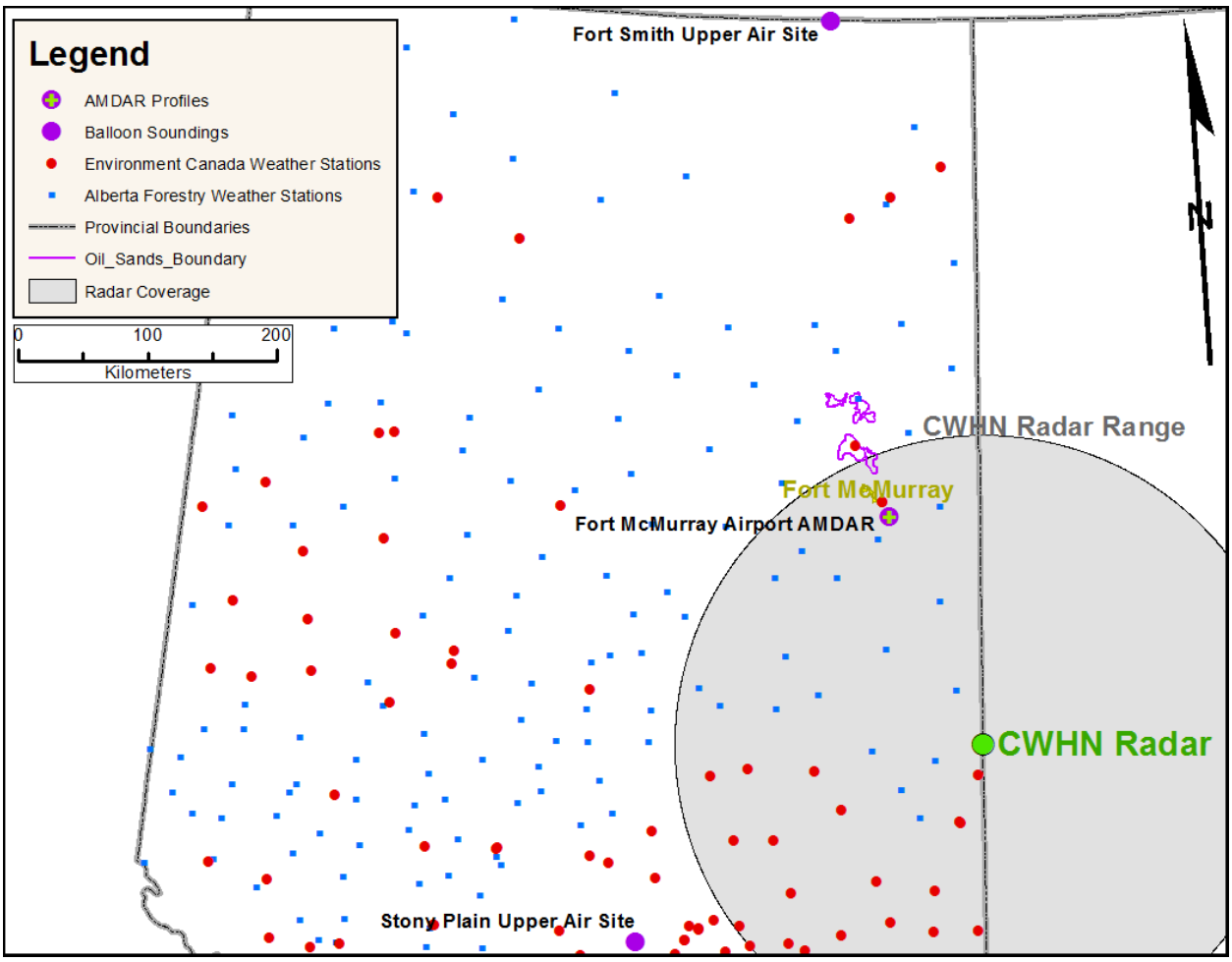

Figure 1.6: Weather data available around the oil sands development. There are many forestry weather stations, but they only operate intermittently during the summer, which makes the analysis difficult.

2. Characteristics of surface conditions affecting convection

2.1. Evapotranspiration in the prairies and the boreal forest

Raddatz (1993) provides a detailed discussion on modelling the process of transpiration in plants. The following is a summary of the discussion. Raddatz (1993) describes an evapotranspiration model that could be used to estimate evapotranspiration at climate sites. The water vapour from transpiration is supplied by the stomata on the underside of the plants leaves. The stomata are generally the same temperature as the air; however, the air in the stomatal cavity is usually fully saturated with water vapour. The amount of transpiration is usually modelled using a stomatal resistance, which depends mostly on the plant species. The transpiration rate can be generalized to an entire population of plants by using both the stomatal resistance and the leaf area index. In this way, the rate of transpiration from large areas can be tracked throughout the year as plants grow and mature. Transpiration can also be adjusted for the predominant plant species (Raddatz 1993).

The Boreal Ecosystem-Atmosphere Study (BOREAS) was a major field campaign that showed important feedbacks between the boreal forest and weather systems (Sellers et al., 1995). The southern BOREAS study area had mostly broadleaf deciduous aspen or birch with some needle-leaf trees mixed in; whereas the northern BOREAS study area was composed mostly of evergreen needle-leaf black spruce trees in the Canadian Shield. A major finding of BOREAS was characterizing the distribution of the Bowen Ratio and energy balance amongst different boreal forest regions (Table 2.1). Barr et al. (1997) found that evergreen needleleaf forests had a higher Bowen Ratio than deciduous broadleaf forests. Betts et al. (2007) showed that deciduous

broadleaf forests had Bowen Ratios in between that of cropped land and needle-leaf forests, and in general, the boreal forest has lower evapotranspiration than cropped lands and grasslands. Barr and Betts (1997) used soundings in Candle Lake, Saskatchewan and Thompson, Manitoba to conclude that the southern area had a higher Bowen Ratio than the northern Canadian Shield area, which should translate into more moisture available and lower condensation levels for convective clouds. They also showed that when mixing begins, soundings actually cool in the upper portions of the boundary layer due to adiabatic cooling of the thermals as they rise.

Transpiration from various types of vegetation can add large amounts of water vapour to the atmosphere. In western Canada, some of the highest transpiration rates are associated with crops (particularly wheat). In the peak transpiration season, evapotranspiration can be 3-6 mm/d, and on some days can peak as high as 8-10 mm/day (Raddatz 1993, Strong 1997). However, transpiration rates in the parkland and boreal forest are not as high. Deciduous broadleaf trees such as aspen, birch, and poplar have the highest boreal transpiration rates. Aspen forests can transpire 2-4 mm/day with peaks to 5 mm/day (Hogg et al. 1997). Needleleaf trees transpired the least. For example, jack pine only transpired 1-2 mm/day with peaks up to 4 mm/day (Baldocchi et al. 1997).

Barr and Betts (1997) showed an interesting phenomena associated with the boreal forest. Although the boreal forest has lower evapotranspiration than the cropland to the south, it transpires for considerably longer because it stays green longer. This effect is similar to the effect found by Raddatz and Cummine (2003). They found that grasslands also had lower evapotranspiration than cropland. Annual crops transpire water vapour at a faster peak rate than forests or perennial grasses. However the length of time they transpire is less because they are slower to start growing and they ripen sooner. Barr and Betts (1997) also noted that broadleaf deciduous forest has a minimum Bowen ratio in the middle of summer when its leaves are

producing the most energy. This also happens to be at the peak of the lightning season. Strong (1997) showed that transpiration alone can add enough humidity to significantly affect thunderstorms. The Bowen ratio for areas with pure broadleaf deciduous trees is somewhat higher than the values reported by Barr and Strong (1996) for cropped land. Thus, transpiration from broadleaf deciduous trees is somewhat less than that of crops.

2.2. Effects of the land surface on thunderstorms

The spatial distribution of thunderstorms is greatly affected by the characteristics of the underlying surface. Topographical features, vegetation cover, soil cover, and water bodies determine heat and humidity fluxes near the surface, as well as the atmospheric circulation and boundary layer wind profile. Thunderstorms are very sensitive to heat and humidity fluxes at the surface along with the surface and boundary layer winds. The most important controlling geographical features that affect thunderstorm formation, development, and dissipation will be discussed in the coming paragraphs.

Prominent topographic features such as hills and ridges significantly affect the distribution of thunderstorms. Topography can cause stronger solar heating on sun-facing slopes, and orographic lifting; both of which can trigger thunderstorm initiation (Figure 2.1). As an example, the morning mountain-plain circulation in southern Alberta is caused by solar heating of the east slopes of the Rocky Mountain. The easterly flow induced by the circulation causes moisture convergence and ascent near the Alberta foothills (Smith and Yau 1993). Burrows and Kochtubajda (2010) found that the Swan Hills in Alberta and Riding Mountain in Manitoba enhanced cloud-to-ground lightning. Hanesiak et al. (2004) found that deep convection on the Canadian prairies was initiated much more often over higher terrain than lower elevation areas.

Brown (2012) documented many topographical features in Saskatchewan that affected cloud-to-ground lightning density. In northern Alberta, the Caribou Mountains are well known for initiating cumulus development and thunderstorms earlier than the surrounding lowlands. Thielan and Gadian (1997) used numerical simulations to show that hills in mid-latitude regions can augment convection mainly due to enhanced solar heating of the sun-facing slopes.

Water bodies also have important effects on thunderstorm initiation and development. Typical examples are lake and sea breezes, which are caused when the land surface is heated faster than the water surface (Curry et al. 2015). The surface of the water is cooler because it has a much higher heat capacity than the land. Because water is clear, heating from the solar radiation is distributed through a much greater depth than the land. Thus, the heating is concentrated in a shallow skin over the land surface, but through a great depth in the water, and contributes to greater surface temperatures on land. The land then heats the air in contact with the surface more than the water, creating lower pressure over the land. The pressure gradient force causes the air over the water to flow over the land (Figure 2.2) (Curry et al. 2015). The boundary between the land air and the lake air is called the lake breeze front, and it tends to be a very sharp transition with strong surface convergence than can penetrate over 100 km inland (Sills et al. 2011). The transition between the cool and warm air usually occurs over less than 1 km, and can be over less than 100 m (Curry et al. 2017).

The effects of lake breezes on thunderstorm initiation are frequently documented. Steiger et al. (2002) speculated that a convergence of different sea breezes could lead to enhanced lightning over Houston, Texas. Curry et al. (2017) measured strong upward velocities of 2-3 m/s at a lake breeze front in Manitoba, and Sills et al. (2011) suggests that the uplift at the lake breeze front sometimes initiates deep convection. King et al. (2003) showed that areas of lake breeze convergence in the Great Lakes region of Ontario were more prone to tornadoes. Sun

et al. (1997) used aircraft transects to document many well-defined lake breezes in the southern boreal forest in Saskatchewan. Numerical modelling of the circulation over Candle Lake, Saskatchewan confirmed the lake breeze forcing mechanism (Vidale et al., 1997).

However, lake and sea breezes are not the only effects of water bodies. Burrows and Kochtubajda (2010) and Hanuta and LaDochy (1989) reported "lightning shadows" downwind of large lakes such as Lake Winnipeg and Great Slave Lake likely due to the cooler lake stabilizing the lower atmosphere. Even small lakes and reservoirs can cause an absence of cumulus clouds in a larger cumulus field, although their effect is greatly reduced in stronger winds (Rabin et al. 1990).

Even more subtle variations in the land surface can affect thunderstorms and convection. One of the most classic examples is that of a dark field heating the ground more than the surrounding vegetated fields, which creates stronger ascent. However, lower albedo is not the only cause of greater surface heating. A barren field surrounded by vegetation of the same albedo will heat up faster because more solar radiation is converted to sensible heat rather than latent heat (i.e. it has a higher Bowen ratio). As an example, Rabin et al. (1990) used numerical simulations and satellite images to show that cumulus clouds formed earlier over a field of wheat stubble compared to the surrounding deciduous forest, even though the wheat field had a higher albedo (Figure 2.3). Pielke et al. (2007) suggested that wildfire burn areas in the boreal forest could cause preferential cumulus formation.

Researchers have also investigated the effect of soil moisture and vegetation variations on thunderstorm frequency and severity. Raddatz (2005) showed that most summertime precipitation on the Canadian Prairies originates from convective showers and thunderstorms. Convective showers and thunderstorms feed partially on moisture supplied to the atmosphere by transpiration from vegetation. In fact, Hanesiak et al. (2010) showed that precipitable water in

southern Manitoba followed a diurnal cycle that was caused by the diurnal cycle of evapotranspiration. Raddatz (2005) also showed that humidity originating from transpiration resulted in 15-30 % of the summertime rainfall on the Canadian prairies. Thus, dry weather results in lower transpiration, lower humidity, lower convective rainfall, and thus, continued dry weather. Wet weather tends to bring more wet weather. Brimelow et al. (2011a) explicitly found that drought contributed to reduced vegetation vigour, and resulted in less lightning. However, the drought had to be over a large enough area (more than about 18 000 km^2).

Soil moisture has been found to significantly influence convection in western Canada. Hanesiak et al. (2004) found that convection was initiated earlier in regions with higher soil moisture. Hanesiak et al. (2009) and Brimelow et al. (2011b) found that regions with a lower Bowen ratio (wetter) created more convection because of higher moisture, and thus, higher instability and lower cloud bases. However, it is not the surface soil moisture (surface to 0.1 meters deep in the soil) that is most important. It was the root zone soil moisture (0.1 to 1.2 meters deep) that had the most influence on enhancing or diminishing convection (Hanesiak et al. 2004). Hanesiak et al. (2009) found that the amount of severe thunderstorm hazards was most correlated with the root zone soil moisture from earlier in the year, rather than the soil moisture during thunderstorm season.

Rather than comparing different land surfaces, some researchers have investigated the effect of the *boundaries* between the different land covers. Brown and Arnold (1998) used satellite images to find that cumulus initiation in Illinois tends to be clustered near land cover boundaries on days with little synoptic forcing. They speculated that weak mesoscale circulations caused convergence at the land cover boundaries, and that cumulus clouds tended to form on the moist side of the boundaries. Hanesiak et al. (2004) found that weak mesoscale circulations at land cover boundaries tended to initiate thunderstorms on the moist side of the boundary. Most

thunderstorms on the Canadian prairies that were initiated away from topographic variations formed near large evapotranspiration gradients. Kellner and Niyogi (2015) found that even tornadoes tend to cluster along land cover boundaries in Indiana. Carleton et al. (2008) found that convection occurred preferentially along crop-forest boundaries mainly in the early summer when vigorous vegetative growth made the boundaries the most distinct. The quantifiable effect of such subtle land cover differences on thunderstorms and thunderstorm initiation suggests that artificial land cover differences could also have an effect on thunderstorms.

2.3. The effects of anthropogenic land cover variations on thunderstorms

Human activities affect the land in many different ways. Probably the most significant land modification that humans have made in North America is the large scale transformation of native prairie and parkland into agricultural farmland. This transformation has affected the seasonal Bowen ratio and albedo of the region, along with the roughness and runoff characteristics. The majority of the Canadian prairies has been transformed from perennial prairie grasses into cropland which is mostly annual crops. This transformation has increased transpiration overall. It has also changed the temporal distribution by creating much higher transpiration in late June and July, but lower transpiration at other times of the year – particularly after harvest (Raddatz 1998). In fact, Raddatz and Cummine (2003) found that the enhanced transpiration in July due to agriculture could lead a shorter, but more intense, tornado season on the Canadian Prairies. Shrestha et al. (2012) found that less summer fallow and more continuous cropping has led to higher humidity and a greater chance of convection since the 1970s on the Canadian Prairies.

Convective weather and precipitation patterns have been affected by urbanization. Changnon et al. (1976) examined rainfall, thunderstorms, and hail in the St. Louis, Missouri area, and found statistically significant enhancements downwind. Similarly, Westcott (1995) documented that there was higher cloud-to-ground lightning densities in the downtown cores than in the surrounding areas of some major cities. Steiger et al. (2002) found that the lightning enhancement was particularly conspicuous around Houston, Texas. Ashley et al. (2012) confirmed the urban effects using radar reflectivities. Niyogi et al. (2011) showed that existing thunderstorms changed their radar signatures when they passed over Indianapolis, Indiana. Dow and DeWalle (2000) suggested that enough urban areas exist in the eastern United States to decrease the humidity and change the Bowen ratio for entire watersheds. Other researchers used numerical simulations to quantify the effect of urban areas on thunderstorms. Niyogi et al. (2006) used numerical simulations and factor separation to show that Oklahoma City, Oklahoma affected the structure of a mesoscale convective system, while Li et al. (2013) also used aircraft meteorological data relay (AMDAR) for Baltimore, Maryland. Schmid and Niyogi (2013) used numerical simulations to show that cities sometimes cause reduced precipitation and convection. Numerical simulations by Guan and Reuter (1995) showed that latent and sensible heat released by a factory could enhance rainshowers. Researchers have generally proposed three possible reasons for lightning or precipitation enhancement near downtown cores: increased convergence due to the urban heat island, increased convergence due to a higher surface roughness, and increased cloud condensation nuclei (Changnon et al. 1976).

Oke (1973) found that most major cities in mid latitudes create an urban heat island, and the heat island strength (difference between the temperature at the centre and the surroundings) rises with the logarithm of city population. Bornstein and Lin (2000) found that convergence caused by the urban heat island of Atlanta, Georgia caused higher precipitation. However,

Nkemdirim (1981) did not find any such enhancement in Calgary, Alberta. Steiger and Orville (2003) reject that urban enhanced lightning in Houston, Texas or Lake Charles, Louisiana is caused by an urban heat island. They rejected this because both cities are co-located with areas of lightning enhancement, but Lake Charles has a very small population. However, using the population of both cities in the formula by Oke (1973), the urban heat island intensity of Lake Charles (population 0.2 million) is still 9 °C, while the logarithmic relation gives an urban heat island intensity of only 13°C for Houston (population 4.5 million). Thus, Steiger and Orville (2003) may not be justified in excluding the urban heat island.

The removal of vegetation from urban areas causes another interesting phenomena related to urban heat islands: lower transpiration in urban or industrial areas causes lower surface humidity. Rozoff et al. (2003) reported lower modelled Convective Available Potential Energy (CAPE) near city centres because of lower humidity. Usually lower humidity at the city centre is caused by less transpiring vegetation. Schmid and Niyogi (2013) suggested that the strength of numerically modelled urban dry islands is related linearly with land area size of the city. Dow and DeWalle (2000) found that this effect has even influenced regional climate in the northeastern United States. An increase in surface roughness due to the tall buildings in the downtown core blocking the flow has been proposed as a possible mechanism for the enhancement of precipitation or thunderstorms over cities. However, few researchers have studied it in depth. Rozoff et al. (2003) used factor separation of numerical simulations to find that higher surface roughness values slightly increased moisture convergence. They also found that increased surface roughness slightly reduces the urban heat island effect.

Various researchers have proposed that cloud condensation nuclei could affect lightning and precipitation enhancement near cities. However, much debate exists over the mechanism, which appears to be very complex (Dixon and Mote 2003). Changnon et al. (1976) suggested that

cloud condensation nuclei could be the main process for precipitation enhancement, and Steiger and Orville (2003) suggested that cloud condensation nuclei could be the dominant process for lightning enhancement. However, it was speculated earlier in this chapter that the Steiger and Orville (2003) reasoning may not be valid. In fact in numerical simulations by Reuter and Guan (1995), cloud condensation nuclei were found to have little effect on industrial rainshowers. The main argument against this proposal is that cloud condensation nuclei tend to cause many small cloud particles to form which limits precipitation formation (Dixon and Mote 2003). Zhong et al. (2015) may have found a better explanation. They studied the effect of aerosols using WRF-CHEM numerical simulations in Beijing, China, and found that cloud condensation nuclei caused two distinct effects: a reduction in precipitation at the city centre, and an enhancement of precipitation downwind. The precipitation reduction downtown was caused by the "aerosol direct effect", where aerosols make many small cloud droplets reducing precipitation. The precipitation enhancement downwind was caused by the "aerosol indirect effect", where the release of latent heat by the cloud droplets freezing downwind enhanced convection. Because the convection takes some time to organize, the precipitation enhancement occurs downwind, and is greater than the heat island effect (Zhong et al. 2015).

2.4. References

Ashley, W. S., M. L. Bentley, and T. Stallins, 2012: Urban induced thunderstorm modification in the southeast United States. *Climatic Change*, **113**, 481-498.

Baldocchi, D. D., and C. A. Vogel, 1997: Seasonal variation of energy and water vapor exchange rates above and below a boreal jack pine forest canopy. *Journal of Geophysical* Research, **102**, D24, 28939-28951.

Barr, A. G., and A. K. Betts, 1997: Radiosonde boundary layer budgets above a boreal forest. *Journal of Geophysical Research*, **102**, D24, 29205-29212.

Barr, A. G., A. K. Betts, R. L. Desjardins, and J. I. MacPherson, 1997: Comparison of regional surface fluxes from boundary-layer budgets and aircraft measurements above boreal forest. *Journal of Geophysical Research*, **102**, D24, 29213-29218.

Barr, A. G., and G. S. Strong, 1997: Estimating regional surface heat and moisture fluxes above prairie cropland from surface and upper air measurements. *Journal of Applied Meteorology*, **35**, 1716-1735.

Betts, A. K., R. L. Desjardins, and D. Worth, 2007: Impact of agriculture, forest, and cloud feedback on the surface energy budget in BOREAS. *Agriculture and Forest Meteorology*, **142**, 156-169.

Bornstein, R. and Q. Lin, 2000: Urban heat islands and summertime convective thunderstorms in Atlanta: Three case studies. *Atmospheric Environment*, **34**, 507-516.

Brimelow, J. C., J. M. Hanesiak, and W. R. Burrows, 2011a: On the surface-convection feedback during drought periods on the Canadian Prairies. *Earth Interactions*, **15**, 1-26.

Brimelow, J. C., J. M. Hanesiak, and W. R. Burrows, 2011b: Impacts of land-atmosphere on deep, moist convection on the Canadian Prairies. *Earth Interactions*, **15**, 1-29.

Brown, D. M., 2012: Analysis of spatial and temporal lightning frequency and patterns in Saskatchewan. Internal Report for the Saskatchewan Ministry of the Environment.

Brown, M. E., and D. L. Arnold, 1998: Land-surface – atmosphere interactions associated with deep convection in Illinois. *International Journal of Climatology*, **18**, 1637-1653.

Burrows, W. R., and B. Kochtubajda, 2010: A decade of cloud-to-ground lightning in Canada: 1999-2008. Part 1: Flash density and occurrence. *Atmosphere-Ocean*, **48**, 3, 177-194.

Carleton, A. M., D. J. Travis, J. O. Adegoke, D. L. Arnold, and S. Curran, 2008: Synoptic circulation and land surface influences on convection in the Midwest U.S. "Corn Belt" during the summers of 1999 and 2000. Part II: role of vegetative boundaries. *Journal of Climate*, **21**, 3617-3640. DOI: 10.1175/2007JCLI1584.1

Changnon, S. A. Jr., R. G. Semonin, and F. A. Huff, 1976: A hypothesis for urban rainfall anomalies. *Journal of Applied Meteorology*, **15**, 544-560.

Curry, M., J. Hanesiak, and D. Sills, 2015: A radar-based investigation of lake breezes in southern Manitoba, Canada. *Atmosphere-Ocean*, **53**, 2, 237-250.

Curry, M., J. Hanesiak, S. Kehler, D. M. L. Sills, and N. M. Taylor, 2017: Ground-based observations of the thermodynamic and kinematic properties of lake-breeze fronts in southern Manitoba, Canada. *Boundary Layer Meteorology*, **163**, 1, 143-159.

Dixon, P. G., and T. L. Mote, 2003: Patterns and causes of Atlanta's urban heat island-initiated precipitation. *Journal of Applied Meteorology*, **42**, 1273-1284.

Dow, C. L. and D. R. DeWalle, 2000: Trends in evaporation and Bowen ratio on urbanizing watersheds in eastern United States. *Water Resources Research*, **36**, 7, 1835-1843.

Guan, S., and G. W. Reuter, 1995: Numerical simulation of a rain shower affected by waste energy released from a cooling tower complex in a calm environment. *Journal of Applied Meteorology*, **34**, 131-142. DOI: 10.1175/1520-0450-34.1.131.

Hanesiak, J. M., R. L. Raddatz, and S. Lobban, 2004: Local initiation of deep convection on the Canadian Prairie Provinces. *Boundary Layer Meteorology*, **110**, 455-470.

Hanesiak, J., Tat, A., and R. L. Raddatz, 2009: Initial soil moisture as a predictor of subsequent severe summer weather in the cropped grassland of the Canadian Prairie provinces. *International Journal of Climatology*, **29**, 899-909.

Hanesiak, J., M. Melsness, and R. Raddatz, 2010: Observed and modeled growing-season diurnal precipitable water vapor in south-central Canada. *Journal of Applied Meteorology and Climatology*, **49**, 2301-2314.

Hanuta, S., and S. LaDochy, 1989: Thunderstorm climatology based on lightning detector data, Manitoba, Canada. Physical *Geography,* **10**, 101-109.

Hogg, E. H., T. A. Black, G. den Hartog, H. H. Neumann, R. Zimmermann, P. A. Hurdle, P. D. Blanken, Z. Nesic, P. C. Yang, R. M. Staebler, K. C. McDonald, and R. Oren, 1997: A comparison of sap flow and eddy fluxes of water vapor from a boreal deciduous forest. *Journal of Geophysical Research*, **102**, D24, 28929-28937.

Kellner, O. and D. Niyogi, 2015: Land surface heterogeneity signature in tornado climatology? An illustrative analysis over Indiana, 1950-2012. *Earth Interactions*, **18**, 10, 1-32.

King, P. W. S., M. J. Leduc, D. M. L. Sills, N. R. Donaldson, D. R. Hudak, P. Joe, and B. P. Murphy, 2003: Lake breezes in southern Ontario and their relation to tornado climatology. *Weather and Forecasting*, **18**, 795-807.

Li, D., E. Bou-Zeid, and M. L. Baeck, 2013: Modeling land surface processes and heavy rainfall in urban environments: Sensitivity to urban surface representations. *Journal of Hydrometeorology*, **14**, 1098-1117.

Niyogi, D., T. Holt, S. Zhong, P. C. Pyle, and J. Basara, 2006: Urban and land surface effects on the 30 July 2003 mesoscale convective system event observed in the southern great plains. *Journal of Geophysical Research*, **111**, D19107, 1-20. DOI: 10.1029/2005JD006746.

Niyogi, D., P. Pyle, M. Lei, S. P. Arya, C. M. Kishtawal, M. Shepherd, F. Chen, and B. Wolfe, 2011: Urban modification of thunderstorms – an observational storm climatology and model case study for the Indianapolis urban region. *Journal of Applied Meteorology and Climatology*, **50**, 1129-1144. DOI: 10.1175/2010JAMC1836.1.

Nkemdirim, L. C., 1981: Extra urban and intra urban rainfall enhancement by a medium sized city. *Water Resources Bulletin*, **17**, 5, 753-759.

Oke, T. R., 1973: City size and the urban heat island. *Atmospheric Environment*, 7, 769-779.

Pielke, R. A., J. Adegoke, A. Beltrán-Przekurat, C. A. Hiemstra, J. Lin, U. S. Nair, D. Niyogi, T. E. Nobis, 2007: An overview of regional land-use and land-cover impacts on rainfall. *Tellus*, **59B**, 587-601.

Rabin, R. M., S. Stadler, P. J. Wetzel, D. J. Stensrud, and M. Gregory, 1990: Observed effects of landscape variability on convective clouds. *Bulletin of the American Meteorological Society*, **71**, 3, 272-280.

Raddatz, R. L., 1993: Prairie agroclimate boundary-layer model: A simulation of the atmosphere/crop-soil interface, *Atmosphere-Ocean*, **31**, 4, 399-419.

Raddatz, R. L., 1998: Anthropogenic vegetation transformation and the potential for deep convection on the Canadian Prairies. *Canadian Journal of Soil Science*, **78**, 4, 657-666.

Raddatz, R. L., 2005: Moisture recycling on the Canadian Prairies for summer droughts and pluvials from 1997 to 2003. *Agriculture and Forest Meteorology*, **131**, 13-26.

Raddatz, R. L., and J. D. Cummine, 2003: Inter-annual variability of moisture flux from the prairie agro-ecosystem: Impact of crop phenology on the seasonal pattern of tornado days. *Boundary Layer Meteorology*, **106**, 283-295.

Reuter G. W., and S. Guan, 1995: Effects of industrial pollution on cumulus convection and rain showers: A numerical study. *Atmospheric Environment*, **29**, 18, 2467-2474.

Rozoff, C. M., W. R. Cotton, and J. O. Adegoke, 2003: Simulation of St. Louis, Missouri, land use impacts on thunderstorms. *Journal of Applied Meteorology*, **42**, 716-738.

Schmid, P. E., and D. Niyogi, 2013: Impact of city size on precipitation-modifying potential. *Geophysical Research Letters*, **40**, 5263-5267.

Sellers, P., F. Hall, H. Margolis, B. Kelly, D. Baldocchi, G. den Hartog, J. Cihlar, M. G. Ryan, B. Goodison, P. Crill, K. J. Ranson, D. Lettermaier, D. E. Wickland, 1995: The boreal ecosystem – atmosphere study (BOREAS): An overview and early results from the 1994 field year. *Bulletin of the American Meteorological Society*, **76**, 9, 1549-1577.

Shrestha, B. M., R. L. Raddatz, R. L. Desjardins, and D. E. Worth, 2012: Continuous cropping and moist deep convection on the Canadian Prairies. *Atmosphere*, **3**, 4, 573-590. DOI: 10.3390/atmos3040573

Sills, D. M. L., J. R. Brook, I. Levy, P. A. Makar, J. Zhang, and P. A. Taylor, 2011: Lake breezes in the southern Great Lakes region and their influence during BAQS-Met 2007. *Atmospheric Chemistry and Physics*, **11**, 7955-7973.

Smith, S. B., and M. K. Yau, 1993: The causes of severe convective outbreaks in Alberta. Part I: A comparison of a severe outbreak with two non-severe events and part II: Conceptual model and statistical analysis. *Monthly Weather Review*, **121**, 1099-1133.

Steiger, S. M., and R. E. Orville, 2003: Cloud-to-ground lightning enhancement over southern Louisiana. *Geophysical Research Letters*, **30**, 1975, DOI: 10.1029/2003GL017923.

Steiger, S. M., R. E. Orville, and G. Huffines, 2002: Cloud-to-ground lightning characteristics over Houston, Texas: 1989-2000. *Journal of Geophysical Research*, **107**, 4117, DOI: 10.1029/2001JD001142.

Strong, G. S., 1997: Atmospheric moisture budget estimates of regional evapotranspiration from RES-91. *Atmosphere-Ocean*, **35**, 1, 29-63

Sun, J., D. H. Lenschow, L. Mahrt, T. L. Crawford, K. J. Davis, S. P. Oncley, J. I. MacPherson, Q. Wang, R. J. Dobosy, and R. L. Desjardins, 1997: Lake-induced atmospheric circulations during BOREAS. *Journal of Geophysical Research*, **102**, D4, 29155-29166.

Thielan, J., and A. Gadian, 1997: Influence of topography and urban heat island effects on the outbreak of convective storms under unstable meteorological conditions: A numerical study. *Meteorology Applications*, **4**, 139-149.

Vidale, P. L., R. A. Pielke, L. T. Steyaert, and A. Barr, 1997: Case study modeling of turbulent and mesoscale fluxes over the BOREAS region. *Journal of Geophysical Research*, **102**, D24, 29167-29188.

Westcott, N. E., 1995: Summertime cloud-to-ground lightning activity around major Midwestern urban areas. *Journal of Applied Meteorology*, **34**, 1633-1642.

Zhong, S., Y. Qian, C. Zhao, R. Leung, and X.-Q. Yang, 2015: A case study of urbanization impact on summer precipitation in the greater Beijing metropolitan area: Urban heat island versus aerosol effects. *Journal of Geophysical Research*, **120**, 10903-10914. DOI: 10.1002/2015JD023753.

2.5. Tables

Table 2.1: Energy balance from various vegetation and land cover types. The data is summarized from Barr and Betts (1997), and Barr and Strong (1996).

	Northern Boreal Regions (Thompson, MB)	Southern Boreal Regions (Candle Lake, SK)	Cropped Lands (Saskatoon, SK)	Cropped Lands (Kenaston, SK)
Sensible Heat Flux (Wm^{-2})	227	166	88	117
Latent Heat Flux (Wm^{-2})	182	185	306	283
Bowen Ratio	1.24	0.90	0.29	0.41

2.6. Figures

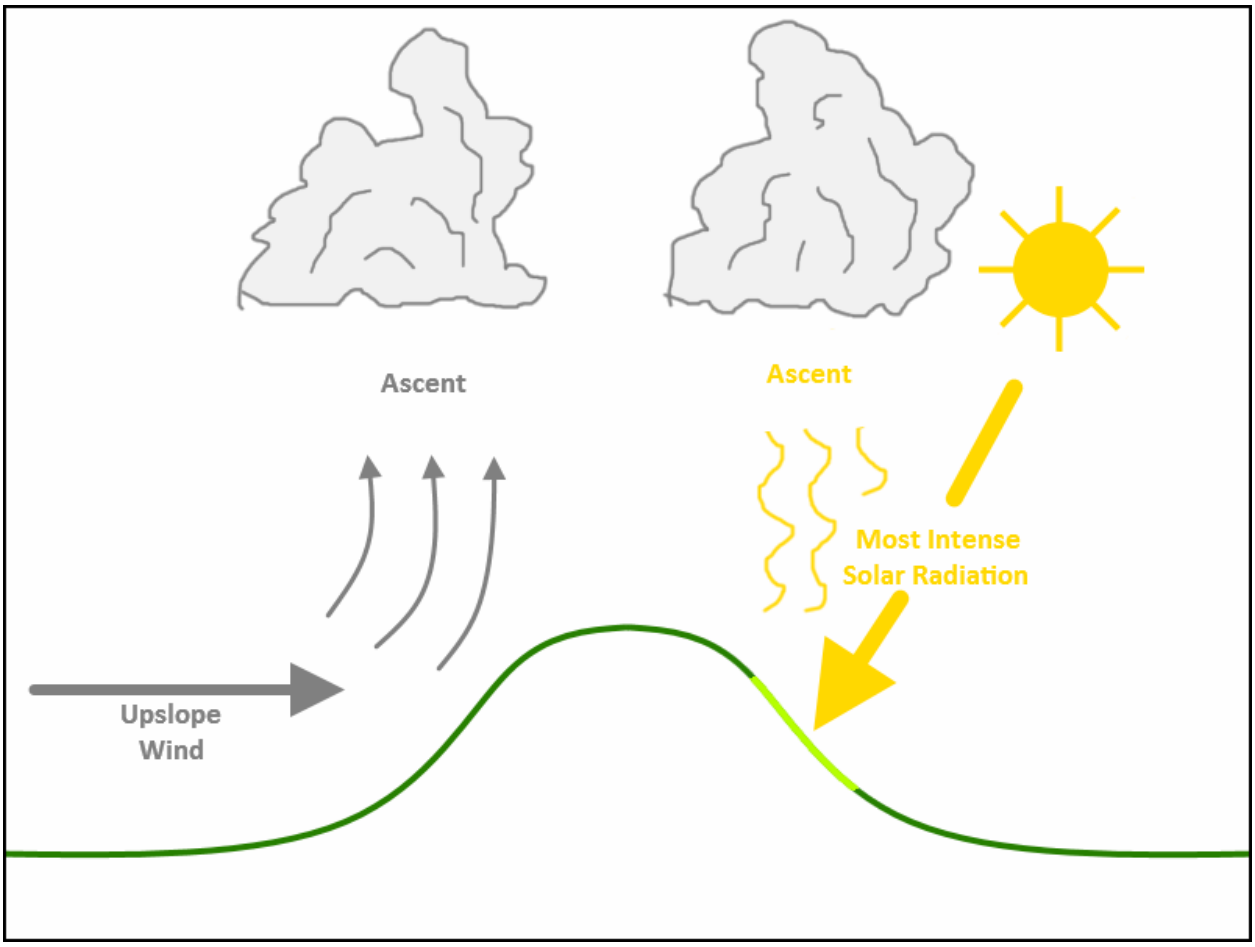

Figure 2.1: An illustration of two different ways that topographic variations can enhance ascent and trigger convection: upslope flow, and intensified solar heating of the slope facing the sun. These ascent methods could happen separately or combined with one another.

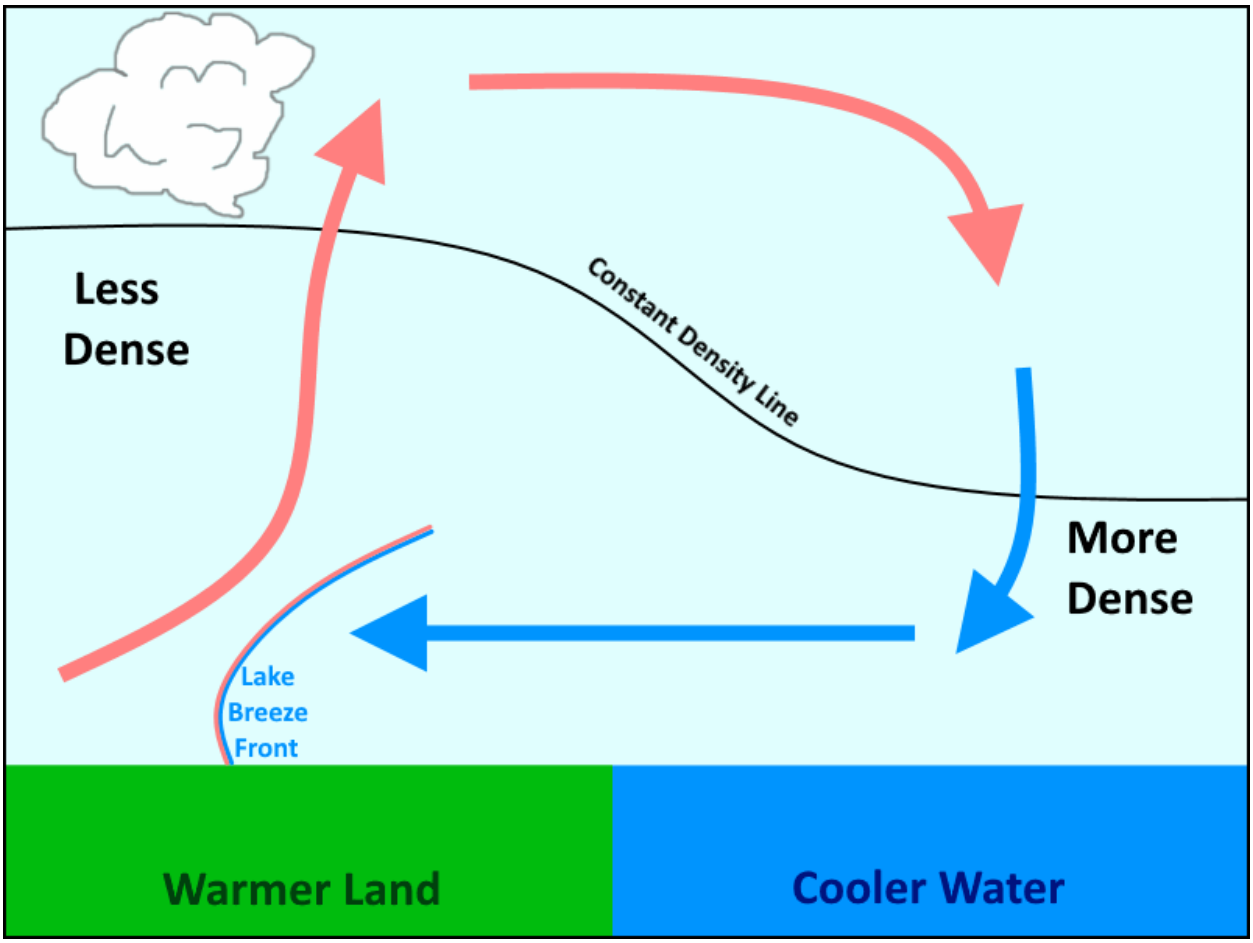

Figure 2.2: An illustration of the lake breeze. The cooler denser air over the water undercuts the warmer less dense air over the land and forms a solenoidal circulation. Ascent over the land at the lake breeze front may cause preferential cumulus formation, and trigger thunderstorms.

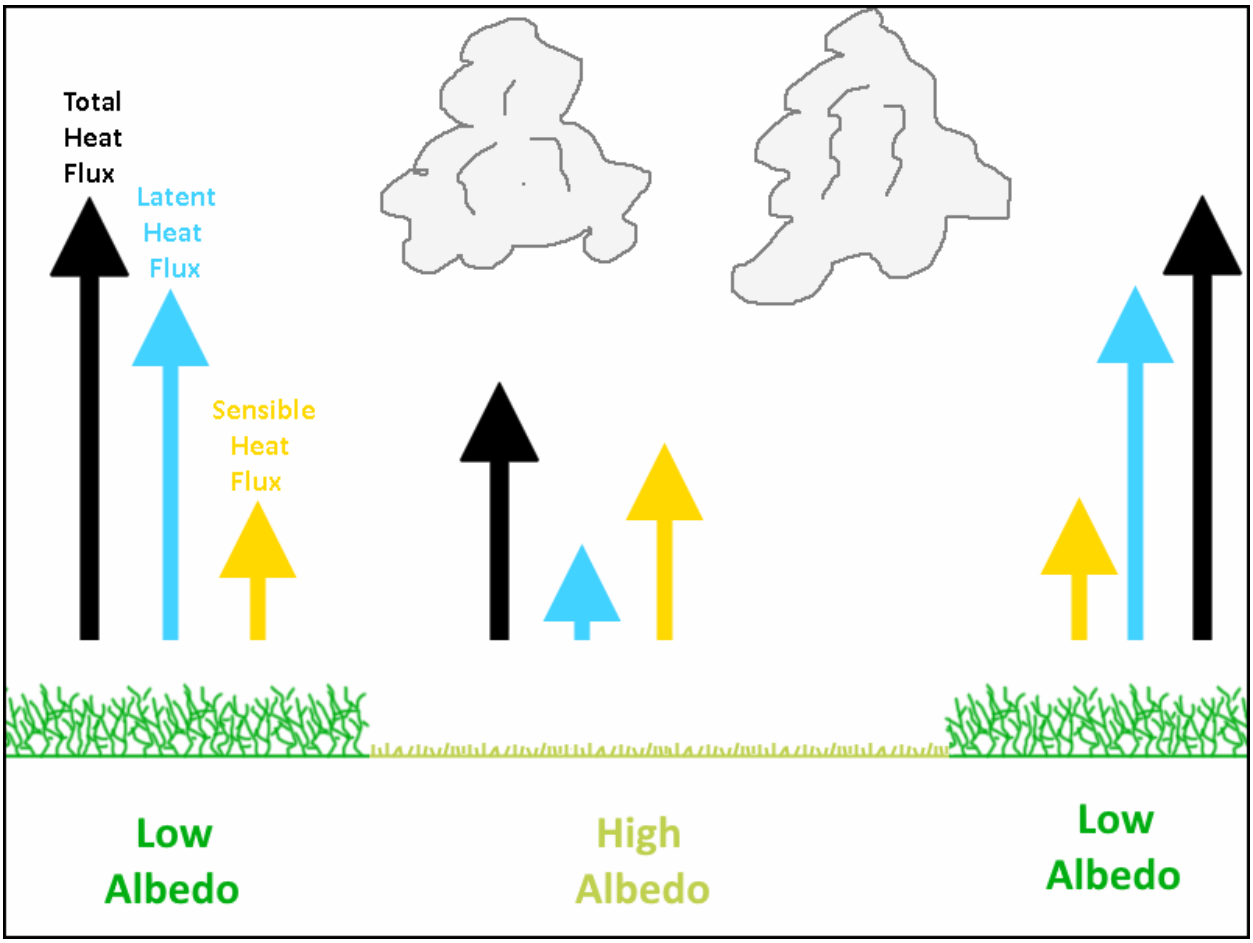

Figure 2.3: An illustration of how the proportion of sensible to latent heat can cause more ascent in a higher albedo area than an area with a lower albedo. If most of the energy emitted from the area with lower albedo is put into the latent heat flux, then there is very little sensible heat flux left over to heat the air. Because the area with high albedo is dry, almost all of the energy goes to sensible heat flux.

3. Background on lightning

3.1. Lightning properties and formation

Lightning in thunderstorms occurs when a large static electricity discharge is forced in cumulonimbus clouds. The temperature within a lightning bolt can reach 30000 K, causing a bright visible flash. The rapidly heated air expands quickly and creates a shockwave in the atmosphere known as thunder (Bürgesser et al. 2006). Cloud-to-ground lightning occurs between a charged cloud and the ground. Cloud lightning occurs within the same charged cloud, or between two different clouds.

In order to create lightning, charge separation must occur within the cloud. Williams (1989) describes a tripole charge arrangement. The anvil at the top of the thunderstorm is positively charged. Mid-levels of the cloud and portions of the base of the cloud are negatively charged. However a small pocket of positive charge exists at the base of the cloud (Figure 1). Scavuzzo et al. (1995) used a numerical model to simulate fracture charging, which reproduced the tripole structure. However, Stolzenburg et al. (1998) found that more complicated charge structures can exist. They also found that the charge structures could vary between updraft and downdraft regions of the thunderstorm complex

Negative cloud-to-ground lightning strokes connect the ground to the middle negatively charge portion of the cloud. A typical stroke transfers several Coulombs of charge at an average peak current of 30 kA. Often there are numerous subsequent lightning strokes following the same path (Bürgesser et al. 2006). Positive cloud-to-ground lightning strokes connect the ground to either the upper or lower positively charged portion of the cloud. Positive strokes from the top of

the cloud can be 10 times as powerful as negative strokes creating a peak current closer to 300 kA, but subsequent strokes rarely occur (Bürgesser et al. 2006). These strokes are shown in Figure 1.

There are various charge separation mechanisms for producing electric charges in thunderstorms. Lightning almost always arises when ice is present in the cloud (Saunders 1993). Charge separation seems to occur when a graupel (small hail) particle collides with small cloud-ice particles (Latham 1981). The smaller cloud-ice particles acquire one charge, and the larger particles acquire another charge. The different sized particles have very different terminal velocities, and are thus separated by the updraft and gravity to the top and bottom of the cloud (Illingworth 1985). Jayaratne et al. (1983) found that charging was strongest in the presence of supercooled liquid water droplets. At temperatures colder than the "charge reversal temperature", graupel particles pick up a negative charge and cloud-ice particles pick up a positive charge. However at warmer temperatures the opposite occurs, leading to the thunderstorm tripole structure (Illingworth 1985). The "charge reversal temperature" is a function of liquid water content and ranges between -10°C and -20°C (Jayaratne et al. 1983).

None of the previous discussion, however, describes the *mechanism* of charge separation. Many of the charge separation theories rely on the thermoelectric effect, which happens when there is a temperature gradient in ice, as described by Wallace and Hobbs (1977). At warmer temperatures, more water molecules are dissociated into hydrogen and hydroxyl ions. The smaller hydrogen ions travel faster by diffusion to colder regions where the concentration of hydrogen ions is less. This mechanism gives positive charge in colder regions and negative charge in warmer regions of the ice crystal (Wallace and Hobbs 1977). Latham and Mason (1961) originally proposed that the production of splinters from collisions may be important. Caranti et al. (1991) described in detail one of the more recent methods of charge separation. Graupel particles growing by riming and deposition have warm extremities due to the release of latent

heat, and thus acquire negative charge. However, graupel particles that are experiencing evaporation or sublimation have cooler extremities and thus acquire positive charge (Figure 2). Through many experiments, Caranti et al (1991) showed that when rising smaller particles collided with the falling graupel particles, small charged protrusions on the outside of the graupel particles shatter and rise in the updraft. Jayaratne (1991) also showed that the charging was independent of the particle that was causing the shattering (sometimes sand was used).

Recently, Gurevich et al. (1992) proposed that when a thunderstorm's electric field approaches a certain value, relativistic electrons produced by cosmic rays accelerate past the threshold velocity and cause an avalanche of relativistic electrons that create an ionization path for the lightning bolt to flow through. Milikh and Roussel-Dupré (2010) show that accounting for the relativistic electron avalanche causes the electric field necessary to initiate a lightning discharge to be ten times lower, closer to what is observed. In fact, somewhat random ionization trails caused by the relativistic electrons may account for the irregular path that lightning takes from one charge region to another. Scott et al. (2014) found that lightning activity was correlated to solar activity. They proposed that the solar wind plasma affected the amount of cosmic rays that made it to the atmosphere, which affected the amount of lightning that could occur. Jungwirth et al. (2005) suggested that the charge distribution can even be affected by ions introduced by aerosols, because lightning in forest fire smoke had different positive to negative stroke ratios. Kochtubajda et al. (2011) found a much higher ratio of positive lightning flashes during the record breaking 2004 Yukon forest fire season when large amounts of smoke were emitted.

3.2. Lightning Detection

There is great interest of having reliable lightning detection systems, because in Canada, lightning causes significant damage to electrical infrastructure, ignites about half of the forest fires, poses a hazard to aviation related activities, and injures about 100 people per year. Cummins et al. (2000) and Rakov (2013) described different lightning detection systems. Some systems are designed to detect cloud-to-ground lightning, while others are designed to detect cloud lightning. It is difficult to construct a single system that detects both effectively (Cummins et al. 2000). There are various lightning detection networks around the world. The National Lightning Detection Network (NLDN) is the main network used in the United States (Orville 1991b). In Alberta, there are three main commercial lightning detection networks: the Canadian Lightning Detection Network (CLDN) (Burrows and Kochtubajda 2010), the Pelmorex Lightning Detection Network (PLDN) (The Weather Network, 2016), and the Alberta Wildfire Lightning Network (Alberta Agriculture and Forestry 2016). In addition, various volunteer networks provide some coverage, such as Blitzortung (Blitzortung 2016).

The cloud-to-ground lightning stroke is the most dangerous stroke. It causes all damage, injuries, and wildfires on the ground. Cloud-to-ground lightning strokes are the easiest to detect because they have the largest currents, and cause the strongest low frequency emissions (Cummins et al. 2000). Most lightning detection networks are tuned to detect mostly cloud-to-ground lightning strokes because they are most dangerous.

The cloud lightning stroke has been studied less because it does not cause as much damage. However, recently there has been interest in detecting cloud lightning to investigate its relation to severe weather (Cummins et al. 2000). Cloud lightning causes the strongest high frequency emissions, and is more difficult to detect because it produces lower peak currents

(Cummins et al. 2000). Some lightning networks now specialize in total lightning detection, which includes both cloud and cloud-to-ground lightning strokes. For example the Earth Networks Total Lightning Network attempts to detect most lightning strokes and classifies them into cloud and cloud-to-ground strokes (Rakov 2013). Gatlin and Goodman (2010) used an algorithm based on the total lightning to predict severe weather events.

Two lightning detection methods are used operationally. The magnetic direction finding method (Figure 3 - top) uses two orthogonal magnetic loop antennae at one location provide the vector components of the direction of the low frequency radiation generated by the lightning stroke (Cummins et al. 2000). Thus, the lightning stroke is located somewhere along the line defined by the direction. If two or more detectors at different locations detect the same stroke, then the intersection of the lines created by each detector gives the geographical location coordinates of the lightning stroke (Orville 1991a).

Time-of-arrival methods are another way to ascertain the location of a lightning stroke by comparing the differences in the arrival time of the lightning-produced microwave radiation at sensors at different geographical locations (Figure 3 - middle) (Lee, 1986). The time-of-arrival method requires an exact time of the arrival of the signal; however, radio frequency radiation produced by a lightning stroke will produce a waveform with a duration on the order of 100 microseconds. The time-of-arrival method works best if the lightning waveform can be closer to a Dirac-Delta function, which is possible using a wide bandwidth (Mazur et al. 1997). However, researchers can also implement waveform matching algorithms to get a consistent result on the signal arrival time (Lee 1986). Because only arrival time *differences* can be calculated between sensors, the arrival time needs to be recorded by four different lightning sensors in order to get a unique location for the lightning stroke (Lee, 1986). Lee (1986) also suggested that the lightning signals are attenuated significantly by non-conducting dry ground.

Most networks now use a combination of the time-of-arrival and magnetic direction finding methods to provide greater accuracy in lightning location (Figure 3 - bottom). Both methods can provide information that can help refine the location of the lightning stroke (Cummins et al. 2000). Most sensors in the National Lightning Detection Network and the Canadian Lightning Detection network use both methods (Rakov 2013).

The previous described lightning sensing systems generally have their sensors placed at a maximum of 400-500 km because more distant lightning signals are attenuated too much due to the curvature of the earth and the underlying land cover (Lee 1986; Cummins et al. 2000). This poses a problem for lightning detection in remote areas because there may not be enough infrastructure to set up a detection system. Lightning also produces signals on a very low frequency band that travels many thousands of kilometres because it is continually reflected between the ionosphere and the ground (Cummins et al. 2000). Said et al. (2010) provides a detailed description of a long range lightning detection system. The GLD360 lightning detection network uses this method (Rakov 2013). In theory, only 10 sensors are required to cover the entire world (Dowden et al. 2002).

Some lightning detection systems are capable of detecting the fine-scale structure of a single lightning bolt, and are known as Lightning Mapping Arrays. A network of sensors uses the time-of-arrival method to detect very high frequency microwave radiation from the path of the lightning bolt (Thomas et al. 2004). These lightning networks can only work at smaller scale (10s of km) because of the nature of the microwave radiation used (Cummins et al. 2000). Thomas et al. (2004) found that although there could be location errors on the order of a kilometre, most errors were closer to 10-30 metres, and the system is able to map out the path of the entire lightning bolt. Data from this type of lightning detection system will not be used in this thesis.

Lightning strokes produce electromagnetic radiation at much higher frequencies; however, this radiation is not as useful for mapping lightning strokes. For example, visible radiation is only useful for short distances because a line of sight is needed. Additionally, infrared and visible radiation is contaminated by solar and terrestrial sources. Lightning strokes are also known to produce x-rays and gamma rays, however these are quickly absorbed by the atmosphere and are difficult to observe. Terrestrial gamma ray bursts caused by lightning have been observed from orbiting satellites (Milikh and Roussel-Dupré 2010).

3.3. Influence of land cover on lightning and lightning detection

Researchers have studied various mechanisms by which the land cover can affect the amount of cloud-to-ground lightning detected by lightning detection networks. The land cover affects the frequency and intensity of thunderstorms, the efficiency of the lightning detection network, and the electrical characteristics of the thunderstorms.

Some researchers have correlated land cover or soil types with the amount of cloud-to-ground lightning. Land cover type in the Mediterranean significantly influences cloud-to-ground lightning. This effect is speculated to be caused by variations in higher moisture in land cover types with lusher vegetation causing more humid, more unstable weather conditions (Kotroni and Lagouvardos 2008). Dissing and Verbyla (2013) found similar results in the boreal forest in Alaska. Bourscheidt et al. (2008) found that land cover instead of soil type primarily influenced lightning density in Brazil, while Mora García et al. (2015) found that both were responsible in Spain.

However, other researchers have speculated that the land cover, specifically the soil electrical conductivity, can influence the quality of the lightning detection. Nag et al. (2015) state

that elevation changes and soil electrical conductivity are the main factors that cause timing errors in the time-of-arrival technique. Schueler and Thompson (2006) found that the location accuracy of lightning detection systems can be improved by accounting for ground electrical conductivity. Errors in lightning location caused by ground conductivity variability were highest in time-of-arrival sensors because the ground conductivity introduced a time lag. Scheftic et al. (2008) found that soil electrical conductivity depended most strongly on soil moisture. In fact, Scheftic et al. (2008) developed a method of inferring changes in soil moisture using the rise-time of the lightning waveform.

The lightning waveform rise-time is the amount of time for the waveform to rise from 10 percent to its peak amplitude (Figure 4), and it appears to be strongly influenced by the ground surface conductivity. Low conductivity ground causes a longer rise-time and a lower peak amplitude of the lightning waveform and could contribute to attenuation of the lightning signal (Herodotou et al. 1993; Scheftic et al. 2008). Scheftic et al. (2008) and Bardo et al. (2004) both show maps of the lightning rise-times over the United States and southern Canada and note that both the Rocky Mountains and the Canadian Shield regions have particularly large rise-times. Similar results were found for the waveform peak-to-zero time (Figure 4). Chisholm et al. (2001) suggested that areas with a lower lightning density seemed to correspond with areas with a higher electrical resistivity. However there is no research or speculation on whether this could translate to a lower detection efficiency.

Some researchers have looked at whether the characteristics of lightning strokes themselves could be affected by the land surface. Lightning strokes over salt water tend to have higher peak electrical currents (Orville and Huffines 2003). Tyahla and López (1994) found that the peak current of lightning strokes was affected slightly by the ground conductivity. Chisholm et al. (2001) suggests that low cloud-to-ground lightning density tends to be found in areas with a

high soil electrical resistivity (low conductivity). Nelson et al. (2013) claim to be able to use the lightning waveform rise-time and lightning density maps to find oil and gas deposits. However, even though the Canadian Shield exists just below the surface in many regions, Scheftic et al. (2008) still found that the rise time was mostly affected by the electrical conductivity of the land surface. This finding suggests that the subsurface probably has little effect.

3.4. References

Alberta Agriculture and Forestry, 2016: Lightning Detection. Accessed 27 August 2016. [Available online at http://wildfire.alberta.ca/fire-weather/lightning-detection/default.aspx.]

Bardo, E. A., K. L. Cummins, and W. A. Brooks, 2004: Lightning current parameters derived from lightning location systems. *International Conference on Lightning Detection*, Helsinki, Finland.

Blitzortung, 2016: Network for lightning and thunderstorms in real time. Accessed 27 August 2016. [http://en.blitzortung.org/contact.php.]

Bourscheidt, V., O. Pinto Jr., K. P. Naccarato, I. R. C. A. Pinto, 2008: Dependence of CG lightning density on altitude, soil type, and land surface temperature in south of Brazil. *20th International Lightning Detection Conference*, Tucson, Arizona.

Bürgesser, R. E., R. G. Pereyra, and E. E. Avila, 2006: Charge separation in updraft region of convective thunderstorms. *Geophysical Research Letters*, **33**, L03808, 1-4.

Burrows, W. R., and B. Kochtubajda, 2010: A decade of cloud-to-ground lightning in Canada: 1999-2008. Part 1: Flash Density and occurrence. *Atmosphere-Ocean*, **48**, 3, 177-194.

Caranti, G. M., E. E. Avila, and M. A. Ré, 1991: Charge transfer during individual collisions in ice growing from vapor deposition. *Journal of Geophysical Research*, **96**, D8, 15365-15375.

Chisholm, William. A., Stephen L. Cress, and Janusz Polak, 2001: Lightning-caused distribution outages. Proceedings of the IEEE Power Engineering Society Transmission Distribution Conference, pp. 1041-1046.

Cummins, K. L., M. J. Murphy, and J. V. Tuel, 2000: Lightning detection methods and meteorological applications. Preprints, fourth international symposium on military meteorology, Marbork, Poland, WMO, 85-100.

Dissing, D. and D. L. Verbyla, 2013: Spatial patterns of lightning strikes in interior Alaska and their relations to elevation and vegetation. *Canadian Journal of Forest Research*, **33**, 770-782.

Dowden, R. L., J. B. Brundell, and C. J. Rodger, 2002: VLF lightning location by time of group arrival (TOGA) at multiple sites. *Journal of Atmospheric and Solar-Terrestrial Physics*, **64**, 817-830.

Gatlin, P. N., and S. J. Goodman, 2010: A total lightning trending algorithm to identify severe thunderstorms. *Journal of Atmospheric and Oceanic Technology*, **27**, 1-22. DOI: 10.1175/2009JTECHA1286.1

Gurevich, A. V., G. M. Milikh, and R. Roussel-Dupré, 1992: Runaway electron mechanism of air breakdown and preconditioning during a thunderstorm. *Physics Letters A*, **165**, 463-468.

Herodotou, N., W. A. Chisholm, and W. Janichewskyj, 1993: Distribution of lightning peak stroke currents in Ontario using an LLP system. *IEEE Transactions on Power Delivery*, **8**, 3, 1331-1339

Illingworth, A. J. 1985: Charge separation in thunderstorms: Small scale processes. *Journal of Geophysical Research*, **90**, D4, 6026-6032.

Jayaratne, E. R., 1991: Charge separation during the impact of sand on ice and its relevance to theories of thunderstorm electrification. *Atmospheric Research*, **26**, 407-424.

Jayaratne, E. R, C. P. R. Saunders, and J. Hallett, 1983: Laboratory studies of the charging of soft-hail during ice crystal interactions. *Quarterly Journal of the Royal Meteorological Society*, **109**, 609-630.

Jungwirth, P., D. Rosenfeld, and V. Buch, 2005: A possible new molecular mechanism of thunderstorm electrification. *Atmospheric Research*, **76**, 190-205.

Kochtubajda, B., W. R. Burrows, D. Green, A. Liu, K. R. Anderson, and D. McLennan, 2011: Exceptional cloud-to-ground lightning during an unusually warm summer in Yukon, Canada. *Journal of Geophysical Research*, **116**, D21206, 1-20, doi:10.1029/2011JD016080.

Kotroni, V. and K. Lagouvardos, 2008: Lightning occurrence in relation with elevation, terrain slope, and vegetation cover in the Mediterranean. Journal of Geophysical Research*,* **113**, D21118, 1-7, doi:10.1029/2008JD010605

Latham, J., 1981: The electrification of thunderstorms. *Quarterly Journal of the Royal Meteorological Society*, **107**, 452, 277-298.

Latham, J., and B. J. Mason, 1961: Generation of electric charge associated with the formation of soft hail in thunderclouds. *Proceedings of the Royal Society of London. Series A, Mathematical and Physical Sciences*, **260**, 1303, 537-549.

Lee, A. C. L., 1986: An operation system for the remote detection of lightning flashes using a VLF arrival time difference technique. *Journal of Atmospheric and Oceanic Technology*, **3**, 630-642.

Mazur, V., E. Williams, R. Boldi, L. Maier, D. E. Proctor, 1997: Initial comparison of lightning mapping with operational time-of-arrival and interferometric systems. *Journal of Geophysical Research*, **102**, D10, 11071-11085.

Milikh, G., and R. Roussel-Dupré, 2010: Runaway breakdown and electrical discharges in thunderstorms. *Journal of Geophysical Research*, **115**, A00E60, 1-15.

Mora García, M., J. Riesco Martín, L. Rivas Soriano, and F. de Pablo Dávila, 2015: Observed impacts of land uses and soil types on cloud-to-ground lightning in Castilla-Leon (Spain). *Atmospheric Research*, **166**, 233-238.

Nag, A., M. J. Murphy, W. Schulz, and K. L. Cummins, 2015: Lightning locating systems: Insights on characteristics and validation techniques. *Earth and Space Sciences*, **2**, 65-93.

Nelson, H. R., D. J. Siebert, and L. R. Denham, 2013: Lightning data – a new geophysical data type. *Search and Discovery Article*, 41184, 1-19.

Orville, R. E., 1991a: Calibration of a magnetic direction finding network using measured triggered lightning return stroke peak currents. *Journal of Geophysical Research*, **96**, D9, 17135-17142.

Orville, R. E., 1991b: Lightning ground flash density in the contiguous United States – 1989. *Monthly Weather Review*, **119**, 573-577.

Orville, R. E., and Huffines, G. R., 2001: Cloud-to-ground lightning in the United States: NLDN results in the first decade, 1989-1998. *Monthly Weather Review*, **129**, 1179-1193.

Rakov, V. A., 2013: Electromagnetic methods of lightning detection. *Surveys of Geophysics*, **34**, 731-753.

Said, R. K., U. S. Inan, and K. L. Cummins, 2010: Long-range lightning geolocation using a VLF radio atmospheric waveform bank. *Journal of Geophysical Research*, **115**, D23108, 1-19.

Saunders, C. P. R., 1993: A review of thunderstorm electrification processes. *Journal of Applied Meteorology*, **32**, 642-655.

Scavuzzo, C. M., E. E. Avila, and G. M. Caranti, 1995: Cloud electrification by fracture in ice-ice collisions: A 3D model. *Atmospheric Research*, **37**, 325-342.

Scheftic, W. D., Cummins, K. L., Krider, P. E., Sternberg, B. K., Goodrich, D., Moran, S., R. Scott, 2008: Wide-area soil moisture estimation using the propagation of lightning generated low-frequency electromagnetic signals. 20th International Lightning Detection Conference, 1-8.

Schueler, J. R. and Thompson, E. M., 2006: Estimating ground conductivity and improving lightning location goodness of fit by compensating propagation effects. *Radio Science*, **41**, RS1001, 1-13.

Scott, C. J., R. G. Harrison, M. J. Owens, M. Lockwood, and L. Barnard, 2014: Evidence for solar wind modulation of lightning. *Environmental Research Letters*, **9**, 1-12.

Stolzenburg, M., W. D. Rust, and T. C. Campbell, 1998: Electrical structure in thunderstorm convective regions 3. Synthesis. *Journal of Geophysical Research*, **103**, D12, 14097-14108.

The Weather Network, 2016: Pelmorex lightning detection network. Accessed 27 August 2016. [Available online at http://data.twncs.com/Solutions/Lightning/lightning.html.]

Thomas, R. J., P. R. Krehbiel, W. Rison, S. J. Hunyady, W. P. Winn, T. Hamlin, and J. Harlin, 2004: Accuracy of a lightning mapping array. *Journal of Geophysical Research*, **109**, D14207, 1-34.

Tyahla, L. J., and R. E. López, 1994: Effect of surface conductivity on the peak magnetic field radiated by first return strokes in cloud-to-ground lightning. *Journal of Geophysical Research*, **99**, D5, 10517-10525.

Wallace, J. M., and P. V. Hobbs, 1977: *Atmospheric Science: An Introductory Survey.* San Diego, California, Elsevier Science, 467 pp.

Williams, E. R., 1989: The tripole structure of thunderstorms. *Journal of Geophysical Research*, **94**, D11, 13151-13167.

3.5. Figures

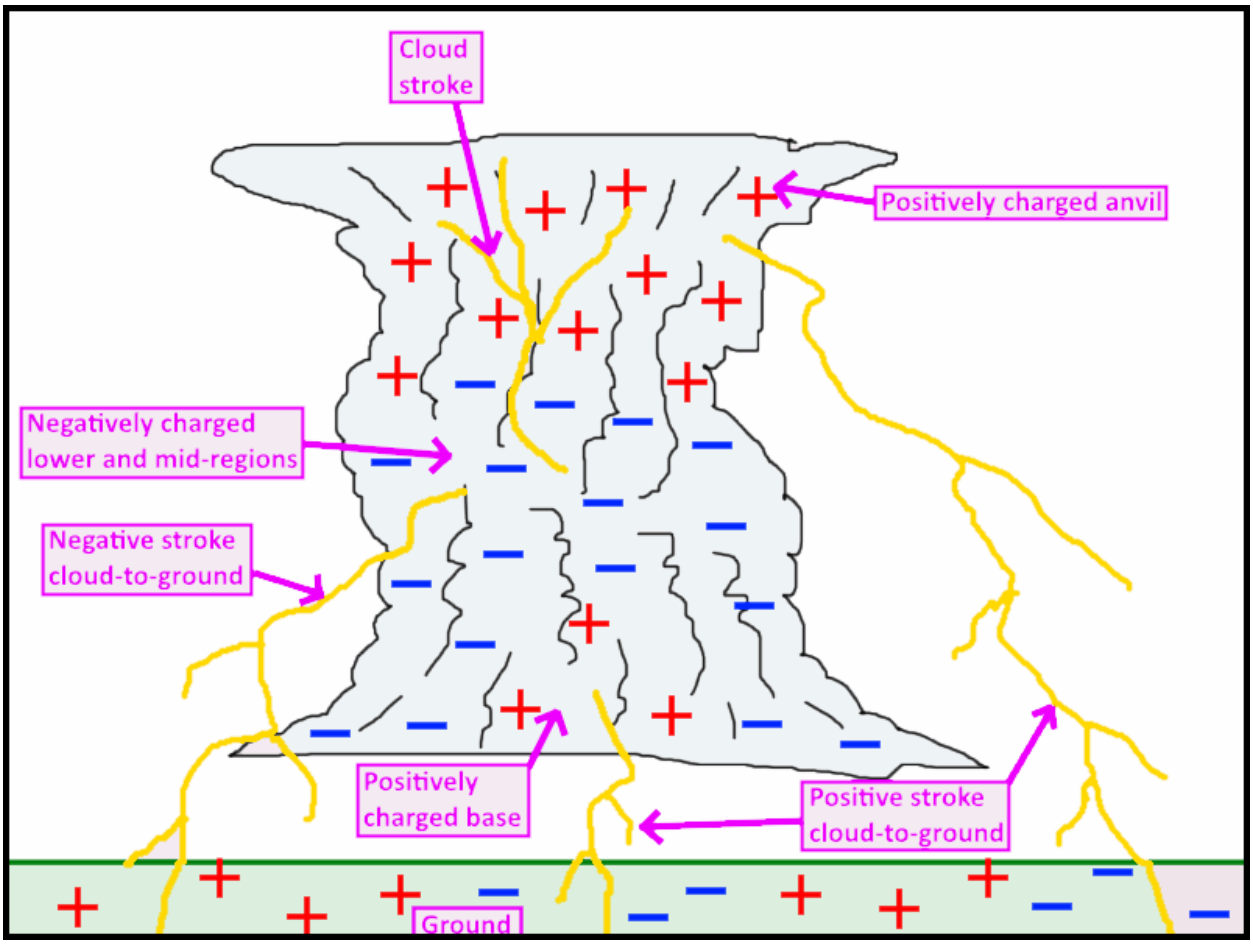

Figure 3.1: The charge structure of the tripole thunderstorm (adapted from Williams 1989), and a diagram of the most common types of lightning.

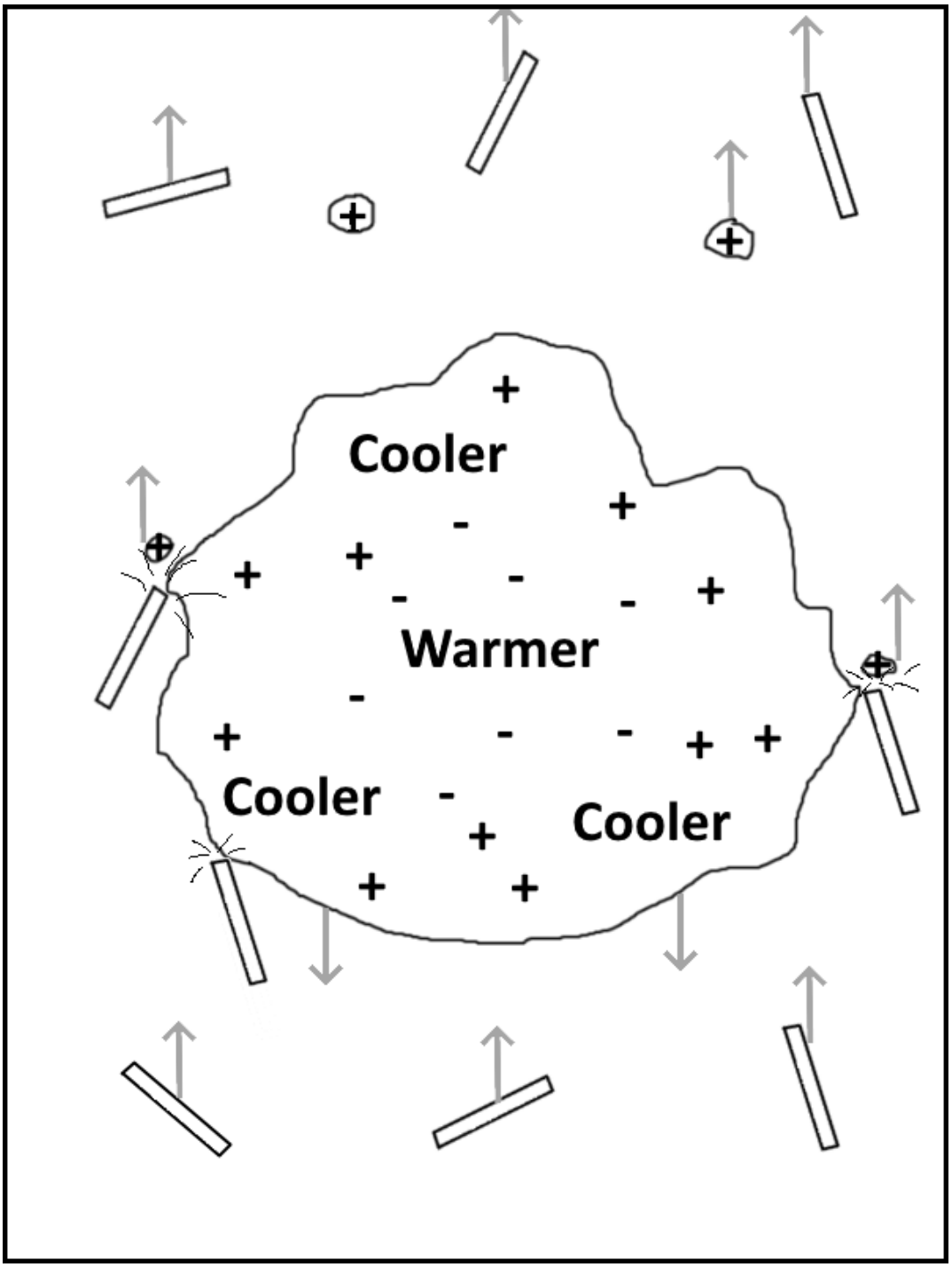

Figure 3.2: An illustration of the thunderstorm charging mechanism proposed by Caranti et al. (1991). Small ice particles break off positively charged shards from an evaporating hailstone. For a hailstone undergoing deposition, the charges and temperatures would be reversed.

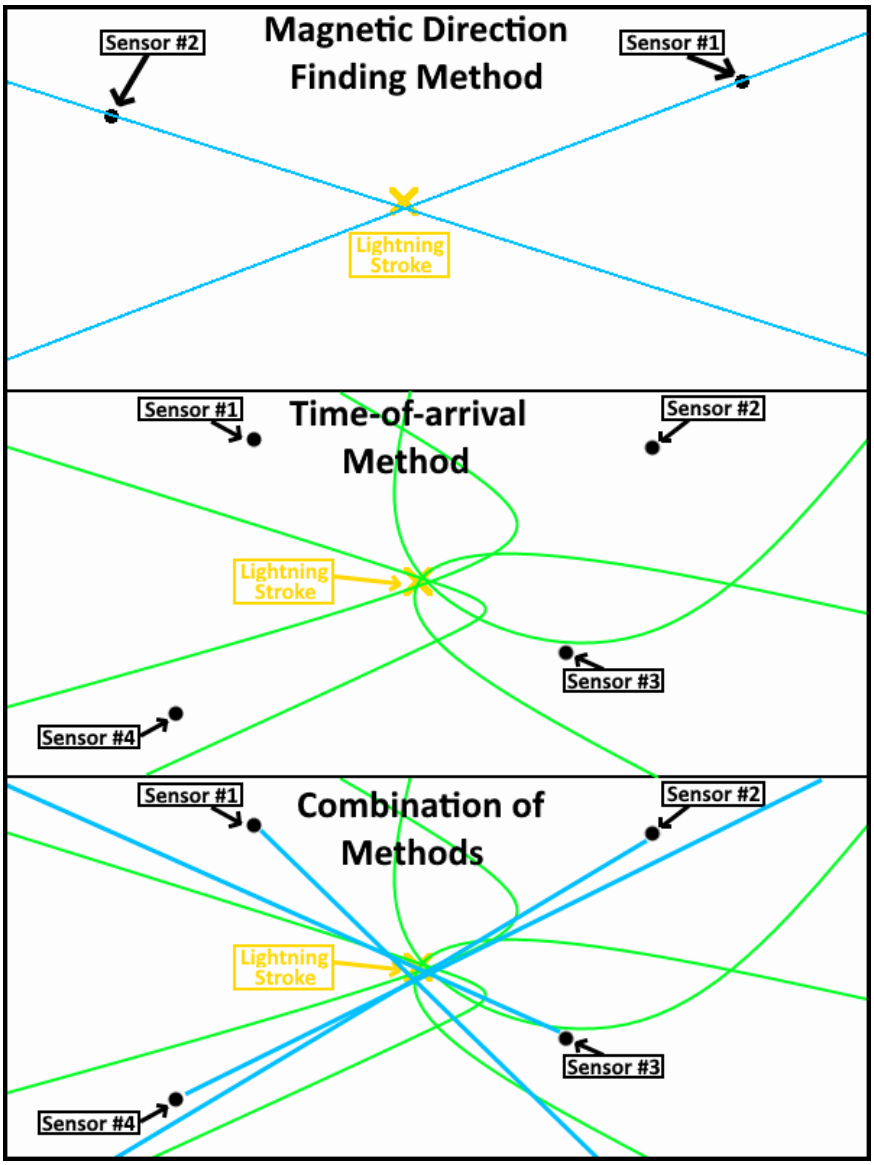

Figure 3.3: An illustration of three methods of lightning detection. Top: the magnetic direction finding method. A sensor consists of two orthogonal loops which detect the direction of a lightning stroke. Only two sensors are needed to locate a stroke (Orville 1991a). Middle: The time-of-arrival method. Each sensor records the time of arrival of the electromagnetic radiation caused by the lightning stroke. The arrival time differences give hyperbolae, of which 4 are needed to locate a stroke (Lee 1986). Bottom: Both methods combined. When both methods are combined, a more accurate result can be obtained (Cummins et al. 2000).

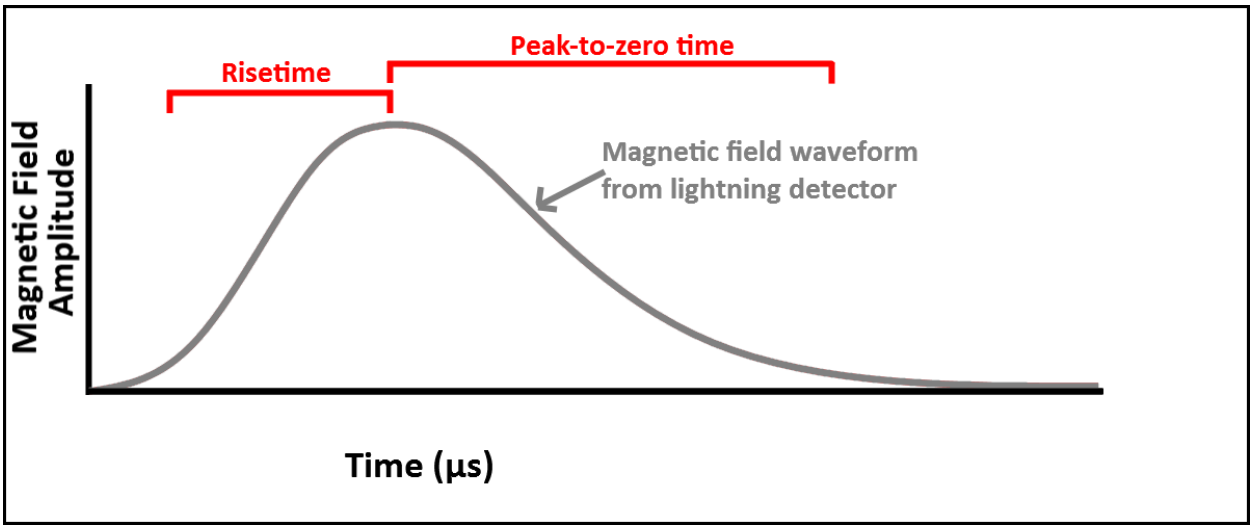

Figure 3.4: A diagram showing an idealized lightning waveform and how the rise-time and peak-to-zero time is calculated (Adapted from Herodotou et al. 1993 and Bardo et al. 2004). If the ground conductivity is low, then the lightning waveform is stretched longer and has a lower amplitude. This results in lower peak currents and longer rise-times and peak-to-zero times.

4. Temperature, precipitation, and lightning modification in the vicinity of the Athabasca oil sands

Daniel M. Brown, Gerhard W. Reuter, and Thomas K. Flesch

This chapter has been published in the journal *Earth Interactions*.

Brown, D. M., G. W. Reuter, and T. K. Flesch, 2011: Temperature, precipitation, and lightning modification in the vicinity of the Athabasca oil sands. *Earth Interactions*, **15**, 1–14. doi: 10.1175/2011EI412.1.

Abstract

The Athabasca oil sands development in northeast Alberta, Canada has disturbed more than 500 km^2 of boreal forest through surface mining and tailings ponds development. In this paper we compare the time series of temperatures and precipitation measured over oil sands and non–oil sands locations from 1994 to 2010. In addition, we analyzed the distribution of lightning strikes from 1999 to 2010. The oil sands development has not affected the number of lightning strikes or precipitation amounts, but has affected the temperature regime. Over the past 17 years, the summer overnight minimum temperatures near the oil sands have increased by about 1.2 °C compared to the regional average. We speculate that this is caused by a combination of the industrial addition of waste heat to the atmosphere above the oil sands, and changing the surface type from boreal forest to open pit mines with tailings ponds.

Key Words

Lightning, Oil sands, Land cover, Weather, Heat island

4.1. Introduction

The Athabasca oil sands development in Canada contains one of the largest known petroleum deposits in the world. It is located about 30 km north of the town of Fort McMurray in northern Alberta (Figure 1A). Bitumen is recovered from the oil sands through surface mining, and is then upgraded into synthetic crude oil. The surface mining results in a dramatic disturbance to the land, and has expanded from about 200 km^2 in 1992, to 380 km^2 in 2001 (Latifovic et al., 2005), to 530 km^2 in 2008 (Kelly et al., 2009). The mined area of the oil sands is separated into two sections of approximately equal area (Latifovic et al., 2005), and consists of a

combination of surface mines, barren land, oil upgrading refineries, and large tailings ponds (Figure 1B). Tailings ponds cover more than 130 km^2 (Kelly et al., 2009).

There has been concern from the public regarding the environmental impacts of the oil sands development. A recent public report (Grant et al., 2010) states "…oil sands activity merits special attention as it is rapidly growing in critical headwaters of the broader Mackenzie River Basin and uses significant amounts of water, while leaving behind toxic sludge. Oil sands development also results in land disturbance and air pollution." (p. 7). Scientific studies have also focused on the environmental effects of the oil sands. Latifovic et al. (2005) found that the oil sands caused vast land cover changes and that vegetation near the oil sands was less productive than vegetation farther away. Kelly et al. (2009) suggest that the oil sands are responsible for considerable toxic water pollution in the Athabasca River, which runs through the development. Hazewinkel et al. (2008) speculated that oil sands emissions of sulphur and nitrogen oxides could cause acid rain which would acidify lakes downwind. The scale of the land disturbance led us to wonder whether the oil sands could also cause inadvertent weather modification.

Inadvertent weather modification due to changes in land cover has been studied extensively. "Urban heat island" is a term used to describe how urban environments cause warmer temperatures in the city centre than in the surrounding rural areas. Oke (1982) found that the magnitude of an urban heat island is related to population, with warming ranging from about 1 °C for smaller cities to over 10 °C for larger cities. These heat islands tend to be strongest in the overnight, and weakest in the afternoon (Oke, 1982).

Researchers have also found increases in precipitation downwind of large cities. Changnon et al. (1976) found this in the St Louis, Missouri area, thought to be caused by surface convergence over the city (caused by an urban heat island and surface roughness changes) and an increase in condensation nuclei due to human activities. Charlton and Park (1984) found increases

in snowfall downwind of Edmonton, Alberta could be caused by the industrial input of heat and moisture into cold arctic air. In contrast, Nkemdirim (1981) found that the city of Calgary, Alberta does not enhance summer precipitation; in fact Calgary has a reduction in summer precipitation in the city centre. Researchers have documented areas of enhanced lightning within and extending downwind of large cities in the United States (Rose et al., 2008; Steiger et al., 2002; Westcott, 1995). Steiger et al. (2002) speculated that enhanced lightning near Houston, Texas may be associated with an increase in cloud condensation nuclei released from industrial activity. Steiger and Orville (2003) hypothesized that industrial activity in Louisiana is responsible for enhancing lightning as well. Reuter (2010) quantified the relative contributions of waste heat, enhanced vapor fluxes, and pollution on convective precipitation for a cluster of power stations.

The literature provides abundant examples describing how a land surface disturbance can result in inadvertent weather modification. The purpose of this paper is to answer the following question: has the development of the Athabasca oil sands had an impact on the local weather; in particular, the surface temperature, precipitation amounts, and cloud-to-ground lightning strikes. Here we compare data from locations in the vicinity of the oil sands relative to the surrounding area, and look for statistically significant trends in the *difference* in daily maximum and minimum surface temperatures, seasonal precipitation amounts, and cloud-to-ground lightning strikes.

4.2. Method of analysis

4.2.1) Observations of surface temperature and precipitation amounts

The study focused on weather stations in the vicinity of the Athabasca oil sands development (Figure 2). The Mildred Lake (57° 02.5’ N, 111° 33.5’ W) weather station is located near the center of the southern portion of the oil sands development. A basic assumption of our analysis is that the Mildred Lake weather data are representative of the conditions within the area

of oil sands development. The only year round observations within the region, but outside the oil sands development are at the Fort McMurray airport (56° 39.2' N, 111° 13.4' W). We assume that the weather conditions measured at this station are representative of the natural state of the region and unaffected by development. Cloud amount and cloud type are recorded at Fort McMurray, but not at Mildred Lake. Thus a comparison was not feasible.

We were initially concerned that the weather data from the Fort McMurray station may be contaminated by the urban heat island of the town of Fort McMurray, which is about 10 km to the west of the Fort McMurray weather station, and has more than doubled in size over the 17 year analysis time period. During the summer, Alberta Sustainable Resource Development operates seasonal forestry weather stations at fire towers in the region. We used these data to compare our results from Fort McMurray with the forestry data in the summer, and our study results (for summer) are similar regardless of which weather stations were used. We thus conclude that the weather data from Fort McMurray is representative of the natural larger region.

Our analysis is limited by the record of the Mildred Lake weather station, which dates back to 1994. The analysis was completed for four seasons: spring (March, April, and May), summer (June, July, and August), autumn (September, October, and November), and winter (December, January, and February). We calculated the average of the daily maximum and minimum temperatures for each season, and the accumulated precipitation. In addition, we calculated the average water vapor mixing ratio for each summer.

We have not used satellite data to augment the surface temperature measurements because the GOES west infrared images have a horizontal spatial resolution of greater than 10 km at Fort McMurray (57 °N). Furthermore, it is difficult to distinguish between cloud and snow making temperature estimates difficult.

4.2.2) Lightning

To determine whether the oil sands development affects lightning, we analyzed data from the Canadian Lightning Detection Network, which has been operating since 1999 (Burrows and Kochtubajda 2010). We analyzed cloud-to-ground lightning strikes detected by the Canadian Lightning Detection Network in an area centered over Fort McMurray. The analysis of lightning was completed for the summer only (June, July, and August), when the vast majority of lightning takes place in the boreal forest.

A number of different methods were employed to test whether the oil sands development affected lightning density. The spatial distribution of lightning density was mapped to find the location of hot spots. A shortcoming of this method is that a single storm can have thousands of lightning strikes, and its influence can dominate the lightning map. To eliminate the influence of prolific lightning storms, we also calculated the number of days with lightning in the region. Both lightning density and lightning days are common ways of quantifying lightning (Burrows and Kochtubajda, 2010).

In addition to visually analyzing maps, we compared the amount of lightning in the vicinity of the Athabasca oil sands with that in the larger region. We created three different analysis areas centered over the oil sands (Figure 2). The smallest area (2500 km^2) encompasses most of the oil sands development. The larger area is about four times as big as the smallest area, and the biggest is about nine times larger. If oil sands development affects lightning, we hypothesize that we will see a difference in lightning trends between the different areas.

4.2.3) The Mann-Kendall statistical test

The Mann-Kendall statistical test is commonly used in meteorology to detect linear trends in a time series of yearly data. This non-parametric test does not require normally distributed data (Yue et al., 2002). The Mann-Kendall test allows us to determine whether the trends are

statistically significant. We used the commonly chosen 95% confidence level to define significance for this study.

4.3. Results

4.3.1) Temperature trends

Figure 3A shows the average summer (June, July, and August) daily maximum and minimum temperatures for Mildred Lake and Fort McMurray from 1994 to 2010. Over the 17 years, the average summer maximum temperatures vary between 21 °C and 25 °C at both stations with less than one degree difference between the two stations. Neither location shows any statistically significant trends in maximum temperature over the 17 years of data. Figure 3B shows the summer temperature *differences* between Fort McMurray and Mildred Lake. We see that maximum temperatures are cooling in Mildred Lake relative to Fort McMurray, and we found this trend significant at the 95 % confidence level (Mann-Kendall test), although the magnitude is small.

The average summer overnight minimum temperatures range from 7 to 12 °C, with substantial differences between the two weather stations. Mildred Lake is between one and four degrees warmer than Fort McMurray. The minimum temperatures do not show any statistically significant trends over the 17 years at either location. Figure 3B shows the summer temperature *differences* between Fort McMurray and Mildred Lake. The minimum temperatures in Mildred Lake are warming relative to Fort McMurray, and this trend is significant at the 95 % confidence level. The magnitude of the trend in the summer minimum temperature difference is much larger than that of the maximum temperature difference.

The results of our analysis for the fall, winter, and spring season temperature *differences* are shown in Table 1. In all cases, any trends in the maximum temperature differences between

Mildred Lake and Fort McMurray are small, and even if the trends are significant they tend to change less than a degree over the 17 years of measurements. Minimum temperatures differences are trending upward in all seasons, but the trends fall just shy of significant in the spring and fall. The minimum temperature trends are larger than the maximum temperature trends; more than two degrees in winter and more than a degree in the summer.

4.3.2) Precipitation trends

Figure 4A compares summer precipitation accumulations at Mildred Lake and Fort McMurray from 1994 to 2010. The precipitation at either of these stations does not appear to show any trends over time, but trend detection is complicated by the large year-to-year variability in precipitation amounts, which varies from about 70 mm to 300 mm. Again, our interest is the temporal trend of the *differences* in precipitation between Mildred Lake and Fort McMurray. Figure 4B shows this for the summer. There are no significant trends in precipitation differences over the summer or any other seasons, but considering the variability in the data, it is likely that the precipitation record is too short to detect subtle trends. We analyzed the precipitation for the other seasons, and also found no significant trends in precipitation differences in any other season.

We also analyzed the water vapor mixing ratio at the two weather stations for each summer (Figure 5A). The average humidity value for both stations was around 8 g kg^{-1} without significant trends. Figure 5B shows the difference of water vapor mixing ratio. Mildred Lake has become 1.5 g kg^{-1} drier compared to Fort McMurray. This trend was found to be statistically significant.

4.3.3) Lightning trends

The lightning density in northeast Alberta is shown in Figure 6A, while Figure 6B shows the number of days with lightning, both between 1999 and 2010. The highest lightning density and lightning days are found in the southern portion of the analysis area. This appears to be caused by lightning enhancement by higher terrain in the southwest (Swan Hills). The lowest area of lightning density and lightning days are in the northeast, which is likely caused by a lightning shadow from large lakes (Lake Athabasca) in the north (Burrows and Kochtubajda 2010). If there is any impact of the oil sands development on lightning, it cannot be visually distinguished from the background noise in the 12 years of lightning data in these maps. Further analysis was completed on other lightning properties (polarity, multiplicity, and first stroke peak current) and again, no clear signal was found.

In Figure 7A we show the total lightning strikes by year in the large box regional analysis area (150 by 150 km). The amount of lightning is highly variable, with some years having almost four times as much lightning as others. We found no significant trends in the total amount of lightning with time. Using the Mann-Kendall test, we calculated whether there were statistically significant trends in the *difference* between lightning in the smallest analysis area (near the oil sands) and in the larger regional areas (far from the oil sands) (Figure 2). We found no statistically significant trends in lightning activity between areas near the oil sands and the greater region (Figure 7B and 7C). We conclude that the oil sands development has little impact on lightning over the development area.

4.4. Discussion and conclusions

Based on the analysis described above, we conclude that the oil sands development has raised local overnight temperatures in all seasons (statistically significant in the summer and winter), and has slightly lowered daytime temperatures in the spring and summer. In contrast to the temperatures, the precipitation and lightning over the oil sands do not appear to be changing relative to that of the larger region.

4.4.1) Temperature

Previous studies have found that inadvertent modification of the weather is common (Oke, 1982; Changnon et al., 1977; Westcott et al., 1995). The warming effect of cities and industry has been well documented as the "urban heat island" effect (Oke, 1982). Urban/rural temperature differences tend to be of the highest magnitude during the night, when a stable atmosphere prevents mixing and confines the heat input to the lowest few hundred meters (Oke, 1982). During the day, deep vertical mixing disperses the heat through a greater volume of air, reducing the magnitude of the urban/rural surface temperature differences to the point where urban heat islands often cannot be found during the day (Oke, 1982). In some cases, slight "urban cool islands" have been reported during the day, thought to be caused by shadows cast by tall buildings, but the magnitude of the daytime "urban cool island" is much smaller than nighttime urban heat islands (Oke, 1982). The temperature observations near the oil sands have similar characteristics as urban heat islands. Two possible explanations for rising temperatures over the oil sands are the following: 1) the direct industrial addition of waste heat to the atmosphere, and 2) modification of the surface energy balance due to land cover changes associated with the large mines (e.g. albedo, heat capacity).

The extraction and production of oil from the Athabasca oil sands uses massive amounts of energy. The oil sands produce about 1.3 million barrels of bitumen per day (Kelly et al., 2009).

We will assume that it takes 1 GJ (de Bruijn, 2010) to produce a barrel of oil. If we roughly estimate that 10 % of this energy is emitted as waste heat and it is distributed over the 530 km^2 land disturbance, then we have a heat flux of about 3 W/m^2. If this were distributed through a 1 km deep boundary layer in the daytime, then the temperature could potentially warm by 0.2 °C, and if we assume a nighttime boundary layer depth of 200 m then this could be 1.1 °C warming.

The development of oil sands has replaced the boreal forest with large mines, which consist of bare ground and large water-filled tailings ponds, which will change the surface energy balance. As the albedo of the bare ground differs from the forested area, it will affect the surface energy budget. It could possibly warm the air by raising the Bowen ratio and reducing the latent heat flux (i.e. no vegetative transpiration). Changing the surface from forest to tailings ponds will increase the heat capacity, and would cause the surface to stay warmer than the surrounding forest at night and cooler during the day. This type of effect was seen by Scott and Huff (1996), who found that during the summer, weather stations near large lakes had warmer overnight and cooler daytime temperatures than stations farther away. This change in surface heat capacity could be a factor in the overnight temperatures near the oil sands, and could be the cause of slightly cooler daytime temperatures.

Our analysis showed that the oil sands project area has become drier compared to the surrounding area during the summer. The trend was 1.5 g kg^{-1} over the 17 years. It seems that the removal of vegetation (causing reduced transpiration) had more impact than the evaporation from the tailings ponds.

4.4.2) Precipitation and lightning

The observed precipitation data provided no evidence that the oil sands inadvertently modify seasonal precipitation amounts. Similar to precipitation, we found no evidence that lightning is modified by the oil sands development. This is in contrast to other studies that

indicated that cities and industrial developments have affected lightning strike densities. Two explanations for urban lightning enhancement have been proposed in the literature: surface convergence over the city (caused by an urban heat island and increased roughness), and increased cloud condensation nuclei caused by urban pollution (Stallins and Rose, 2008). While a heat island and air pollution are both present during the summer near the oil sands development, we find no trend in lightning. Westcott (1995) suggested that complex topography may make it more difficult to distinguish inadvertent lightning modification. The complex topography around the oil sands includes a river valley and areas of elevated terrain (more than 500 m higher than the river) so this may indeed be a possibility. Studies of enhanced lightning have primarily looked at areas which are warmer and more humid with more thunderstorms than the Fort McMurray area. It is possible that lightning enhancement would be easier at these locations with greater convective instability.

4.4.3) Conclusions and further research

The Athabasca oil sands development in northeast Alberta has disturbed more than 500 km^2 of boreal forest through surface mining and tailings ponds development. The areal extent of the tailings ponds has grown to larger than 100 km^2. There has been a significant impact on the toxic water pollution (Kelly et al., 2009), vegetative production (Latifovic et al., 2005), and air pollution (Hazewinkel et al., 2008). The focus of this paper is on the possible meteorological impact of the disturbance. A comparison was made on the time series of air temperature, humidity, and precipitation measured at weather stations in oil sands and non-oil sands locations. Furthermore we analyzed the temporal and spatial distribution of the lightning strikes over the oil sands region.

Our main finding was that the meteorological impact was most noticeable in the summertime. Daytime maximum temperature values tended to be cooler for the oil sands

disturbed area compared to the undisturbed outside region. In contrast, the overnight minimum temperatures were warmer for the oil sands location. In terms of humidity, the summer observations suggest that the oil sands disturbed region was drier compared to the undisturbed outside region. Mann-Kendall tests showed that the temporal trend in the differences in summertime temperature and water vapor mixing ratio values were statistically significant. Our analysis showed that the oil sands development had no detectable effect on daily accumulated precipitation or lightning.

It should be stressed that the results presented here were based primarily on the observations sampled at two surface weather stations: Mildred Lake, and Fort McMurray. Thus our analysis is based on the assumption that the meteorological data recorded at Mildred Lake is representative of the atmospheric conditions of the oil sands environment, while the observations at the Fort McMurray weather station are representative of the natural undisturbed environment. The validity of this key assumption likely holds for the summertime based on our intercomparison with measurements at weather stations operated by the Alberta forestry department. However, for the spring, fall, and wintertime these additional measurements were not available. Our finding about the impact on the occurrence and frequency of lightning is not limited by our assumptions about the two weather stations.

Further understanding of the possible effects of future oil sands development on the weather could be made with a numerical weather prediction model. The Athabasca oil sands project is forecast to more than double in the near future (Kelly et al., 2009). Modeling studies would allow an estimation of the sensitivity of the weather to the oil sands development. Modeling sensitivity studies may allow us to determine which factors are most important for controlling temperature, precipitation, and convection.

4.5. Acknowledgements

The authors would like to acknowledge William Burrows from Environment Canada for his suggestions for analyzing the lightning data. We also wish to thank Environment Canada for their generous permission to use Canadian Lightning Detection Network (CLDN) data and software, and for providing the climate data from Mildred Lake and Fort McMurray. We also thank Alberta Environment for supplying the data used to create the oil sands maps.

4.6. References

Burrows, W. R., and B. Kochtubajda, 2010: A decade of cloud-to-ground lightning in Canada: 1999-2008. Part 1: Flash density and occurrence. *Atmosphere-Ocean*, **48**, 3, 177-194, doi:10.3137/AO1118.2010

Changnon, Jr., S. A., R. G. Semonin, and F. A. Huff, 1976: A hypothesis for urban rainfall anomalies. *Journal of Applied Meteorology*, **15**, 544-560.

Charlton, R. B., and C. Park, 1984: Observations of industrial fog, cloud, and precipitation on very cold days. *Atmosphere-Ocean*, **22**, 1, 106-121.

De Bruijn, T. J. W., 2010: Estimated life cycle GHG and energy use for oil-sands-derived crudes versus conventional light crude using GHGenius. *Natural Resources Canada*, Canmet Energy. 38 pp.

Grant, J., J. Dagg, S. Dyer, and N. Lemphers, 2010: Northern lifeblood: Empowering northern leaders to protect the Mackenzie River basin from oil sands risks. *Pembina Institute*, Drayton Valley, Alberta, Canada. 77 pp.

Hazewinkel, R. R. O., A. P. Wolfe, S. Pla, C. Curtis, and K Hadley, 2008: Have atmospheric emissions from the Athabasca oil sands impacted lakes in northeastern Alberta, Canada? *Canadian Journal of Fisheries and Aquatic Sciences*, **65**, 1554-1567, doi:10.1139/F08.074

Kelly, E. N., J. W. Short, D. W. Schindler, P. V. Hodson, M. Ma, A. K. Kwan, and B. L. Fortin, 2009: Oil sands development contributes polycyclic aromatic compounds to the Athabasca River and its tributaries. *Proceedings of the National Academy of Sciences*, **106**, 52, 22346-22351, doi:10.1073/pnas0912050106

Latifovic, R., K. Fytas, J. Chen, and J. Paraszczak, 2005: Assessing land cover change resulting from large surface mining development. *International Journal of Applied Earth Observation and Geoinformation,* 7, 29-48, doi:10.1016/j.jag.2004.11.003

Nkemdirim, L. C., 1981: Extra urban and intra urban rainfall enhancement by a medium sized city. *Water Resources Bulletin*, **17**, 5, 753-759.

Oke, T. R., 1982: The energetic basis of the urban heat island. *Quarterly Journal of the Royal Meteorological Society*, **108**, 1-24.

Reuter, G. W., 2010: Application of the factor separation methodology to quantify the effect of waste heat, vapor and pollution on cumulus convection, in *Factor Separation in the Atmosphere: Applications and Future Prospects*, edited by P. Alpert and T. Sholokhman, pp. 163-170, Cambridge University Press, Cambridge, UK.

Rose, L. S., J. A. Stallins, and M. L. Bentley, 2008: Concurrent cloud-to-ground lightning and precipitation enhancement in the Atlanta, Georgia (United States), urban region. *Earth Interactions*, **12**, 1-30, doi:10.1175/2008EI265.1

Scott, R. W., and F. A. Huff, 1996: Impact of the great lakes on regional climate conditions. *Journal of Great Lakes Research*, **22**, 4, 845-863.

Stallins, J. A., and L. S. Rose, 2008: Urban lightning: Current research, methods, and the geographical perspective. *Geography Compass*, **2**, 3, 620-639, doi:10.1111/j.1749-8198.2008.00110.x

Steiger, S. M. and R. E. Orville, 2003: Cloud-to-ground lightning enhancement over southern Louisiana. *Geophysical Research Letters*, **30**, 19, 1975, doi:10.1029/2003GL017923

Steiger, S. M., R. E. Orville, and G. Huffines, 2002: Cloud-to-ground lightning characteristics over Houston, Texas: 1989-2000. *Journal of Geophysical Research*, **107**, D11, 4117, doi:10.1029/2001JD001142.

Westcott, N. E., 1995: Summertime cloud-to-ground lightning activity around major Midwestern urban areas. *Journal of Applied Meteorology*, **34**, 1633-1642.

Yue, S., P. Pilon, and G. Cavadias, 2002: Power of the Mann-Kendall and Spearman's rho tests for detecting monotonic trends in hydrological series. *Journal of Hydrology*, **259**, 254-271.

4.7. Tables

Season	Daytime High	Overnight Low	Precipitation	Lightning
Spring	Cooler	No Trend	No Trend	N/A
Summer	Cooler	Warmer	No Trend	No Trend
Fall	No Trend	No Trend	No Trend	N/A
Winter	No Trend	Warmer	No Trend	N/A

Table 4.1: Summary of the impact of oil sands development on temperature, precipitation, and lightning. This is a comparison of the Mildred Lake weather station with the Fort McMurray weather station, where warmer means Mildred Lake is becoming significantly warmer than Fort McMurray at the 95 % confidence interval (Mann-Kendall statistical test).

4.8. Figures

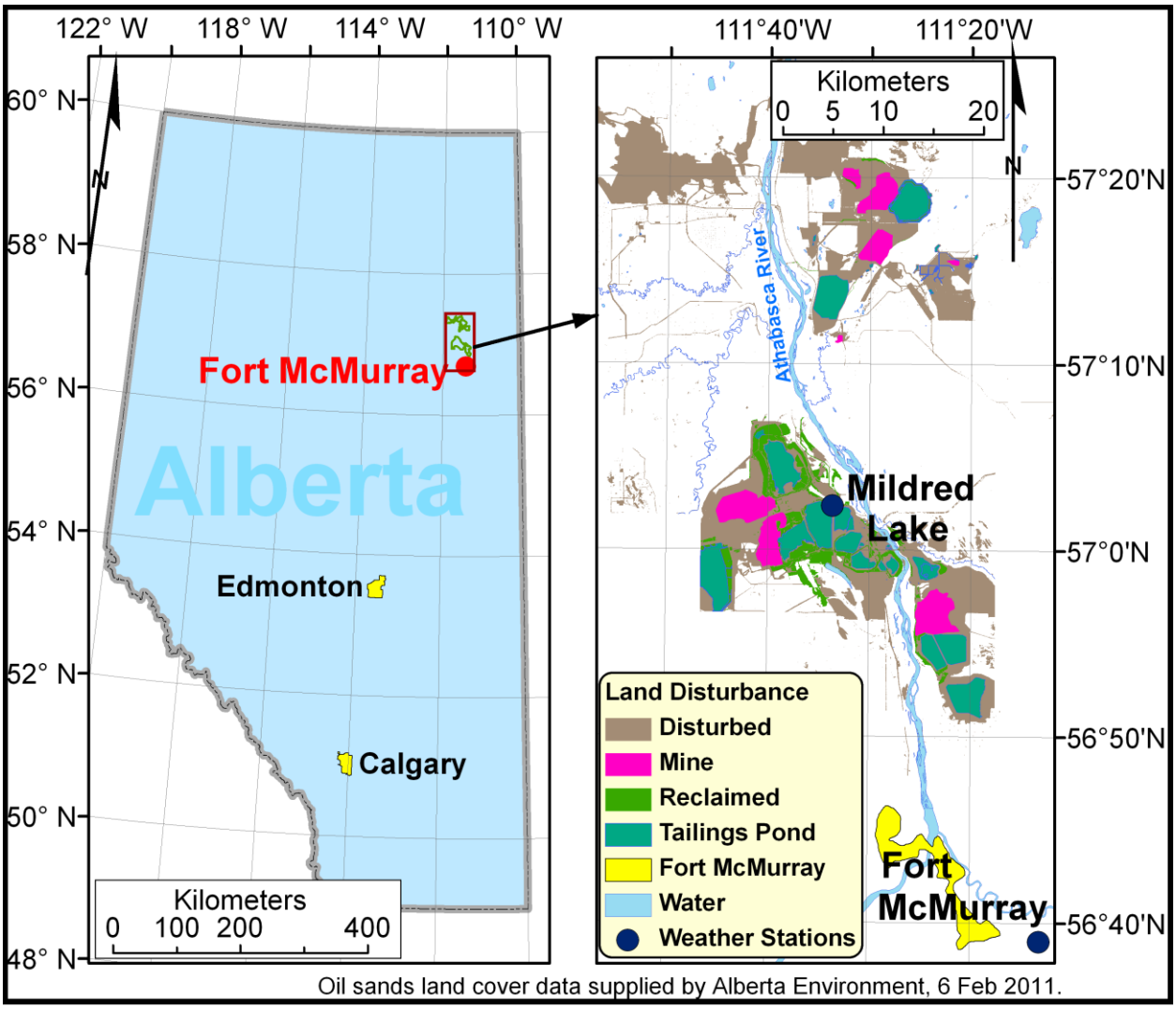

Figure 4.1: Map of the oil sands development near Fort McMurray, Alberta. The type of development is coloured according to the legend, and relevant weather stations are also located on the map.

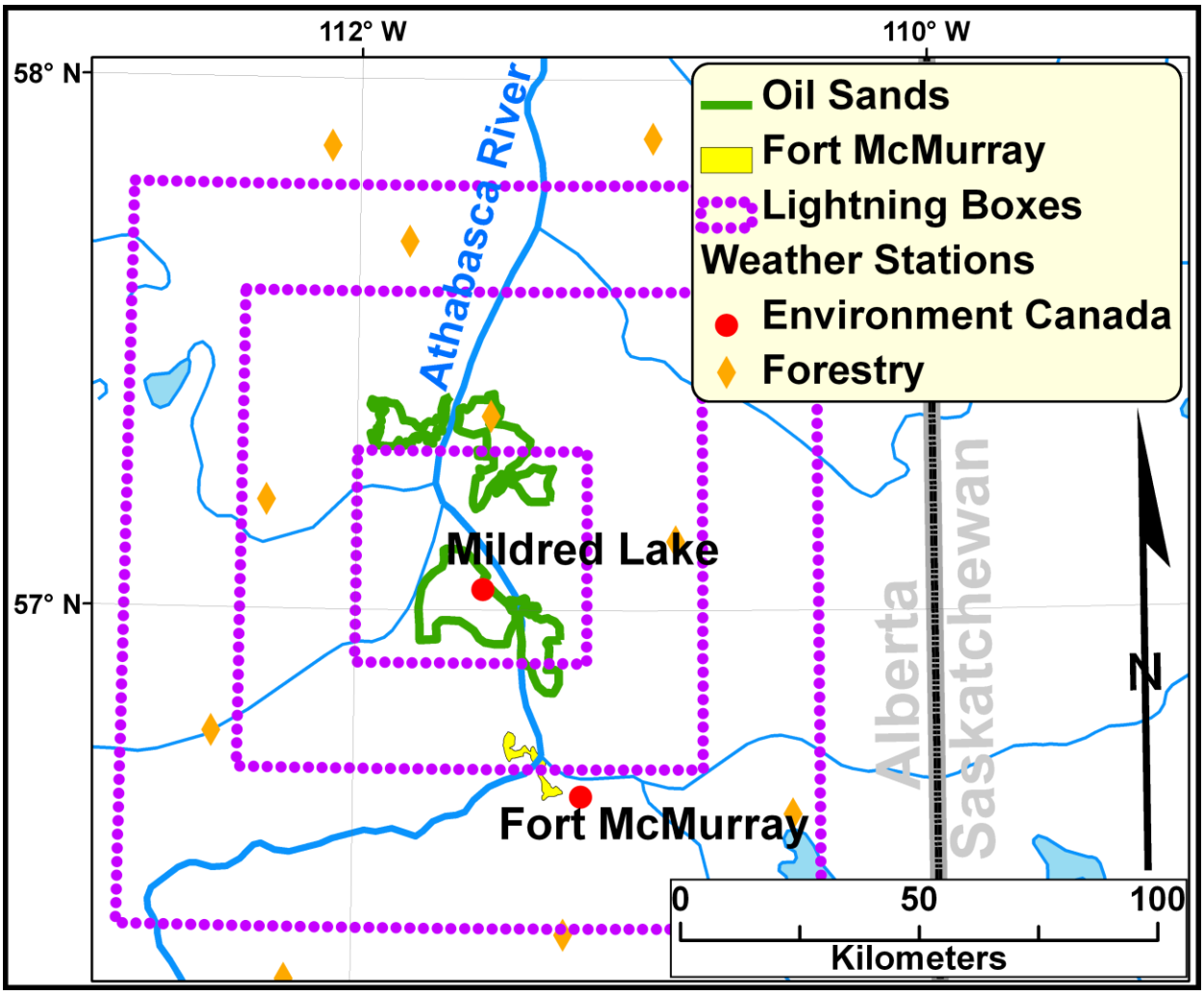

Figure 4.2: Lightning analysis boxes. The smallest lightning box was designed to approximately include the area of the oil sands disturbance (about 2500 km^2). The two larger boxes are approximately 10000 km^2 and 22500 km^2.

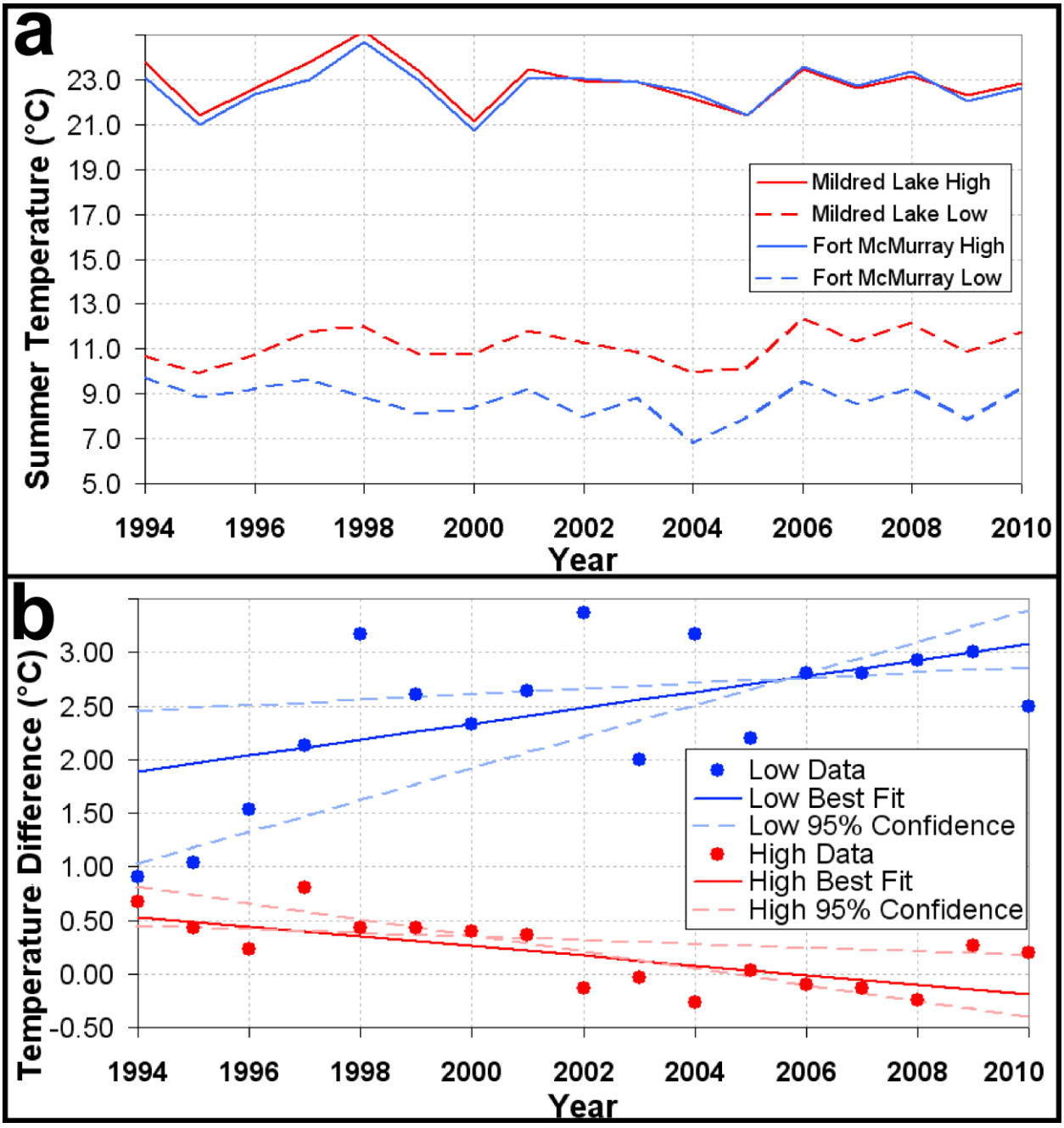

Figure 4.3: Summer temperatures at Mildred Lake and Fort McMurray. a) The average high and low temperatures by year. b) The difference between Mildred Lake and Fort McMurray for the average high and low temperatures, including the linear trend and 95 % confidence intervals.

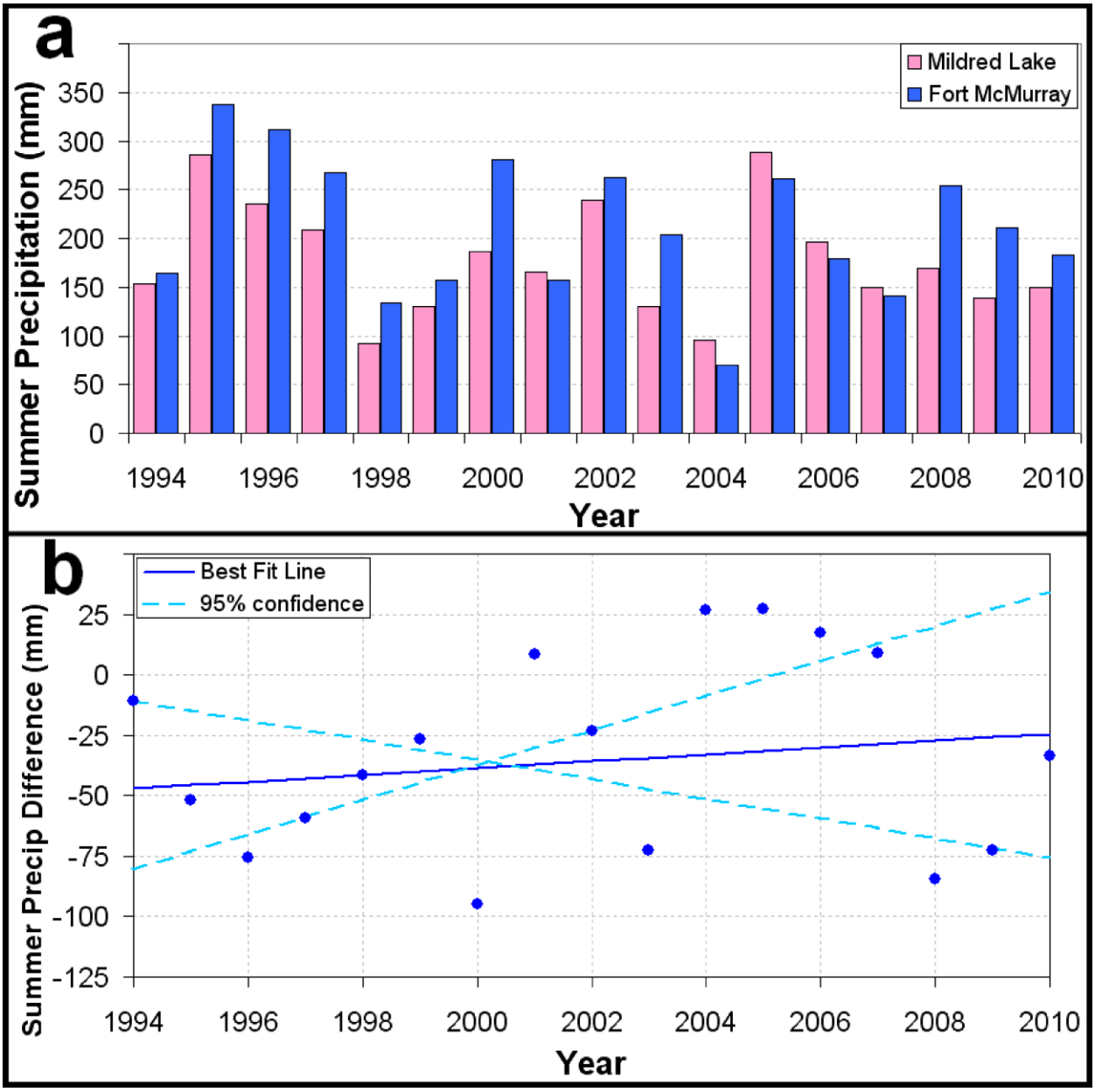

Figure 4.4: Summer precipitation at Mildred Lake and Fort McMurray. a) The total precipitation by year. b) The difference in precipitation between Mildred Lake and Fort McMurray, including the linear trend and 95 % confidence intervals.

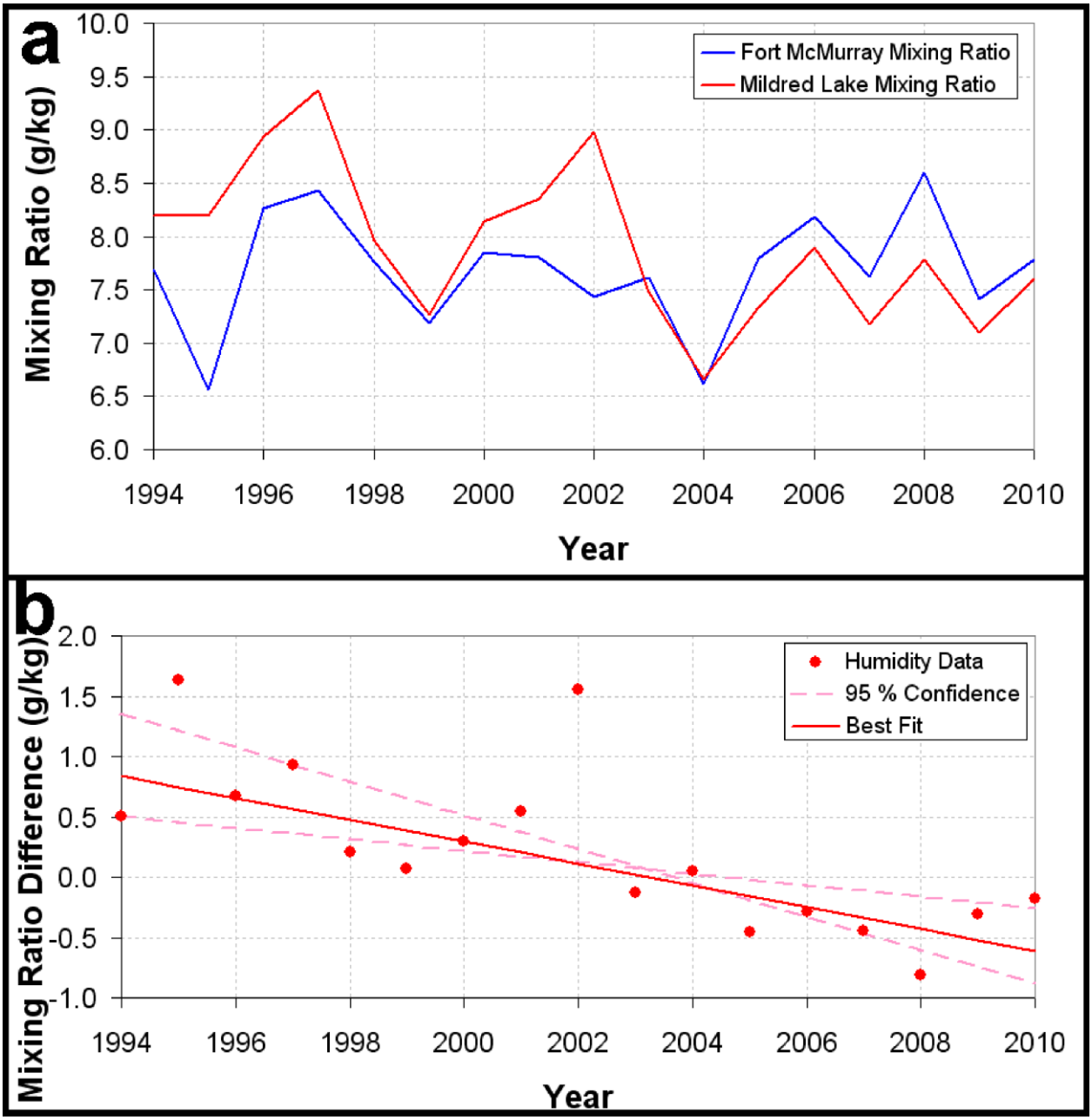

Figure 4.5: Summer humidity at Mildred Lake and Fort McMurray. A) The average water vapor mixing ratio by year. B) The water vapor mixing ratio difference between Mildred Lake and Fort McMurray including the linear trend and 95 % confidence intervals.

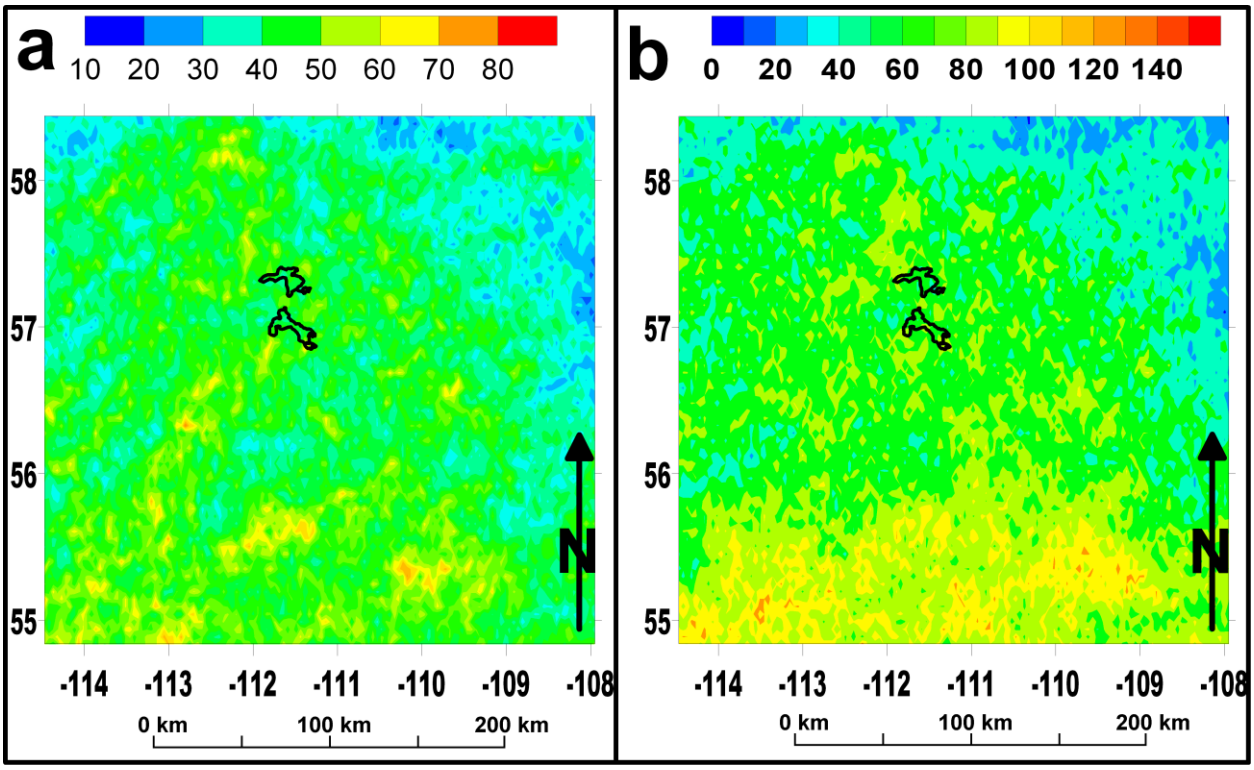

Figure 4.6: a) Summer cloud-to-ground lightning strike density (strikes per 10 km^2) in northeast Alberta from 1999 to 2010. b) Cloud-to-ground lightning days. The main disturbance due to the Athabasca oil sands is located at -111.5° and 57.0°, and is outlined in black.

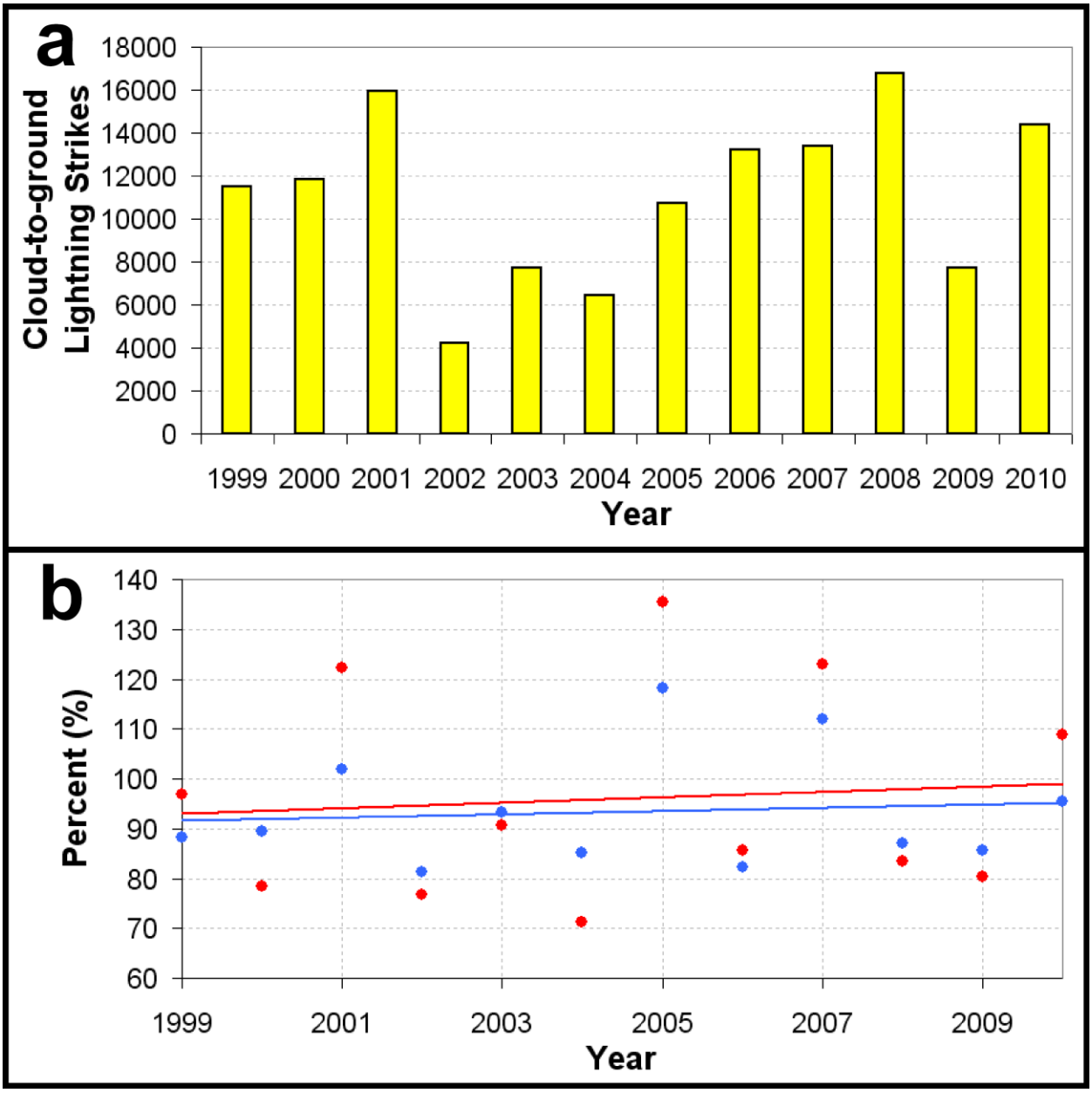

Figure 4.7: Summer lightning trends near the oil sands from 1999 to 2010. a) The number of lightning strikes each year in the biggest box (defined in Figure 2). b) Blue lines are the ratio (percentage) of the lightning density in the innermost area to that in the middle ring. The bottom panel is the ratio of the lightning density in the innermost area to that in the outer ring. The areas and rings are defined in Figure 2.

5. WRF model simulations of the influence of the Athabasca oil sands development on convective storms

Daniel Brown and Gerhard Reuter

A version of this chapter has been submitted for review to Earth Interactions.

Abstract

The Athabasca oil sands development has created a surface disturbance of almost 900 km^2 in northeastern Alberta. The main meteorological impact of the oil sands development is that of releasing waste heat and lowering the surface humidity due to the removal of boreal forest vegetation. The Weather Research and Forecasting (WRF) model was used to simulate the effects of the oil sands on thunderstorm intensity, initiation time, and duration on ten case study days. The results show that the oil sands development did not cause substantial increases in thunderstorm intensity on all case study days. However, including the oil sands development in the simulations caused thunderstorm initiation time to be a few hours earlier on two of the case study days. Furthermore, the duration of the thunderstorms was increased. On both of these case study days, the model simulation most closely matches reality only if the simulation includes the oil sands. Data from the model simulations along with data from commercial aircraft show that if the 850-500 mb temperature difference was greater than 30 °C, then the oil sands development seemed to have a greater effect on thunderstorm initiation time and duration. A large 850-500 mb temperature difference occurs in extremely unstable environments. These days were rare enough that they did not appear to affect the thunderstorm climatology.

5.1. Introduction

The Athabasca oil sands development is a large oil mining and upgrading operation in northeastern Alberta, located in the boreal forest just north of Fort McMurray. A mixture of bitumen and sand is mined from just beneath the surface. Then the bitumen is extracted from the sand mixture and is upgraded into synthetic crude oil; a process which causes a large environmental disturbance and uses enormous amounts of energy (Kelly et al. 2009). Figure 5.1 (left and centre) shows the surface disturbance of the oil sands development in 2007, when the surface disturbance was about 530 km^2. The Government of Alberta (2016) reports that the disturbed area increased to 895 km^2 in 2013, 88 km^2 of which consisted of tailings ponds.

The province of Alberta is prone to thunderstorms, and many regions in Alberta have experienced significant damages due to severe thunderstorms (Smith et al. 1998). However, most thunderstorm research in Alberta is focused in the Rocky Mountain foothills and the populated Edmonton-Calgary corridor (Taylor et al. 2011). But, thunderstorms can occur in other areas of the province; the sparse observation network and low population often makes thunderstorms more difficult to detect (Cheng et al. 2013). For example, baseball sized hail from a severe thunderstorm caused $15 million in damage to Fort McMurray, Alberta (Crewe 2008).

Some research has shown that oil refineries can influence convection. For example, Guan and Reuter (1995) found that cooling towers from oil refineries could cause enhanced rainshowers from cumulus clouds. Further research by Guan and Reuter (1996) suggested that sensible heat emissions were the dominant factor, but the combined effect of cloud condensation nuclei and sensible heat also needed to be considered. However, Steiger and Orville (2003) found that enhanced lightning near oil refineries near Lake Charles, Louisiana, caused enhanced lightning mainly due to cloud condensation nuclei emissions alone. They concluded that the heat island

was not a significant factor. In fact, Brown et al. (2011) found that the oil sands development did not affect climatological cloud-to-ground lightning. These contradictory results suggest that more research is needed to fully understand how industry can affect convection and thunderstorms.

Many researchers have found that urban areas can enhance convection and increase rainfall. For example, Changnon et al. (1976) documented enhanced rainfall, thunderstorms, and hail downwind of St. Louis, Missouri. Westcott (1995) found that city centres caused enhanced cloud-to-ground lightning. Ashley et al. (2002) confirmed that enhanced precipitation was the cause by documenting the same effect with radar reflectivity. Niyogi et al. (2011) showed that thunderstorm radar signatures were modified over the city of Indianapolis, Indiana. Niyogi et al. (2006) used a numerical model to remove Oklahoma City, Oklahoma. They found that the structure of a mesoscale convective system was significantly affected by the city. However, not all research shows that cities cause thunderstorm or precipitation enhancement. For example, Nkemdirim (1981) could not find evidence that Calgary, Alberta enhances precipitation. Numerical simulations by Schmid and Niyogi (2013) showed that in some cases cities caused lower precipitation. Researchers often suggest three possibilities for urban rainfall or thunderstorm enhancement: the urban heat island, an increase in surface roughness, and emissions of cloud condensation nuclei (Changnon et al. 1976, Steiger et al. 2002).

Heat islands have been studied extensively for many years. Oke (1973) documented strong heat islands in many small and large mid-latitude cities in North America. Heat islands and waste heat emissions have been suspected to enhance thunderstorms. Bornstein and Lin (2000) found that an urban heat island was responsible for enhanced precipitation in Atlanta, Georgia. Guan and Reuter (1996) found that heat output from an oil refinery was the dominant cause of rainshower enhancement. Baik et al. (2007) suggested that an urban heat island affects thunderstorms by causing enhanced surface convergence. They also suggested that the urban

heat island circulation can be strongest in the mid-afternoon, when the rural-urban surface temperature difference is weakest. Brown et al. (2011) found that a heat island caused by the oil sands development is strengthening as the development increases in size. Lower vegetation coverage in urban areas can cause an "urban dry island" (Schmid and Niyogi 2013). Rozoff et al. (2003) found that lower evapotranspiration caused lower humidity and less instability in city centres. Brown et al. (2011) found that the oil sands development is causing an increasingly strong dry island as the development increases in size.

Much less research has discussed the effect of surface roughness. Rozoff et al. (2003) found that higher surface roughness in the city centre slightly increased moisture convergence and slightly reduced the urban heat island effect. Overall, its contribution to thunderstorm enhancement was small. The surface roughness of the oil sands development is not known. The roughness might be less because the surrounding forests have been cleared to barren land and tailings ponds. However concentrations of upgrading facilities and open pit mines might cause higher roughness.

Cloud condensation nuclei have been suggested as a cause for precipitation enhancement (Changnon et al. 1976, Steiger and Orville 2003). Many researchers have investigated the effect of cloud condensation nuclei; however, most of the results have either been inconclusive or do not agree with other studies. For example, Steiger and Orville (2003) concluded that the prevailing reason for lightning enhancement was emissions of cloud condensation nuclei, but Reuter and Guan (1995) found that the effect was small. The effect of cloud condensation nuclei appears to be complex (Dixon and Mote 2003). Zhong et al. (2015) found that cloud condensation nuclei reduced precipitation at the city centre and enhanced it downwind. The oil sands development emits large amounts of sulphur dioxide and nitrogen oxides into the atmosphere (Hazewinkel et al. 2008). Howell et al. (2014) found that emissions from the bitumen upgrading facilities in the oil

sands development do not release much cloud condensation nuclei, but as the plume of emissions ages, a substantial amount of cloud condensation nuclei form.

In this study, we investigate how the oil sands development can affect thunderstorms. The oil sands development has a massive land disturbance and emits large quantities of waste heat (Kelly et al. 2009). The Weather Research and Forecasting (WRF) numerical weather prediction model is used to assess the relative contributions of the land cover modifications and the waste heat separately and together using Stein and Alpert's (1993) method of factor separation on a number of case study days. The effect of cloud condensation nuclei is outside the scope of this research, and will not be further assessed in this paper. Not enough is known about the emissions of cloud condensation nuclei from the oil sands development, and the process is too complex to be assessed in conjunction with the rest of this study. We do not expect to find any drastic modification of thunderstorms caused by the oil sands development because Brown et al. (2011) did not find any climatological lightning enhancement. However, we think that it may be possible to find certain cases where the heat island caused by the oil sands could serve as a trigger for thunderstorm initiation if the atmosphere was unstable with a weak capping inversion.

5.2. Experimental design and hypothesis

5.2.1) The Weather Research and Forecasting (WRF) model

We used the Weather Research and Forecasting (WRF) model to carry out sensitivity experiments near the oil sands development. Pennelly and Reuter (2017) found that the WRF model is suited to forecast daily weather conditions for Alberta and could simulate heavy precipitation events (Pennelly et al. 2014). The WRF model is a non-hydrostatic regional numerical weather prediction model (Shamarock et al. 2008). Three nested domains were

centred on the oil sands development (Figure 5.2), and the North American Regional Reanalysis (NARR) (NCEP/NWS/NOAA, 2005) data were used for our initial and boundary conditions. On each day, the simulation started at 0600 UTC (midnight local), and ran for 36 hours, which allowed for about 12 hours of spin-up and captured all of the storms until they dissipated the next evening.

The physics scheme configurations are listed in Table 5.1. The purpose of this paper is not to evaluate the merits of different physics schemes; thus, some of the schemes were chosen simply because they were the defaults, or they worked well with the other chosen defaults. Probably the most important choice was the convective scheme. The Grell-Freitas scheme was chosen because it is designed to adjust its parameterization strategy for different scales, and it is valid at some of the smaller scales that we use in our simulations (Grell and Freitas 2014). We did not use a convective scheme in our smallest domain because the grid spacing was 2 km; lower than what is needed for a convective scheme. The Noah land surface model was used because it is the most advanced land surface model included in WRF. The Noah land surface model includes sophisticated representations of soil-vegetation-atmosphere interactions and urban or barren ground physics (Chen and Dudhia 2001). The high-resolution convective simulations require a precipitation microphysics scheme that includes snow and graupel, thus the Lin et al. (1983) microphysics scheme was used. The default rapid radiative transfer model was used to parameterize the shortwave and longwave radiation. The default MM5 surface layer scheme, and the default Yonsei University planetary boundary layer scheme were also used.

5.2.2) WRF land cover and waste heat emissions

The land cover of the oil sands development was not classified adequately in the WRF database, and the data is too old to include the rapid land cover changes that have occurred in the

oil sands development in the past 10 years. We changed the land surface in WRF by creating a new "oil sands" land surface type. The WRF model framework allows us to modify the properties of this land surface type in a simple text file. The "oil sands" land surface type was given the same land surface parameters as the 'Barren' land surface category included in WRF. We wrote a new module for the WRF model that allowed us to specify our waste heat amount in W m^{-2} in a configuration file and add it to the lowest eta level of the atmosphere (about 50 m thick). A constant 100 W m^{-2} was added to one tenth of the oil sands area (The blue area in Figure 5.1 - right), equivalent to an average of 10 W m^{-2} over the entire area (discussed further below). Even though the oil sands development was rapidly increasing in size during our case study days, the waste heat value was kept the same because we are not studying the temporal changes in thunderstorm modification. The objective is to compare different, but arbitrary days using the current oil sands development characteristics.

Since data on the waste heat emissions from the oil sands facilities were unavailable, we made an estimate using the following method. Using De Bruijn`s (2010) estimate of 1 GJ of energy for producing one barrel of oil, Brown et al. (2011) calculated that the total waste heat flux from the oil sands development to be about 3 W m^{-2}. The assumptions for this estimate were that the waste heat released into the atmosphere was 10% of the production energy and that it was spread over the entire area. New developments have caused the disturbed area and the total energy to increase significantly in recent years, thus we decided to use an average of 10 W m^{-2} in our simulations. However, there could be a large amount of error on this estimate.

It does not appear realistic to distribute the emitted energy over the entire area of the oil sands development. Satellite images and map data suggest that only a small percentage of the disturbed area is covered with upgrading and refining equipment, thus in our simulations we applied 100 W m^{-2} of waste heat to 10 percent of the area. This sensible heating area is much

larger and much less concentrated than Guan and Reuter (1995), but we believe it more accurately represents the actual conditions. In reality, the upgrading facilities are in a number of different clumps in the oil sands development. For our sensitivity experiments we felt it was more instructive just to make one idealized clump. We changed an area of 650 km^2 in the WRF model into our oil sands land use type. Rather than trying to replicate the footprint of the oil sands development exactly, we instead modified one large circular area. The additional waste heat was added into a smaller area of 65 km^2 in the centre of the large land disturbance area.

5.2.3) Case study days and method of analysis

Since Brown et al. (2011) showed little impact on climatological lightning, we expected it to be difficult to find suitable case study days that could show thunderstorm enhancement. We used weather radar (from Environment and Climate Change Canada 2016), weather stations and upper air data to find days when thunderstorms occurred in the oil sands area. However, radar and surface data were used to exclude days when a synoptic scale trigger, like a cold front triggered thunderstorms. These restrictions ensured that the thunderstorms were mainly caused by daytime heating. We restricted our days to when one of the two nearest soundings indicated moderate Convective Available Potential Energy (CAPE), and some, but not too much Convective Inhibition (CIN). However, the nearest soundings are still 300 km away. Weather radar was an invaluable tool for confirming convection, thus we limited our analysis to days when historical radar data is available from Environment Canada's external website (2007-2014). We tried to find days where the storm radar reflectivities were at least 40 dBZ. We also checked precipitation measurements from nearby weather stations for evidence of precipitation. A lack of recorded precipitation at a weather station did not necessarily exclude a day because the sparse precipitation network may not lie within the track of a storm. Using a combination of soundings, weather radar, and precipitation measurements, we were able to narrow our choice of days to

those suitable for thunderstorm enhancement. We settled on 10 case study days: 14 July 2007, 29 July 2007, 08 August 2009, 29 July 2010, 30 July 2010, 14 August 2011, 30 June 2013, 23 July 2014, 29 July 2014, and 6 August 2014.

In this paper we will use the Stein and Alpert (1993) method of factor separation to quantify the differences in the pure and the combined effects between our numerical simulations. Factor separation requires that all factors, and all factor combinations be considered. Thus, on each day we had four numerical experiments (Figure 5.1, right): one with no heat or land cover changes (Case-0), one with heat added to the atmosphere (Case-H), one with the land cover changed to barren (Case-B), and one with both (Case-HB). It is necessary to have a simulation with neither of the factors activated, and one with both of the factors activated because the combined effect of both factors may not equal the sum of the individual factors. The simulation with both factors activated (the "control") is the most important because it should represent the actual geographical and meteorological conditions at the oil sands development.

5.2.4) Difficulties modelling thunderstorms

Thunderstorms and convection are highly non-linear processes that are some of the most difficult meteorological phenomena to simulate using even the most sophisticated numerical models. The non-linear synergistic interactions of weather systems typically increase with a smaller grid spacing, and small perturbations quickly amplify in moist convection (Hohenegger and Schär 2007). However, Elmore et al. (2002) found a few cases where large perturbations seemed to have little effect on thunderstorm development. Numerical model simulations of convective initiation continue to improve, but even the most sophisticated now-casting systems in data-rich areas continue to struggle with convective initiation (Sun et al. 2014). Although numerical simulations in the 1-4 km range can forecast convection explicitly (without parameterization), they

still struggle with convective precipitation amount and distribution (Bryan et al. 2003). Weisman et al. (2008) found both success and failure using WRF to explicitly simulate convection on a 4 km grid in the United States Midwest.

Much of the recent research on numerical simulations of convection has the luxury of dense observation, upper air, and radar networks to create accurate initialization analyses (Sun et al. 2014). In fact, Xue et al. (2013) showed that ingesting radar data was required to simulate the convective precipitation accurately. Even with a dense observation network, storms investigated by Rozoff et al. (2003) still occurred 2 hours earlier than their simulated storms. Real data is scarce near the Fort McMurray oil sands development. Because thunderstorms are difficult to model, we will not be concerned with the exact agreement of the modelled thunderstorms with reality. Instead, we will consider it "good enough" if the initiation time is close (within a few hours), the storm motion is close (within 45 degrees), and the storm intensities are close. On all days there were both real and simulated storms with greater than 40 dBZ; however, the exact locations and timing was not necessarily the same. Before we present our results in the next section we will attempt to ensure that each of our "control" simulations somewhat match the observed convection from the radar and precipitation measurements.

5.3. Numerical simulation results

5.3.1) Agreement with observations

To examine the simulated release of waste heat and convection, we analyzed vertical sections of temperature and water vapor mixing ratio for all case study days. The cross sections were on a latitude line approximately through the centre of the oil sands development. To catch the strongest modifications of temperature and mixing ratio, we had to vary the actual latitude

somewhat depending on the wind direction, but it was usually between 57.0 and 57.1 degrees north. The cross section for 29 July 2010 (Figure 5.3) is shown. The two panels on the far left show the temperature (top), and water vapour mixing ratio (bottom) from the Boreal forest case (Case 0). The three panels on the right show the difference between each of the three modified cases (Case H, B, and HB) and the natural boreal forest case (Case 0) at 1815 UTC. When the land cover is changed to barren (middle-left panels), heat is input into the atmosphere by changing the land surface from boreal forest to barren. Barren ground has a much lower Bowen ratio and thus converts more solar radiation into sensible heat rather than latent heat, which also causes the mixing ratio to be much lower. When we added waste heat directly to the atmosphere (middle-right panels), a concentrated heat plume formed, but the mixing ratio was essentially the same. When both factors are activated (far right panels), the resulting temperature field is approximately the sum of the temperature or mixing ratio field produced by each individual factor. All case study days showed similar results with minor variations.

In all cases, the warming effect of the land cover change was substantially larger than that of the added waste heat. While the sensible waste heat emissions did not change on the water vapour mixing ratio, the land cover modification significantly reduced the mixing ratio values. On all case study days, the total heat island effect was about 1°C, while the total dry island effect was about 2 g kg^{-1}. The plume of warm dry air caused by the heat and dry island mixed up above the 800 mb level in most cases. At the top of the plume there was always relatively cooler and moister air, caused by the higher reaching updraft and possibly cloud formation. Thus we are confident that enhanced lift possibly causing cloud formation is being caused by the simulated oil sands development. If we add much more heat (about 5 times more), the effect of the waste heat becomes equal or greater than that of the land cover. The modelled heat and dry island strength appear to be consistent with the results and predictions of Brown et al. (2011).

However, the mechanisms influencing convection are complex. The sum of the modification of land cover and emissions of waste heat create a significant heat island and plume that could add energy to or trigger thunderstorms. However, the presence of the dry island due to the removal of vegetation causes significant drying that would reduce energy for thunderstorms. Thus, the effect on thunderstorms depends strongly on whether the thunderstorm enhancement mechanism is: increased instability due to the warmer conditions, decreased instability due to the drier conditions, or a trigger due to the heat island. Brimelow et al. (2011) found that the size of a drought-induced vegetative disturbance should be greater than 18000 km^2 to affect instability enough to modify thunderstorms. However, Knowles (1993) found that forest fire burn areas (which are significantly higher impact than drought) at 400 km^2 could create convective circulations that could trigger thunderstorms. Pielke and Uliasz (1993) showed that larger disturbance sizes had a greater impact on the vertical velocity. Thus, at just under 1000 km^2, the oil sands may be more suited to triggering thunderstorms rather than causing widespread instability modification.

We further examined the convection produced by the model by comparing model simulated radar images with both actual radar images and precipitation measurements. Our analysis is still hampered by data sparsity. In the Fort McMurray area there are few rainfall measurements and the nearest weather radar is far away. This causes the radar to only detect the top half of the storms. The sparsity of the data affects our comparison with the model and the amount of data used in model initialization.

Table 5.2 compares the initiation time of the simulation with no oil sands development (Case-0) to that of the real radar data. We defined the initiation time from the real radar as when convective cells in the general vicinity of the oil sands development had a reflectivity greater than about 40 dBZ (a thunderstorm), and we want to see whether the actual initiation time is similar to

the modelled initiation time. Data from both the innermost domain and the middle domain was used. We also compared the storm motion between the real radar and the simulated radar. Again, we want to stress that our focus is on the general convective characteristics rather than the exact location of the storms, because it is very difficult (if not impossible) to accurately simulate exact observed storm locations using a numerical model many hours in advance.

The results of Table 5.2 show that on six case study days, the difference in time between model initiation and reality (from radar) was less than an hour. On most of these cases, the model forecasted the convection slightly earlier than it actually occurred. However, on the other four case study days, the model initiated convection four or more hours later than reality. These four days needed further investigation. As we will see in the next section, the initiation time results from three of these four days were improved by adding the fluxes from the oil sands development. On all days, the motion of the real storms was very similar to the modelled storms (Table 5.2); the minor variations are likely due to misinterpretations of right-moving multi-cell or supercell storms. We feel that the model performed as adequately as it could on all of these case study days. However, the model does not, and is not expected to perform well enough to reproduce the specific storm tracks. The fact that it initiated reasonable convection, and generally forecasted the track well is impressive in itself given the sparse initialization data.

5.3.2) Summary of all case study days

Table 5.3 shows the results of the effect of the oil sands development on thunderstorm intensity. Three variables were examined: the maximum simulated radar reflectivity, the average total condensate in the atmosphere, and the average total surface rainfall. The maximum simulated radar reflectivity was used as a proxy for the maximum storm strength. However average values likely better summarize the total impact on the oil sands development, thus we

used the average total condensate and average surface accumulated rainfall. All of the columns in Table 5.3 are the result of factor separation. For example, on 29 July 2010, the maximum reflectivity in Case 0 was 49.5 dBZ. The value for Case B was 2.3 dBZ less than the value for Case 0, and the value for Case H was 0.5 dBZ less than the value for Case 0. However, the value for Case HB was 0.5 greater than the sum of Case 0, Case B, and Case H.

The maximum simulated radar reflectivity was the maximum value at any time of the day at any grid cell in domain 3. The results of the maximum reflectivity are inconclusive. Some days had slightly higher values (29 July 2014) when the oil sands development was activated, while other days had slightly lower values (29 July 2010). Most often, the HB simulation was less than the sum of both the H and B simulations. The largest reduction was 2.3 dBZ, and the largest increase was 1.8 dBZ. These changes are very small, almost inconsequential, and there is no trend in either direction. Thus, we cannot find any discernable impact on the maximum simulated radar reflectivity.

The average condensate was calculated as the average of the total condensate in domain 3 (rain, snow, hail, cloud water, cloud ice) over the entire three dimensional domain, and over the total time of the simulation. Again, the results are inconclusive. When the oil sands development was activated, some days had slightly higher values of total condensate (30 July 2014). However, other days had lower values (14 July 2007). The HB simulation was sometimes positive and sometimes negative. Again, all changes were small and the oil sands development does not appear to have any discernable impact on the total condensate.

The total average rainfall was the total accumulated rainfall for the day averaged over all grid cells in domain 3. There was a large variability because some days had short-lived fast-moving storms over a small area (resulting in very low average rainfall), whereas other days had

long-lived slower moving storms and multiple rounds of back-building storms (with a larger average rainfall). Again, the results were inconclusive. On some days the oil sands simulations had slightly higher values (30 July 2007), while on other days there were slightly lower values (14 July 2007). However, the differences were only a few mm. The oil sands development did not appear to cause any discernable impact on the average total rainfall measurements.

Overall, the oil sands development does not affect the intensity of thunderstorms. We could not find any impact on the maximum radar reflectivity, the average total condensate, or the average accumulated rainfall. The oil sands development is likely too small to cause widespread changes to the convective instability.

In contrast to the results on thunderstorm intensity, there were some large differences in the thunderstorm initiation time and duration. Thunderstorm initiation and duration are related. The initiation is mostly affected by triggering, but the duration shows the total impact of the thunderstorm (for example, a storm that lasts twice as long could produce double the precipitation). Table 5.4 shows the initiation time and storm duration for the four sensitivity simulations on each case study day. Here we considered the initiation time of the storm to be when the maximum reflectivity in the innermost domain was greater than 20 dBZ. In 8 of the case study days, thunderstorm initiation and duration was not affected by the oil sands development. However, two of the case study days experienced large changes in the initiation time and duration. When the oil sands were activated, thunderstorms on 29 July 2010 were initiated 2 hours earlier, while thunderstorms on 29 July 2014 were initiated 1 hour earlier. It appears that the oil sands development has some influence on thunderstorm triggering. We will explore these two days in greater detail and suggest why these two days had such a greater impact on thunderstorms in the next two sections.

5.3.3) Most interesting case study days

The two most interesting days in the analysis were 29 July 2010 and 29 July 2014. The conditions on these two days seemed particularly sensitive to land cover modifications and industrial waste heat emissions. We will explore these two days in greater detail in this section, which will include a detailed analysis of the initiation time, duration, and storm motion. The reasons for the thunderstorm sensitivity to the oil sands development will be examined in the next sub-section.

On 29 July 2010, radar from the Cold Lake weather radar (Figure 5.4, left panels) showed a thunderstorm develop directly over the oil sands development at about 1830 UTC. This thunderstorm passed directly over the automated weather station at the Fort McMurray airport about an hour later. The radar echoes were 50-55 dBZ, and the storms dropped about 20 mm of heavy rain with a visibility as low as 400 m when it passed over the airport weather station between 1949 and 2024 UTC. As the storm continued to the southeast, it slowly weakened and eventually dissipated. Other isolated thunderstorms were observed on the radar images after the first storm, but none of them were triggered over the oil sands development.

The development of the storm simulated by the WRF model is shown in Figures 5.5 and 5.6. Figure 5.5 (left) shows the simulated column maximum radar reflectivity for the four simulations at 2145 UTC on 29 July 2010; about the time when the simulated storms initiated. We used Stein and Alpert's (1993) method of factor separation to further quantify the results (Table 5.5). Figure 5.6 (top) shows a time-series of the maximum simulated radar reflectivity from all grid cells within the innermost domain. When the land cover is the natural boreal forest and no waste heat is added, thunderstorms were initiated at 2315 UTC. However, when we added the waste heat, a small short-lived storm was initiated 1.5 hours earlier. When we changed the land use to

barren, the storm was also initiated 1.5 hours earlier, but it was a little stronger and lasted longer. The land cover modification had a greater effect than the addition of waste heat in this case. The simulated thunderstorms are initiated earliest when both factors are activated, a full 2 hours earlier than the case with no factors activated. In this case, turning on both factors at the same time had a weaker effect than the sum of each factor by itself. These numbers are an improvement on the no oil sands case, but they are still later than the actual radar observations. The earliest simulated storm developed at 2115 UTC; a full 2.8 hours later than the observed storm. We used the most realistic amount of waste heat that we could come up with in the results that we present. In other experiments (not shown), the simulated storm developed much closer to the observed time if much more heat is added, which suggests that this particular case is very sensitive to the heat island input.

The other case study day when the initiation time seemed sensitive to the oil sands development was 29 July 2014. Some images from the Cold Lake weather radar for this day are shown in Figure 5.4 (right side). Thunderstorms developed close to, but not immediately over the oil sands development. However, it is difficult to pinpoint the exact location of initiation because the initial development stages of the thunderstorm would occur below the level that the radar could detect. Three separate thunderstorms developed. The first storm formed at 1910 UTC about 40 km south of Fort McMurray. Some weak thunderstorms formed about 90 km to the east of Fort McMurray around 2030 UTC. A very weak shower formed about 10 km east of Fort McMurray at 0030 UTC, and some thunderstorms formed about 40 km east of Fort McMurray at about 0100 UTC. All storms moved slowly to the southeast, and none appeared to form directly over the oil sands development based on radar data.

The simulations of 29 July 2014 are shown alongside the simulations for 29 July 2010 in Figures 5.5 and 5.6. Figure 5.5 (right) shows the simulated column maximum radar reflectivity for

the four simulations at 2315 UTC on 29 July 2014, and Figure 5.6 (bottom) shows a time-series of the maximum simulated radar reflectivity from all grid cells within the innermost domain. The difference between the simulations with the oil sands development and those without is very apparent. The simulations with the barren land cover initiated storms about 1 hour earlier. In fact, the storms that were initiated earlier would not exist if the oil sands development was not present. Interestingly, the new storms only formed when the land cover was changed to barren. The simulation with the waste heat added was very close to the simulation with no oil sands development. The factor separation of the initiation time and duration did not show any difference between the sum of the individual factor simulations and the simulation with both factors activated at the same time. The effect of the oil sands development on this case study day was less than that on 29 July 2010. The earliest simulated storm was at 21:45, which was still 2.6 hours later than the observed 19:10 initiation on the radar. Similar to 29 July 2010, other experiments (not shown) where we added much more waste heat moved the initiation time much closer to the observed initiation time on the radar. However, we could not justify adding that much heat based on the information that we were able to obtain about the oil sands development.

We would like to briefly discuss the results of 06 August 2014. The analysis did not show anything particularly unusual about this day. However, some of the simulations where we added a much higher than realistic heat flux (not shown) caused a thunderstorm to initiate over the oil sands over an hour earlier. In our results with the realistic heat flux, we do see an area with a reflectivity of less than 20 dBZ form over an hour earlier only with the oil sands activated, but it was dismissed as a weak cumulus cloud. These results suggest that 06 August 2014 was partially susceptible to thunderstorm modification. Thunderstorms were not affected at all by the unrealistic increased heat flux on any of the other seven case study days.

On four case study days, the initiation time from the numerical model did not agree with what was observed on radar. In all four case study days, the model initiated thunderstorms too late by more than 4 hours. However, three of those four days seemed sensitive to boundary layer triggering, and adding heat fluxes associated with the oil sands development triggered convective clouds or thunderstorms significantly earlier, and much closer to the observed initiation time. 29 July 2007 was the only day that was simulated poorly for which we do not have an explanation, which also happened to be the day with the baseball-sized hailstorm that caused $15 million in insured damages (Crewe 2008).

5.3.4) Analysis of aircraft measurements

A natural question arising from our results is why do some case study days seem to be affected by the oil sands development, while the remainder are not? We computed the difference in thunderstorm *duration* between the simulation with zero factors activated and the simulation with both factors activated, which we used to represent the magnitude of the oil sands effect on thunderstorm duration. Thunderstorm duration was used rather than initiation time because it better describes the total impact of the thunderstorm, but the results would be similar either way. We calculated the temperature difference between 850 mb and 500 mb (also known as the *vertical totals index*) from commercial aircraft measurements at the Fort McMurray airport, and used it as a proxy for mid-level instability. Dixon and Mote (2003) investigated many days with urban enhanced precipitation in Atlanta, Georgia. They found that days with more urban enhancement tended to have higher lapse rates below 600 mb, and higher humidity between 900 and 600 mb.

Aircraft meteorological data relay (AMDAR) soundings (ESRL/GSD, 2016) were obtained from the National Oceanic and Atmospheric Administration website at http://amdar.noaa.gov/.

Benjamin et al. (1999) found that AMDAR data can be as accurate as radiosonde sounding data. Schwartz et al. (2000) used AMDAR data to evaluate forecast model accuracy. Radiosonde balloons are not regularly launched near Fort McMurray, but between 2 and 8 aircraft submitted AMDAR soundings from the Fort McMurray airport on each of our case study days. Data had to be interpolated to the 850 and 500 mb levels because AMDARS may not take measurements at those exact levels. We computed the difference between the 850 mb and 500 mb temperatures for all AMDAR soundings after 1800 UTC on each day and used the median for our model comparison so that outlier values did not skew the results.

Figure 5.7 shows the relationship between the 850 – 500 mb temperature difference and how much the oil sands development affected the thunderstorm duration on each case study day. The highest temperature difference was on 29 July 2010 (30.6), while the second highest temperature difference was on 29 July 2014 (30.5). On both of these days the oil sands development caused the thunderstorm duration to be increased the most. Thus, days with an 850 – 500 mb temperature difference greater than 30 °C certainly affected thunderstorms initiation time and duration to some degree. In fact, the only two days that were strongly affected by the oil sands development were the only two days with an 850 – 500 mb temperature difference greater than 30. However, there were some days with a temperature difference slightly less than 30 °C that did not affect thunderstorms (30 July 2010, and 14 July 2007). Additionally, the day that affected thunderstorms when much more heat was added (06 August 2014) was also less than 30°C. There seems to be some association between days with very high lapse rates and strong modification of thunderstorm initiation time by the oil sands. However, it is difficult to make strong conclusions based on only ten case study days.

5.4. Discussion and conclusion

Our research lead to the following findings:

1) Waste heat created by the oil sands development does not cause significant changes to the thunderstorm intensity by directly adding sensible heat to the atmosphere to increase buoyancy.
2) Land cover modification by the oil sands development also does not cause significant changes to the thunderstorm intensity by adding sensible heat to the atmosphere by increasing the Bowen ratio.
3) In rare cases, both land cover modifications and waste heat created by the oil sands development cause thunderstorms to initiate substantially earlier and last longer.
4) Stein and Alpert's (1993) method of factor separation helped us determine the relative contributions of the land cover modification and the waste heat to thunderstorm initiation time and intensity.
5) Days in which the oil sands development significantly modified thunderstorms had a 850 – 500 mb temperature difference greater than 30 °C.

The WRF model adequately simulated the heat and dry islands produced by the oil sands development. The heat and dry islands were about the expected magnitude and extended fully throughout the boundary layer by the afternoon. The WRF model also simulated convection and convection initiation reasonably well most of the time. On six of the ten case study days, convection was initiated at nearly the same time as reality. On two of the four case study days where convection was not initiated at the expected time, the time is significantly closer to reality when the oil sands development is added into the model. On a third day, if much more heat was added to the model, the timing of convective initiation was improved as well. However the case

study day with the massive baseball-sized hailstorm was not simulated well regardless of the amount of heat added.

In all cases, there was minimal modification to convection intensity, regardless of which factors were activated in the model. Sometimes a factor slightly increased or decreased the intensity of the convection, but there were no patterns. Thus, the oil sands do not seem to be causing more thunderstorms or stronger thunderstorms.

On two case study days, adding the oil sands development into the model caused the convective initiation time to be earlier than without it. These results seem to be caused mostly by the change in land cover, and only partially by the waste heat emissions. However, these cases are rare. The timing of thunderstorm modification by the oil sands seems most likely when large mid-level lapse rates exist. We found that days with significant modification had an 850 – 500 mb temperature difference greater than 30 °C. We are confident that the oil sands land cover and waste heat modifications to the atmosphere caused these changes to occur.

In this study, we did not account for cloud condensation nuclei because research on this effect has given conflicting results, and Dixon and Mote (2003) suggest that the effect of cloud condensation nuclei could be more complex. Zhong et al. (2015) suggest that cloud condensation nuclei could increase precipitation downwind of the emission site, and Howell et al. (2014) found that pollution from the oil sands development could cause cloud condensation nuclei to form downwind. Thus, it is possible that the increased amount of cloud condensation nuclei could help to initiate convection even earlier. This could partly account for the discrepancies between the observed convection and the modelled convection on the days when the model initiated convection too late.

We also are unsure of our estimates of waste heat emissions from the oil sands development. We have shown that 3 case study days can be sensitive to extra waste heat emissions over and above the ten percent waste that was input. There is a large uncertainty on the amount of waste heat, and these results suggest that the amount of waste heat could be significantly higher than our estimates. We added what we thought was reasonable, but a combination of more waste heat and the inclusion of cloud condensation nuclei could explain why the model results differed from reality some of the case study days.

We note that in our study, the main mechanism for thunderstorm modification seems to be triggering, rather than a direct modification of the thunderstorm environment. Few studies have specifically implicated triggering as a means of thunderstorm modification. We also note that we used a high resolution three dimensional numerical model for an industrial surface mine site, while most studies look at large cities. Industrial sites differ from cities in that they have few people, few buildings, and sometimes much less vegetation. We specifically did not use an urban model to represent the conditions at the oil sands development because of the lack of tall buildings retaining heat by re-emission. Also, almost no studies have looked at artificial weather modification in the boreal forest. Most studies looked at agricultural areas with a much warmer climate, like St Louis, Missouri.

It would be interesting to test how often the conditions for thunderstorm duration enhancement exist in both the Athabasca oil sands development and in the Houston and Louisiana cases. Maybe that would help understand why the oil refineries cause such strong climatological lightning enhancement in Houston and Louisiana, but not at the oil sands development in Alberta. We think that there is little climatological lightning enhancement at the oil sands development because there appear to be only 1-2 days per year that are conducive to modifying thunderstorms. Maybe the conditions for thunderstorm enhancement (an 850 – 500 mb

temperature difference greater than 30°C) are more common near the Gulf of Mexico, causing the sum of the thunderstorm durations to be higher so it can impact climatological lightning.

5.5. Acknowledgements

We would like to acknowledge that some paid time was provided by the Meteorological Service of Environment and Climate Change Canada to complete this project. We would also like to acknowledge the Department of Atmospheric Sciences at the University of Utah for providing insight into modifying the WRF model code.

5.6. References

Ashley, W. S., M. L. Bentley, and T. Stallins, 2012: Urban induced thunderstorm modification in the southeast United States. *Climatic Change*, **113**, 481-498. DOI: 10.1007/s10584-011-0324-1

Baik, J. J., Y. H. Kim, J. J. Kim, and J. Y. Han, 2007: Effects of boundary-layer stability on urban heat island-induced circulation. *Theoretical and Applied Climatology*, **89**, 73-81. DOI: 10.1007/s00704-006-0254-4.

Benjamin, S. B., B. E. Schwartz, and R. E. Cole, 1999: Accuracy of ACARS wind and temperature observations determined by collocation. *Weather and Forecasting*, **14**, 1032-1038. DOI: 10.1175/1520-0434(1999)014<1032:AOAWAT>2.0.CO;2.

Bornstein, R. and Q. Lin, 2000: Urban heat islands and summertime convective thunderstorms in Atlanta: Three case studies. *Atmospheric Environment*, **34**, 507-516. DOI: 10.1016/S1352-2310(99)00374-X

Brimelow, J. C., J. M. Hanesiak, and W. R. Burrows, 2011: On the surface convection feedback during drought periods on the Canadian Prairies. *Earth Interactions*, **15**, 1-26. DOI: 10.1175/2010EI381.1

Brown, D. M., G. W. Reuter, and T. K. Flesch, 2011: Temperature, precipitation, and lightning modification in the vicinity of the Athabasca oil sands. *Earth Interactions*, **15**, 1–14. DOI: 10.1175/2011EI412.1.

Bryan, G. H., J. C. Wyngaard, and J. M. Fritsch, 2003: Resolution requirements for deep moist convection. *Monthly Weather Review*, **131**, 2394-2416. DOI: 10.1175/1520-0493(2003)131<2394:RRFTSO>2.0.CO;2

Changnon, S. A. Jr., R. G. Semonin, and F. A. Huff, 1976: A hypothesis for urban rainfall anomalies. *Journal of Applied Meteorology*, **15**, 544-560. DOI: 10.1175/1520-0450(1976)015<0544:AHFURA>2.0.CO;2

Chen, F., and J. Dudhia, 2001: Coupling an advanced land surface hydrology model with the Penn State-NCAR MM5 modelling system. *Monthly Weather Review*, **129**, 569-604. DOI: 10.1175/1520-0493(2001)129<0569:CAALSH>2.0.CO;2

Cheng, V. Y. S., G. B. Arhonditsis, D. M. L. Sills, H. Auld, R. W. Shephard, W. A. Gough, and J. Klaassen, 2013: Probability of tornado occurrence across Canada. *Journal of Climate*, **26**, 9415-9428. DOI: 10.1175/JCLI-D-13-00093.1

Crewe, Ashley, 2008: Hailstorm a year later: It can happen again. *Fort McMurray Today*. Accessed 01 February 2016. [Available online at http://www.fortmcmurraytoday.com/2008/07/29/hailstorm-a-year-later-it-can-happen-again-2.]

De Bruijn, T.J.W., 2010: Estimated life cycle GHG emissions and energy use for oil sands derived crudes versus conventional light crude using GHGenius, NRC, Canmet Energy, 38 pp.

Dixon, P. G., and T. L. Mote, 2003: Patterns and causes of Atlanta's urban heat island-initiated precipitation. *Journal of Applied Meteorology*, **42**, 1273-1284. DOI: 10.1175/1520-0450(2003)042<1273:PACOAU>2.0.CO;2

Elmore, K. L., D. J. Stensrud, K. C. Crawford, 2002: Explicit cloud-scale models for operational forecasts: a note of caution. *Weather and Forecasting*, **17**, 873-884. DOI: 10.1175/1520-0434(2002)017<0873:ECSMFO>2.0.CO;2

Environment and Climate Change Canada, 2016: Canadian historical weather radar. Meteorological Service of Canada Data Services Section, accessed 15 March 2016. [Available online at http://climate.weather.gc.ca/radar/index_e.html].

ESRL/GSD, 2016: Aircraft data web. Earth System Research Laboratory, Global Systems Division, accessed 25 March 2016. [Available online at http://amdar.noaa.gov/].

Government of Alberta, 2016: Alberta energy: Facts and statistics. Accessed 31 January 2016. [Available online at http://www.energy.alberta.ca/OilSands/791.asp.]

Grell, G. A., and S. R. Freitas, 2014: A scale and aerosol aware stochastic convective parameterization for weather and air quality modeling. *Atmospheric Chemistry and Physics*, **14**, 5233-5250. DOI: 10.5194/acp-14-5233-2014.

Guan, S., and G. W. Reuter, 1995: Numerical simulation of a rain shower affected by waste energy released from a cooling tower complex in a calm environment. *Journal of Applied Meteorology*, **34**, 131-142. DOI: 10.1175/1520-0450-34.1.131.

Guan, S., and G. W. Reuter, 1996: Numerical simulation of an industrial cumulus affected by heat, moisture, and CCN released from an oil refinery. *Journal of Applied Meteorology*, **35**, 1257-1264. DOI: 10.1175/1520-0450(1996)035<1257:NSOAIC>2.0.CO;2

Hazewinkel, R. R. O., A. P. Wolfe, S. Pla, C. Curtis, and K Hadley, 2008: Have atmospheric emissions from the Athabasca oil sands impacted lakes in northeastern Alberta, Canada? *Canadian Journal of Fisheries and Aquatic Sciences*, **65**, 1554-1567, DOI:10.1139/F08.074

Hohenegger, C., and C. Schär, 2007: Predictability and error growth dynamics in cloud-resolving models. *Journal of the Atmospheric Sciences*, **64**, 4467-4478. DOI: 10.1175/2007JAS2143.1

Howell, S. G., A. D. Clarke, S. Freitag, C. S. McNaughton, C. Kapustin, V. Brekovskikh, J.-L. Jimenez, and M. J. Cubison, 2014: An airborne assessment of atmospheric particulate emissions from the processing of the Athabasca oil sands. *Atmospheric Chemistry and Physics*, **14**, 5073-5087. DOI: 10.5194/acp-14-5073-2014

Kelly, E. N., J. W. Short, D. W. Schindler, P. V. Hodson, M. Ma, A. K. Kwan, and B. L. Fortin, 2009: Oil sands development contributes polycyclic aromatic compounds to the Athabasca River and its tributaries. *Proceedings of the National Academy of Sciences*, 106, **52**, 22346–22351. DOI: 10.1073/pnas.0912050106.

Knowles, J. B., 1993: The influence of forest fire induced albedo differences on the generation of mesoscale circulations. *M.Sc. Thesis*, Department of Atmospheric Sciences, Colorado State University, 94 pp.

Lin, Y., R. D. Farley, and H. D. Orville, 1983: Bulk parameterization of the snow field in a cloud model. *Journal of Applied Meteorology and Climatology*, **22**, 1065-1092. DOI: 10.1175/1520-0450(1983)022<1065:BPOTSF>2.0.CO;2.

NCEP/NWS/NOAA, 2005: NCEP North American Regional Reanalysis (NARR). Research data archive at the national center for atmospheric research, computational and information systems laboratory, accessed 15 December 2016. [Available online at http://rda.ucar.edu/datasets/ds608.0/].

Niyogi, D., T. Holt, S. Zhong, P. C. Pyle, and J. Basara, 2006: Urban and land surface effects on the 30 July 2003 mesoscale convective system event observed in the southern great plains. *Journal of Geophysical Research*, **111**, D19107, 1-20. DOI: 10.1029/2005JD006746.

Niyogi, D., P. Pyle, M. Lei, S. P. Arya, C. M. Kishtawal, M. Shepherd, F. Chen, B. Wolfe, 2011: Urban modification of thunderstorms –an observational storm climatology and model case study for the Indianapolis urban region. *Journal of Applied Meteorology and Climatology*, **50**, 1129-1144. DOI: 10.1175/2010JAMC1836.1.

Nkemdirim, L. C., 1981: Extra urban and intra urban rainfall enhancement by a medium sized city. *Water Resources Bulletin*, **17**, 5, 753-759. DOI: 10.1111/j.1752-1688.1981.tb01294.x

Oke, T. R., 1973: City size and the urban heat island. *Atmospheric Environment*, **7**, 769-779. DOI: 10.1016/0004-6981(73)90140-6

Pennelly, C., G. W. Reuter, and T. Flesch, 2014: Verification of the WRF model for simulating heavy precipitation in Alberta. *Atmospheric Research*, **135-136**, 172-192. DOI: 10.1016/j.atmosres.2013.09.004.

Pennelly, C. and G.W. Reuter, 2017: Verification of the Weather Research and Forecasting Model when forecasting daily surface conditions in southern Alberta. *Atmosphere-Ocean*, **55**, 31-41. DOI: 10.1080/07055900.2017.1282345.

Pielke, R. A., and M. Uliasz, 1993: Influence of landscape variability on atmospheric dispersion. *Journal of the Air and Waste Management Association*, **43**, 989-994. DOI: 10.1080/1073161X.1993.10467181

Reuter G. W., and S. Guan, 1995: Effects of industrial pollution on cumulus convection and rain showers: A numerical study. *Atmospheric Environment*, **29**, 18, 2467-2474. DOI: 10.1016/1352-2310(95)00169-Y

Rozoff, C. M., W. R. Cotton, and J. O. Adegoke, 2003: Simulation of St. Louis, Missouri, land use impacts on thunderstorms. *Journal of Applied Meteorology*, **42**, 716-738. DOI: 10.1175/1520-0450(2003)042<0716:SOSLML>2.0.CO;2

Schmid, P. E., and D. Niyogi, 2013: Impact of city size on precipitation-modifying potential. *Geophysical Research Letters*, **40**, 5263-5267. DOI: 10.1002/grl.50656

Schwartz, B. E., S. G. Benjamin, S. M. Green, and M. R. Jardin, 2000: Accuracy of RUC-1 and RUC-2 wind and aircraft trajectory forecasts by comparison with ACARS observations. *Weather and Forecasting*, **15**, 313-326.

Shamarock, W. C., J. B. Klemp, J. Dudhia, D. O. Gill, D. M Barker, M. G. Duda, X.-Y. Huang, W. Wang, and J. G. Powers, 2008: A description of the Advanced Research WRF Version 3. *NCAR Technical Note.*

Smith, S. B., G. W. Reuter, M. K. Yau, 1998: The episodic occurrence of hail in central Alberta and the Highveld of South Africa. Research Note: *Atmosphere-Ocean*, **36**, 2, 169-178. DOI:10.1080/07055900.1998.9649610.

Steiger, S. M., and R. E. Orville, 2003: Cloud-to-ground lightning enhancement over southern Louisiana. *Geophysical Research Letters*, **30**, 1975, DOI: 10.1029/2003GL017923.

Steiger, S. M., R. E. Orville, and G. Huffines, 2002: Cloud-to-ground lightning characteristics over Houston, Texas: 1989-2000. *Journal of Geophysical Research*, **107**, 4117, DOI: 10.1029/2001JD001142.

Stein, U. and P. Alpert, 1993: Factor separation in numerical simulations. *Journal of the Atmospheric Sciences*, **50**, 14, 2107-2115. DOI: 10.1175/1520-0469(1993)050<2107:FSINS>2.0.CO;2.

Sun, J., D. H. Lenschow, L. Mahrt, T. L. Crawford, K. J. Davis, S. P. Oncley, J. I. MacPherson, Q. Wang, R. J. Dobosy, and R. L. Desjardins, 1997: Lake-induced atmospheric circulations during BOREAS. *Journal of Geophysical Research*, **102**, D4, 29155-29166. DOI: 10.1029/97JD01114

Taylor, N. M., D. M. L. Sills, J. M. Hanesiak, J. A. Milbrandt, C. D. Smith, G. S. Strong, S. H. Scone, P. J. McCarthy, and J. C. Brimelow, 2011: The understanding severe thunderstorms and Alberta boundary layer experiment (UNSTABLE) 2008. *Bulletin of the American Meteorological Society*, June, 739-763. DOI: 10.1175/2011BAMS2994.1

Weisman, M. L., C. Davis, W. Wang, K. W. Manning, and J. B. Klemp, 2008: Experiences with 0-36-h explicit convective forecasts with the WRF-ARW model. *Weather and Forecasting*, **23**, 407-437. DOI: 10.1175/2007WAF2007005.1

Westcott, N. E., 1995: Summertime cloud-to-ground lightning activity around major Midwestern urban areas. *Journal of Applied Meteorology*, **34**, 1633-1642. DOI: 10.1175/1520-0450-34.7.1633

Xue, M., F. Kong, K. W. Thomas, J. Gao, Y. Wang, K. Brewster, K. K. Droegemeier, 2013: Prediction of convective storms over continental United States with radar data assimilation: An example case of 26 May 2008 and precipitation forecasts from spring 2009. *Advances in Meteorology,* 2013, 1-9. DOI: 10.1155/2013/259052

Zhong, S., Y. Qian, C. Zhao, R. Leung, and X.-Q. Yang, 2015: A case study of urbanization impact on summer precipitation in the greater Beijing metropolitan area: urban heat island versus aerosol effects. *Journal of Geophysical Research*, **120**, 10903-10914. DOI: 10.1002/2015JD023753.

5.7. Tables

Table 5.1: The WRF configuration for our model runs. The cumulus scheme was developed by Grell and Freitas (2014). The Microphysics scheme was developed by Lin et al. (1983). The default Rapid Radiative Transfer Model (RRTM) was used for the longwave and shortwave schemes.

Domain	**Outer Domain**	**Middle Domain**	**Inner domain**
Horizontal Grid Spacing (km)	*18 km*	*6 km*	*2 km*
Time-step	*108 s*	*36 s*	*12 s*
Grid Dimensions (Grid cells)	*30 x 30*	*34 x 34*	*40 x 40*
Vertical Levels	*30*	*30*	*30*
Cumulus Scheme	*Grell-Freitas*	*Grell-Freitas*	*None*
Microphysics Scheme	*Lin et al.*	*Lin et al.*	*Lin et al.*
Land-Surface Scheme	*Noah*	*Noah*	*Noah*
Short and Longwave Radiation Scheme	*RRTM*	*RRTM*	*RRTM*
Surface Layer	*MM5 scheme*	*MM5 scheme*	*MM5 scheme*
Planetary Boundary Layer	*Yonsei University*	*Yonsei University*	*Yonsei University*

Table 5.2: A comparison of the storm motion and the initiation time of the simulated thunderstorms and the real thunderstorms. The cases where the simulated and real thunderstorms differed by more than four hours are bolded. The simulated initiation times are from a combination of the innermost and middle domain to give a larger areal sample of convective initiation.

Date	Storm Motion		First Echoes		Time Difference
	(Radar)	(Simulated)	(Radar)	(Simulated)	
2007-07-14	SE	E	20:20	20:30	-0.2
2007-07-29	NE	NE	22:10	02:45	**-4.6**
2009-08-09	E	E	22:10	21:15	0.9
2010-07-29	SE	E	18:40	23:45	**-5.1**
2010-07-30	E	E	18:50	19:15	-0.4
2011-08-14	NE	NE	17:20	17:00	0.3
2013-06-30	SE	SE	20:20	20:00	0.3
2014-07-23	N	N	22:40	22:00	0.7
2014-07-29	SE	E	19:10	23:15	**-4.1**
2014-08-06	NE	NE	18:30	23:00	**-4.5**

Table 5.3: The results of the factor separation for each case study day. The factor separation was method was applied for three variables: maximum reflectivity (dBZ), average total condensate (g/kg), and the total average rainfall (mm).

Date	Variable	0	B	H	HB	Actual
14-Jul-2007	**Maximum Reflectivity**	**54.3**	**0.8**	**0.6**	**-0.6**	**58**
	Average Condensate	*0.77*	*-0.03*	*0.02*	*0.00*	*n/a*
	Total Average Rainfall	25.1	-3.0	0.3	0.7	*n/a*
29-Jul-2007	**Maximum Reflectivity**	**57.4**	**-0.2**	**-1.3**	**0.4**	**62**
	Average Condensate	*0.53*	*-0.01*	*-0.01*	*0.02*	*n/a*
	Total Average Rainfall	18.1	-0.4	-0.2	1.0	*n/a*
09-Aug-2009	**Maximum Reflectivity**	**48.0**	**1.5**	**1.2**	**-1.1**	**53**
	Average Condensate	*0.05*	*0.00*	*0.01*	*-0.01*	*n/a*
	Total Average Rainfall	0.6	0.1	0.1	-0.1	*n/a*
29-Jul-2010	**Maximum Reflectivity**	**49.5**	**-2.3**	**-0.5**	**0.5**	**56**
	Average Condensate	*0.07*	*-0.02*	*-0.01*	*0.03*	*n/a*
	Total Average Rainfall	0.5	-0.3	-0.2	0.4	*n/a*
30-Jul-2010	**Maximum Reflectivity**	**53.3**	**1.8**	**-0.1**	**-1.4**	**60**
	Average Condensate	*0.44*	*0.07*	*0.08*	*-0.07*	*n/a*
	Total Average Rainfall	14.3	3.4	4.0	-2.8	*n/a*
14-Aug-2011	**Maximum Reflectivity**	**53.8**	**-0.4**	**-0.9**	**1.1**	**60**
	Average Condensate	*0.45*	*-0.01*	*-0.01*	*0.01*	*n/a*
	Total Average Rainfall	14.2	-0.6	-0.5	0.2	*n/a*

30-Jun-2013	**Maximum Reflectivity**	**54.2**	**0.1**	**1.5**	**-2.1**	**55**
	Average Condensate	*0.16*	*0.03*	*0.05*	*-0.03*	*n/a*
	Total Average Rainfall	3.5	1.1	1.4	-0.9	*n/a*
23-Jul-2014	**Maximum Reflectivity**	**51.4**	**0.1**	**-0.5**	**0.5**	**50**
	Average Condensate	*0.11*	*0.00*	*-0.01*	*0.00*	*n/a*
	Total Average Rainfall	2.2	0.2	-0.2	0.0	*n/a*
29-Jul-2014	**Maximum Reflectivity**	**50.1**	**1.5**	**0.3**	**-0.9**	**52**
	Average Condensate	*0.05*	*0.02*	*0.01*	*-0.01*	*n/a*
	Total Average Rainfall	0.4	0.4	0.2	-0.2	*n/a*
06-Aug-2014	**Maximum Reflectivity**	**47.4**	**1.8**	**0.1**	**-2.5**	**52**
	Average Condensate	*0.03*	*0.00*	*0.00*	*0.00*	*n/a*
	Total Average Rainfall	0.1	0.0	0.0	0.0	*n/a*
Average	**Maximum Reflectivity**	**51.9**	**0.5**	**0.0**	**-0.6**	**55.8**
	Average Condensate	*0.27*	*0.01*	*0.01*	*-0.01*	*n/a*
	Total Average Rainfall	7.9	0.1	0.5	-0.2	*n/a*

Table 5.4: The initiation time (UTC), and the storm duration (hours) for each model run for each case study day. The initiation time and duration difference columns are the difference between the "0" and the "HB" cases. The two days with the largest initiation time and duration differences are bolded and italicized. The initiation times are from the innermost domain only, and thus might not match the numbers from table 5.2.

Date	Storm Initiation Time (UTC)				Initiation Difference	Storm Duration (Hours)				Duration Difference
	0	B	H	HB		0	B	H	HB	
07-14-2007	21:00	21:00	21:00	21:00	0.00	9.75	10.25	9.25	10.00	0.25
07-29-2007	03:15	03:15	03:15	03:15	0.00	3.75	3.75	3.75	3.50	-0.25
08-09-2009	19:15	19:15	19:15	19:15	0.00	10.00	10.25	10.25	10.50	0.50
07-29-2010	**23:15**	**21:45**	**21:45**	**21:15**	**-2.00**	**5.50**	**7.00**	**6.75**	**7.25**	**1.75**
07-30-2010	19:15	19:15	19:15	19:15	0.00	9.75	9.75	9.75	9.75	0.00
08-14-2011	22:45	23:00	22:45	22:45	0.00	5.25	5.25	5.50	5.50	0.25
06-30-2013	19:00	19:00	19:00	19:00	0.00	7.00	7.00	7.25	7.25	0.25
07-23-2014	21:45	21:45	21:45	21:45	0.00	4.75	4.75	4.50	4.75	0.00
07-29-2014	**22:45**	**22:00**	**22:45**	**21:45**	**-1.00**	**3.00**	**3.75**	**3.25**	**4.00**	**1.00**
08-06-2014	22:45	23:00	22:45	23:00	0.25	1.25	1.00	1.25	1.00	-0.25

Table 5.5: The results of our factor separation analysis on the initiation time and duration data for 29 July 2010 and 29 July 2014 for each of the model runs. The factor separation results are bolded.

Date	Model Run	Initiation Time	**Separated Factors**	Duration	**Separated Factors**
29-Jul-10	0	23:15	**23.25**	4.75	**4.75**
	H	21:45	**-1.50**	6.25	**1.50**
	B	21:45	**-1.50**	6.00	**1.25**
	HB	21:15	**1.00**	6.25	**-1.25**
29-Jul-14	0	22:45	**22.75**	3.00	**3.00**
	H	22:00	**-0.75**	3.75	**0.75**
	B	22:45	**0.00**	3.25	**0.25**
	HB	21:45	**-0.25**	4.00	**0.00**

5.8. Figures

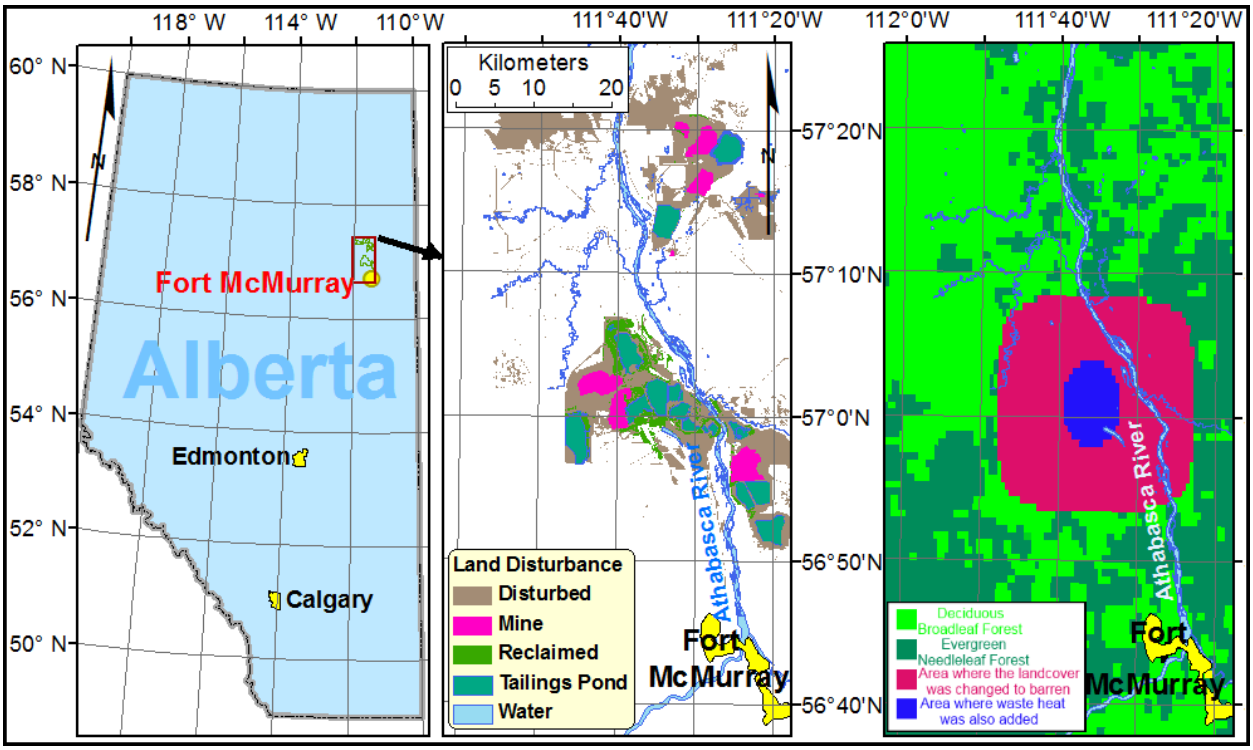

Figure 5.1: Left: The location of the oil sands and Fort McMurray in Alberta (reprinted from Brown et al. 2011). Centre: the oil sands land cover in 2007 (reprinted from Brown et al. 2011). Right: The model modifications. We modelled the oil sands development approximately as a circular 650 km^2 disturbance of barren ground (pink area). We added waste heat to the atmosphere in a smaller area in the centre of the disturbance (blue area).

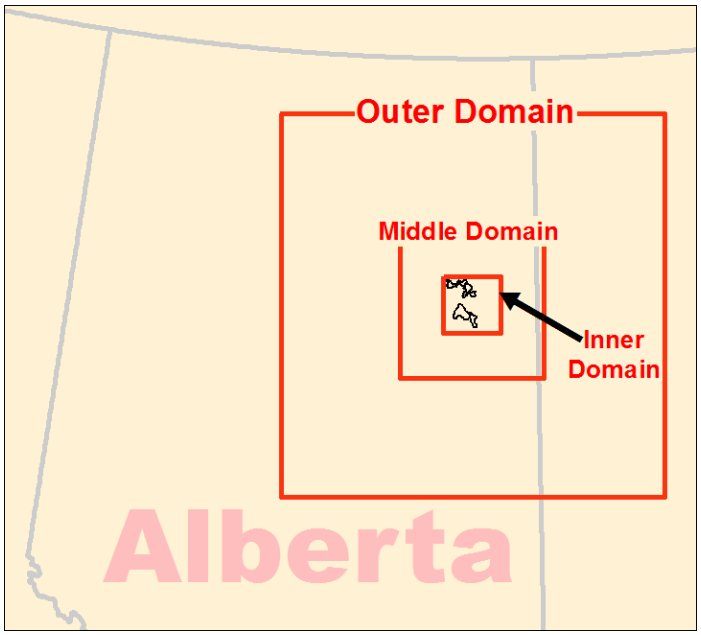

Figure 5.2: A map of our three nested model domains in relation to the oil sands development in northeastern Alberta.

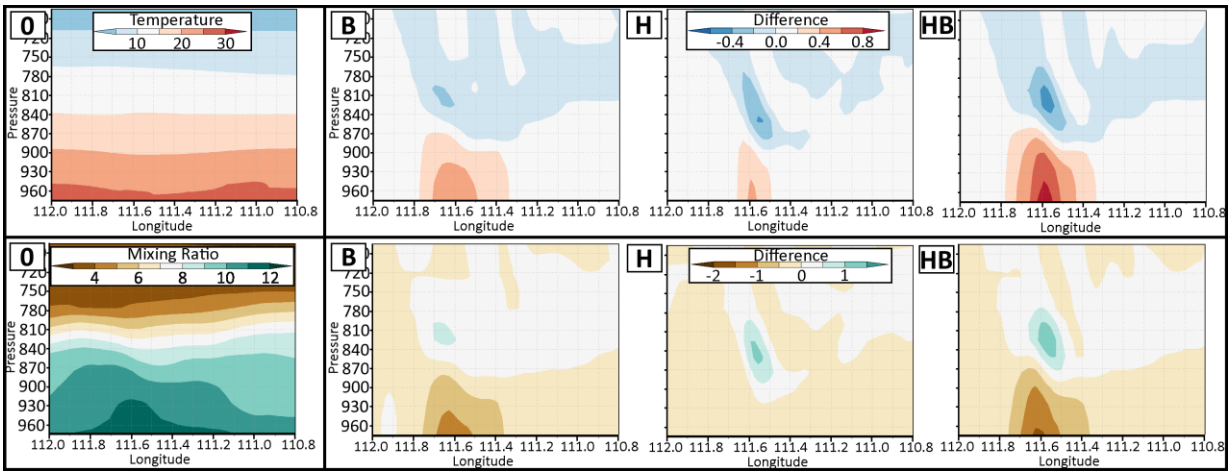

Figure 5.3: Upper left: A cross section of the model simulated temperature (°C) near the oil sands development from the case with no barren modifications or waste heat. Next three upper row images: The difference between the three modified simulations and the first one. Bottom row: Same as above, but with the water vapour mixing ratio (g kg^{-1}) instead of the temperature. All images are at 1815 UTC 29 July 2010, and the cross section was take at latitude 57.1 °N.

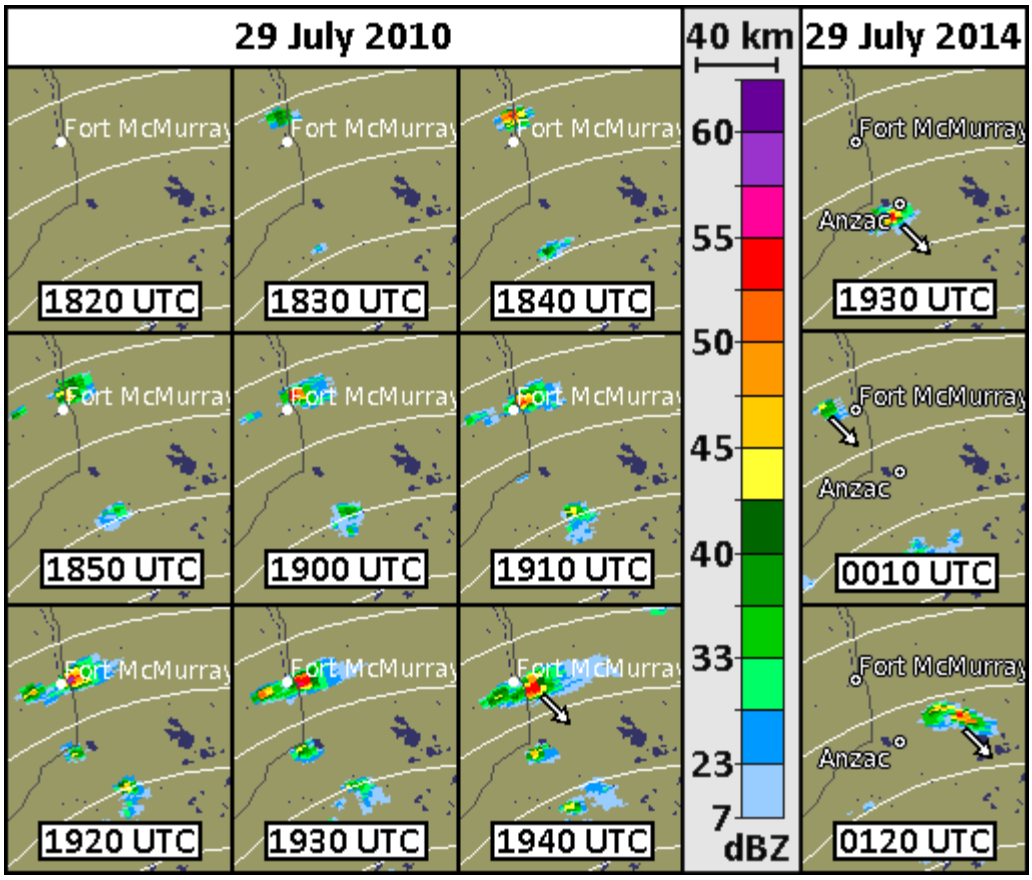

Figure 5.4: Observed radar images of the thunderstorm that initiated near the oil sands development on 29 July 2010 and 29 July 2014 (Environment and Climate Change Canada, 2016). Arrows indicate the storm motion.

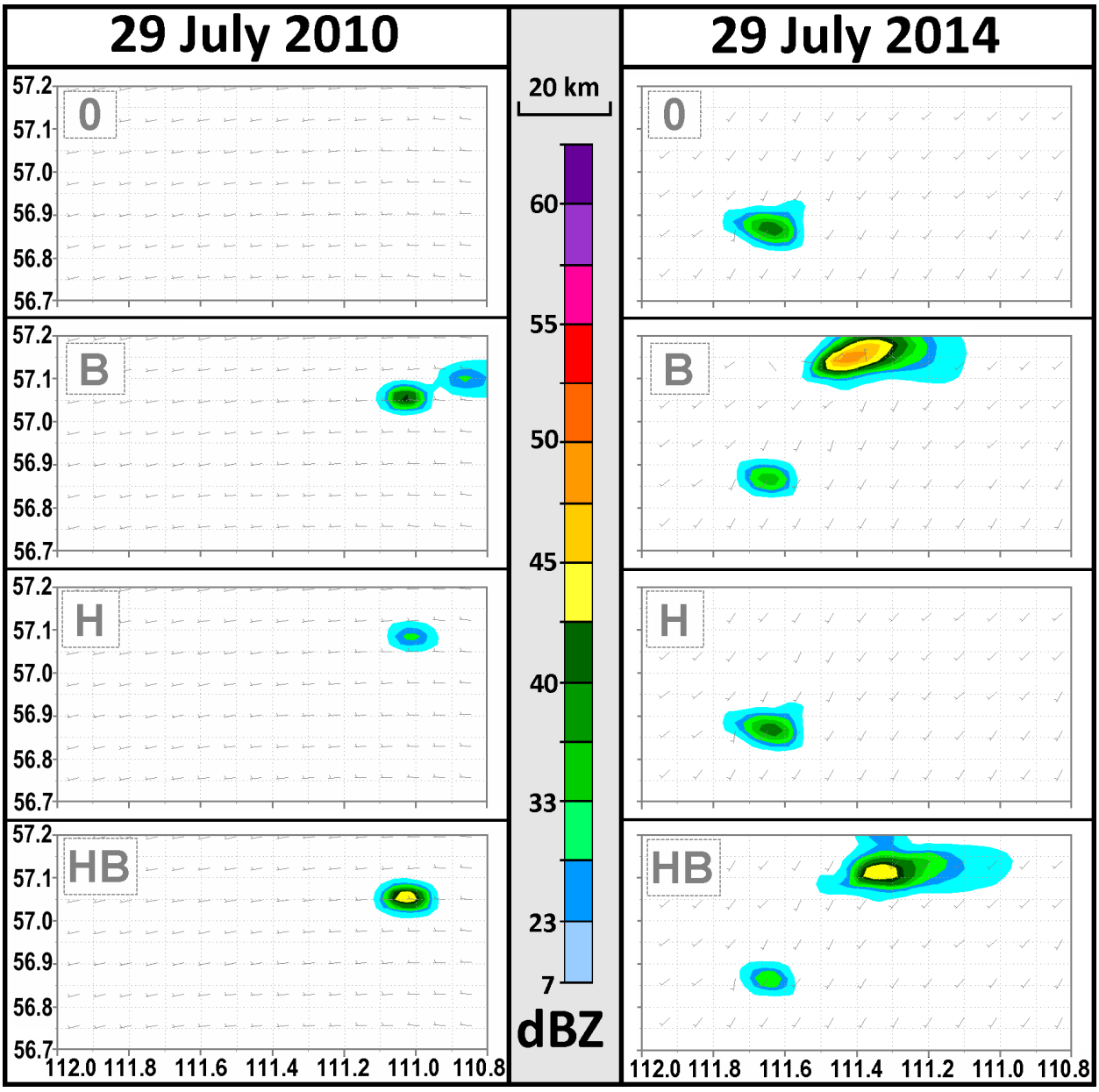

Figure 5.5: Simulated model radar images for 2145 UTC 29 July 2010 (right), and for 2315 UTC 29 July 2014 (left). Simulation 0 is the simulation with no factors activated. Simulation B is the simulation with the land cover changed to barren. Simulation H is the simulation with the waste heat emissions. Simulation HB is the simulation with both factors activated.

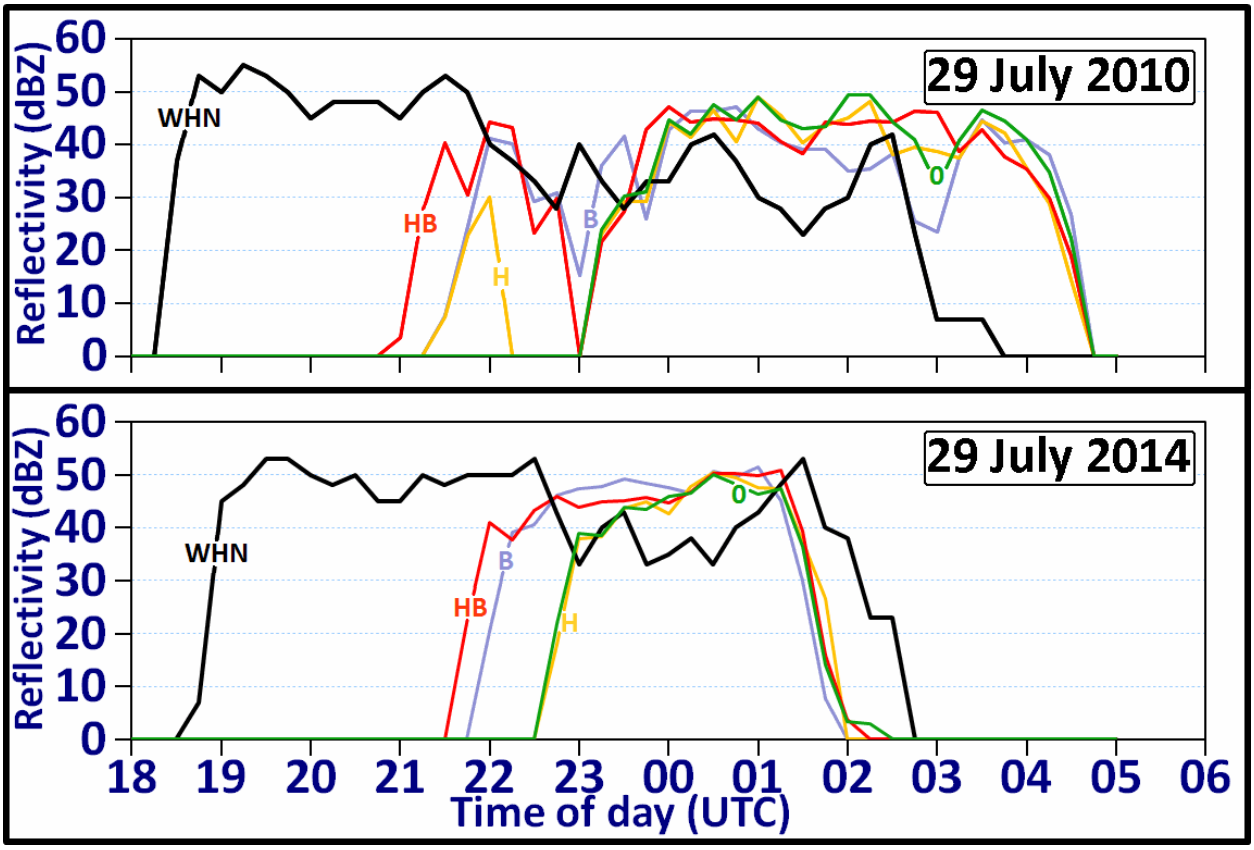

Figure 5.6: The maximum simulated radar reflectivity on 29 July 2010 (top) and 29 July 2014 (bottom) for the four simulations. 0 is the simulation with no factors activated. B is the case with the land surface changed to barren. H is the case with the waste heat added. HB is the case where both factors were activated. Also shown is the observed maximum radar reflectivity from the Jimmy Lake Radar Station (WHN).

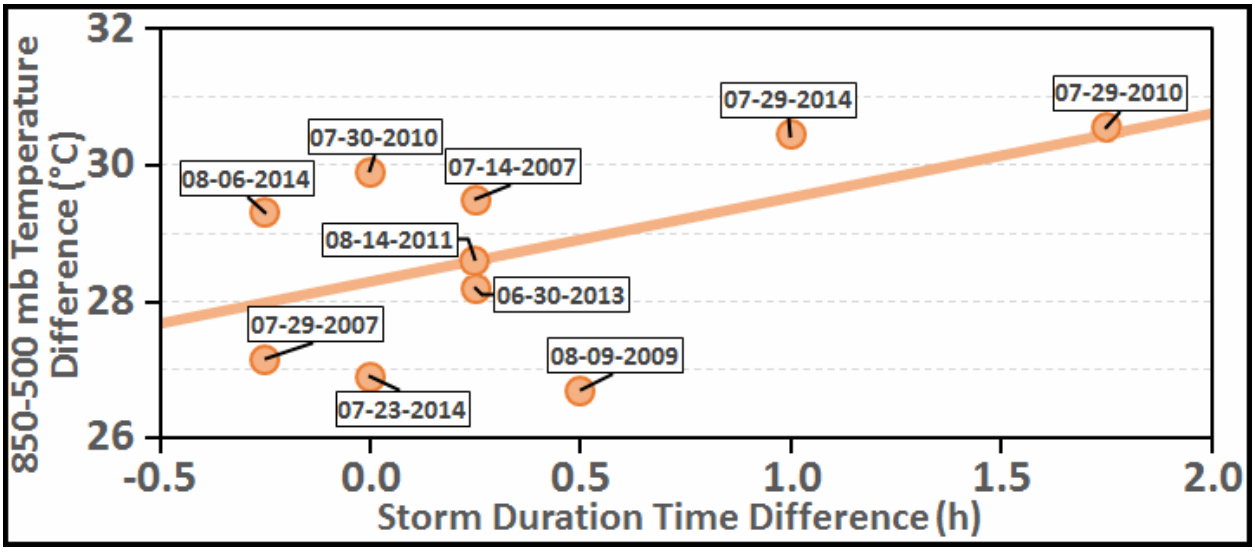

Figure 5.7: The storm duration difference versus the 850 – 500 mb temperature difference.

6. The effect of the Canadian Shield on cloud-to-ground lightning density

Daniel Brown and Gerhard Reuter

This chapter has been published in the journal *Atmosphere-Ocean*.

Brown, D. M. and G. W. Reuter, 2017: The effect of the Canadian Shield on cloud-to-ground lightning density. *Atmosphere-Ocean*, 53, 3, 133-143.

DOI: 10.1080/07055900.2017.1316699.

Abstract

The Canadian Shield is a large area of exposed bedrock that covers a significant portion of Canada. The focus of this research is on the Canadian Shield in northeastern regions of the Canadian Prairie provinces, the Northwest Territories, and northwestern Ontario. Observations of cloud-to-ground lightning flashes show a distinct reduction in lightning density when crossing the southern boundary of the Canadian Shield. Statistical tests were used to determine whether there was a statistically significant change between the average cloud-to-ground lightning density gradient near the Canadian Shield and away from it. Most regions had a statistically significant change at the 95% confidence level across the boundary. However, regions that contained large lakes or significant topography did not, suggesting that the large open water and rough topography have a greater effect than the Canadian Shield.

Three reasons for the distinct change across the Canadian Shield were explored: less lightning is detected, less lightning occurs with the same number of thunderstorms, and less lightning occurs because fewer thunderstorms occur. Some evidence suggested that less lightning is detected because the Canadian Shield has lower electrical conductivity. The low conductivity distorts the lightning waveform and contributes to higher errors and lower detection efficiency. There is also some evidence that a sharp change in land cover from lusher, higher transpiring forest to sparser lower transpiring forest could be reducing the instability causing fewer, weaker thunderstorms.

Keywords

Convection, Lightning, Continental, Lakes, Regional, Observation

6.1. Introduction

Lightning is responsible for igniting most large wildfires in Canada (Stocks et al. 2003), and, on average, lightning injures 100 and kills 10 persons per year in Canada (Mills et al. 2008). Thus, we need to further our understanding of when and why lightning occurs and determine how we can detect lightning in real time. However, the initiation of convective storms that produce lightning is not fully understood. In fact, recent field projects such as the Understanding Severe Thunderstorms and Alberta Boundary Layer Experiment (Taylor et al. 2011) are still investigating thunderstorm initiation. Kozak (1998) analyzed the spatial distribution of cloud-to-ground lightning density and found that there is a strong gradient in lightning flash density in northeastern Alberta. Similarly, Brown (2012) found that the cloud-to-ground lightning density suddenly dropped at the Canadian Shield boundary in northern Saskatchewan. This paper incorporates the work from Brown's study and expands on it to include the Canadian Shield boundary from Great Bear Lake in the Northwest Territories southeast to Lake of the Woods on the Manitoba-Ontario-Minnesota border from 1999 to 2015. Specifically, we focus on whether there is a marked reduction in cloud-to-ground lightning density along the entire Canadian Shield boundary, and examine what controls the spatial distribution of lightning flashes in these northern regions.

All thunderstorms require three ingredients: low-level humidity, convective instability, and a lifting mechanism. Low-level humidity is typically supplied to western Canada by moisture transport from the Gulf of Mexico (Brimelow and Reuter 2008), or by evapotranspiration from crops, deciduous trees, and soils (Strong 1997). A combination of low-level humidity, warm surface temperatures, and cool temperatures aloft creates convective instability. Surface

temperatures can be increased by warm air advection or solar heating, while cool temperatures aloft can be caused by an approaching longwave or shortwave upper trough (Smith and Yau 1993). Even when low-level humidity and convective instability are present, thunderstorms still need a lifting mechanism to initiate convection. Some of the most common lifting mechanisms are convergence due to frontal passages and upper level disturbances (Wilson and Roberts 2006). Other lifting mechanisms are lake breeze fronts, differential surface heating, orographic lifting and mountain breezes, drylines and outflow of pre-existing mid-level cumulus convection. Severe thunderstorms require the three ingredients above as well as strong wind shear between the surface and the mid-levels of the atmosphere (around 500 mb). This strong wind shear causes storms to undergo a mesoscale organization that separates the updraft and downdraft, causing more intense longer lasting storms. Severe thunderstorms can produce much more lightning than non-severe thunderstorms (Reap and MacGorman 1989).

Thunderstorms are always convective in nature, that is, most of the ascent is driven directly by buoyancy caused by density differences. Large density differences between warm moist air at the surface and cool dry air aloft create large vertical velocities at small scales. In particular, strong updrafts and downdrafts cause electric charge separation in thunderstorms. Strong thunderstorm updrafts are efficient at sorting the small cloud-ice particles from the larger graupel (snow pellet) particles, and the interactions between these particles transfer charge from one to the other (Latham 1981). Convective storms are the only weather phenomena that can provide an updraft sufficiently strong to suspend graupel particles long enough to build up enough static electricity to produce lightning (Illingworth 1985). Even with plentiful research, the exact mechanism of charge transfer has not yet been determined (Saunders 1993). However, positive charge is generally transferred to the top and bottom of the cloud, while negative charge settles to the lower-middle part of the cloud (Williams 1989).

In contrast, lightning detection is fairly well understood. Lightning can be detected by either time-of-arrival or magnetic direction finding detectors. Time-of-arrival sensors triangulate the location by comparing the arrival time differences of radio frequency waves radiated by a lightning stroke (Lee 1986). Magnetic direction finding sensors use two orthogonal loops to vector the direction of the radio frequency waves (Orville 1991). Most lightning detection networks use a combination of these methods to provide greater accuracy (Cummins et al. 2000). In our analysis, we used data from the Canadian Lightning Detection Network (CLDN). Vaisala operates the CLDN, which uses a number of different sensors. Some of the sensors use only the time-of-arrival method, while other sensors add magnetic direction finding to help fine-tune the accuracy. The sensors of the CLDN are continually being upgraded, making trend analysis difficult (Burrows and Kochtubajda 2010). The detection efficiency of the CLDN is generally greater than 80 percent in our study area. However, in most of the Northwest Territories and Nunavut the detection efficiency decreases to below 70% because only the strongest lightning strokes are detected. The median location accuracy of the CLDN is approximately 500 m. (Burrows and Kochtubajda 2010).

The Canadian Shield zone covers a significant portion of Canada and primarily consists of Precambrian bedrock exposed at the ground surface partially covered with patchy thin soils. The land to the southwest of the Canadian Shield is covered with sedimentary rocks with deeper soil on top (Shilts et al. 1987). In most regions, the Centre for Land and Biological Resources Research (1996) shows that the soil suddenly changes from mostly Luvisolic or Chernozemic (well-developed soils supporting higher biomass) southwest of the Canadian Shield to Brunisolic or Unclassified (poorly developed soils supporting a lower biomass or barren rock) in the Canadian Shield (Soil Classification Working Group, 1998). However, a portion of the Canadian Shield north of Lake Winnipeg is classified as Luvisolic, and the region between Great Slave Lake and Great Bear Lake is difficult to interpret because there is a large amount of frozen soil. The change in soil

type likely causes a sudden change in surface land cover at the boundary between the Canadian Shield and the more heavily forested or agricultural lands to the southwest. The Canadian Shield is rocky, vegetated with mostly needle-leaf trees, and dotted with numerous deep cold lakes. The land southwest of the Canadian Shield is mostly soil, and much more fertile. There are fewer lakes and lusher vegetation including higher transpiring broadleaf trees and shrubs (Sellers et al. 1995). Lightning-caused fires are common in the Canadian Shield (Stocks et al. 2003), thus we need to learn more about lightning and thunderstorms in the Canadian Shield region.

The Canadian Shield region has unusually low ground conductivity. The conductivity of the Canadian Shield ranges from 1 to 2 mSm^{-1} in most regions, but higher values are found in central Manitoba. Ground conductivity values to the southwest of the Canadian Shield range from 8 to 15 mSm^{-1} (International Telecommunication Union 2015). Nag et al. (2015) found that ground conductivity and elevation caused the majority of errors when using the time-of-arrival method, and Schueler and Thompson (2006) found that incorporating these factors significantly improved lightning location accuracy.

Herodotou et al. (1993) showed that the lightning signal waveform displays much more attenuation travelling over rock than over water. Scheftic et al. (2008) showed that lightning signals propagate poorly over ground with low conductivity. The rise-time of the lightning waveform is strongly affected by the ground conductivity, and is defined as the time (usually in μs) for the waveform to rise from 10% of its peak value to the peak value. Low ground conductivity distorts the lightning waveform, which results in a longer rise-time, and can affect the results of the time-of-arrival method (Scheftic et al. 2008). The rise time of lightning waveforms is much longer inside the Canadian Shield than outside (Scheftic et al. 2008, Bardo et al. 2004).

In this paper we will examine whether a sharp cloud-to-ground lightning density gradient exists along the Canadian Shield boundary. Burrows and Kochtubajda (2010) showed that Lake Winnipeg and Great Slave Lake had a significantly lower lightning density in their lee because the cool water supressed thunderstorms. We expect it will be difficult to find conclusive evidence that the Canadian Shield affects lightning flash density in the vicinity of large lakes. We will explore the possibility that the low conductivity of the Canadian Shield causes fewer lightning flashes to be detected, in addition to the possibility that the surface land cover influences the amount of convection.

6.2. Study area and method of analysis

We defined our study area as the region 200 km on either side of the boundary separating the Canadian Shield from the boreal forest between Great Bear Lake in the Northwest Territories and the Canadian side of Lake of the Woods in Manitoba and Ontario. We divided our study area into eight regions in order to examine the regional variability of the Canadian Shield lightning effect (Figure 6.1). Because we expect different behaviour near large lakes, we purposely arranged our regions such that Great Slave Lake, Lake Athabasca, and Lake Winnipeg were contained within their own regions (Lake Winnipeg took two regions). We can then compare our analysis for the regions containing large lakes with those that do not.

In most of our analyses, we used lightning flash data. A lightning flash consists of one or more individual lightning strokes grouped together at the same location within a short time interval (usually no more than a few seconds). The number of strokes in a flash is the multiplicity. For our first analysis we calculated the cloud-to-ground lightning flash density in 10 km by 10 km squares annually and in total for the years 1999 through 2015. We used these gridded data to

create lightning flash density maps along the Canadian Shield boundary in the various sub-regions to help visualize the Canadian Shield lightning effect.

We also quantified the sharp change in cloud-to-ground lightning flash density across the Canadian Shield boundary using a statistical analysis of the lightning density gradient. For our statistical analysis, we divided each region into 10 km wide strips from 0 to 200 km on either side of the Canadian Shield boundary (Figure 6.1, inset). Then we calculated the cloud-to-ground lightning flash density within each strip annually and for the total time period. Of course, we needed to divide by the area of each strip (which varied) to properly calculate the density.

A gradual gradient in lightning density from southwest to northeast exists in our study region (Burrows and Kochtubajda 2010), but we are interested in a step change along the Canadian Shield boundary. In order to detect this step change we calculated the lightning flash density gradient to see whether it is enhanced along the Canadian Shield boundary. The lightning density gradient was calculated by subtracting the lightning densities from the two adjacent strips and dividing by the total distance (20 km).

We used various statistical tests to detect whether the lightning density gradient near the Canadian Shield boundary (within 30 km) was significantly different from that away from the boundary (30 to 100 km). We chose the area within 30 km to be considered "near the boundary" because we preferred to have a sample size greater than five for our various statistical tests, and our preliminary analysis indicated this distance was reasonable. Only data up to 100 km were considered as "away from the boundary" because we did not want to have too large a discrepancy between our sample sizes for the Student's t-test, and we did not want to include other influences on lightning that could not be accounted for. The most basic statistical test to use is the one-tailed Student's t-test. Clodman and Chisholm (1996) also used the Student's t-test to test

differences in lightning density. However, we are not certain whether the assumption of a normal distribution is valid, so we also present data from the non-parametric equivalent of the Student's t-test: the one-tailed Mann-Whitney U test. The Kolmogorov-Smirnov (KS) test was used by Kochtubajda et al. (2011) to determine whether lightning from different geographical regions came from the same distribution, and we also present results from that test. A significance level of 0.05 was used for all our tests.

6.3. Relating the lightning flash density with the Canadian Shield boundary

Figure 6.2 shows the spatial distribution of the cloud-to-ground lightning flash density for western Canada. As expected, the cloud-to-ground lightning flash density was generally highest in the southern and western sections and lowest in the northeastern sections, similar to the findings of Burrows and Kochtubajda (2010). However, the feature we focus on here is the relatively sharp *discontinuity* in the cloud-to-ground lightning flash density that appears to occur along the Canadian Shield boundary. The results shown in Figure 6.2 show that location and orientation of the discontinuity agree well with the Canadian Shield boundary, particularly over northern Saskatchewan. The sharp discontinuity in lightning flash density almost exactly follows the Canadian Shield boundary throughout western Canada.

We want to discuss the Clearwater River region further because it showed one of the strongest signals in our analysis. Figure 6.3 shows the cloud-to-ground lightning flash density and density gradient in each of the strips versus the distance to the Canadian Shield boundary in the Clearwater River region, along with a few other regions. Any sudden change will appear as a spike in the lightning flash density gradient, whereas a steady change will appear as a constant.

Therefore, we need to quantify and compare the magnitude of the spike in the cloud-to-ground lightning flash density gradient relative to the background.

The lightning density gradient in the Clearwater River region near the Canadian Shield boundary was 0.00250 flashes km^{-2} km^{-1} yr^{-1}, while it was 0.00106 flashes km^{-2} km^{-1} yr^{-1} away from it, both with a sample standard deviation of about 0.0012 (Table 6.1). These means are statistically different at the 95% confidence level using all three statistical tests. The results suggest that there is a sharp cloud-to-ground lightning density gradient at the Canadian Shield boundary in the Clearwater River sub-region and that lightning seems to be affected by the Canadian Shield in this region. We can see the sharp gradient on the lightning density map shown in Figure 6.2. However, we need to investigate all regions to determine whether this result is consistent.

Table 6.1 shows our statistical analysis for all the regions. We found that five of our eight regions had statistically significant higher values of cloud-to-ground lightning density gradient near the shield boundary and lower values away from it. Two of the three regions that do not show a statistical significance had large lakes, as expected. This is consistent with the observations reported by Hanuta and LaDochy (1989) and Burrows and Kochtubajda (2010). The Lake Athabasca region did not show statistical significance, while another region where we did not expect to find statistical significance was one of the most significant of all (Lake Winnipeg South). The sudden drop in lightning density also existed regardless of the orientation of the Canadian Shield boundary. The Canadian Shield is oriented mostly east-west in Saskatchewan, while it is mostly north-south in the Tlicho and Lake of the Woods regions. All these regions still showed a sudden drop across the boundary.

We need to take a further look at the two regions that did not produce the expected result: the Lake Athabasca region and the Lake Winnipeg South region. We expected a statistically significant result in the Lake Athabasca region but did not find one. It is tempting to assume that Lake Athabasca was sufficiently large to affect the lightning, but it is located mostly in the Canadian Shield region. The lightning density map (Figure 6.2) shows a sharp lightning density gradient at the north and south ends of the region. However in the middle of the region, the lightning density seems to be more affected by the Peace River Valley, Lake Claire, and the Peace-Athabasca delta wetland system. In fact, the Peace River Valley in northern Alberta has almost half the lightning flashes of the higher terrain areas north and south of it. Both the Caribou and Birch Mountains are known to enhance lightning at the expense of the Peace River Valley. We suspect that the land cover and terrain has a larger influence on the lightning than the Canadian Shield in this region.

Contrary to expectations, we found a statistically significant result in the Lake Winnipeg South region. This region contains a very large lake, but recorded an unexpected statistically significant change in cloud-to-ground lightning flash density across where we think the Canadian Shield boundary should be. However, it appears that the change in lightning density is actually caused by the configuration of the lake. Lake Winnipeg is long and narrow, and positioned parallel to and in line with the Canadian Shield boundary. We think that the lake effect and the Canadian Shield effect both cause a sharp discontinuity in cloud-to-ground lightning flash density. In fact, Figure 6.3 shows that the lightning density steps down twice: once over Lake Manitoba to the west, and again over Lake Winnipeg.

6.4. Possible reasons for the Canadian Shield affecting lightning

We have established that the cloud-to-ground lightning flash density is lower inside the Canadian Shield than outside, and it is statistically significant. We will now investigate three possible reasons for this effect:

1) The same density of lightning flashes may occur on either side of the Canadian Shield boundary, but the CLDN did not detect them for some reason,

2) The sudden change in lightning density is real; the number of thunderstorms has not decreased, but they produce less cloud-to-ground lightning,

3) The sudden change in lightning density is real because there are fewer thunderstorms.

6.4.1) Lightning detection efficiency

Some research hints at the possibility that the CLDN is not detecting lightning flashes in the Canadian Shield, and we need to investigate this. Herodotou et al. (1993) and Scheftic et al. (2008) showed that the lightning waveform received by the detection system is considerably modified by ground with low conductivity, such as rock. This modification results in an increased rise-time to the peak amplitude. In fact, both Scheftic et al. (2008), and Bardo et al. (2004) showed that the southern part of the Canadian Shield in Manitoba and Ontario has much longer waveform rise-times than nearby regions, but their analysis did not cover northern regions in Canada because their map did not extend farther into northern Canada. The ground conductivity map of Canada provided by the International Telecommunications Union (2015) shows that most of the Canadian Shield in Manitoba, Saskatchewan, Alberta, and the Northwest Territories has much lower ground conductivity than adjacent regions. Nag et al. (2015) found that ground conductivity and elevation caused the majority of errors when using the time-of-arrival method,

and Schueler and Thompson (2006) found that incorporating these factors significantly improved accuracy. The CLDN consists of a combination of LPATS-IV, IMPACT, and LS7000 sensors (Burrows and Kochtubajda 2010), all of which, at least partially, use the time-of-arrival detection method (Cummins et al. 2000) and could be susceptible to errors caused by the low ground conductivity of the Canadian Shield.

Inspection of Figure 6.3 suggests that the sharpest density gradient seems to occur over about 50km on either side of the boundary in the Clearwater River and Lake of the Woods region. The lightning flash density changes from about 0.55 to 0.35 flashes km^{-2} yr^{-1} across the Canadian Shield boundary in the Clearwater River region, and it decreases from 0.95 to 0.65 flashes km^{-2} yr^{-1} in the Lake of the Woods region. Thus, the effect of the Canadian Shield seems to cause the detection of 30-40% fewer lightning flashes in these two regions. We found similar numbers in the other regions significantly affected by the Canadian Shield.

We investigated three properties of lightning strokes to determine whether or not the reduced detection efficiency caused by lower ground conductivity could cause such a large amount of lightning flashes to be missed. We looked at: the normalized chi-square error, the waveform rise-time, and the waveform peak-to-zero time (Figure 6.4). The waveform rise-time and peak-to-zero time data were not available before 2011 and were not available in the flash data. Thus, we had to use stroke data for these two properties. We calculated these values in approximately 10 km^2 grid boxes in the peak lightning season. The normalized chi-square error is consistently high in two areas: the Canadian Shield, and the Rocky Mountains. Figure 6.4 also shows much longer waveform rise-times and peak-to-zero times in the Canadian Shield. These values indicate a more distorted waveform with a lower amplitude and more error possibilities, and increase the possibility that a stroke may be rejected by the quality control system. We also

plotted maps, of the semi-major axis of the error ellipse and the number of sensors for each stroke (not shown), but we did not find any relation to geographic features.

To further investigate the possibility of reduced lightning detection efficiency in the Canadian Shield, we looked at the histogram distribution of these three properties in northern Saskatchewan (Figure 6.5). As before, we separated our data into 30-100 km north of the Canadian Shield boundary and 30-100 km south of it. The normalized chi-square values were skewed toward higher values inside the Canadian Shield than outside it, and Cummins et al. (1998) suggested that lightning strokes with a chi-square value greater than 15 would be removed from the database. However, the shape of the distribution suggests that the number of lightning strokes having a value greater than 15 is much lower than 30%. Thus, it is unlikely that this is the cause of the detection efficiency issues. The rise-time and peak-to-zero time values were also skewed toward higher values in the Canadian Shield, suggesting distortion in the lightning waveform. However, we are not convinced that the differences are sufficient to account for as much as a 30-40 % reduction in lightning flashes.

We also found that the effect of the Canadian Shield does not appear in every year. Figure 6.6 shows the yearly effect of the Canadian Shield in the Clearwater River and Lake of the Woods regions. We see that the effect of the Canadian Shield exists in some years, but not all years. However, when we compared the annual average chi-square errors, rise-times, and peak-to-zero times, we found consistently high values in the Canadian Shield in every year (Figure 6.6).

There is, however, some interesting evidence from the Hudson Bay Plains ecozone that suggests that the Canadian Shield affects lightning detection. The Hudson Bay Plains ecozone has a widespread layer of clay and organic matter on top of the Canadian Shield bedrock. The soil data from the Centre for Land and Biological Resources Research (1996) shows a large area of

primarily organic soils in that ecozone; the International Telecommunications Union (2015) shows a corresponding higher ground conductivity (8 mS m^{-1}), and Bardo et al. (2004) report much lower waveform rise-times. Figure 6.4 also shows a lower normalized chi-square error in this region. This evidence suggests that low ground conductivity distorts the waveform and causes the longer rise times and higher chi-square errors, but we still cannot conclude that these effects cause a lower detection efficiency in the Canadian Shield. However, some analysis from Kochtubajda and Burrows (2010) provides further insight. Analysis of the lightning flash multiplicity shows high multiplicity southwest of the Canadian Shield, low multiplicity in the Canadian Shield, and high multiplicity in the Hudson Bay Plains ecozone. Their analysis also shows that lightning flashes with a current greater than 100 kA and a multiplicity greater than 10 primarily occur southwest of the Canadian Shield and in the Hudson Bay Plains (Kochtubajda and Burrows 2010). These results give more weight to the possibility that lightning flashes are missed by the CLDN, but we have no way of knowing if this can account for as much as a 30-40% reduction.

6.4.2) Less cloud-to-ground lightning

Some research has investigated whether land surface variations can affect lightning triggered in thunderstorms. In this case, we are not investigating whether there are fewer thunderstorms, only whether less lightning is produced by those thunderstorms. Tyahla and López (1994) researched the effect of ground conductivity on lightning strokes. They found that the peak current was slightly affected by ground conductivity, but this effect was not statistically significant. Orville and Huffines (2001) found an abrupt change to higher peak currents over saltwater, but could not provide a reason for it. Chisholm et al. (2001) found that lightning density in Ontario was much lower in areas with higher ground resistivity, but did not speculate on the reason. Scott et al. (2014) showed that the amount of lightning is affected by ionizing radiation caused by the solar wind and galactic cosmic rays, so we also briefly speculated that a different

level of terrestrial ionizing radiation may exist in the Canadian Shield. However, we could not find enough evidence that there was a sudden change in the amount of terrestrial radiation in the Canadian Shield. We do not see sufficient evidence in the literature and we do not have any evidence of our own to suggest that cloud-to-ground lightning in thunderstorms is somehow inhibited by the Canadian Shield.

6.4.3) Fewer thunderstorms

We also believe it is possible that the number of thunderstorms could be lower because of a change in land cover and vegetation. The land cover in the Canadian Shield tends to be barren rock, needle-leaf evergreen trees, and deep cold lakes. Betts et al. (2007) showed that these regions tend to have lower transpiration rates. Land cover to the southwest of the Canadian Shield tends to have deeper moister soil, a higher percentage of broadleaf deciduous trees, and fewer deep cold lakes. Betts et al. (2007) showed that these regions tend to have higher transpiration rates. The transpiration rate of broadleaf deciduous trees is particularly high in mid-summer, when the majority of thunderstorms occur. Strong (1997) suggested that transpiration from cropped lands can significantly affect thunderstorms. Barr and Strong (1996) showed that broadleaf deciduous trees transpire somewhat less than cropped land, but still significantly more than needle-leaf evergreen trees.

We think it conceivable that lower transpiration from the sparser needle-leaf forests northeast of the Canadian Shield could contribute to fewer thunderstorms, and could cause existing thunderstorms to dissipate as they cross the boundary. In fact, other researchers have found correlations between lightning activity and vegetation or soil cover. For example, Clodman and Chisholm (1996) found much lower lightning density in non-agricultural areas and the Canadian Shield than in agricultural areas in southern Ontario. Kotroni and Lagouvardos (2008)

found that lightning density in the Mediterranean was influenced by land cover type, and speculated that soil moisture was the driving force. Bourscheidt et al. (2008) found that land cover had some effect on lightning in Brazil, but soil type had little effect there. Mora García et al. (2015) found that both land cover and soils affected lightning density in Spain.

However, to get such a strong sharp effect in lightning along the Canadian Shield boundary, we would need a sudden change in vegetation. No literature has discussed in detail whether this is the case; however, it is likely that the vegetation changes rapidly because the soil types change so rapidly across the boundary (Centre for Land and Biological Resources Research 1996). This effect might be similar to the lightning shadows observed by Burrows and Kochtubajda (2010) downwind of large lakes.

6.5. Discussion and conclusions

After analyzing cloud-to-ground lightning observations between 1999 and 2015, we found that lightning density is related to the Canadian Shield in the following ways:

1) There is a significantly lower cloud-to-ground lightning flash density inside the Canadian Shield than outside of (in most regions 30-40 % less), and most of the change occurs in a band with a width less than 60 km.
2) The sudden change in lightning flash density occurs regardless of geographical location of the boundary, the orientation of the boundary, or the mean lightning flash density in the area.
3) The lightning flash density gradient is steepest in northern Saskatchewan.
4) The Canadian Shield lightning effect is overshadowed in the presence of Great Slave Lake and northern Lake Winnipeg along with areas with more significant topography.

5) The sharp gradient does not necessarily show up in individual years, and there are no temporal trends in the strength of the effect. Many years of data need to be accumulated to see the results.

We established that the cloud-to-ground lightning density drops off near the Canadian Shield boundary throughout western Canada in areas away from large lakes. This finding gives more weight to the idea that the Canadian Shield affects the amount of lightning detected. We found that the strongest effects occurred in northern Saskatchewan and the Lake of the Woods region. Effects in other regions were not as sudden or distinct as in northern Saskatchewan, but were still statistically significant. In fact, the effect was statistically significant in both the Tlicho region and the Lake of the Woods region, even though they are almost 2000 km apart and the Lake of the Woods region has almost ten times as much lightning. The effect occurred regardless of whether the Canadian Shield boundary was oriented north-south or east-west.

We have shown that it is possible that the Canadian Shield reduces the detection efficiency of the CLDN, which is caused by the low ground conductivity of the Canadian Shield region. The low conductivity causes a higher chi-square error, longer waveform rise-times, and a lower waveform amplitude (Bardo et al. 2004, Scheftic et al. 2008), which leads to reduced detection efficiency and higher location error. Data from the Hudson Bay Plains ecozone suggests that this is indeed *part* of what is happening in the Canadian Shield region. The Hudson Bay Plains are farther north and east of the Canadian Shield in Manitoba and Ontario and consist of mostly clay and organic soils (Centre for Land and Biological Resources Research, 1996). In the Hudson Bay Plains region, we found a lower chi-square error, and Kochtubajda and Burrows (2010) reported higher multiplicity and more large current flashes with high multiplicity than in the Canadian Shield. These results indicate that some strokes and flashes are definitely being missed. However, we found 30 to 40 % fewer lightning flashes inside the Canadian Shield, and it is not

obvious whether a lower detection efficiency can account for this much missing lightning. Our investigation of the waveform rise-time and peak-to-zero time distribution makes it difficult to conclude that the lightning network is missing 30 to 40 % of lightning flashes in the Canadian Shield.

A natural question arising from this study is, do other lightning detection networks show the same lightning density change across the Canadian Shield boundary as the CLDN? Cecil et al. (2014) summarized lightning flash density data collected by the Tropical Rainfall Measuring Mission satellite. The data from this satellite only cover our study region from 1995 to 2000, and the spatial resolution is very coarse. There appears to be a lightning density gradient near the Canadian Shield boundary in northern regions, but it is more difficult to distinguish in southern Manitoba and Ontario. Holle (2016) presented lightning stroke density data from the Global Lightning Dataset (GLD360) covering 2011–2014. Again, a change in lightning density appears near the Canadian Shield boundary. However, an area of higher lightning density exists in northern Ontario that is not on any of the other charts. Hutchins et al. (2012) presented lightning stroke density data from the World Wide Lightning Location Network. Again, a similar pattern seems to appear along the Canadian Shield boundary.

One of the findings in this paper is that the Canadian Shield lightning effect does not appear every year. Thus, the short observation periods of the lightning datasets described in the previous paragraph may make detection of the Canadian Shield effect difficult. All three papers cited show that it is possible that the Canadian Shield effect exists in the other networks, but interpretation is difficult. Future research should involve completion of a detailed investigation to compare one or more other lightning networks with the CLDN. Further analysis of other lightning

networks will provide more insight into whether the Canadian Shield effect is an artifact of lightning detection efficiency or whether it is caused by land cover change.

This same effect appears possible in the Rocky Mountains, because the same conductivity, rise-time, and error conditions exist there. However, complex thunderstorm triggering mechanisms would make further study in the Rocky Mountains difficult. It would be very unsettling if 30-40 % of lightning went undetected in the Canadian Shield or in the Rocky Mountains because lightning detection is very important for forest fire detection.

We were unable to find evidence for or against the possibility of reduced cloud-to-ground lightning flashes caused by modification of the charge separation mechanisms. We cannot say whether or not this is possible, but it seems unlikely because no literature has described such an effect. Bourscheidt et al. (2008) suggested that there is insufficient evidence for such an effect yet.

It seems possible that the sudden change in soil (Centre for Land and Biological Resources Research, 1996) across the Canadian Shield boundary causes a sudden change in vegetation and a sudden change in transpiration (Betts et al. 2007). It is reasonable to think that this could reduce the frequency and intensity of thunderstorms in the Canadian Shield simply by reducing the amount of instability, which is similar to the reduction in lightning observed by Burrows and Kochtubajda (2010) downwind of large lakes in Canada. A few examples exist in the literature of land cover or soil type affecting lightning flash density (Bourscheidt et al. 2008, Mora García et al. 2015, and Kotroni and Lagouvardos 2008); thus, it is possible that the land cover change also affects lightning density. Further research would need to be completed to produce more definitive conclusions, because whether or not the sudden land cover change causes sufficient sudden change in weather to influence instability needs to be determined.

We conclude that the Canadian Shield seems to reduce the detected cloud-to-ground lightning flash density by 30 to 40 %. It is likely that the Canadian Shield affects the detection efficiency of the CLDN, but we do not know by how much or whether it is sufficient to account for the observed lightning differences. It seems unlikely that the Canadian Shield affects charge separation processes. However, the Canadian Shield influences soils, and likely vegetation. Thus, it seems possible that the Canadian Shield can influence humidity and thus instability, and can decrease the amount of lightning. Again, we do not know the magnitude of the climatological effect. The most likely scenario is that both detection efficiency and land cover affect the cloud-to-ground lightning density in the Canadian Shield. However, it is difficult to separate the two effects. Both are caused by the same land cover change but the reasons for the reduction in lightning flashes detected are very different.

6.6. Acknowledgements

The authors would like to acknowledge Daniel Poirier, Henri Dagenais, and Saskatchewan Wildfire Management for encouraging work on this project during the time of Daniel Brown's employment with them and also for providing valuable feedback. We would also like to thank Bob Kochtubajda for expert input on the content of the manuscript. We would like to acknowledge support from Environment and Climate Change Canada for providing paid time to work on this project. The CLDN is operated by Vaisala, and the lightning data are the property of Environment and Climate Change Canada. We thank Environment and Climate Change Canada for providing the lightning data from the CLDN, and we thank Ryan Lagerquist for creating the software used to extract data from the lightning database. We also acknowledge the constructive suggestions of the anonymous reviewers that significantly improved this manuscript.

6.7. References

Bardo, E. A., K. L. Cummins, and W. A. Brooks, 2004: Lightning current parameters derived from lightning location systems. *International Conference on Lightning Detection*, Helsinki, Finland.

Barr, A. G., and G. S. Strong, 1997: Estimating regional surface heat and moisture fluxes above prairie cropland from surface and upper air measurements. *Journal of Applied Meteorology*, **35**, 1716-1735, doi:10.1175/1520-0450(1996)035<1716:ERSHAM>2.0.CO;2

Betts, A. K., R. L. Desjardins, and D. Worth, 2007: Impact of agriculture, forest, and cloud feedback on the surface energy budget in BOREAS. *Agricultural and Forest Meteorology*, **142**, 156-169, doi:10.1016/j.agrformet.2006.08.020

Bourscheidt, V., O. Pinto Jr., K. P. Naccarato, I. R. C. A. Pinto, 2008: Dependence of CG lightning density on altitude, soil type, and land surface temperature in south of Brazil, *20th International Lightning Detection Conference*, Tucson, Arizona.

Brimelow, J. C., and G. W. Reuter, 2008: Moisture sources for extreme rainfall events over the Mackenzie Basin. Cold Regions and Hydrologic Studies: The Mackenzie GEWEX Experience, Volume 1, *Atmospheric Dynamics*, edited by M.-K. Woo, pp 127-136, Springer, Berlin.

Brown, D. M., 2012: Analysis of spatial and temporal lightning frequency and patterns in Saskatchewan. *Internal Saskatchewan Ministry of the Environment Report for Wildfire Management*: unpublished. Available on request from the author.

Burrows, W. R., and B. Kochtubajda, 2010: A decade of cloud-to-ground lightning in Canada: 1999-2008. Part 1: Flash Density and occurrence. *Atmosphere-Ocean*, **48**, 3, 177-194, doi:10.3137/AO1118.2010

Cecil, D. J., D. E Buechler, and R. J. Blakeslee, 2014: Gridded lightning climatology from TRMM-LIS and OTD: Dataset description. *Atmospheric Research*, **135-136**, 404-414.

Centre for Land and Biological Resources Research, 1996: Soil Landscapes of Canada, v.2.2. *Research Branch, Agriculture and Agri-Food Canada. Ottawa.*

Chisholm, W. A., S L. Cress, and J. Polak, 2001: Lightning-caused distribution outages. *Proceedings of the IEEE Power Engineering Society Transmission Distribution Conference*, pp. 1041-1046.

Clodman, S., and W. Chisholm, 1996: Lightning flash climatology in the southern great lakes region. *Atmosphere-Ocean*, **32**, 2, 345-377, doi:10.1080/07055900.1996.9649568.

Cummins, K. L., M. J. Murphy, E. A. Bardo, W. L. Hiscox, R. B. Pyle, A. E. Pifer, 1998: A combined TOA/MDF technology upgrade of the U.S. National Lightning Detection Network. *Journal of Geophysical Research*, **103**, D8, 9035-9044.

Cummins, K. L., M. J. Murphy, and J. V. Tuel, 2000: Lightning detection methods and meteorological applications. Preprints, *Fourth International Symposium on Military Meteorology*, Marbork, Poland, WMO, 85-100.

Hanuta, S., and S. LaDochy, 1989: Thunderstorm climatology based on lightning detector data, Manitoba, Canada. *Physical Geography,* **10**, 101-109.

Herodotou, N., W. A. Chisholm, and W. Janichewskyj, 1993: Distribution of lightning peak stroke currents in Ontario using an LLP system. *IEEE Transactions on Power Delivery*, **8**, 3, 1331-1339.

Holle, R. L., 2016: A summary of recent national-scale lightning fatality studies. *Weather, Climate, and Society*, **8**, 35-42.

Hutchins, M. L., R. H. Holzworth, J. B. Brundell, and C. J. Roger, 2012: Relative detection efficiency of the World Wide Lightning Location Network. *Radio Science*, **47**, RS6005.

Illingworth, A. J., 1985: Charge separation in thunderstorms: Small scale processes. *Journal of Geophysical Research*, **90**, D4, 6026-6032, doi:10.1029/JD090iD04p06026.

International Telecommunication Union, 2015: Recommendation ITU-R P.832.4. *World Atlas of Ground Conductivities*, 51 pp.

Kochtubajda, B., and W. R. Burrows, 2010: A decade of cloud-to-ground lightning in Canada: 1998-2008. Part 2: Polarity, multiplicity, and first-stroke peak current. *Atmosphere-Ocean*, **48**, 3, 195-209, doi: 10.3137/AO1119.2010.

Kochtubajda, B., W. R. Burrows, D. Green, A. Liu, K. R. Anderson, and D. McLennan, 2011: Exceptional cloud-to-ground lightning during an unusually warm summer in Yukon, Canada. *Journal of Geophysical Research*, **116**, D21206, 1-20, doi:10.1029/2011JD016080.

Kotroni, V. and K. Lagouvardos, 2008: Lightning occurrence in relation with elevation, terrain slope, and vegetation cover in the Mediterranean. *Journal of Geophysical Research,* **113**, D21118, 1-7, doi:10.1029/2008JD010605.

Kozak, S. A., 1998: Lightning strikes in Alberta thunderstorms: Climatology and case studies. *MSc Thesis*, University of Alberta, 129pp.

Latham, J., 1981: The electrification of thunderstorms. *Quarterly Journal of the Royal Meteorological Society*, **107**, 452, 277-298, doi:10.1002/qj.49710745202.

Lee, A. C. L., 1986: An operation system for the remote detection of lightning flashes using a VLF arrival time difference technique. *Journal of Atmospheric and Oceanic Technology*, **3**, 630-642, doi: 10.1175/1520-0426(1986)003<0630:AOSFTR>2.0.CO;2.

Mills, B., D. Unrau, C. Parkinson, B. Jones, J. Yessis, K. Spring, L. Pentelow, 2008: Assessment of lightning-related fatality and injury risk in Canada. *Natural Hazards*, **47**, 157-183, doi:10.1007/s11069-007-9204-4.

Mora García, M., J. Riesco Martín, L. Rivas Soriano, and F. de Pablo Dávila, 2015: Observed impacts of land uses and soil types on cloud-to-ground lightning in Castilla-Leon (Spain). *Atmospheric Research*, **166**, 233-238.

Nag, A., M. J. Murphy, W. Schulz, and K. L. Cummins, 2015: Lightning locating systems: Insights on characteristics and validation techniques. *Earth and Space Science*, **2**, 65-93, doi:10.1002/2014EA000051.

Orville, R. E., 1991: Calibration of a magnetic direction finding network using measured triggered lightning return stroke peak currents. *Journal of Geophysical Research*, **96**, D9, 17135-17142, doi:10.1029/91JD00611.

Orville, R. E., and Huffines, G. R., 2001: Cloud-to-ground lightning in the United States: NLDN results in the first decade, 1989-1998. *Monthly Weather Review,* **129**, 1179-1193, doi:10.1175/1520-0493(2001)129<1179:CTGLIT>2.0.CO;2.

Reap, R. M. and D. R. MacGorman, 1989: Cloud-to-ground lightning: Climatological characteristics and relationships to model fields, radar observations, and severe local storms. *Monthly Weather Review,* **117**, 518-535, doi:10.1175/1520-0493(1989)117<0518:CTGLCC>2.0.CO;2.

Saunders, C. P. R., 1993: A review of thunderstorm electrification processes. *Journal of Applied Meteorology*, **32**, 642-655, doi:10.1175/1520-0450(1993)032<0642:AROTEP>2.0.CO;2.

Scheftic, W. D., Cummins, K. L., Krider, P. E., Sternberg, B. K., Goodrich, D., Moran, S., Scott, R., 2008: Wide-area soil moisture estimation using the propagation of lightning generated low-frequency electromagnetic signals. *20th International Lightning Detection Conference*, 1-8.

Schueler, J. R. and E. M. Thompson, 2006: Estimating ground conductivity and improving lightning location goodness of fit by compensating propagation effects. *Radio Science*, **41**, RS1001, 1-13, doi:10.1029/2004RS003113.

Scott, C. J., R. G. Harrison, M. J. Owens, M. Lockwood, and L. Barnard, 2014: Evidence for solar wind modulation of lightning, *Environmental Research Letters*, **9**, 1-12, doi:10.1088/1748-9326/9/5/055004.

Sellers, P., F. Hall, H. Margolis, B. Kelly, D. Baldocchi, G. den Hartog, J. Cihlar, M. G. Ryan, B. Goodison, P. Crill, K. J. Ranson, D. Lettermaier, D. E. Wickland, 1995: The boreal ecosystem – atmosphere study (BOREAS): An overview and early results from the 1994 field year. *Bulletin of the American Meteorological Society*, **76**, 9, 1549-1577, doi:10.1175/1520-0477(1995)076<1549:TBESAO>2.0.CO;2.

Shilts, W. W., J. M. Aylsworth, C. A. Kaszycki, and R. A. Klassen, 1987: Canadian Shield. *Geomorphic Systems of North America*, Boulder, Colorado, Geological Society of America, Centennial Volume 2.

Smith, S. B., and M. K. Yau, 1993: The causes of severe convective outbreaks in Alberta. Part I: A comparison of a severe outbreak with two non-severe events and part II: Conceptual model and statistical analysis. *Monthly Weather Review*, **121**, 1099-1133, doi:10.1175/1520-0493(1993)121<1099:TCOSCO>2.0.CO;2.

Soil Classification Working Group, 1998: The Canadian System of Soil Classification, 3rd ed. *Agriculture and Agri-Food Canada Publication 1646,* 187 pp.

Stocks, B. J., J. A. Manson, J. B. Todd, E. M. Bosch, B. M. Wotton, B. D. Amiro, M. D. Flannigan, K. G. Hirsch, K. A. Logan, D. L. Martell, and W. R. Skinner, 2003: Large forest fires in Canada, 1959-1997. *Journal of Geophysical Research*, **108**, D1, 8159, 1-12, doi:10.1029/2001JD000484.

Strong, G. S., 1997: Atmospheric moisture budget estimates of regional evapotranspiration from RES-91. *Atmosphere-Ocean*, **35**, 1, 29-63, doi:10.1080/07055900.1997.9649584.

Taylor, N. M., D. M. L. Sills, J. M. Hanesiak, J. A. Milbrandt, C. D. Smith, G. S. Strong, S. H. Scone, P. J. McCarthy, and J. C. Brimelow, 2011: The understanding severe thunderstorms and Alberta boundary layer experiment (UNSTABLE) 2008. *Bulletin of the American Meteorological Society*, **92**, 6, 739-763, doi:10.1175/2011BAMS2994.1.

Tyahla, L. J., and R. E. López, 1994: Effect of surface conductivity on the peak magnetic field radiated by first return strokes in cloud-to-ground lightning. *Journal of Geophysical Research*, **99**, D5, 10517-10525, doi:10.1029/94JD00384.

Williams, E. R., 1989: The tripole structure of thunderstorms. *Journal of Geophysical Research*, **94**, D11, 13151-13167, doi:10.1029/JD094iD11p13151.

Wilson, J. W., and R. D. Roberts, 2006: Summary of convective storm initiation and evolution during IHOP: Observation and modeling perspective. *Monthly Weather Review*, **134**, 23-47, doi:10.1175/MWR3069.1.

6.8. Figures

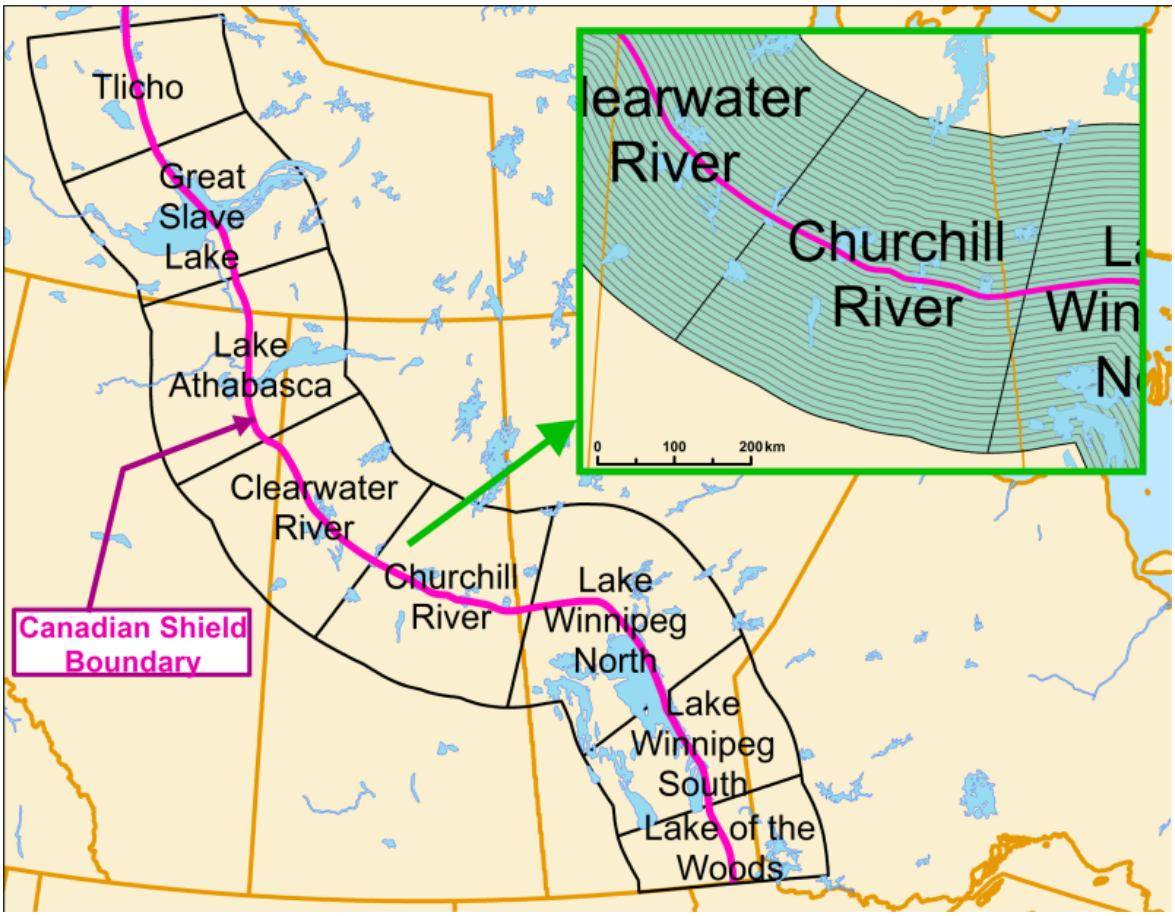

Figure 6.1: Map showing the study region (outlined in black) within 200 km of the Canadian Shield boundary divided into the various regions. The inset map shows the 10 kilometer wide polygon strips that each region was divided into.

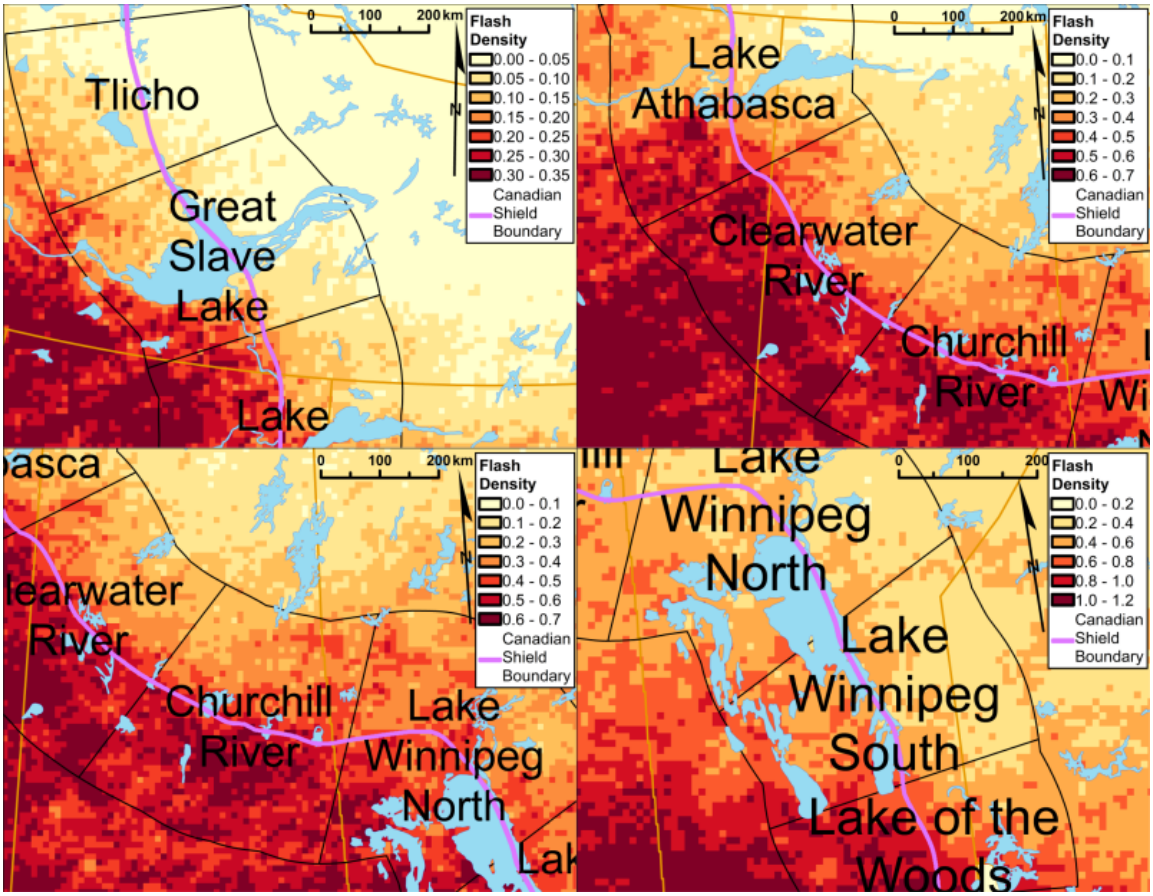

Figure 6.2: Cloud-to-ground lightning flash density (flashes km^{-2} yr^{-1}) from 1999 until 2015 along the Canadian Shield boundary between Great Bear Lake and Lake of the Woods. The Canadian Shield Boundary is identified by the purple line. Upper left: The Northwest Territories. Upper Right: Alberta and Saskatchewan. Lower Left: Saskatchewan and Manitoba. Lower Right: Southern Manitoba. Note that the colour scales had to be different to because of the large variation in lightning density between the northern and southern regions.

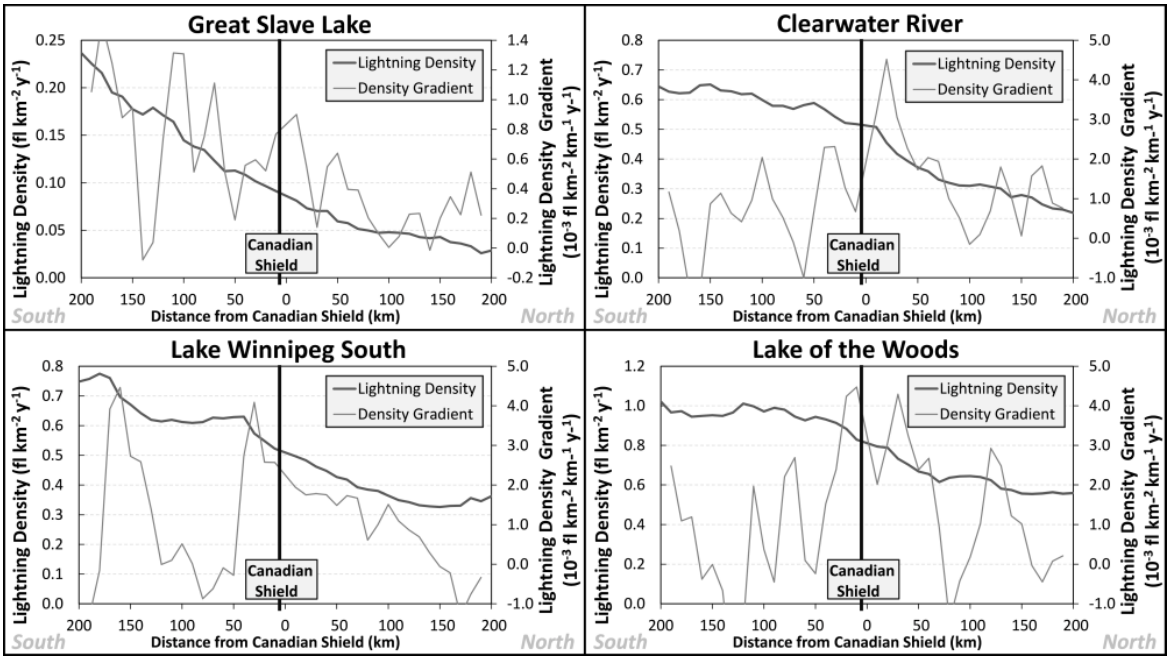

Figure 6.3: Lightning density and density gradient versus distance from the Canadian Shield boundary for selected regions. The units of lightning density are flashes km^{-2} yr^{-1}, and the units of the lightning density gradient are 10^{-3} flashes km^{-2} km^{-1} yr^{-1}. Note that the scales are different on some regions because of the large differences in lightning density between the northern and southern regions.

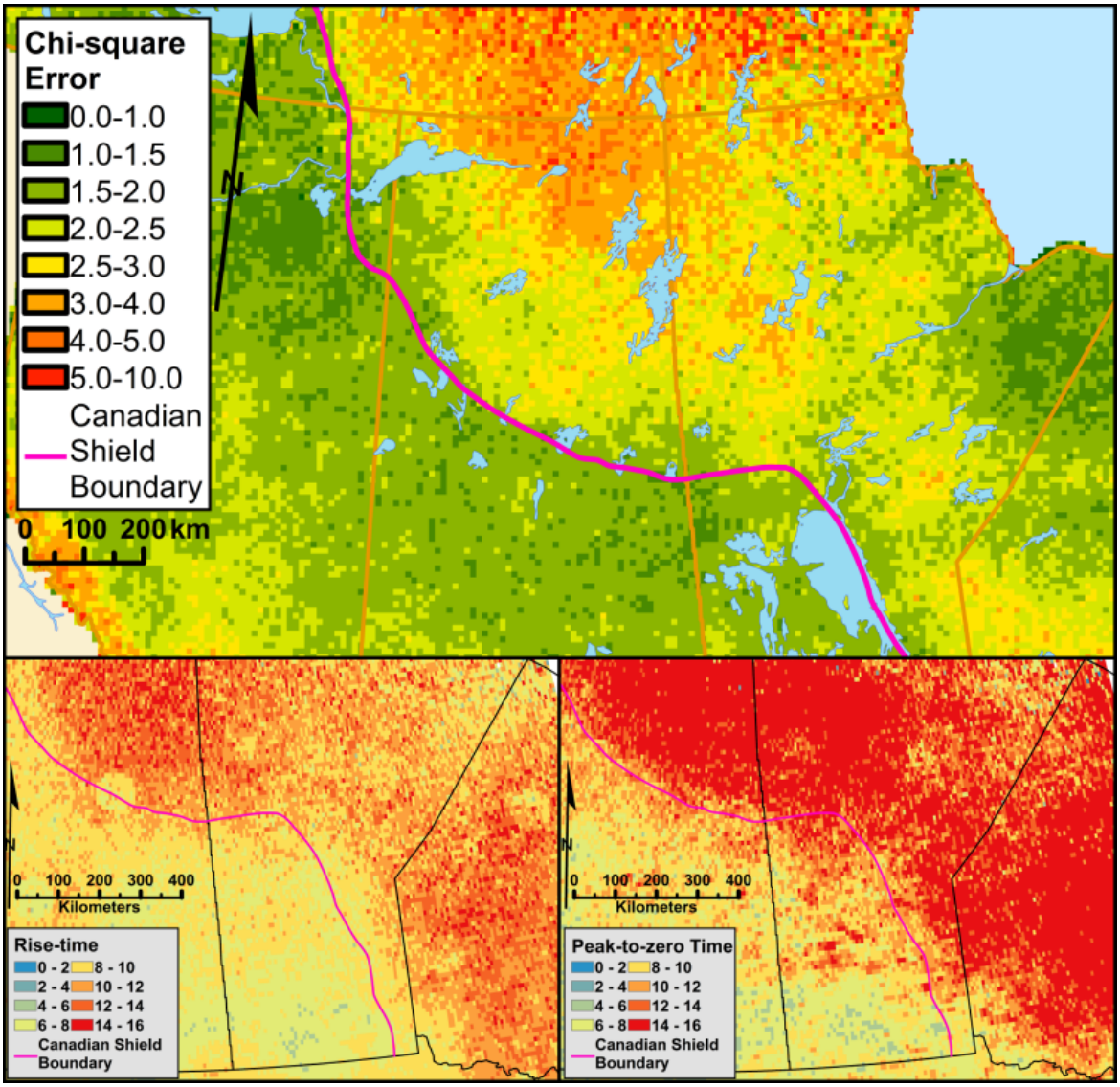

Figure 6.4: Maps of various parameters of lightning flashes and strokes in 10 by 10 km grid boxes the Canadian Shield area. Top: The average normalized chi-square error from 1999-2015. Bottom-left: The waveform rise-time (μs) from 2011-2015. Bottom-right: The waveform peak-to-zero time (μs) from 2011-2015.

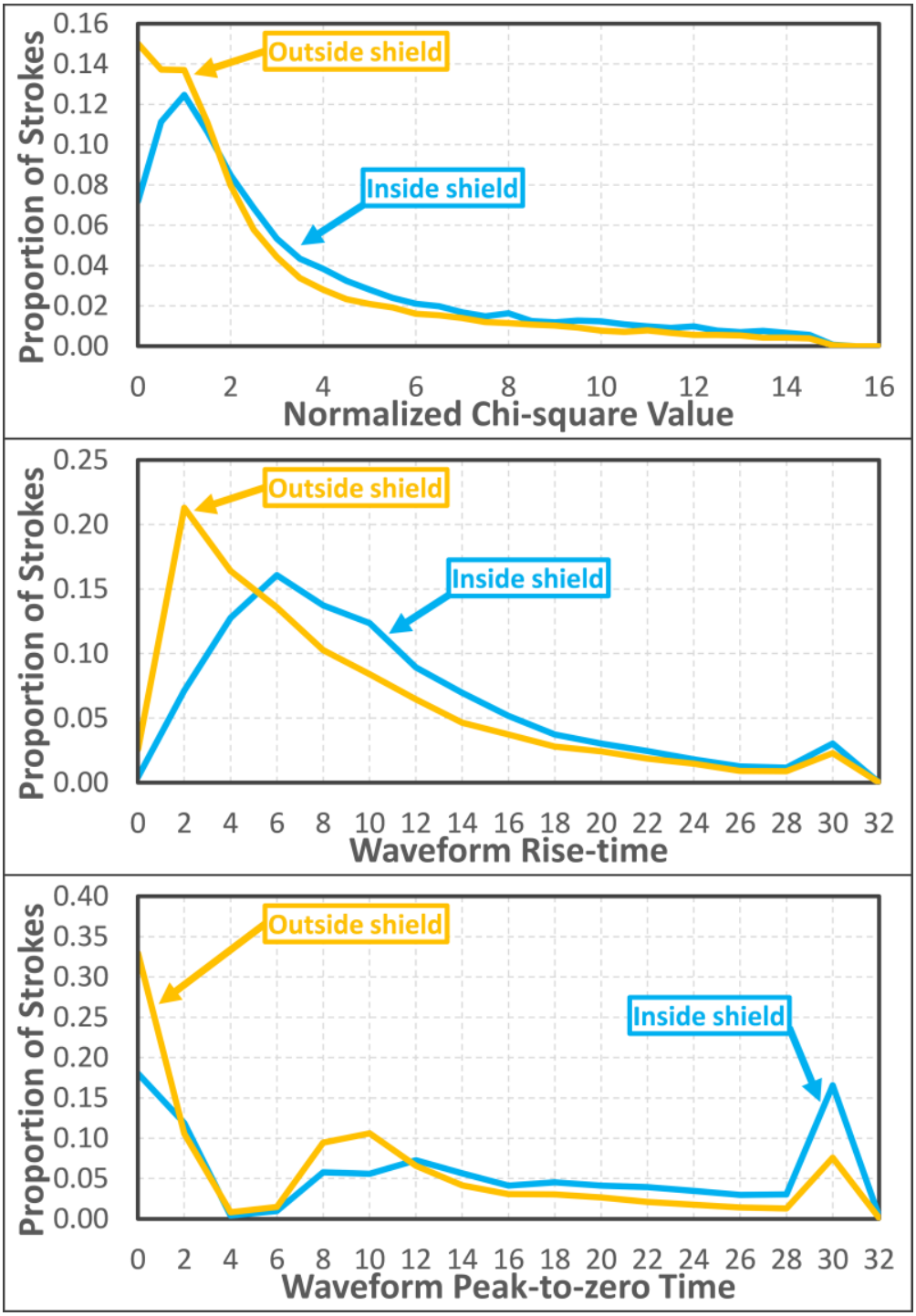

Figure 6.5: Histograms of various lightning stroke parameters within and outside of the Canadian Shield. Top: Normalized chi-square value. Middle: Waveform rise-time (μs). Bottom: Waveform peak-to-zero time (μs).

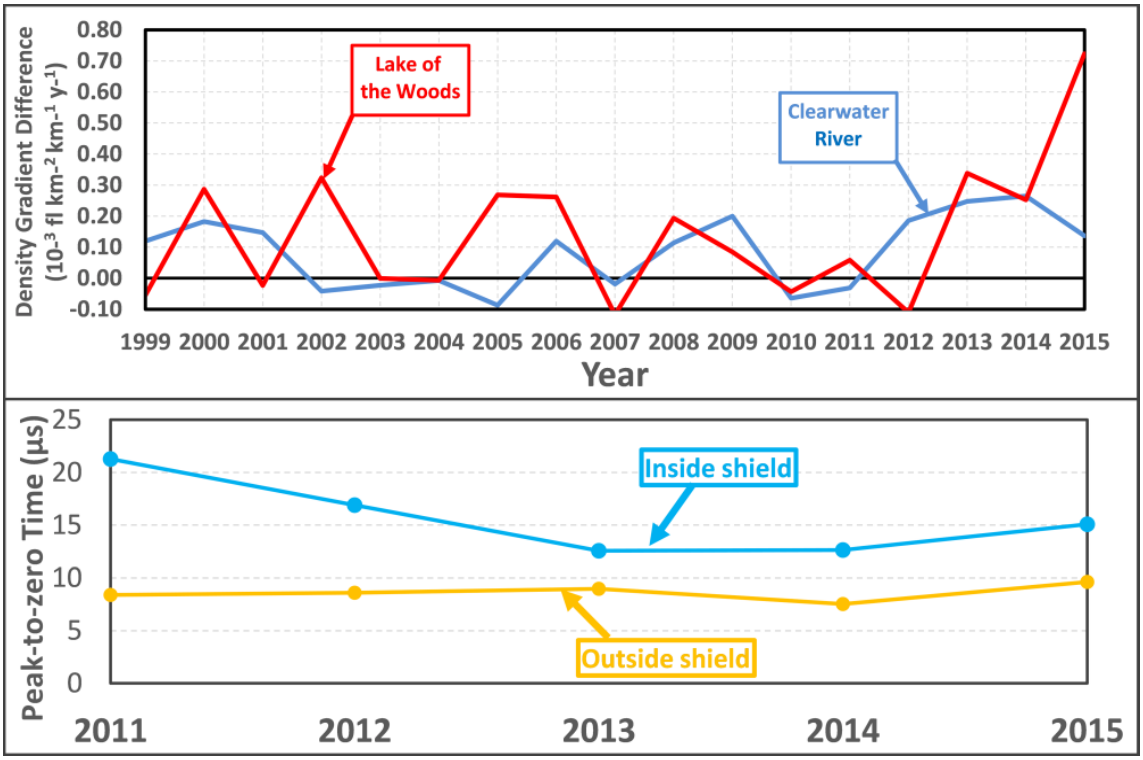

Figure 6.6: Top: Lightning flash density gradient difference (10^{-3} flashes km^{-2} km^{-1} yr^{-1}) between areas within 30 km (near) of the Canadian Shield boundary, and areas between 30 and 100 km (away) from the boundary. Bottom: For each available year, the average peak-to-zero time (µs) within the Canadian Shield and outside of it is plotted.

6.9. Tables

	Tlicho	Great Slave Lake	Lake Athabasca	Clearwater River	Churchill River	Lake Winnipeg North	Lake Winnipeg South	Lake of the Woods
Mean Near	0.47	0.58	1.21	2.50	2.34	0.84	2.45	3.41
Mean Away	0.22	0.52	0.99	1.06	0.80	0.89	0.80	0.98
Mean Ratio	2.1	1.1	1.2	2.4	2.9	0.9	3.1	3.5
σ Near	0.30	0.26	1.06	1.39	1.23	0.59	0.88	1.07
σ Away	0.14	0.36	1.38	1.03	1.06	0.77	1.07	1.46
T Statistic	1.94*	0.43	0.39	2.28*	2.68*	-0.16	3.59*	4.15*
U Statistic	19*	32	39	15*	13*	39	6*	21*
KS Statistic	0.690*	0.262	0.262	0.667*	0.500	0.238	0.762*	0.643

Table 6.1: Various statistical analyses of the mean cloud-to-ground lightning density gradient near the Canadian Shield boundary. The units on the means and standard deviations are 10^{-3} flashes km^{-2} km^{-1} yr^{-1}. The mean ratio is the ratio of the mean near the Canadian Shield divided by the mean away from it. In the last three rows, statistically significant values at the 0.05 threshold are identified by an asterisks. The one-tailed t-statistic requires values greater than 1.73 to be significant. The one tailed U-statistic requires values less than 21 to be significant. The KS statistic requires values greater than 0.664 to be significant.

7. Discussion and conclusions

Thunderstorm development in boreal forest regions is influenced by surface land cover variations, including lake breezes and orographic effects. In this thesis, the role of the Athabasca oils sands development (a human made effect) and the Canadian Shield bedrock (a natural effect) in thunderstorm development is examined. There is evidence from other geographical regions that similar land cover variations stimulate the formation of thunderstorms (Steiger and Orville 2003, Raddatz 1998). The findings as reported in this thesis present compelling evidence that the Canadian Shield affects thunderstorms, and some evidence that the oil sands development could affect thunderstorms under rare circumstances.

The Athabasca oil sands development uses large amounts of energy and creates a massive land surface disturbance (Kelly et al. 2009). Anthropogenic land disturbances in other regions have been shown to affect thunderstorm initiation. For example, large cities often enhance lightning at the city centre (Westcott 1995). Concentrations of oil refineries sometimes modify thunderstorms (Steiger et al. 2002). However, no one has investigated the effect of the oil sands development on thunderstorm initiation and development prior to this thesis. In fact, there was very little research at all on the effect of large industrial developments in boreal forest regions. Most research is performed farther south in the United States. The effects of industry on thunderstorm development may not be the same as in other regions given the differing latitude, surface weather conditions, atmospheric instability, and thunderstorm season. A portion of this thesis investigated how the oil sands development can affect thunderstorms. It is separated into two papers: one using past observations and another using numerical modelling.

To the east of Fort McMurray and the oil sands development, a sharp change in land cover and geology occurs: deeper soil supporting lusher vegetation to the southwest suddenly changes

to exposed Canadian Shield bedrock with sparser vegetation to the northeast. The boundary marking the start of the Canadian Shield runs from Great Bear Lake in the Northwest Territories southeastward to Lake of the Woods in Manitoba. Corn fields (Carleton et al. 2008), land cover boundaries (Brown and Arnold 1998), lake edges (King et al. 2003), and topography (Thielan and Gadian 1997) have been shown to affect thunderstorms. However, no one has examined how the Canadian Shield boundary affects thunderstorms. The thunderstorm dataset with the most consistent coverage in the Canadian Shield region is cloud-to-ground lightning detection. Using lightning detection as a proxy for thunderstorms is more complicated because the surface conductivity of the Canadian Shield bedrock could also interfere with lightning detection (Bardo et al. 2004). This thesis investigated differences in cloud-to-ground lightning between areas in the Canadian Shield and those away from it.

7.1. Modification of past temperature, precipitation, and lightning by the oil sands development

Chapter 3 showed that the oil sands development does not affect precipitation or lightning climatology. This finding was surprising because other researchers have found that urban areas or large industrial facilities do have an effect on lightning and precipitation (Changnon et al. 1976, Steiger et al. 2002, Steiger and Orville 2003). However, the oil sands development did affect the temperature and humidity at a weather station near the oil sands development. Specifically, the temperature increased and the humidity decreased at the oil sands weather station compared to a station away from the oil sands development as the amount of oil sands development increased over time. This effect appears to be partially due to a lower Bowen ratio caused by the massive surface land disturbance in the oil sands development, which removed the

boreal forest vegetation and left mostly barren land. It could also be partly due to the emission of industrial waste heat from bitumen upgrading and processing in the oil sands development, however it was difficult to separate the two effects due to the lack of observations.

This research showed that oil sands development does not have a statistically significant effect on lightning and precipitation climatology. However, the existence of a heat island and dry island could sporadically affect individual thunderstorms. Urban heat islands and urban dry islands have been shown to affect individual thunderstorms in the Midwestern United States (Schmid and Niyogi 2013). If the oil sands development affected individual thunderstorms only occasionally, it might not statistically significantly affect the climatology given the short study timescale. Thus, in Chapter 4, a numerical model was used to simulate the effect of the oil sands development on thunderstorm initiation and development on individual case study days.

7.2. Case studies of numerical model simulations of thunderstorms near the oil sands development

The numerical modelling study in Chapter 4 used sensitivity experiments to examine ten individual thunderstorm case studies near the oil sands development. The criteria for selecting case study days were: convective instability, weak synoptic scale forcing, and observations of thunderstorm occurrence. The Weather Research and Forecasting Model (WRF) (Shamarock et al. 2008) was used with a new module to include waste heat from the oil sands in WRF. Each case study day had four simulations: a simulation with no effects of the oil sands development, a simulation with only the waste heat activated, a simulation with only the land disturbance activated, and a simulation with both activated at the same time. Factor separation, which is used

in this study, is a common technique to quantify differences in the results of numerical model sensitivity experiments (Stein and Alpert 1993).

The results of the numerical modelling study showed that the oil sands did not have a dramatic impact on thunderstorm initiation and development in most cases. When the oil sands development was activated in the numerical model, the initiation time of thunderstorms was significantly impacted in only two of the ten case studies, and the thunderstorm intensity was not affected at all. On those two days, the oil sands development mostly affected the timing of the thunderstorm initiation, suggesting that the oil sands development primarily affects thunderstorm triggering. There was little evidence that thunderstorm intensity was affected. The factor separation results showed that the effect of land cover was slightly more significant compared to the effect of the waste heat. When both were activated together, the initiation time was about the same as when either one was activated alone. Commercial aircraft measurements were used to investigate why specifically those two days affected thunderstorm initiation but the other days did not. When thunderstorm initiation was strongly affected, aircraft measurements indicated considerable mid-level instability (specifically, the 850-500 mb temperature difference was greater than 30 °C). The results were similar whether the mid-level instability was calculated using model data or aircraft measurements.

It is interesting that the oil sands development had such a little effect on thunderstorms, in contrast to previous findings that industrial facilities impact thunderstorm development (Steiger and Orville 2003, Guan and Reuter 1995). The strength of the effect is likely related to the amount of convective instability in the atmosphere, which depends on many factors, including the amount of humidity. Thus it is possible that more southern regions may have more days with sufficient humidity and instability and can thus influence thunderstorms more often.

7.3. The effect of the Canadian Shield on cloud-to-ground lightning density

The study in Chapter 5 showed that a sharp gradient in detected cloud-to-ground lightning density exists along the Canadian Shield boundary. The sudden drop-off in cloud-to-ground lightning density exists along the boundary from Great Bear Lake in the Northwest Territories to Lake of the Woods in Manitoba/Ontario/Minnesota regardless of latitude, cloud-to-ground lightning flash density, or orientation of the boundary. If the cloud-to-ground lightning density changed drastically at the Canadian Shield, a spike in the lightning density gradient should exist. A variety of statistical analysis shows that the lightning flash density gradient near the Canadian Shield boundary is higher than that away from it, and that difference is statistically significant. However in regions with large lakes, the result was not statistically significant because the lake shadowing effect overpowered the Canadian Shield effect. In the regions that were statistically significant, 30-40 percent less lightning occurred in the Canadian Shield region than outside of it.

Two plausible reasons for this effect were proposed: less lightning is detected in the Canadian Shield, or less thunderstorms occur in the Canadian Shield. It is possible that less lightning is detected because the low conductivity of the ground surface causes timing errors in the lightning detection system and reduces the peak current. This would cause more lightning strokes to be rejected by the quality control system (Nag et al. 2015). An analysis of the normalized chi-square lightning location errors, the waveform rise-time, and the waveform peak-to-zero time suggests that detection efficiency could be partially responsible for the observed differences in lightning density. However, further analysis suggested that it is unlikely that the lower detection efficiency could be responsible for 30-40 percent fewer flashes. Thus, it is also possible that less thunderstorms occur because the land cover changes so drastically at the Canadian Shield boundary. The area southwest of the Canadian Shield consists of deeper, more

developed soils supporting lusher, higher transpiring vegetation. The Canadian Shield is mostly exposed bedrock with poorly developed soils supporting sparser, lower transpiring vegetation with many lakes (Sellers et al. 1995). This land cover change suggests a sharp gradient in surface heat and humidity, and thus instability. The Canadian Shield had a much larger effect on thunderstorms than was expected, and this may be partially due to the unexpected effect of the Canadian Shield bedrock on lightning detection efficiency.

7.4. Discussion

Similar to the more heavily studied agricultural areas in southern Canada and the United States, the previous research has demonstrated that artificial and natural land cover variations in the boreal forest can affect thunderstorms. However, the oil sands development did not affect thunderstorms to the extent that was expected. This finding was surprising because the oil sands development has such a large-scale ground disturbance. In other regions, disturbances with a much smaller footprint, such as the refineries in Lake Charles, Louisiana, had much more significant impacts on thunderstorms (Steiger and Orville 2003). Conversely, the Canadian Shield influenced lightning much more significantly than expected. This finding might be partially due to reduced lightning detection efficiency in the Canadian Shield. However, there was not enough evidence to show that the reduction in lightning detection efficiency in the Canadian Shield could account for all of the reduction in cloud-to-ground lightning density. Some of it also appeared to be related to the change in land cover, similar to results by Raddatz (1998) and Dow and DeWalle (2000).

Part of the difference between the oil sands results and the Canadian Shield results may arise from the direction of the effect that the studies were trying to show. The oil sands

development research was trying to show that the oil sands could *enhance* thunderstorms. However, the boreal climate might not be conductive to thunderstorm enhancement because it is significantly cooler and drier, and has a shorter, less intense thunderstorm season than the locations of the studies in the United States. In fact, it was difficult to find many days that were unstable enough for strong thunderstorms that were not associated with a strong cold front. However, the research on the Canadian Shield was trying to show that it could *dissipate* thunderstorms. The Canadian Shield is filled with deep cold lakes and sparse low-transpiring vegetation, which seemed to inhibit thunderstorms. Since thunderstorms in boreal regions are often marginal air-mass thunderstorms, it might take only a little forcing to dissipate them; thus, the relatively strong signal from the Canadian Shield research.

7.5. Implications for the future

New or expanding industries may want to consider the results of this thesis on the oil sands development (Chapters 3 and 4) and plan for the possibility of inadvertent weather modification. In fact, many expansion projects are planned at the oil sands development in Alberta that could double the size of the land disturbance (Kelly et al. 2009). These could have greater impacts on the weather and thunderstorms. Modelling experiments (not shown) suggest that much larger amounts of waste heat can influence thunderstorms much more near the oil sands development in cases where thunderstorms already seem prone to modification. Both the land cover disturbance and the emission of waste heat should be considered when planning for inadvertent weather modification because the results found that both are about equally important. Thus, a large land disturbance with very little waste heat emissions (such as a large bare field) could have as much of an impact on weather modification as a large oil refinery with a

relatively small land disturbance, but with very high waste heat emissions. However, combining the two might not have a much larger effect than one or the other.

The results from Chapter 5 add to the literature suggesting that variations in land cover can affect thunderstorms. In this case, a geological variation induced a vegetation variation which in turn induced a surface weather variation and influenced the instability available to thunderstorms. Further research should be performed on other land cover boundaries. However, a more significant finding from Chapter 5 may be the possibility of reduced lightning detection efficiency in the Canadian Shield. The reduced lightning detection efficiency in the Canadian Shield *must* be considered for activities that rely on lightning data, such as forest fire detection, public safety, and damage to electrical power infrastructure. Further research should be initiated to investigate how much of the Canadian Shield lightning effect is due to detection efficiency issues, and how can these issues be resolved. Accurate lightning detection in the boreal forest is vital for predicting and investigating forest fires, especially in the more remote Canadian Shield regions.

7.6. Recommendations for future research

The research that has been presented in this thesis has answered some questions about how variations in land cover affect thunderstorms in the boreal forest. However, it has also created more questions, and more possibilities for further research. Some of these questions and research possibilities will be presented here. This section is far from a comprehensive list of all research that needs to be done, but it addresses some of the key questions that arose from this research.

Because the oil sands development causes thunderstorm enhancement in some situations, it is worth investigating whether other large scale artificial surface disturbances or releases of waste heat and moisture in the boreal forest could do the same. However, there are few projects in the North American boreal forest that can compare in magnitude with the oil sands development. There are a number of large open pit mines in the Northwest Territories that may have some impact on weather modification. Additionally, there has been substantial clearing of the boreal forest in northwestern Alberta for agricultural purposes. There are also some areas (such as near Edmonton, Alberta) with concentrations of oil refineries that emit waste heat. These refineries have been shown to have an effect on winter snowfall (Charlton and Park 1984), but no studies have specifically looked at summer thunderstorms.

One of the surprising results from this thesis was the minor impact of the oil sands development on thunderstorms in the boreal forest. The results from Chapter 4 found that when the oil sands development did modify thunderstorms, there was a very steep mid-level temperature lapse rate. Thus, a natural extension of this study would be to find whether steep mid-level lapse rates exist more often in Houston or Louisiana where thunderstorms are known to be modified much more by industrial developments. These weather conditions exist only a few days per year in Fort McMurray, which was a major contributor to the difficulty finding suitable case study days. However, their frequency in more southern locations has not been catalogued. Histories of atmospheric soundings from various locations could be used to find out how often the conditions conductive to industrial thunderstorm enhancement exist in various locations.

The possibility of a lower lightning detection efficiency in the Canadian Shield needs to be investigated further. The number of lightning strokes that are rejected by quality control methods needs to be analyzed to compare Canadian Shield regions with regions outside, but currently this data is not available from the proprietary lightning detection systems. However, it is very

important to know whether the reduced cloud-to-ground lightning is an artefact of the lightning detection system or a real phenomenon. The future research should determine how much lightning is not being detected, and should devise techniques for increasing the detection efficiency in high resistivity ground environments. These data should be investigated using a variety of lightning detection networks, such as the Pelmorex network, the Earth Networks network, or the GLD360 long-range network.

Given that there is an actual change (i.e. the change is not just an artefact of the detection efficiency of the network) in lightning density across the Canadian Shield boundary, then further analysis of weather could provide some clues to the origin of that change. There are enough fire weather stations along the Canadian Shield boundary to explore temperature and humidity gradients in the vicinity. These stations may be sufficient to ascertain the changes in weather conditions along the boundary, but for more detail it may be necessary to install a mesonet of weather stations along the Canadian Shield boundary in the most affected area in Saskatchewan. This method should be able to capture the small-scale variation that occurs along the boundary.

7.7. References

Bardo, E. A., K. L. Cummins, and W. A. Brooks, 2004: Lightning current parameters derived from lightning location systems. *International Conference on Lightning Detection*, Helsinki, Finland.

Brown, M. E., and D. L. Arnold, 1998: Land-surface – atmosphere interactions associated with deep convection in Illinois. *International Journal of Climatology*, **18**, 1637-1653.

Carleton, A. M., D. J. Travis, J. O. Adegoke, D. L. Arnold, and S. Curran, 2008: Synoptic circulation and land surface influences on convection in the Midwest U.S. "Corn Belt" during the summers of 1999 and 2000. Part II: Role of vegetative boundaries. *Journal of Climate*, **21**, 3617-3640. DOI: 10.1175/2007JCLI1584.1

Changnon, S. A. Jr., R. G. Semonin, and F. A. Huff, 1976: A hypothesis for urban rainfall anomalies. *Journal of Applied Meteorology*, **15**, 544-560.

Charlton, R. B., and C. Park, 1984: Observations of industrial fog, cloud, and precipitation on very cold days. *Atmosphere-Ocean*, **22**, 1, 106-121.

Dow, C. L. and D. R. DeWalle, 2000: Trends in evaporation and Bowen ratio on urbanizing watersheds in eastern United States. *Water Resources Research*, **36**, 7, 1835-1843.

Guan, S., and G. W. Reuter, 1995: Numerical simulation of a rain shower affected by waste energy released from a cooling tower complex in a calm environment. *Journal of Applied Meteorology*, **34**, 131-142. DOI: 10.1175/1520-0450-34.1.131.

Kelly, E. N., J. W. Short, D. W. Schindler, P. V. Hodson, M. Ma, A. K. Kwan, and B. L. Fortin, 2009: Oil sands development contributes polycyclic aromatic compounds to the Athabasca River and

its tributaries. *Proceedings of the National Academy of Science*, 106, **52**, 22346–22351. DOI: 10.1073/pnas.0912050106.

King, P. W. S., M. J. Leduc, D. M. L. Sills, N. R. Donaldson, D. R. Hudak, P. Joe, and B. P. Murphy, 2003: Lake breezes in southern Ontario and their relation to tornado climatology. *Weather and Forecasting*, **18**, 795-807.

Nag, A., M. J. Murphy, W. Schulz, and K. L. Cummins, 2015: Lightning locating systems: Insights on characteristics and validation techniques. *Earth and Space Sciences*, **2**, 65-93.

Raddatz, R. L., 1998: Anthropogenic vegetation transformation and the potential for deep convection on the Canadian Prairies. *Canadian Journal of Soil Science*, **78**, 4, 657-666.

Schmid, P. E., and D. Niyogi, 2013: Impact of city size on precipitation-modifying potential. *Geophysical Research Letters*, **40**, 5263-5267.

Sellers, P., F. Hall, H. Margolis, B. Kelly, D. Baldocchi, G. den Hartog, J. Cihlar, M. G. Ryan, B. Goodison, P. Crill, K. J. Ranson, D. Lettermaier, D. E. Wickland, 1995: The boreal ecosystem – atmosphere study (BOREAS): An overview and early results from the 1994 field year. *Bulletin of the American Meteorological Society*, **76**, 9, 1549-1577.

Shamarock, W. C., J. B. Klemp, J. Dudhia, D. O. Gill, D. M Barker, M. G. Duda, X.-Y. Huang, W. Wang, and J. G. Powers, 2008: A description of the Advanced Research WRF Version 3. *NCAR Technical Note.*

Steiger, S. M., and R. E. Orville, 2003: Cloud-to-ground lightning enhancement over southern Louisiana. *Geophysical Research Letters*, **30**, 1975, DOI: 10.1029/2003GL017923.

Steiger, S. M., R. E. Orville, and G. Huffines, 2002: Cloud-to-ground lightning characteristics over Houston, Texas: 1989-2000. *Journal of Geophysical Research*, **107**, 4117, DOI: 10.1029/2001JD001142.

Stein, U. and P. Alpert, 1993: Factor separation in numerical simulations. *Journal of the Atmospheric Sciences*, **50**, 14, 2107-2115. doi:10.1175/1520-0469(1993)050<2107:FSINS>2.0.CO;2.

Thielan, J., and A. Gadian, 1997: Influence of topography and urban heat island effects on the outbreak of convective storms under unstable meteorological conditions: A numerical study. *Meteorology Applications*, **4**, 139-149.

Westcott, N. E., 1995: Summertime cloud-to-ground lightning activity around major Midwestern urban areas. *Journal of Applied Meteorology*, **34**, 1633-1642.

References

Alberta Agriculture and Forestry, 2016: Lightning Detection. Accessed 27 August 2016. [Available online at http://wildfire.alberta.ca/fire-weather/lightning-detection/default.aspx.]

Alpert, P, and T. Sholokhman, 2011: *Factor Separation in the Atmosphere.* Cambridge University Press. New York, 274 pp.

Ashley, W. S., M. L. Bentley, and T. Stallins, 2012: Urban induced thunderstorm modification in the southeast United States. *Climatic Change*, **113**, 481-498.

Baik, J. J., Y. H. Kim, J. J. Kim, and J. Y. Han, 2007: Effects of boundary-layer stability on urban heat island-induced circulation. *Theoretical and Applied Climatology*, **89**, 73-81. DOI: 10.1007/s00704-006-0254-4.

Baldocchi, D. D., and C. A. Vogel, 1997: Seasonal variation of energy and water vapor exchange rates above and below a boreal jack pine forest canopy. *Journal of Geophysical* Research, **102**, D24, 28939-28951.

Bardo, E. A., K. L. Cummins, and W. A. Brooks, 2004: Lightning current parameters derived from lightning location systems. *International Conference on Lightning Detection*, Helsinki, Finland.

Barr, A. G., and A. K. Betts, 1997: Radiosonde boundary layer budgets above a boreal forest. *Journal of Geophysical Research*, **102**, D24, 29205-29212.

Barr, A. G., A. K. Betts, R. L. Desjardins, and J. I. MacPherson, 1997: Comparison of regional surface fluxes from boundary-layer budgets and aircraft measurements above boreal forest. *Journal of Geophysical Research*, **102**, D24, 29213-29218.

Barr, A. G., and G. S. Strong, 1997: Estimating regional surface heat and moisture fluxes above prairie cropland from surface and upper air measurements. *Journal of Applied Meteorology*, **35**, 1716-1735.

Benjamin, S. B., B. E. Schwartz, and R. E. Cole, 1999: Accuracy of ACARS wind and temperature observations determined by collocation. *Weather and Forecasting*, **14**, 1032-1038.

Betts, A. K., R. L. Desjardins, and D. Worth, 2007: Impact of agriculture, forest, and cloud feedback on the surface energy budget in BOREAS. *Agriculture and Forest Meteorology*, **142**, 156-169.

Blitzortung, 2016: Network for lightning and thunderstorms in real time. Accessed 27 August 2016. [http://en.blitzortung.org/contact.php.]

Bornstein, R. and Q. Lin, 2000: Urban heat islands and summertime convective thunderstorms in Atlanta: Three case studies. *Atmospheric Environment*, **34**, 507-516.

Bourscheidt, V., O. Pinto Jr., K. P. Naccarato, I. R. C. A. Pinto, 2008: Dependence of CG lightning density on altitude, soil type, and land surface temperature in south of Brazil. *20th International Lightning Detection Conference*, Tucson, Arizona.

Brimelow, J. C., J. M. Hanesiak, and W. R. Burrows, 2011a: On the surface-convection feedback during drought periods on the Canadian Prairies. *Earth Interactions*, **15**, 1-26.

Brimelow, J. C., J. M. Hanesiak, and W. R. Burrows, 2011b: Impacts of land-atmosphere on deep, moist convection on the Canadian Prairies. *Earth Interactions*, **15**, 1-29.

Brimelow, J. C., and G. W. Reuter, 2008: Moisture sources for extreme rainfall events over the Mackenzie Basin. Cold Regions and Hydrologic Studies: The Mackenzie GEWEX Experience, Volume 1, *Atmospheric Dynamics*, edited by M.-K. Woo, pp 127-136, Springer, Berlin.

Brown, D. M., 2012: Analysis of spatial and temporal lightning frequency and patterns in Saskatchewan. Internal Report for the Saskatchewan Ministry of the Environment.

Brown, D. M., G. W. Reuter, and T. K. Flesch, 2011: Temperature, precipitation, and lightning modification in the vicinity of the Athabasca oil sands. *Earth Interactions*, **15**, 1–14. DOI: 10.1175/2011EI412.1.

Brown, M. E., and D. L. Arnold, 1998: Land-surface – atmosphere interactions associated with deep convection in Illinois. *International Journal of Climatology*, **18**, 1637-1653.

Bryan, G. H., J. C. Wyngaard, and J. M. Fritsch, 2003: Resolution requirements for deep moist convection. *Monthly Weather Review*, **131**, 2394-2416. DOI: 10.1175/1520-0493(2003)131<2394:RRFTSO>2.0.CO;2

Bürgesser, R. E., R. G. Pereyra, and E. E. Avila, 2006: Charge separation in updraft region of convective thunderstorms. *Geophysical Research Letters*, **33**, L03808, 1-4.

Burrows, W. R., P. King, P. J. Lewis, B. Kochtubajda, B. Snyder, and V. Turcotte, 2002: Lightning occurrence patterns over Canada and adjacent United States from lightning detection network observations. *Atmosphere-Ocean*, **40**, 1, 59-81.

Burrows, W. R., and B. Kochtubajda, 2010: A decade of cloud-to-ground lightning in Canada: 1999-2008. Part 1: Flash Density and occurrence. *Atmosphere-Ocean*, **48**, 3, 177-194.

Caranti, G. M., E. E. Avila, and M. A. Ré, 1991: Charge transfer during individual collisions in ice growing from vapor deposition. *Journal of Geophysical Research*, **96**, D8, 15365-15375.

Carleton, A. M., D. J. Travis, J. O. Adegoke, D. L. Arnold, and S. Curran, 2008: Synoptic circulation and land surface influences on convection in the Midwest U.S. “Corn Belt” during the

summers of 1999 and 2000. Part II: role of vegetative boundaries. *Journal of Climate*, **21**, 3617-3640.

Cecil, D. J., D. E. Buechler, and R. J. Blakeslee, 2014: Gridded lightning climatology from TRMM-LIS and OTD: Dataset description. *Atmospheric Research*, **135-136**, 404-414.

Centre for Land and Biological Resources Research, 1996: Soil Landscapes of Canada, v.2.2. *Research Branch, Agriculture and Agri-Food Canada. Ottawa.*

Changnon, Jr., S. A., R. G. Semonin, and F. A. Huff, 1976: A hypothesis for urban rainfall anomalies. *Journal of Applied Meteorology*, **15**, 544-560.

Charlton, R. B., B. M. Kachman, and L. Wojtiw, 1995: Urban hailstorms: A view from Alberta. *Natural Hazards*, **12**, 29-75.

Charlton, R. B., and C. Park, 1984: Observations of industrial fog, cloud, and precipitation on very cold days. *Atmosphere-Ocean*, **22**, 1, 106-121.

Charpentier, A. D., J. A. Bergerson, and H. L. MacLean, 2009: Understanding the Canadian oil sands industry's greenhouse gas emissions. *Environmental Research Letters*, **4**, 1-11.

Chen, F., and J. Dudhia, 2001: Coupling an advanced land surface hydrology model with the Penn State-NCAR MM5 modelling system. *Monthly Weather Review*, **129**, 569-604.

Chen, F., K. Mitchell, J. Schaake, Y. Zue, H.-L. Pan, V. Koren, Q. Y. Duan, M. Ek, and A. Betts, 1996: Modelling of land surface evaporation by four schemes and comparison with FIFE observations. *Journal of Geophysical Research*, **101**, 7251-7268

Cheng, V. Y. S., G. B. Arhonditsis, D. M. L. Sills, H. Auld, R. W. Shephard, W. A. Gough, and J. Klaassen, 2013: Probability of tornado occurrence across Canada. *Journal of Climate*, **26**, 9415-9428.

Chisholm, W. A., S L. Cress, and J. Polak, 2001: Lightning-caused distribution outages. *Proceedings of the IEEE Power Engineering Society Transmission Distribution Conference*, pp. 1041-1046.

Clodman, S., and W. Chisholm, 1996: Lightning flash climatology in the southern great lakes region. *Atmosphere-Ocean*, **32**, 2, 345-377, doi:10.1080/07055900.1996.9649568.

Crewe, A., 2008: Hailstorm a Year Later: It Can Happen Again. Fort McMurray Today. Accessed 01 February 2016. [Available online at http://www.fortmcmurraytoday.com/2008/07/29/hailstorm-a-year-later-it-can-happen-again-2.]

Cummins, K. L., N. Honma, A. E. Pifer, T. Rogers, and M. Tatsumi, 2012: Improved detection of winter lightning in the Tohoku region of Japan using Vaisala's LS700X technology. *IEEJ Transactions on Power and Energy*, **132**, 6, 1-6.

Cummins, K. L., and M. J. Murphy, 2009: An overview of lightning locating systems: history, techniques, and data uses, with an in-depth look at the US NLDN. *IEEE Transactions on Electromagnetic Compatibility*, **51**, 3, 499-518.

Cummins, K. L., M. J. Murphy, E. A. Bardo, W. L. Hiscox, R. B. Pyle, A. E. Pifer, 1998: A combined TOA/MDF technology upgrade of the U.S. National Lightning Detection Network. *Journal of Geophysical Research*, **103**, D8, 9035-9044.

Cummins, K. L., M. J. Murphy, and J. V. Tuel, 2000: Lightning detection methods and meteorological applications. Preprints, fourth international symposium on military meteorology, Marbork, Poland, WMO, 85-100.

Curry, M., J. Hanesiak, S. Kehler, D. M. L. Sills, and N. M. Taylor, 2017: Ground-based observations of the thermodynamic and kinematic properties of lake-breeze fronts in southern Manitoba, Canada. *Boundary Layer Meteorology*, **163**, 1, 143-159.

Curry, M., J. Hanesiak, and D. Sills, 2015: A radar-based investigation of lake breezes in southern Manitoba, Canada. *Atmosphere-Ocean*, **53**, 2, 237-250.

De Bruijn, T. J. W., 2010: Estimated life cycle GHG and energy use for oil-sands-derived crudes versus conventional light crude using GHGenius. *Natural Resources Canada*, Canmet Energy. 38 pp.

Dissing, D. and D. L. Verbyla, 2013: Spatial patterns of lightning strikes in interior Alaska and their relations to elevation and vegetation. *Canadian Journal of Forest Research*, **33**, 770-782.

Dixon, P. G., and T. L. Mote, 2003: Patterns and causes of Atlanta's urban heat island-initiated precipitation. *Journal of Applied Meteorology*, **42**, 1273-1284.

Dow, C. L. and D. R. DeWalle, 2000: Trends in evaporation and Bowen ratio on urbanizing watersheds in eastern United States. *Water Resources Research*, **36**, 7, 1835-1843.

Dowden, R. L., J. B. Brundell, and C. J. Rodger, 2002: VLF lightning location by time of group arrival (TOGA) at multiple sites. *Journal of Atmospheric and Solar-Terrestrial Physics*, **64**, 817-830.

Dupilka, M. L., and G. W. Reuter, 2005: An examination of three severe convective storms that produced significant tornadoes in central Alberta. *National Weather Digest*, **29**, 47-59.

Elmore, K. L., D. J. Stensrud, K. C. Crawford, 2002: Explicit cloud-scale models for operational forecasts: a note of caution. *Weather and Forecasting*, **17**, 873-884. DOI: 10.1175/1520-0434(2002)017<0873:ECSMFO>2.0.CO;2

Environment and Climate Change Canada, 2016: Canadian historical weather radar. Meteorological Service of Canada Data Services Section, accessed 15 March 2016. [Available online at http://climate.weather.gc.ca/radar/index_e.html].

Environmental Protection Agency, 2009: *Statistical Analysis of Groundwater Monitoring Data at RCRA Facilities, Unified Guidance. (*EPA Publication No. 530-R-09-007). Rockville, MD: U.S. Environmental Protection Agency.

ESRL/GSD, 2016: Aircraft Data Web. Earth System Research Laboratory, Global Systems Division, accessed 25 March 2016. [Available online at http://amdar.noaa.gov/].

Fanaki, F., 1986: Simultaneous acoustic sounder measurements at two locations. *Boundary Layer Meteorology*, **37**, 197-207.

Flesch, T.K. and G.W. Reuter, 2012: WRF model simulation of two Alberta flooding events and the impact of topography. *Journal of Hydrometeorology*, **13**, 695-708.

Gatlin, P. N., and S. J. Goodman, 2010: A total lightning trending algorithm to identify severe thunderstorms. *Journal of Atmospheric and Oceanic Technology*, **27**, 1-22. DOI: 10.1175/2009JTECHA1286.1

Geerts, B., D. Parsons, C. L. Ziegler, T. M. Weckwerth, M. I. Biggerstaff, R. D. Clark, M. C. Coniglio, B. B. Demoz, R. A. Ferrare, W. A. Gallus Jr., K Haghi, J. M. Hanesiak, P. M. Klein, K. R. Knupp, K. Kosiba, G. M. McFarquhar, J. A. Moore, A. R. Nehrir, M. D. Parker, J. O. Pinto, R. M. Rauber, R. S. Schumacher, D. D. Turner, Q. Wang, X. Wang, Z. Wang, and J. Wurman, 2017: The 2015 plains elevated convection at night field project. *Bulletin of the American Meteorological Society*, April, 767-786.

Government of Alberta, 2016: Alberta Energy: Facts and Statistics. Accessed 31 January 2016. [Available online at http://www.energy.alberta.ca/OilSands/791.asp.]

Grant, J., J. Dagg, S. Dyer, and N. Lemphers, 2010: Northern lifeblood: Empowering northern leaders to protect the Mackenzie River basin from oil sands risks. *Pembina Institute*, Drayton Valley, Alberta, Canada. 77 pp.

Grell, G. A. and D. Dévényi, 2002: A generalized approach to parameterizing convection combining ensemble and data assimilation techniques. *Geophysical Research Letters*, **29**, 14, 38-1 – 38-4.

Grell, G. A., J. Dudhia, and D. R. Stauffer, 1994: A description of the Fifth-Generation Penn State/NCAR Mesoscale Model (MM5). *NCAR Technical Note*.

Grell, G. A., and S. R. Freitas, 2014: A scale and aerosol aware stochastic convective parameterization for weather and air quality monitoring. *Atmospheric Chemistry and Physics*, **14**, 5233-5250.

Guan, S., and G. W. Reuter, 1995: Numerical simulation of a rain shower affected by waste energy released from a cooling tower complex in a calm environment. *Journal of Applied Meteorology*, **34**, 131-142.

Guan, S., and G. W. Reuter, 1996: Numerical simulation of an industrial cumulus affected by heat, moisture, and CCN released from an oil refinery. *Journal of Applied Meteorology*, **35**, 1257-1264.

Gurevich, A. V., G. M. Milikh, and R. Roussel-Dupré, 1992: Runaway electron mechanism of air breakdown and preconditioning during a thunderstorm. *Physics Letters A*, 165, 463-468.

Hanesiak, J., M. Melsness, and R. Raddatz, 2010: Observed and modeled growing-season diurnal precipitable water vapor in south-central Canada. *Journal of Applied Meteorology and Climatology*, **49**, 2301-2314.

Hanesiak, J. M., R. L. Raddatz, and S. Loban, 2004: Local initiation of deep convection on the Canadian Prairie Provinces. *Boundary Layer Meteorology*, **110**, 455-470.

Hanesiak, J., Tat, A., and R. L. Raddatz, 2009: Initial soil moisture as a predictor of subsequent severe summer weather in the cropped grassland of the Canadian Prairie provinces. *International Journal of Climatology*, **29**, 899-909.

Hanuta, S., and S. LaDochy, 1989: Thunderstorm climatology based on lightning detector data, Manitoba, Canada. *Physical Geography,* **10**, 101-109.

Hazewinkel, R. R. O., A. P. Wolfe, S. Pla, C. Curtis, and K Hadley, 2008: Have atmospheric emissions from the Athabasca oil sands impacted lakes in northeastern Alberta, Canada? *Canadian Journal of Fisheries and Aquatic Sciences*, **65**, 1554-1567

Herodotou, N., W. A. Chisholm, and W. Janichewskyj, 1993: Distribution of lightning peak stroke currents in Ontario using an LLP system. *IEEE Transactions on Power Delivery*, **8**, 3, 1331-1339

Hogg, E. H., T. A. Black, G. den Hartog, H. H. Neumann, R. Zimmermann, P. A. Hurdle, P. D. Blanken, Z. Nesic, P. C. Yang, R. M. Staebler, K. C. McDonald, and R. Oren, 1997: A comparison of sap flow and eddy fluxes of water vapor from a boreal deciduous forest. *Journal of Geophysical Research*, **102**, D24, 28929-28937.

Hohenegger, C., and C. Schär, 2007: Predictability and error growth dynamics in cloud-resolving models. *Journal of the Atmospheric Sciences*, **64**, 4467-4478. DOI: 10.1175/2007JAS2143.1

Holle, R. L., 2016: A summary of recent national-scale lightning fatality studies. *Weather, Climate, and Society*, **8**, 35-42.

Howell, S. G., A. D. Clarke, S. Freitag, C. S. McNaughton, C. Kapustin, V. Brekovskikh, J.-L. Jimenez, and M. J. Cubison, 2014: An airborne assessment of atmospheric particulate emissions from the processing of the Athabasca oil sands. *Atmospheric Chemistry and Physics*, **14**, 5073-5087. DOI: 10.5194/acp-14-5073-2014

Hutchins, M. L., R. H. Holzworth, J. B. Brundell, and C. J. Roger, 2012: Relative detection efficiency of the World Wide Lightning Location Network. *Radio Science*, **47**, RS6005.

Illingworth, A. J. 1985: Charge separation in thunderstorms: Small scale processes. *Journal of Geophysical Research*, **90**, D4, 6026-6032.

International Telecommunication Union, 2015: Recommendation ITU-R P.832.4. *World Atlas of Ground Conductivities*, 51 pp.

Jacquemin, B., and J. Noilhan, 1990: Sensitivity study and validation of a land surface parameterization using the Hapex-Mobilhy data set. *Boundary Layer* Meteorology, **52**, 93-134.

Jayaratne, E. R., 1991: Charge separation during the impact of sand on ice and its relevance to theories of thunderstorm electrification. *Atmospheric Research*, **26**, 407-424.

Jayaratne, E. R, C. P. R. Saunders, and J. Hallett, 1983: Laboratory studies of the charging of soft-hail during ice crystal interactions. *Quarterly Journal of the Royal Meteorological Society*, **109**, 609-630.

Joe, P., and S. Lapczak, 2002: Evolution of the Canadian operational radar network. *Proceedings of the 2002 European Conference on Radar in Meteorology and Hydrology (ERAD)*, Delft, Netherlands.

Jungwirth, P., D. Rosenfeld, and V. Buch, 2005: A possible new molecular mechanism of thunderstorm electrification. *Atmospheric Research*, **76**, 190-205.

Kellner, O. and D. Niyogi, 2015: Land surface heterogeneity signature in tornado climatology? An illustrative analysis over Indiana, 1950-2012. *Earth Interactions*, **18**, 10, 1-32.

Kelly, E. N., J. W. Short, D. W. Schindler, P. V. Hodson, M. Ma, A. K. Kwan, and B. L. Fortin, 2009: Oil sands development contributes polycyclic aromatic compounds to the Athabasca River and its tributaries. *Proceedings of the National Academy of Science*, **106**, 52, 22346–22351.

King, P. W. S., M. J. Leduc, D. M. L. Sills, N. R. Donaldson, D. R. Hudak, P. Joe, and B. P. Murphy, 2003: Lake breezes in southern Ontario and their relation to tornado climatology. *Weather and Forecasting*, **18**, 795-807.

Knowles, J. B., 1993: The influence of forest fire induced albedo differences on the generation of mesoscale circulations. *M.Sc. Thesis*, Department of Atmospheric Sciences, Colorado State University, 94 pp.

Kochtubajda, B., and W. R. Burrows, 2010: A decade of cloud-to-ground lightning in Canada: 1998-2008. Part 2: Polarity, multiplicity, and first-stroke peak current. *Atmosphere-Ocean*, **48**, 3, 195-209.

Kochtubajda, B., W. R. Burrows, D. Green, A. Liu, K. R. Anderson, and D. McLennan, 2011: Exceptional cloud-to-ground lightning during an unusually warm summer in Yukon, Canada. *Journal of Geophysical Research*, **116**, D21206, 1-20,

Kotroni, V. and K. Lagouvardos, 2008: Lightning occurrence in relation with elevation, terrain slope, and vegetation cover in the Mediterranean. *Journal of Geophysical Research,* **113**, D21118, 1-7.

Kozak, S. A., 1998: Lightning strikes in Alberta thunderstorms: Climatology and case studies. *MSc Thesis*, University of Alberta, 129pp.

Krauss, T. W., and J. Renick, 1997: The new Alberta hail suppression project. *Journal of Weather Modification*, **29**, 100-105.

Kumar, A., J. Dudhia, R. Rotunno, D. Niyogi, and U. C. Mohanty, 2008: Analysis of the 26 July 2005 heavy rain event over Mumbai, India using the Weather Research and Forecasting (WRF) model. *Quarterly Journal of the Royal Meteorological Society*, **134**, 1897-1910.

Latham, J., 1981: The electrification of thunderstorms. *Quarterly Journal of the Royal Meteorological Society*, **107**, 452, 277-298.

Latham, J., and B. J. Mason, 1961: Generation of electric charge associated with the formation of soft hail in thunderclouds. *Proceedings of the Royal Society of London. Series A, Mathematical and Physical Sciences*, **260**, 1303, 537-549.

Latifovic, R., K Fytas, J. Chen, and J. Paraszczak, 2005: Assessing land cover change resulting from large surface mining development. *International Journal of Applied Earth Observation and Geoinformation*, **7**, 29-48.

Leahey, D. M., and M. C. Hansen, 1982: Influences of terrain on plume level winds in the Athabasca oil sands area. *Atmospheric Environment*, **16**, 12, 2849-2854.

Lee, A. C. L., 1986: An operation system for the remote detection of lightning flashes using a VLF arrival time difference technique. *Journal of Atmospheric and Oceanic Technology*, **3**, 630-642.

Li, D., E. Bou-Zeid, and M. L. Baeck, 2013: Modeling land surface processes and heavy rainfall in urban environments: Sensitivity to urban surface representations. *Journal of Hydrometeorology*, 14, 1098-1117.

Lin, C.-Y., F. Chen, J. C. Huang, W.-C. Chen, Y.-A. Liou, W.-N. Chen, S.-C. Liu, 2008: Urban heat island effect and its impact on boundary layer development and land-sea circulation in northern Taiwan. *Atmospheric Environment*, **42**, 5635-5649.

Lin, Y.-L., R. D. Rarley, and H. D. Orville, 1983: Bulk parameterisation of the snow field in a cloud model. *Journal of Climate and Applied Meteorology*, **22**, 1065-1092.

Massey, F. J. Jr., 1951: The Kolmogorov-Smirnov test for goodness of fit. *Journal of the American Statistical Association*, **46**, 253, 68-78.

Mazur, V., E. Williams, R. Boldi, L. Maier, D. E. Proctor, 1997: Initial comparison of lightning mapping with operational time-of-arrival and interferometric systems. *Journal of Geophysical Research*, **102**, D10, 11071-11085.

Milikh, G., and R. Roussel-Dupré, 2010: Runaway breakdown and electrical discharges in thunderstorms. *Journal of Geophysical Research*, **115**, A00E60, 1-15.

Mills, B., D. Unrau, C. Parkinson, B. Jones, J. Yessis, K. Spring, L. Pentelow, 2008: Assessment of lightning-related fatality and injury risk in Canada. *Natural Hazards*, **47**, 157-183.

Mölders, N., 2008: Suitability of the Weather Research and Forecasting (WRF) model to predict the June 2005 fire weather for interior Alaska. *Weather and Forecasting*, **23**, 953-973.

Moninger, W. R., R. D. Mamrosh, and T. S. Daniels, 2006: Automated weather reports from aircraft: TAMDAR and the U.S. AMDAR fleet. 12th Conference on Aviation, Range, and Aerospace Meteorology, January 2006, Atlanta, Georgia. 6 pp.

Mora García, M., J. Riesco Martín, L. Rivas Soriano, and F. de Pablo Dávila, 2015: Observed impacts of land uses and soil types on cloud-to-ground lightning in Castilla-Leon (Spain). *Atmospheric Research*, **166**, 233-238.

Nag, A., M. J. Murphy, W. Schulz, and K. L. Cummins, 2015: Lightning locating systems: Insights on characteristics and validation techniques. *Earth and Space Sciences*, **2**, 65-93.

NCEP/NWS/NOAA, 2005: NCEP North American Regional Reanalysis (NARR). Research data archive at the national center for atmospheric research, computational and information systems laboratory, accessed 15 December 2016. [Available online at http://rda.ucar.edu/datasets/ds608.0/].

Nelson, H. R., D. J. Siebert, and L. R. Denham, 2013: Lightning data – a new geophysical data type. *Search and Discovery Article*, 41184, 1-19.

Niyogi, D., T. Holt, S. Zhong, P. C. Pyle, and J. Basara, 2006: Urban and land surface effects on the 30 July 2003 mesoscale convective system event observed in the southern great plains. *Journal of Geophysical Research*, **111**, D19107, 1-20.

Niyogi, D., P. Pyle, M. Lei, S. P. Arya, C. M. Kishtawal, M. Shepherd, F. Chen, and B. Wolfe, 2011: Urban modification of thunderstorms –an observational storm climatology and model case study for the Indianapolis urban region. *Journal of Applied Meteorology and Climatology*, **50**, 1129-1144.

Nkemdirim, L. C., 1981: Extra urban and intra urban rainfall enhancement by a medium sized city. *Water Resources Bulletin*, **17**, 5, 753-759.

Oke, T. R., 1973: City size and the urban heat island. *Atmospheric Environment*, 7, 769-779.

Oke, T. R., 1982: The energetic basis of the urban heat island. *Quarterly Journal of the Royal Meteorological Society*, **108**, 1-24.

Orville, R. E., 1991a: Calibration of a magnetic direction finding network using measured triggered lightning return stroke peak currents. *Journal of Geophysical Research*, **96**, D9, 17135-17142.

Orville, R. E., 1991b: Lightning ground flash density in the contiguous United States – 1989. *Monthly Weather Review*, **119**, 573-577.

Orville, R. E., and Huffines, G. R., 2001: Cloud-to-ground lightning in the United States: NLDN results in the first decade, 1989-1998. *Monthly Weather Review*, **129**, 1179-1193.

Pennelly, C. and G. W. Reuter, 2017: Verification of the Weather Research and Forecasting Model when forecasting daily surface conditions in southern Alberta. *Atmosphere-Ocean*, **55**, 1, 31-41.

Pennelly, C., G. W. Reuter, and T. Flesch, 2014: Verification of the WRF model for simulating heavy precipitation in Alberta. *Atmospheric Research*, **135-136**, 172-192.

Pielke, R. A., J. Adegoke, A. Beltrán-Przekurat, C. A. Hiemstra, J. Lin, U. S. Nair, D. Niyogi, T. E. Nobis, 2007: An overview of regional land-use and land-cover impacts on rainfall. *Tellus*, **59B**, 587-601.

Pielke, R. A., and M. Uliasz, 1993: Influence of landscape variability on atmospheric dispersion. *Journal of the Air and Waste Management Association*, **43**, 989-994.

Rabin, R. M., S. Stadler, P. J. Wetzel, D. J. Stensrud, and M. Gregory, 1990: Observed effects of landscape variability on convective clouds. *Bulletin of the American Meteorological Society*, **71**, 3, 272-280.

Raddatz, R. L., 1993: Prairie agroclimate boundary-layer model: A simulation of the atmosphere/crop-soil interface, *Atmosphere-Ocean*, **31**, 4, 399-419.

Raddatz, R. L., 1998: Anthropogenic vegetation transformation and the potential for deep convection on the Canadian Prairies. *Canadian Journal of Soil Science*, **78**, 4, 657-666.

Raddatz, R. L., 2005: Moisture recycling on the Canadian Prairies for summer droughts and pluvials from 1997 to 2003. *Agriculture and Forest Meteorology*, **131**, 13-26.

Raddatz, R. L., and J. D. Cummine, 2003: Inter-annual variability of moisture flux from the prairie agro-ecosystem: Impact of crop phenology on the seasonal pattern of tornado days. *Boundary Layer Meteorology*, **106**, 283-295.

Rahn, D. A., and C. J. Mitchell, 2016: Diurnal climatology of the boundary layer in southern California using AMDAR temperature and wind profiles. *Journal of Applied Meteorology and Climatology*, **55**, 1123-1137.

Rakov, V. A., 2013: Electromagnetic methods of lightning detection. *Surveys of Geophysics*, 34, 731-753.

Reap, R. M. and D. R. MacGorman, 1989: Cloud-to-ground lightning: Climatological characteristics and relationships to model fields, radar observations, and severe local storms. *Monthly Weather Review,* **117**, 518-535.

Reuter G. W., and S. Guan, 1995: Effects of industrial pollution on cumulus convection and rain showers: A numerical study. *Atmospheric Environment*, **29**, 18, 2467-2474.

Reuter, G. W., 2010: Application of the factor separation methodology to quantify the effect of waste heat, vapor and pollution on cumulus convection, in *Factor Separation in the Atmosphere: Applications and Future Prospects*, edited by P. Alpert and T. Sholokhman, pp. 163-170, Cambridge University Press, Cambridge, UK.

Rose, L. S., J. A. Stallins, and M. L. Bentley, 2008: Concurrent cloud-to-ground lightning and precipitation enhancement in the Atlanta, Georgia (United States), urban region. *Earth Interactions*, **12**, 1-30.

Rozoff, C. M., W. R. Cotton, and J. O. Adegoke, 2003: Simulation of St. Louis, Missouri, land use impacts on thunderstorms. *Journal of Applied Meteorology*, **42**, 716-738.

Said, R. K., U. S. Inan, and K. L. Cummins, 2010: Long-range lightning geolocation using a VLF radio atmospheric waveform bank. *Journal of Geophysical Research*, **115**, D23108, 1-19.

Saunders, C. P. R., 1993: A review of thunderstorm electrification processes. *Journal of Applied Meteorology*, **32**, 642-655.

Scavuzzo, C. M., E. E. Avila, and G. M. Caranti, 1995: Cloud electrification by fracture in ice-ice collisions: A 3D model. *Atmospheric Research*, **37**, 325-342.

Scheftic, W. D., Cummins, K. L., Krider, P. E., Sternberg, B. K., Goodrich, D., Moran, S., R. Scott, 2008: Wide-area soil moisture estimation using the propagation of lightning generated low-frequency electromagnetic signals. *20th International Lightning Detection Conference*, 1-8.

Schmid, P. E., and D. Niyogi, 2013: Impact of city size on precipitation-modifying potential. *Geophysical Research Letters*, **40**, 5263-5267.

Schueler, J. R. and E. M. Thompson, 2006: Estimating ground conductivity and improving lightning location goodness of fit by compensating propagation effects. *Radio Science*, **41**, RS1001, 1-13.

Schwartz, B. E., S. G. Benjamin, S. M. Green, and M. R. Jardin, 2000: Accuracy of RUC-1 and RUC-2 wind and aircraft trajectory forecasts by comparison with ACARS observations. *Weather and Forecasting*, **15**, 313-326.

Schwartz, B., and S. G. Benjamin, 1995, A comparison of temperature and wind measurements from ACARS-equipped aircraft and rawinsondes. *Weather and Forecasting*, **10**, 528-544.

Scott, C. J., R. G. Harrison, M. J. Owens, M. Lockwood, and L. Barnard, 2014: Evidence for solar wind modulation of lightning. *Environmental Research Letters*, **9**, 1-12.

Scott, R. W., and F. A. Huff, 1996: Impact of the great lakes on regional climate conditions. *Journal of Great Lakes Research*, **22**, 4, 845-863.

Sellers, P., F. Hall, H. Margolis, B. Kelly, D. Baldocchi, G. den Hartog, J. Cihlar, M. G. Ryan, B. Goodison, P. Crill, K. J. Ranson, D. Lettermaier, D. E. Wickland, 1995: The boreal ecosystem – atmosphere study (BOREAS): An overview and early results from the 1994 field year. *Bulletin of the American Meteorological Society*, **76**, 9, 1549-1577.

Shamarock, W. C., J. B. Klemp, J. Dudhia, D. O. Gill, D. M Barker, M. G. Duda, X.-Y. Huang, W. Wang, and J. G. Powers, 2008: A description of the Advanced Research WRF Version 3. *NCAR Technical Note.*

Shilts, W. W., J. M. Aylsworth, C. A. Kaszycki, and R. A. Klassen, 1987: Canadian Shield. *Geomorphic Systems of North America*, Boulder, Colorado, Geological Society of America, Centennial Volume 2.

Shrestha, B. M., R. L. Raddatz, R. L. Desjardins, and D. E. Worth, 2012: Continuous cropping and moist deep convection on the Canadian Prairies. *Atmosphere*, **3**, 4, 573-590. DOI: 10.3390/atmos3040573

Sills, D. M. L., J. R. Brook, I. Levy, P. A. Makar, J. Zhang, and P. A. Taylor, 2011: Lake breezes in the southern Great Lakes region and their influence during BAQS-Met 2007. *Atmospheric Chemistry and Physics*, **11**, 7955-7973.

Smith, B. L., and J. L. Blaes, 2015: Examination of a winter storm using a micro rain radar and AMDAR aircraft soundings. *Journal of Operational Meteorology*, **3**, 14, 156-171.

Smith, S. B., and M. K. Yau, 1993: The causes of severe convective outbreaks in Alberta. Part I: A comparison of a severe outbreak with two non-severe events and part II: Conceptual model and statistical analysis. *Monthly Weather Review*, **121**, 1099-1133.

Smith, S. B., G. W. Reuter, M. K. Yau, 1998: The episodic occurrence of hail in central Alberta and the Highveld of South Africa. Research Note: *Atmosphere-Ocean*, **36**, 2, 169-178.

Soil Classification Working Group, 1998: The Canadian System of Soil Classification, 3rd ed. *Agriculture and Agri-Food Canada Publication 1646,* 187 pp.

Stallins, J. A., and L. S. Rose, 2008: Urban lightning: Current research, methods, and the geographical perspective. *Geography Compass*, **2**, 3, 620-639.

Steiger, S. M. and R. E. Orville, 2003: Cloud-to-ground lightning enhancement over southern Louisiana. *Geophysical Research Letters*, **30**, 19, 1975.

Steiger, S. M., R. E. Orville, and G. Huffines, 2002: Cloud-to-ground lightning characteristics over Houston, Texas: 1989-2000. *Journal of Geophysical Research*, **107**, 4117, DOI: 10.1029/2001JD001142.

Stein, U. and P. Alpert, 1993: Factor separation in numerical simulations. *Journal of the Atmospheric Sciences*, **50**, 14, 2107-2115.

Stocks, B. J., J. A. Manson, J. B. Todd, E. M. Bosch, B. M. Wotton, B. D. Amiro, M. D. Flannigan, K. G. Hirsch, K. A. Logan, D. L. Martell, and W. R. Skinner, 2003: Large forest fires in Canada, 1959-1997. *Journal of Geophysical Research*, **108**, D1, 8159, 1-12.

Stolzenburg, M., W. D. Rust, and T. C. Campbell, 1998: Electrical structure in thunderstorm convective regions 3. Synthesis. *Journal of Geophysical Research*, **103**, D12, 14097-14108.

Strong, G. S., 1986: synoptic to mesoscale dynamics of severe thunderstorm environments: A diagnostic study with forecasting applications. *PhD Thesis*, University of Alberta, Edmonton.

Strong, G. S., 1997: Atmospheric moisture budget estimates of regional evapotranspiration from RES-91. *Atmosphere-Ocean*, **35**, 1, 29-63

Sun, J., D. H. Lenschow, L. Mahrt, T. L. Crawford, K. J. Davis, S. P. Oncley, J. I. MacPherson, Q. Wang, R. J. Dobosy, and R. L. Desjardins, 1997: Lake-induced atmospheric circulations during BOREAS. *Journal of Geophysical Research*, **102**, D4, 29155-29166.

Taylor, N. M., D. M. L. Sills, J. M. Hanesiak, J. A. Milbrandt, C. D. Smith, G. S. Strong, S. H. Scone, P. J. McCarthy, and J. C. Brimelow, 2011: The understanding severe thunderstorms and Alberta boundary layer experiment (UNSTABLE) 2008. *Bulletin of the American Meteorological Society*, June, 739-763

The Weather Network, 2016: Pelmorex lightning detection network. Accessed 27 August 2016. [Available online at http://data.twncs.com/Solutions/Lightning/lightning.html.]

Thielan, J., and A. Gadian, 1997: Influence of topography and urban heat island effects on the outbreak of convective storms under unstable meteorological conditions: a numerical study. *Meteorology Applications*, **4**, 139-149.

Thomas, R. J., P. R. Krehbiel, W. Rison, S. J. Hunyady, W. P. Winn, T. Hamlin, and J. Harlin, 2004: Accuracy of a lightning mapping array. *Journal of Geophysical Research*, **109**, D14207, 1-34.

Tyahla, L. J., and R. E. López, 1994: Effect of surface conductivity on the peak magnetic field radiated by first return strokes in cloud-to-ground lightning. *Journal of Geophysical Research*, **99**, D5, 10517-10525.

Vidale, P. L., R. A. Pielke, L. T. Steyaert, and A. Barr, 1997: Case study modeling of turbulent and mesoscale fluxes over the BOREAS region. *Journal of Geophysical Research*, **102**, D24, 29167-29188.

Wallace, J. M., and P. V. Hobbs, 1977: *Atmospheric Science: An Introductory Survey.* San Diego, California, Elsevier Science, 467 pp.

Walmsley, J. L., and D. L. Bagg, 1978: A method of correlating wind data between two stations with application to the Alberta oil sands. *Atmosphere-Ocean*, **16**, 4, 333-347.

Weckwerth, T. M., D. B. Parsons, S. E. Koch, J. A. Moore, M. A. LeMone, B. B. Demoz, C. Flamant, B. Geerts, J. Wang, and W. F. Feltz, 2004: An overview of the international H_2O project (IHOP_2002) and some preliminary highlights. *Bulletin of the American Meteorological Society*, February, 253-277.

Weisman, M. L., C. Davis, W. Wang, K. W. Manning, and J. B. Klemp, 2008: Experiences with 0-36-h explicit convective forecasts with the WRF-ARW model. *Weather and Forecasting*, **23**, 407-437. DOI: 10.1175/2007WAF2007005.1.

Weismann, M. L., and J. B. Klemp, 1982: The dependence of numerically simulated convective storms on vertical wind shear and buoyancy. *Monthly Weather Review*, **110**, 504-520.

Westcott, N. E., 1995: Summertime cloud-to-ground lightning activity around major Midwestern urban areas. *Journal of Applied Meteorology*, **34**, 1633-1642.

Williams, E. R., 1989: The tripole structure of thunderstorms. *Journal of Geophysical Research*, **94**, D11, 13151-13167.

Wilson, J. W., and R. D. Roberts, 2006: Summary of convective storm initiation and evolution during IHOP: Observation and modeling perspective. *Monthly Weather Review*, **134**, 23-47.

Wurman, J., D. Dowell, Y. Richardson, P. Markowski, E. Rasmussen, D. Burgess, L. Wicker, and H. B. Bluestein, 2012: The second verification of the origins of rotation in tornadoes experiment. *Bulletin of the American Meteorological Society*, August, 1147-1170.

Xue, M., F. Kong, K. W. Thomas, J. Gao, Y. Wang, K. Brewster, K. K. Droegemeier, 2013: Prediction of convective storms over continental United States with radar data assimilation: an example case of 26 May 2008 and precipitation forecasts from spring 2009. *Advances in Meteorology,* 2013, 1-9.

Yue, S., P. Pilon, and G. Cavadias, 2002: Power of the Mann-Kendall and Spearman's rho tests for detecting monotonic trends in hydrological series. *Journal of Hydrology*, **259**, 254-271.

Zhong, S., Y. Qian, C. Zhao, R. Leung, and X.-Q. Yang, 2015: A case study of urbanization impact on summer precipitation in the greater Beijing metropolitan area: Urban heat island versus aerosol effects. *Journal of Geophysical Research*, **120**, 10903-10914.

Appendix A: WRF Modifications

An earlier version of this appendix and the WRF modifications have been posted to the University of Utah WRF users' group website. The files are located on the WRF users group webpage located at http://home.chpc.utah.edu/~u0198116/wrf/modifying.html.

A.1. Introduction

The Weather Research and Forecasting (WRF) model is a numerical weather prediction model that researchers often use for regional weather modelling studies. We plan to use the WRF model to simulate the meteorological effects on thunderstorms of the addition of industrial heat into the atmosphere; however, there is no easy mechanism within the WRF model to do so. In order to add industrial heat to the atmosphere, we needed to create a new physics module and add it to the WRF system. We describe the new module in this appendix.

We followed examples from WRF-Fire to help us learn how the WRF model interacts with added sensible and latent heat. These examples helped us to create the new subroutines and to add them to the WRF modelling system. WRF-Fire is an addition to WRF which incorporates a wildfire propagation model coupled with the WRF atmospheric model. WRF-Fire adds sensible and latent heat to the atmosphere from wildfires, which was very similar to what we wanted to do.

A.2. Modified WRF files

In order to add the industrial heat to the model, we had to modify a number of files within the WRF system. Some of these files were configuration files where we could specify certain variables, like the amount of waste heat. Some of the files were registry files. We had to create one new file to hold our new subroutines. We also had to modify some files to allow our heat to be added to the modelling system. The following files were modified:

1) phys/Makefile,
2) phys/module_ind_heat.F,
3) Registry/Registry.EM_COMMON,
4) run/namelist.input,
5) dyn_em/module_first_rk_step_part1.F,
6) dyn_em/module_first_rk_step_part2.F,
7) phys/module_physics_addtendc.F.

The following sections will explain in detail all of the modifications we made, why we made them, and how they work to achieve the goal of adding industrial heat to the model.

A.3. Setting up "namelist.input"

We decided that we would add the heat to a special 'industrial' land-use type because this allowed us the most flexibility to configure where and how much heat we wanted to add to the atmosphere without recompiling the code every time we wanted to make small changes. We reconfigured an unused land-use type for this purpose. In WRF, the user normally inputs parameters such as physics parameterizations into a file called "namelist.input". We added two

new variables into the physics section of the “namelist.input” file: the amount of industrial heat, “ind_heat_amt” (W/m^2), and the land use type to which we want to add the heat, “lu_type” (an integer). The variables in the “namelist.input” file are visible to most WRF subroutines through the "config_flags" object. The individual “namelist.input” variables are accessed in the WRF subroutines by using “config_flags%variable_name”, where “variable_name” is the name of the variable in the “namelist.input” file (in this case, “ind_heat_amt”).

In order to add the two new variables to the “namelist.input” file we had to add a record for each variable to the “Registry/Registry.EM_COMMON” file. This registry file contains a ‘namelist’ physics section, which is where we added the records. They are listed as "rconfig" variables. The WRF modelling system will not recognize our new variables, and will not compile, unless we register them in the registry file.

A.4. The main ‘grid’ object

The model communicates its current “state” using the “grid” object. The current state of the model includes arrays of data such as the pressure, temperature, density, land use type, radiation, etc. These variables are accessed by using “grid%variable_name”, where “variable_name” is the name of the variable to be accessed. The list of possible variables is stored in the WRF registry. WRF needs to be able to access our industrial heat variable in all modules and all subroutines, so we need to add it as a global variable to WRF as a part of the main “grid” object. We created a new global state variable called, “rthindten”, by adding a record describing the new state variable with ikj dimensions to the "Registry/Registry.EM_COMMON" file. This new

variable is now accessible in many of the WRF subroutines, and represents the industrial heating tendency. How this variable is calculated will be described later.

WRF temperature tendency variables are 3 dimensional variables representing the entire WRF atmosphere at any given time step. We are adding our heat only to the first level of the atmosphere, so we set the industrial temperature tendency to zero at all levels above the surface. It is also zero wherever the WRF land use category does not equal our pre-chosen land use category from the "namelist" file. In this way, we only add heat where we want to do so. All we have to do to change the geographic location of where the heat is added is to modify the land cover type data. In the model's lowest atmospheric level over our chosen land use type, the tendency is calculated as described in the next section.

A.5. New industrial heat physics module

In order to add industrial heat to the atmosphere, we wrote a new physics module: "module_ind_heat", and added it to the "phys" folder. The module contains one subroutine: "ind_heat". It takes as input the main grid for the model ("grid"), the namelist flags ("config_flags"), the indices of the model area, the air density, the ground elevation, and the thickness of the layer. It outputs the industrial heat tendency variable ("rthindten"). Once all the variables and dimensions are specified, the following is done by the subroutine:

1. The "namelist.input" file specifies the industrial heat amount (W/m2) and flags the land use index to which we will add the industrial heat. We pull both of these values out from the "config_flags" object.

2. The program loops through all the tiles on the grid and does the following to each tile:

2.1. The starting and ending indices for all three dimensions of each tile are pulled from the main “grid” object.

2.2. We loop through all dimensions of “rthindten” and set it to zero everywhere. If this does not happen, Fortran seems fill the array with random numbers instead of zeros.

2.3. We loop through all dimensions of “rthindten” again and do the following:

2.3.1. We pull the land use type for the current grid cell from the main "grid" object, and convert it from a real number to an integer to prevent any rounding errors.

2.3.2. We test whether it is equal to the land use index from the namelist file.

2.3.3. If it is the correct type, then we calculate the heating temperature tendency using the following equations:

We start with the heat capacity equation:

$$\Delta Q = mc_p \Delta T \quad (1),$$

where ΔQ is the change in internal energy of the system, m is the mass of air, c_p is the heat capacity of air at constant pressure, and ΔT is the temperature change associated with the change in internal energy. We can find ΔT by rearranging Equation (1) and making the following substitutions:

$$\Delta T = \frac{\Delta Q}{mc_p} \quad (2).$$

Using the relation $m = \rho V$, where ρ is the air density and V is the volume of air, we find:

$$\Delta T = \frac{\Delta Q}{\rho V c_p} \quad (3).$$

We use $V = Ah$ to rewrite the volume as the surface area (A) multiplied by the height (h), giving us the next iteration of the equation:

$$\Delta T = \frac{\Delta Q}{\rho A h c_p} \quad (4).$$

We note that ΔQ divided by the surface area gives us the heat flux (Flx), and arrive at the final equation:

$$\Delta T = \frac{Flx}{\rho h c_p} \quad (5).$$

The heat flux (Flx) is specified in the “namelist.input” file. The air density (ρ), height (h), and the specific heat capacity (c_p) are all pulled out of the main "grid" object. These allow us to calculate the temperature tendency due to the industrial heat input specified in the “namelist.input” file. This is the temperature tendency that we need to add to the main temperature tendency equation in the next section.

Because the WRF equations are in flux form, the tendency equations are coupled with the total air column mass (‘mut’ in the WRF registry). We also need to multiply our tendency by the total air column mass to have it in the same form as the other tendency terms. Our new equation then becomes:

$$\Delta T = M_{ut} \frac{Flx}{\rho h c_p} \quad (6).$$

This is the final step in preparing the equation for input into the modelling code. Our equation in the code becomes: rthindten(i,kk,j) = mu*cp_i*rho_i*heat/dz8w(i,kk,j), where kk = 1 (the lowest level of the atmosphere), i and j are the x and y indices, cp_i is the inverse of the specific heat

capacity ($1/c_p$), rho_i is the inverse of the density ($1/\rho$), heat is the industrial heat flux (Flx), and dz8w is the thickness of the current level of the atmosphere. After we calculate this, we check if it is equal to itself. This is a Fortran trick to make sure that the number is defined. If the number is not equal to itself, it is not defined and we set it to zero. In theory this should never happen.

In order for the WRF system to compile the new code, a line must be added to the 'phys/Makefile' file to include the new 'module_ind_heat.o' module in the list of modules to compile. It is also important to note that the model grid is divided into a number of tiles intended to facilitate tasks for multiple processors. In this case, we just loop through all the tiles at once because the multiple processor portion of WRF was not working properly.

A.6. Communication between the new industrial heat module and WRF

WRF needs to be able to call the new industrial heat module and needs to be able to use the output from the new module. We added a small section of code into the file "dyn_em/module_first_rk_step_part1.F" to call the new industrial heat subroutine. The new subroutine returns the industrial heat tendency which is added into the main "grid" object.

Once the new module and subroutines are executed, a subroutine in the file "dyn_em/module_first_rk_step_part2.F" calls another subroutine, "update_phy_ten". This subroutine sums all the temperature tendencies from the various ongoing meteorological processes and calculates the total temperature tendency for the time step. We just have to add our new heating variable to the call to the "update_phy_ten" subroutine so it can be input into the subroutine.

A number of changes need to be made to the file “phys/module_physics_addtendc.F”. We must accept the new variable send in from “dyn_em/module_first_rk_step_part2.F” in the subroutine header. At the end of the “update_phy_ten” subroutine we call a small new subroutine called “phy_ind_ten”. This subroutine takes our “rthindten” variable and sends it into the ‘add_a2a’ subroutine, which is the final step. The ‘add_a2a’ subroutine adds our industrial heating tendency to the total model temperature tendency, which then updates the entire model temperature based on all the temperature tendencies.

A.7. Summary

1. Modify “Registry/Registry.EM_COMMON” to include the new “state” and “namelist.input” variables.
2. Write code for addition of heat as a “.F” Fortran file in the “phys” directory.
3. Add the name of the new module “.o” file to “phys/Makefile” in the list of modules.
4. Add the new “rthindten” variable to the “Registry/Registry.EM_COMMON” file.
5. Add code to call the new module in "dyn_em/module_first_rk_step_part1.F".
6. Add code to add the new "rthindten" variable to the "update_phy_ten" subroutine call.
7. Modify the "phys/module_physics_addtendc.F" code to accept the “rthindten” variable and add it to the temperature tendency.

Appendix B: Statistical methods

In this appendix, a summary of the various statistical methods that were used in this thesis is provided.

B.1. Mann-Kendall statistical test for temporal trends (used in Chapter 3)

The Mann-Kendall statistical test is often used to detect time-series trends in meteorological data, and is used to determine whether a temporal trend is statistically significant. (Yue et al. 2002). The U. S. Environmental Protection Agency (2009) provides an in-depth summary of this statistical test, and the discussion in this section is based on this report.

The Mann-Kendall statistical test tests for trends in data time series. The test can be performed on any dataset, and the test does not make any assumptions based on the magnitudes of the data. The first step is to compute the differences between all possible data points in the time series, and assign a value of +1 if the difference is positive, 0 if they are the same, and -1 if the difference is negative. This step removes the dependence on the magnitude of the data. Note that the number of pairs is equal to n*(n-1)/2 because every possible combination must be accounted for. The Mann-Kendall statistic is calculated by summing all of these values. If there is an upward trend, then there will be more +1 values, and the sum will be positive. A downward trend will give a negative sum. The Mann-Kendall statistic can be used with a table of significance levels to determine whether or not the temporal trend is significant. The Mann-Kendall test is non-parametric (i.e. it does not require normally distributed data); thus, any dataset can be used with the test.

Because the Mann-Kendall test is a less commonly used test, a short example of its application will be described here. A hypothetical temperature dataset is provided in Table 2. To perform the Mann-Kendall test, the temperature at each time must be subtracted from the temperature at every time later than it. Thus, there are 15 different subtractions for a dataset of size 6. Normally the Mann-Kendall Test should be applied to datasets larger than 10 (Yue et al. 2000), but it is more instructive to show a complete example with fewer data points. By calculating the signs of the differences and summing them up (Table 3), the Mann-Kendall statistic is found to be +8, thus there is an increasing trend. An equation is then used to convert this value into a statistic, whose significance can be looked up in a table. The Mann-Kendall test was used in Chapter 3 to compute trends in the temperature, humidity, and precipitation differences between a weather station near the oil sands and that away from them.

B.2. Factor separation method (used in Chapter 4)

When analysing sensitivity experiments with numerical models using more than one factor, it is recommended that researchers use the Stein and Alpert (1993) factor separation method. This method rigorously quantifies the effect of each individual factor and all of their combinations. Instead of just adding the values of individual factors, the model user must run a new simulation with both factors activated because the effect of two factors might be more or less than the sum of the individual factors. The following descriptions of the factor separation method are summarized from Alpert and Sholokhman (2011).

The Factor separation method depend largely on the number of independent factors. Here we present the method for two factors as it used in Chapter 4. The effect on total accumulated rainfall amount depends on the two factors (Table 1): modification to the land cover

(Factor 1), and emissions of waste heat (Factor 2). The dataset that is used for this is entirely hypothetical. The value of the variable, total accumulated rainfall amount, from the base numerical simulation which had no factors activated will be designated r_0, and in the example has a value of 10 mm. All of the following simulations are compared with this base simulation.

Thus, the results of the simulation with the first factor activated, land cover modification, can be written as the sum of value of the base simulation and the amount induced by the first factor:

$$r_1 = r_0 + f_1 \quad (1).$$

Note that in the example case, the total accumulated rainfall is 13 mm; thus, f_1 is the amount of rainfall induced by factor #1 (3 mm). The same procedure is applied for factor #2:

$$r_2 = r_0 + f_2 \quad (2).$$

However, the procedure is more complex when both factors are activated. In the example case, the total accumulated rainfall depends on the base state (r_0), the amount from factor #1 (f_1), the amount from factor #2 (f_2), and additionally the amount caused by the non-linear interactions (labelled synergism by Alpert and Sholokhman (2011)) of both factors (f_{12}). Thus the equation becomes:

$$r_{12} = r_0 + f_1 + f_2 + f_{12} \quad (3),$$

and the example total accumulated rainfall from the simulation with both factors activated, 11 mm, is the sum of all four components in Table 1. The value, f_{12}, is the amount induced by the non-linear interaction between the two factors, and is in addition to f_1 and f_2. If the interaction was linear, and f_1 and f_2 could simply be added, then f_{12} would simply be zero. Usually the results of the simulation, r0, r1, r2, and r12 are given, and the contributions associated with the factors

are what is required for analysis. These equations can be derived by rearranging equations 1, 2, and 3, and are as follows:

$$f_1 = r_1 - r_0 \quad (4),$$

$$f_2 = r_2 - r_0 \quad (5),$$

$$f_{12} = r_{12} - r_1 - r_2 + r_0 \quad (6).$$

Thus, using four model runs, the contributions of the two factors along with the contribution of the non-linear interactions between the two factors can be calculated. However, factor separation is not limited to only two factors.

In the oil sands development factor separation, a distinction is made between the "natural" state and the "control" state. The "control" state is usually the current, real state. For example, the "control" state is when both the land cover modifications and the waste heat have been added to the oil sands development and the state of the model most represents what is actually there. The "natural" state is when all factors are turned off, and the state of the model represents what would have been there if there was no disturbance. The "natural" state, however, is not the state that currently exists.

Various researchers have used factor separation as a method for organizing the results of numerical simulation sensitivity experiments. Alpert and Sholokhman (2011) provide an exhaustive list of papers that refer to the method. Here, only a few relating to land surface feedbacks will be discussed. Guan and Reuter (1996) used the factor separation technique to measure the relative contributions of waste sensible heat, latent heat and cloud condensation nuclei on cumulus clouds. Niyogi et al. (2006) used factor separation to investigate how Oklahoma City, Oklahoma affected a mesoscale convective system. Rozoff et al. (2003) used

factor separation to compare the results of numerical simulations of thunderstorms over St. Louis, Missouri. They used the urban heat island, the urban roughness, and the topography as their factors. Factor separation is used in Chapter 4 to investigate the effect of the oil sands development on thunderstorms.

B.3. Student's *t*-test (Used in Chapter 5)

The U. S. Environmental Protection Agency (2009) provides an in-depth description of the Student's T test, which will be summarized here. The Student's t-test is used to determine whether or not there exists a statistically significant difference between the means of two populations. The researcher should choose the significance level beforehand, and is often chosen to be 0.05. If the mean, standard deviation, and sample size of each population is known, then the *t* statistic can be calculated. The significance level can be looked up in a probability table and the researcher can find out if the difference in means is statistically significant.

However, there are a number of assumptions required that can make the *t*-test difficult to use. In order to use the *t*-test, the data must approximate a normal distribution, and the samples must be independent. Sometimes these criteria can be difficult to satisfy. Particularly with small sample size, the normality of the distribution is not always clear. Other tests have been devised that are less dependent on the shape of the distribution, and some of them will be discussed next. The *t*-test was used by Clodman and Chisholm (1996) to investigate lightning density in southern Ontario. In this thesis, the *t*-test was used in Chapter 5 to examine the lightning density gradient near the Canadian Shield boundary.

B.4. Mann-Whitney *u*-test (Used in Chapter 5)

Again, the U. S. Environmental Protection Agency (2009) provides an in-depth description of the Mann-Whitney *u*-test (also known as the Wilcoxon rank-sum test), which will be summarized here. The Mann-Whitney *u*-test is in some ways the non-parametric equivalent of the Student's *t*-test. The test is used in cases where the distributions for each sample are not known to be normal (although it works for normal distributions as well), but the distributions for the two samples must be similar. The Mann-Whitney *u*-test compares the two samples by ranking the values of both samples in one table, and then summing the ranks of each sample. Like before, equations are provided for converting the *u* statistic into a probability that can be looked up in a table of probabilities.

In some ways The Mann-Whitney *u*-test is similar to the *t*-test, but it does not provide a significant result as easily as the *t*-test. For large sample sizes, the *u*-test works about as well as the *t*-test, but for small sample sizes, it can be difficult to get a statistically significant result using the *u*-test. The *u*-test assumes that the data come from populations with similar distributions, and that the populations have similar variances. The *u*-test was used in Chapter 5 to examine the lightning density gradient near the Canadian Shield boundary.

B.5. Kolmogorov-Smirnov test (Used in Chapter 5)

If the researcher knows little about the distributions that the samples come from, the Kolmogorov-Smirnov (KS) test gives a little more freedom than the previous two tests. The KS test determines whether or not two data samples come from the same population, and is described in detail by Massey (1951). To perform the test on two samples, the two sample KS test is used and

the cumulative distribution function of each dataset must be calculated. The test compares the cumulative distribution functions of the two datasets. The KS statistic is the maximum difference between the cumulative distribution functions, and the critical values for significance at different significance levels can be looked up in a table. The KS test does not depend on the distribution, nor does it require a normal distribution. Kochtubajda et al. (2011) used the KS test to compare lightning data from different geographical regions. The KS test was used in Chapter 5 to examine the lightning density gradient near the Canadian Shield.

B.6. References

Alpert, P, and T. Sholokhman, 2011: *Factor Separation in the Atmosphere.* Cambridge University Press. New York, 274 pp.

Clodman, S., and Chisholm, W, 1996: Lightning flash climatology in the southern great lakes region, *Atmosphere-Ocean*, **32**, 2, 345-377.

Environmental Protection Agency, 2009: *Statistical Analysis of Groundwater Monitoring Data at RCRA Facilities, Unified Guidance. (*EPA Publication No. 530-R-09-007). Rockville, MD: U.S. Environmental Protection Agency.

Guan, S., and G. W. Reuter, 1995: Numerical simulation of a rain shower affected by waste energy released from a cooling tower complex in a calm environment. *Journal of Applied Meteorology*, **34**, 131-142.

Kochtubajda, B., W. R. Burrows, D. Green, A. Liu, K. R. Anderson, and D. McLennan, 2011: Exceptional cloud-to-ground lightning during an unusually warm summer in Yukon, Canada. *Journal of Geophysical Research*, **116**, D21206, 1-20,

Massey, F. J. Jr., 1951: The Kolmogorov-Smirnov test for goodness of fit. *Journal of the American Statistical Association*, **46**, 253, 68-78.

Niyogi, D., T. Holt, S. Zhong, P. C. Pyle, and J. Basara, 2006: Urban and land surface effects on the 30 July 2003 mesoscale convective system event observed in the southern great plains. *Journal of Geophysical Research*, **111**, D19107, 1-20.

Rozoff, C. M., W. R. Cotton, and J. O. Adegoke, 2003: Simulation of St. Louis, Missouri, land use impacts on thunderstorms. *Journal of Applied Meteorology*, **42**, 716-738.

Stein, U. and P. Alpert, 1993: Factor separation in numerical simulations. *Journal of the Atmospheric Sciences*, **50**, 14, 2107-2115.

Yue, S., P. Pilon, and G. Cavadias, 2002: Power of the Mann-Kendall and Spearman's rho tests for detecting monotonic trends in hydrological series. *Journal of Hydrology*, **259**, 254–271.

B.7. Tables

Run	Factor #1	Factor #2	Equation for total rainfall, **R**	Total Rainfall	Base Amount, **r0**	Induced by Factor #1, **f1**	Induced by Factor #2, **f2**	Induced by Both Factors, **f12**
r_0	Off	Off	$r_0 = r_0$	**10 mm**	10 mm	0 mm	0 mm	0 mm
r_1	On	Off	$r_1 = r_0 + f_1$	**13 mm**	10 mm	3 mm	0 mm	0 mm
r_2	Off	On	$r_2 = r_0 + f_2$	**16 mm**	10 mm	0 mm	6 mm	0 mm
r_{12}	On	On	$r_{12} = r_0 + f_1 + f_2 + f_{12}$	**11 mm**	10 mm	3 mm	6 mm	-8 mm

Table B.1: An example of the factor separation method on a hypothetical dataset.

Time (Z)	0800	1000	1200	1400	1600	1800
Temperature	15	14	12	15	20	24

Table B.2: A hypothetical dataset for the Mann-Kendall test.

Time Differences	Temperature Differences	Sign of the Differences
1000-0800	-1	-1
1200-0800	-3	-1
1400-0800	0	0
1600-0800	5	+1
1800-0800	9	+1
1200-1000	-2	-1
1400-1000	1	+1
1600-1000	6	+1
1800-1000	10	+1
1400-1200	3	+1
1600-1200	8	+1
1800-1200	12	+1
1600-1400	5	+1
1800-1400	9	+1
1800-1600	4	+1
Mann-Kendall Statistic		**+8**

Table B.3: Calculation of the Mann-Kendall statistic.

Appendix C: The Canadian Lightning Detection Network

Burrows and Kochtubajda (2010) describe the Canadian Lightning Detection Network (CLDN). Data from the CLDN was used in Chapter 3, and in Chapter 5. The CLDN was initiated in 1998 and is operated and processed by Vaisala in Tucson, Arizona. The type of sensors, the locations of the sensors, and the geographic coverage of the sensors has evolved from 1998 to 2017, which makes temporal trend analysis somewhat complicated. A list of sensors as of 2010 from Burrows and Kochtubajda (2010) is shown in Table 1, and is displayed in a map format in Figure 1.

The CLDN consists of a mosaic of three types of sensors: the LPATS-IV, IMPACT, and LS7000 sensors. However, the network is continuously changing as older sensors are upgraded, and sensors are installed at new locations (Burrows and Kochtubajda 2010). Readers are referred to the end of Chapter 2 for an overview of the lightning detection techniques discussed in this section. The LPATS-IV sensors are the oldest, and detect lightning via the time-of-arrival method only. The time-of-arrival method provides a high location accuracy (Cummins and Murphy 2009). The magnetic direction finding method has a lower location accuracy because small angular errors translate to large location errors over large distances. However, the magnetic direction finding method provides a higher detection efficiency, and it has the ability to calculate the peak current of the lightning strike (Cummins and Murphy 2009). Thus the IMPACT sensor was developed, which uses both time-of-arrival and magnetic direction finding methods together to locate lightning, resulting in a higher detection efficiency, peak currents, and a better location accuracy (Cummins and Murphy 2009). The LS7000 lightning sensor is newer digital version of the IMPACT sensor, and was designed to be easier to install, modify, and repair (Cummins et al. 2012).

The CLDN currently detects both cloud-to-ground and cloud lightning; however, early in its existence it detected solely cloud-to-ground lightning strikes (Burrows and Kochtubajda 2010). Cloud lightning is more difficult to detect than cloud-to-ground lightning because it produces lower peak currents (Cummins et al. 2000). When the CLDN began detecting cloud lightning, less than five percent of cloud flashes were being detected (Burrows et al. 2002). However, the criteria for detecting cloud flashes have changed over the years, and the CLDN can now detect significantly more of them (Burrows and Kochtubajda 2010). Because of the many changes to the cloud lightning detection by the CLDN, cloud lightning data was not used in any of these analyses; only cloud-to-ground lightning was used.

The CLDN stores both flash and stroke data. A lightning stroke is one single electrical discharge. It may be positive or negative, and it may be cloud lightning or cloud-to-ground lightning. Often, subsequent stroke discharges happen along the same path. As many as 26 subsequent strokes can occur. The CLDN can group these subsequent strokes together into a lightning flash based on their similar location and time. The multiplicity is defined as the number of strokes in the flash (Burrows and Kochtubajda 2010).

The flash dataset produced by the CLDN contains various properties of each lightning flash. An example is shown in Table 2. The data includes the data and time of the lightning strike, the latitude and longitude, the polarity (positive or negative) and peak current (kA), the multiplicity, and various error and uncertainty parameters. The quality of the stroke detection is represented by the normalized chi-square error measurement. The location of each lightning flash is positioned where the chi-square error is at a minimum, which is derived from the data from each sensor that detected the strike. Lightning stokes that have a normalized chi-square value greater than 15 are not included in the dataset (Cummins et al. 1998). The 50 % confidence ellipse is another uncertainty property which consists of three separate values: the semi-major

axis of the ellipse (km), the semi-minor axis (km), and the orientation (degrees clockwise from north). The probability distribution of the location of the lightning strike is assumed to have a Gaussian shape that fits into the error ellipse, and the 50 % confidence ellipse can be scaled to any confidence level (Cummins et al. 1998).

The stroke dataset contains all of the parameters of the flash dataset, along with some other parameters that give some insight into how the stroke was detected. The extra parameters include the following: the number of sensors used to detect the stroke, the waveform rise-time, and waveform peak-to-zero time. The waveform rise-time and peak-to-zero time have units of microseconds, and are defined at the end of Chapter 2. An example of the extra parameters in the stroke dataset is shown in Table 3. Both of these parameters can be strongly affected by the ground conductivity (Bardo et al. 2004).

C.1. References

Bardo, E. A., K. L. Cummins, and W. A. Brooks, 2004: Lightning current parameters derived from lightning location systems. *International Conference on Lightning Detection*, Helsinki, Finland.

Burrows, W. R., P. King, P. J. Lewis, B. Kochtubajda, B. Snyder, and V. Turcotte, 2002: Lightning occurrence patterns over Canada and adjacent United States from lightning detection network observations. *Atmosphere-Ocean*, **40**, 1, 59-81.

Burrows, W. R., and B. Kochtubajda, 2010: A decade of cloud-to-ground lightning in Canada: 1999-2008. Part 1: Flash density and occurrence. *Atmosphere-Ocean*, **48**, 3, 177-194.

Cummins, K. L., and M. J. Murphy, 2009: An overview of lightning locating systems: History, techniques, and data uses, with an in-depth look at the US NLDN. *IEEE Transactions on Electromagnetic Compatibility*, **51**, 3, 499-518.

Cummins, K. L., M. J. Murphy, and J. V. Tuel, 2000: Lightning detection methods and meteorological applications. Preprints, fourth international symposium on military meteorology, Marbork, Poland, WMO, 85-100.

Cummins, K. L., M. J. Murphy, E. A. Bardo, W. L. Hiscox, R. B. Pyle, and A. E. Pifer, 1998: A combined TOA/MDF technology upgrade of the US national lightning detection network. *Journal of Geophysical Research*, **103**, D8, 9035-9044.

Cummins, K. L., N. Honma, A. E. Pifer, T. Rogers, and M. Tatsumi, 2012: Improved detection of winter lightning in the Tohoku region of Japan using Vaisala's LS700X technology. *IEEJ Transactions on Power and Energy*, **132**, 6, 1-6.

C.2. Tables

Yukon			
Old Crow	67.57	139.83	IMPACT
Eagle Plains	66.37	136.72	IMPACT
Dawson City	64.06	139.43	LS7000
Burwash	61.35	138.99	IMPACT
Faro	62.23	133.35	LPATS-IV
Whitehorse	60.72	135.06	LPATS-IV
Watson Lake	60.06	128.71	IMPACT
Northwest Territories			
Fort Simpson	61.86	121.35	IMPACT
Yellowknife	62.45	114.37	LS7000
Fort Smith	60.01	111.88	LPATS-IV
Nunavut			
Arviat	61.11	94.06	IMPACT
British Columbia			
Dease Lake	58.43	130.00	LPATS-IV
Fort Nelson	58.81	122.70	LPATS-IV
Fort St John	56.25	120.85	LPATS-IV
Terrace	54.52	128.60	IMPACT
Sandspit	53.24	131.82	LPATS-IV
Prince George	53.92	122.75	LS7000
Puntzi Mountain	52.11	124.14	LPATS-IV
Sayward	50.38	125.96	LS7000
Revelstoke	51.00	118.20	IMPACT
Langley	49.10	122.66	LS7000
Cranbrook	49.51	115.77	LPATS-IV
Alberta			
High Level	58.52	117.14	IMPACT
Fort McMurray	56.73	111.38	LPATS-IV
Grande Prairie	55.17	118.80	IMPACT
Slave Lake	55.29	114.77	LS7000
Cold Lake	54.46	110.17	IMPACT
Stony Plain	53.53	114.00	LPATS-IV
Springbank	51.10	114.37	LS7000
Medicine Hat	50.04	110.68	LPATS-IV
Saskatchewan			
Stony Rapids	59.26	105.83	IMPACT
La Ronge	55.11	105.29	LPATS-IV
North Battleford	52.78	108.30	LPATS-IV
Yorkton	51.22	102.47	LPATS-IV
Moose Jaw	50.39	105.53	IMPACT
Manitoba			
Churchill	58.77	94.17	LPATS-IV
Lynn Lake	56.85	101.05	LS7000
Thompson	55.74	97.85	IMPACT
Shamattawa	55.86	92.10	LPATS-IV
St Theresa	53.82	94.92	LPATS-IV
Grace Lake	53.82	101.19	LPATS-IV
Dauphin	51.15	100.05	IMPACT
Winnipeg	49.91	97.24	LS7000
Ontario			
Peawanuk	54.99	85.43	IMPACT
Big Trout Lake	53.76	90.08	IMPACT
Kashechewan	52.29	81.64	LPATS-IV
Red Lake	51.01	93.83	LPATS-IV
Pickle Lake	51.47	90.19	LS7000
Moosonee	51.27	80.64	LS7000
Geraldton	49.73	86.95	LPATS-IV
Timmins	48.48	81.33	IMPACT
Thunder Bay	48.38	89.25	IMPACT
Sault St Marie	46.52	84.35	LPATS-IV
North Bay	46.31	79.46	LPATS-IV
Petawawa	45.90	77.29	LPATS-IV
Egbert	44.23	79.78	LS7000
Windsor	42.31	83.04	LS7000
Quebec			
Schefferville	54.82	66.82	LPATS-IV
Kuujjuarapik	55.27	77.76	LS7000
La Grande	53.63	79.03	LS7000
Wemindji	53.05	78.71	IMPACT
Sept-Isle	50.21	66.38	LPATS-IV
Natashquan	50.17	61.82	IMPACT
Chibougamau	49.91	74.37	IMPACT
Gaspe	48.83	64.49	LPATS-IV
Baie Comeau	49.22	68.15	IMPACT
Normandin	48.84	72.53	LS7000
Rouyn	48.23	79.02	LS7000
Valcartier	46.94	71.47	LS7000
Blainville	45.67	73.87	LPATS-IV
New Brunswick			
Fredericton	45.96	66.64	LS7000
Prince Edward Island			
Charlottetown	46.24	63.13	LS7000
Nova Scotia			
Sydney	46.14	60.19	IMPACT
Sable Island	43.93	59.91	LS7000
Yarmouth	43.84	66.12	IMPACT
Newfoundland			
Wabush Lake	53.08	66.87	IMPACT
Churchill Falls	53.59	64.31	LS7000
Goose Bay	53.30	60.33	LPATS-IV
Cartwright	53.71	57.02	IMPACT
St Anthony	51.37	55.60	LS7000
Stephenville	48.55	58.58	LPATS-IV
Gander	48.95	54.61	IMPACT
St John's	47.56	52.71	LS7000

Table C.1: The approximate location of all lightning sensors in Canada as of 2010 (from Burrows and Kochtubajda 2010).

Date and Time Data							Location Data		Peak	Chi-Square	Ellipse Axes and Orientation			
Year	Month	Day	Hour	Minute	Second	Decimal	Latitude	Longitude	Current	Error	Major	Minor	Orientation	Muliplicity
2000	12	12	7	41	10	936561450	42.9652	-79.1922	-34.9	0.3	0.4	0.4	179	1
2000	12	12	7	42	52	550013900	43.5507	-79.327	-23.2	0.7	0.4	0.4	179	1
2000	12	12	7	47	24	204749050	42.855	-79.1754	18.2	0.3	1.1	0.4	85	1
2000	12	12	8	18	24	376965100	44.1498	-81.157	-23.8	0.7	0.4	0.4	17	1
2000	12	12	9	2	16	478452650	44.4119	-79.6109	-29.4	1.8	0.4	0.4	98	1
2000	12	12	10	41	21	489276565	45.4591	-75.5337	-21.2	3.2	0.4	0.4	158	3
2000	12	17	2	30	59	171406300	42.9476	-81.2635	-26.1	0.5	0.4	0.4	111	1
2000	12	17	7	30	46	15730500	45.4119	-74.8191	-28.6	2.6	0.4	0.4	152	4
2000	12	17	7	34	23	498665100	45.4856	-74.7775	-28.7	1.7	0.4	0.4	138	5
2000	12	19	16	32	0	6362850	51.6807	-108.692	-12.3	0.3	0.4	0.4	172	1

Table C.2: A sample of flash data that is stored in the Canadian Lightning Detection Network.

Hour	Minute	Second	Latitude	Longitude	Sensors	Rise-time	Peak-to-zero
19	41	28	57.8507	-90.9085	4	11.6	0.8
19	48	13	57.8339	-90.7923	3	5.2	1
21	33	23	56.5694	-88.3477	15	10.2	22
21	37	38	57.6284	-92.5671	4	7.2	25.8
21	39	37	56.5488	-88.2879	8	14.6	30.2
21	50	20	57.7128	-92.5434	4	10.8	2.2
21	51	27	57.7302	-92.4864	4	12.4	30
21	52	48	57.6859	-92.5977	2	13.8	0.6
21	54	39	57.6764	-92.4767	5	14.6	30.2

Table C.3: A sample of stroke data that is stored in the Canadian Lightning Detection Network.

C.3. Figures

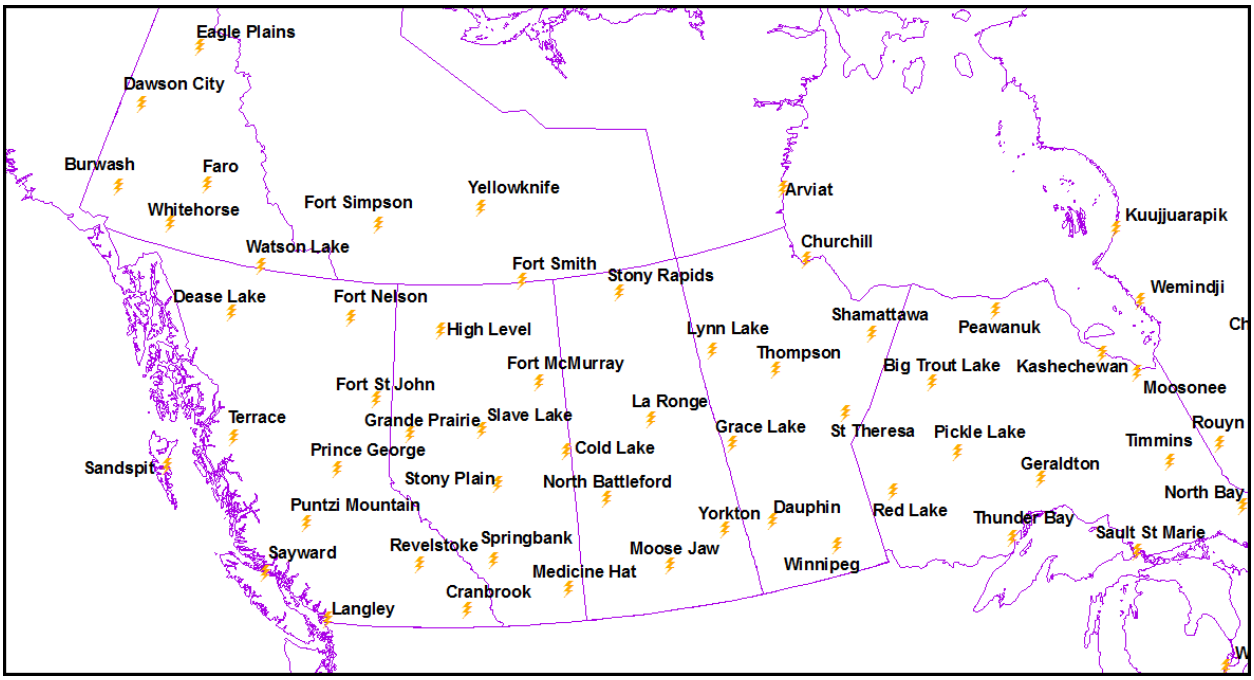

Figure C.1: A map showing the lightning sensor locations in western regions of the Canadian Lightning Detection Network in 2010 (adapted from Burrows and Kochtubajda 2010).

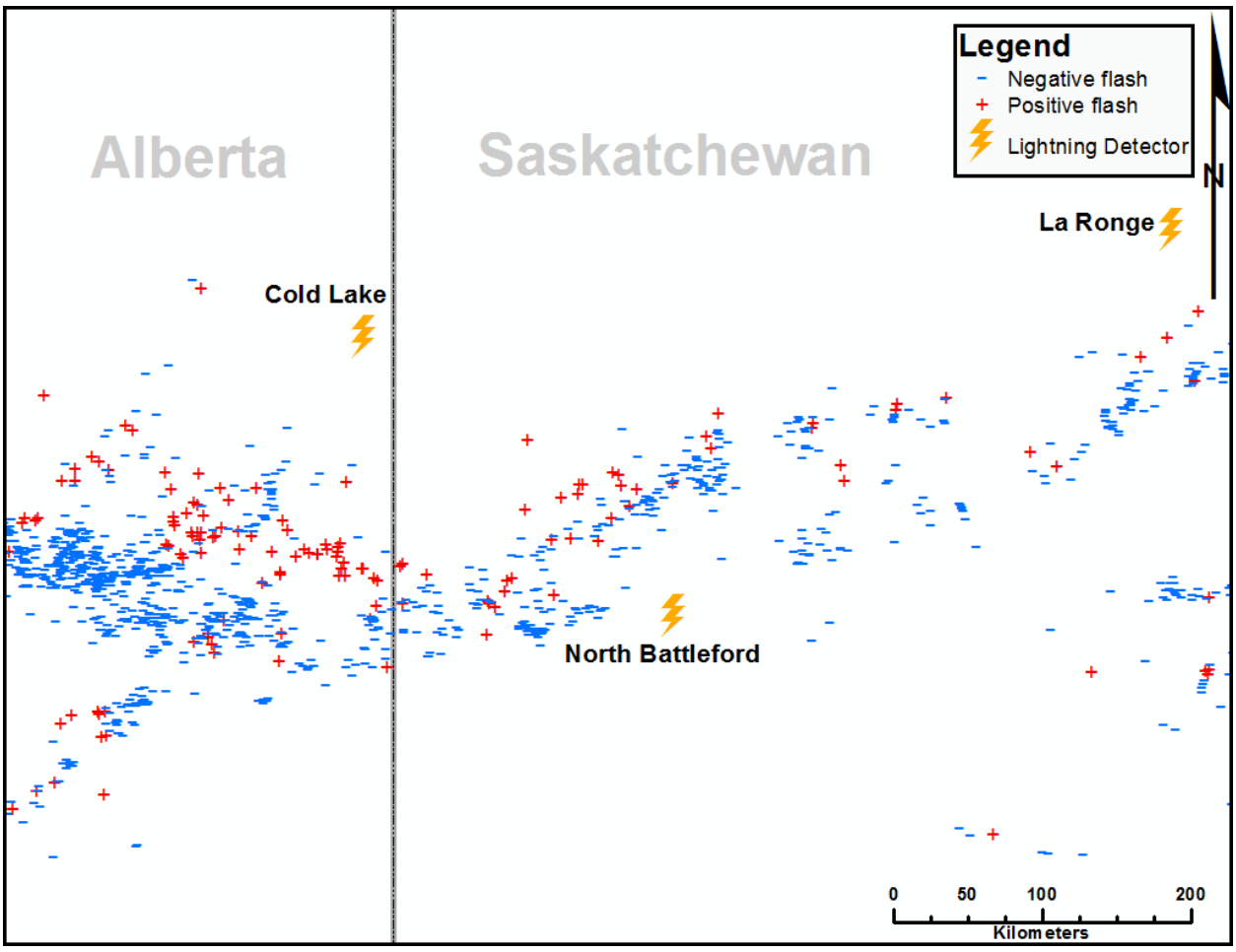

Figure C.2: A map showing a sample of stroke lightning detection data from the Canadian Lightning Detection Network. In this map, lightning data are classified by their polarity, with a plus for positive and a minus for negative. The data is from May 28, 2000.

Appendix D: AMDAR data

The Aircraft Meteorological Data Relay (AMDAR) system uses commercial aircraft as a means of obtaining atmospheric data. AMDAR sensors are often integrated directly into the aircrafts systems, and the data is reported in real time to facilitate operational forecasting (Moninger et al. 2006). AMDAR data are available for operational forecasting and research. Most AMDAR equipped aircraft report the temperature and wind. Only a few aircraft are equipped with humidity sensors, and some are equipped to measure turbulence (Moninger et al. 2006).

Much of the data collected from AMDAR flights is from near or above the tropopause as this is the cruising level for aircraft flights. When aircraft are ascending or descending, they pass through the low and mid-levels, and thus an AMDAR sounding can be constructed (Moninger et al. 2006). AMDAR soundings often occur at airports between sounding sites, and are extremely helpful in data-sparse areas because they fill in the gaps between an extremely sparse upper air balloon sounding network. They can also have a much greater temporal frequency than balloon soundings. Sometimes AMDAR soundings can be recorded every hour, but balloon soundings at synoptic stations occur only at 0000 UTC and 1200 UTC. AMDAR soundings have provided much needed data above the surface in Canada for the past decade or so, but recently there have been much fewer AMDAR-equipped aircraft in Canada. It is also rare to get an AMDAR with humidity data in Canada.

The National Oceanic and Atmospheric Administration (NOAA) provides AMDAR data on a website interface (https://amdar.noaa.gov). Users can retrieve current and historical AMDAR data from the website. However, recent AMDAR data may be restricted to access from only certain networks because the AMDAR data is owned by the airlines who supply it. AMDAR data are included in the analysis data for the various numerical models.

Many research papers have assessed the accuracy of AMDAR data, and how it impacts the accuracy of numerical models. For example, Schwartz and Benjamin (1995) compared AMDAR temperature and nearby upper air balloon soundings and found that they agreed well. Benjamin et al. (1999) compared AMDAR data with other nearby AMDAR data to see if it was consistent with itself, and also found that there was good agreement. Schwartz et al. (2000) found that AMDAR data helped to improve numerical model forecasts.

AMDAR data has not been used in research as much as it could be. Most studies of AMDAR data try to assess the accuracy of the data by comparing it to other data or numerical models. Recently, however, a few studies have used AMDAR data strictly as a research dataset. Smith and Blaes (2015) used AMDAR measurements to assess mixed precipitation from a winter storm in North Carolina. Rahn and Mitchell (2016) used AMDAR data to investigate the atmospheric boundary layer in Southern California. Li et al. (2013) used AMDAR data alongside other measurements to investigate heavy rainfall in Baltimore, Maryland.

D.1. References

Benjamin, S. B., B. E. Schwartz, and R. E. Cole, 1999: Accuracy of ACARS wind and temperature observations determined by collocation. *Weather and Forecasting*, **14**, 1032-1038.

Li, D., E. Bou-Zeid, and M. L. Baeck, 2013: Modeling land surface processes and heavy rainfall in urban environments: sensitivity to urban surface representations. *Journal of Hydrometeorology*, **14**, 1098-1117.

Moninger, W. R., R. D. Mamrosh, and T. S. Daniels, 2006: Automated weather reports from aircraft: TAMDAR and the U.S. AMDAR fleet. 12th Conference on Aviation, Range, and Aerospace Meteorology, January 2006, Atlanta, Georgia. 6 pp.

Rahn, D. A., and C. J. Mitchell, 2016: Diurnal climatology of the boundary layer in southern California using AMDAR temperature and wind profiles. *Journal of Applied Meteorology and Climatology*, **55**, 1123-1137.

Schwartz, B., and S. G. Benjamin, 1995, A comparison of temperature and wind measurements from ACARS-equipped aircraft and rawinsondes. *Weather and Forecasting*, **10**, 528-544.

Schwartz, B. E., S. G. Benjamin, S. M. Green, and M. R. Jardin, 2000: Accuracy of RUC-1 and RUC-2 wind and aircraft trajectory forecasts by comparison with ACARS observations. *Weather and Forecasting*, **15**, 313-326.

Smith, B. L., and J. L. Blaes, 2015: Examination of a winter storm using a micro rain radar and AMDAR aircraft soundings. *Journal of Operational Meteorology*, **3**, 14, 156-171.